University of Strathclyde

Strathclyde Institute of Pharmacy and Biomedical Sciences

Elucidating the function of a conserved gene cluster in a non-pathogenic actinomycete

Laura Clark

Thesis presented in fulfilment of the requirements for the degree of Doctor of Philosophy

2011

Declaration

This thesis is the result of the author's original research. It has been composed by the author and has not been previously submitted for examination which has led to the award of a degree.

Signed:

Date:

Acknowledgements

I would like to thank the many people whose support, help and encouragement made this thesis possible. Thanks firstly to my supervisor Paul Hoskisson for doing so much to make this project so enjoyable, for his advice and encouragement, and for buying me cider. Thanks also to Paul Herron and Nick Tucker for their all-round expertise and advice.

To my many colleagues in R5.21 (and latterly the Penthouse), thank you for making the lab so much fun. In particular, thank you Vinod, Debs, Janet, Gillian and Leena for practical advice at crucial moments and good company all the time.

I would also like to thank my parents and my sister for their neverending support, encouragement, and for valiantly feigning interest in the minutiae of lab work.

To Lawrence, Kirsten, Anna, Liz, Rory, Ben and many other friends from Edinburgh and Bristol, thank you, and I promise to shut up about it now.

Abstract

Streptomyces coelicolor is a soil-dwelling Gram positive saprophytic bacterium of the order *Actinomycetales*, which also includes pathogenic species such as *Mycobacterium tuberculosis*. To survive in the soil environment, *S. coelicolor* must compete with other soil-dwelling organisms. Although a number of mechanisms have been identified for defence against viral, bacterial, fungal and helminthic competitors, no dedicated mechanism has been identified in *S. coelicolor* for resistance to protozoal predation.

The *mce* gene cluster is an operon containing nine core genes and was identified as a virulence factor in *M. tuberculosis*, involved in entry to and survival within macrophages. The *mce* cluster is also present in *S. coelicolor* where its function is unknown.

This thesis details the disruption of several *mce* cluster genes and the construction of a multiple gene knockout in *S. coelicolor*, and the subsequent screening of these mutant strains to determine a *mce* phenotype. It also includes the results of bioinformatic analysis of the operon, as well as transcriptional studies. Development and optimisation of a co-culture assay using the free-living protozoan *Acanthamoeba polyphaga* is described, including idenfication of a hypervirulent *mce* knockout phenotype.

The results of these experiments suggest that the *mce* operon may have evolved as a defence mechanism against protozoal predation in the soil, before undergoing duplication and adaptation in pathogenic species to act as a virulence factor.

Chapter 1: Introduction 1
Overview and project rationale 1
Outline of chapters 2
The actinomycetes 3
Taxonomy of the actinomycetes 4
Actinomycetes as pathogens 7
Inhibition of lysosomal fusion 8
Cell envelope components of *Mycobacterium tuberculosis* 9
The *Mycobacterium tuberculosis* genome sequence 12
Identification of the *mce* locus in *Mycobacterium tuberculosis* 12
Duplication of the operon in *M. tuberculosis* 13
Expression of the *mce* operon in *Mycobacterium tuberculosis* 15
Regulation of the mycobacterial *mce* operons 15
The *mtrAB-lpqB* two-component response regulator 17
The *mce* locus encodes an ABC transporter assembly 18
ABC transport in prokaryotes 18
The Mce ABC assembly in *Mycobacterium tuberculosis* is a cholesterol importer 22
Presence of the *mce* locus in other pathogenic actinomycetes 23
The *Streptomyces* 25
Streptomyces coelicolor 25
Genetic features of *S. coelicolor* A3(2) 26
Development among the actinomycetes 27
Morphological development of *Streptomyces coelicolor* 28
Cell wall components 29
Fatty acid biosynthesis and sterol metabolism 30
Uptake of carbon sources 31
***Streptomyces coelicolor* in the soil** 32
The *mce* operon in *Streptomyces coelicolor* 34
The core cluster 36
The *mce* genes 36
The downstream region 37
Virulence factors in the actinomycetes 37
Aims of project 39
Chapter 2: Materials and Methods 41
Strains, plasmids and cultivation 41
Bacterial growth media 46
Cultivation of *Streptomyces* strains 49
Solid phase growth curves of *Streptomyces* 49
Preparation of *Streptomyces* spore stocks 49
Coverslip cultures for microscopy 50
Dry weight growth curves 50
Cultivation of *E. coli* 50
Storage of *E. coli* stocks 51
Preparation of electrocompetent cells 51
Electroporation of *E. coli* 51
Preparation of chemically competent *E. coli* cells 52
Transformation of *E. coli* 52

Intergenic conjugation of plasmids and cosmids from *E. coli* to *Streptomyces* 52
Screening for double crossovers in *Streptomyces* 53
Isolation of plasmid and cosmid DNA for *E. coli* cultures using the alkaline lysis method 53
Isolation of genomic DNA from *Streptomyces* 54
Agarose gel electrophoresis 55
Southern blotting 56
***Acanthamoeba* co-culture** 58
Plaque assay 59
RNA isolation from *Streptomyces* cultures 60
RT-PCR 62
PCR primers and their design 63
Catalase assay of vacuole catalase activity 65
Bradford assay for protein concentration 65
Spore sensitivity assays 66
Bioinformatics 66
Cloning 67
Overexpression of *mce* cluster genes 67
FTIR 67
Germination assay 68
Plant cultivation 68
Microscopy of plant roots 69
Western blot 69
Chapter 3: Detailed analysis of the *mce* gene cluster in *Streptomyces* 73
Bioinformatic analysis of the *mce* gene cluster 73
The *mce* promoter region 73
Distribution of the *mce* operon 74
Conservation of the *mce* operon in newly-sequenced actinomycetes 74
Constructing phylogenetic trees for the *mce* cluster 77
Regulation of the *mce* operon 83
The *mce* operon encodes an ABC importer 84
Substrate-binding proteins and the MceE lipobox motif 85
Predicted structure of the Mce assembly 87
Chapter 3 summary 89
Chapter 4: Construction of *mce* mutants and phenotypic screening 90
Introduction 90
Construction of single gene disruption mutants 90
Mutation via homologous recombination 100
Construction of a *mce* multiple knockout 102
Construction of a *mce* complementation vector 106
Applications of the complementation vector 111
Analysis of genomic mutations by Southern blot 111
Screening for mutant phenotypes 117
The *mce* operon is not essential in *Streptomyces coelicolor* 118
Phenotypic screening on carbon sources 118
Morphological screening of mutant strains 129
Scanning electron microscopy 130

Germination assay ... 135
FTIR ... 135
Spore sensitivity assay ... 136
Chapter 4 summary ... 141
Chapter 5: Role of the *mce* operon in Streptomycete virulence and interactions ... 142
Introduction to *Acanthamoeba* biology ... 142
***Acanthamoeba polyphaga* in the environment** ... 142
Interaction of *Acanthamoeba* and bacteria ... 146
***Acanthamoeba* and the actinomycetes** ... 148
Investigating the relationship between *S. coelicolor* and a free-living protozoan ... 148
Uptake of wild-type *S. coelicolor* spores leads to lysis of amoebal cells ... 149
Virulence of *Streptomyces coelicolor* is enhanced by disruption of the *mce* genes ... 151
A. polyphaga* does not encyst in co-culture with *S. coelicolor ... 153
Further development of the co-culture assay ... 153
Optimisation of an amoebal plaque assay for use with streptomycetes ... 154
***mce* mutants display hypervirulence in plaque assay** ... 157
An *mtrA* knockout is also resistant to plaquing ... 161
Δ*relA*, Δ*desD* and an *esxBA* mutant show no difference in plaque assay ... 161
Streptomyces scabies* is less resistant to plaquing than *S. coelicolor ... 165
***A. polyphaga* behaves differently in solid and liquid medium** ... 165
Catalase assay ... 166
The role of the *mce* gene cluster in the Rhizosphere ... 168
Establishment of a model plant species ... 169
Impact of *Streptomyces* colonisiation of plant growth and development ... 170
Chapter 5 summary ... 180
Chapter 6: Expression and regulation of the *mce* operon ... 181
Introduction ... 181
***mce* expression during development** ... 181
***mce* expression in the presence of cholesterol** ... 184
Regulation of the *mce* operon ... 190
Transcriptional coupling ... 195
***mce* expression in amoebal co-culture** ... 196
***S. coelicolor mce* expression in plant root-associated bacteria** ... 198
Presence of *mce* genes in pathogenic *Streptomyces* ... 200
Expression of the Mce proteins ... 203
Overexpression of *mce* cluster genes ... 207
Creation of a GFP-promoter fusion ... 211
Chapter 6 summary ... 212
Chapter 7: Discussion ... 213
The *mce* operon is present in many newly-sequenced streptomycetes ... 213
***Streptomyces coelicolor mce* mutants have unusual morphology** ... 214
The *Streptomyces coelicolor* Mce assembly may be a cholesterol importer ... 215
Disruption of the *mce* cluster causes hypervirulence in co-culture with amoebae ... 215
The *mce* phenotype is dose-dependent and rescued by complementation ... 217
The *mtrA* locus encodes a putative regulator of *mce* ... 217

The *mce* operon is involved in the colonisation of plant roots 218
The *mce* operon originated as a survival mechanism in soil 219
Future work 220
Conclusion 221
References 223

Chapter 1: Introduction

Overview and project rationale

The bacterium *Streptomyces coelicolor* spends its life in the soil where it must compete for resources with, and avoid predation by, other soil-dwelling organisms. Some of the diverse mechanisms by which it copes with these pressures have been explored, but others remain unknown.

The soil microbiota is made up of a heterogeneous collection of microscopic life, which can be broadly categorised into viruses, bacteria, archaea, fungi and protozoa (Hartmann *et al.*, 2009; Swanson *et al.*, 2009). Mechanisms have been identified in *S. coelicolor* for defence against the first four categories of organism; however the system or systems which mediate interactions of the bacterium with protozoans remain unclear.

A current area of interest for both environmental and clinical microbiologists is the relationship of environmental bacteria such as the actinomycetes (a group which contains both pathogenic and non-pathogenic taxa) with unicellular protozoans such as the amoebae. A growing body of research has examined the role of these protozoa as environmental reservoirs, vectors and bacterial virulence enhancers (Adekambi *et al.*, 2006; Cirillo *et al.*, 1997; Eddyani *et al.*, 2008).

Concurrently, researchers have been able to exploit the increasing availability of high quality genome sequences to identify genetic virulence factors in important human pathogens such as the mycobacteria. Bioinformatic techniques coupled with novel virulence screens allow large-scale multi-species analysis of virulence determinants.

One such virulence factor is the *mce* (mammalian cell entry) locus, which is widely conserved throughout the actinomycetes. Initially identified in *Mycobacterium tuberculosis*, it is also present in other mycobacteria and widely distributed amongst the actinomycetes including species such as *Nocardia farcinica* and *Streptomyces*

coelicolor. Characterisation of its role in *M. tuberculosis* shows that the operon promotes bacterial entry into and persistence within mammalian macrophages, but its role in other actinomycetes is unknown (Arruda *et al.*, 1993).

This thesis will explore the role of the *mce* operon in *S. coelicolor*, a non-pathogenic organism, with a particular focus on the interaction of the bacterium with the soil-dwelling unicellular protozoan *Acanthamoeba polyphaga*. More broadly, it will examine the distribution of the *mce* loci throughout the actinomycetes, and the possible evolutionary origin of this virulence factor as a survival mechanism in the soil.

Outline of chapters

This first chapter will introduce the bacterial genera which form the actinomycetes. There will be a detailed examination of the mycobacteria, particularly *Mycobacterium tuberculosis* and its mode of infection. There will also be an introduction to the streptomycetes, focusing on *Streptomyces coelicolor* and its ecology and interactions in the environment. The final section of this chapter will examine the origins of virulence factors in the actinomycetes, and virulence factor homologues in *Streptomyces*.

The Materials and Methods chapter (2) will detail the bacterial strains, genetic elements and experimental techniques used in this work.

Chapter 3 will examine the *mce* operon in detail, addressing its genetic structure, its predicted functions at both the molecular and systemic level, and its distribution in the *Actinobacteria*. The data presented here will update and extend the scope of the analysis included in previous reviews of the subject, reflecting the significant number and diversity of actinomycete genomes that have recently been sequenced.

The Results section is divided into three chapters. The first Results chapter (4) describes the creation of *mce* mutant strains of *S. coelicolor*, their verification, and

the initial phenotypic screening of those strains using carbon source screening, spore sensitivity assays and scanning electron microscopy. A *mce* mutant phenotype is described which is further defined in subsequent chapters.

The second Results chapter (5) focuses on the role of the *S. coelicolor mce* cluster in mediating the interactions of the bacterium with the unicellular protozoan *Acanthamoeba polyphaga*. This chapter describes the optimisation of a number of co-culture techniques and the effect of *mce* mutations on the virulence of *S. coelicolor* in co-culture with *A. polyphaga.* This chapter also describes the interaction of *S. coelicolor mce* mutants with plant species *Arabidopsis thaliana* and *Nicotiana tabacum*.

The third Results chapter (6) explores the *S. coelicolor mce* operon on the molecular level using RT-PCR and western blotting. Overexpression of Mce proteins is addressed, as well as the predicted structural features of the Mce ABC assembly.

The Discussion section (chapter 7) reviews the current knowledge of the workings of the *mce* operon in *S. coelicolor* in the light of these experiments. The evolutionary origins of the *mce* cluster are also discussed, as well as its wider role as a virulence factor in the actinomycetes, and the part it plays in environmental interactions between species.

The actinomycetes

The *Actinobacteria* are a phylum of Gram-positive bacteria whose genomic DNA is characterised by a high GC content (Embley and Stackebrandt, 1994) – for a recent review of Actinobacterial systematics see Zhi et al 2009 (Zhi, 2009). Many, although not all, of the actinomycetes will exhibit mycelial growth under appropriate conditions (Kieser *et al.*, 2000). The actinomycetes contain a number of pathogenic organisms, including notable human pathogens such as *Mycobacterium tuberculosis*, *Mycobacterium leprae, Corynebacterium diphtheriae, Nocardia farcinica* and

Streptomyces somaliensis, veterinary pathogens such as *Rhodococcus equi*, and plant pathogens such as *Streptomyces scabies* (Fig. 1.1).

Many actinomycetes spend at least a part of their lifecycle in soil or water, and new actinomycete species are still being isolated from environmental samples; a pubmed search for "novel actinomycete" yields more than 50 publications from 2010 alone. Actinomycetes are found in environments as diverse as mangrove swamps, ocean sediment, crop fields and the Antarctic tundra (Li *et al.*; Liu *et al.*; Xu *et al.*, 2009; Yamamura *et al.*, 2007).

Actinomycetes also have the ability to adapt to radical changes in their environment, for instance from the nutrient-poor soil environment to the eukaryotic intracellular milieu, as is the case for many mycobacterial species. Factors which allow them to do this include siderophores, DNA-binding proteins and transporter assemblies, with large percentages of actinomycete genomes being dedicated to sensing and responding to these changes in environmental conditions (Bentley *et al.*, 2002; Hoskisson and Hutchings, 2006).

Taxonomy of the actinomycetes

The order *Actinomycetales* is divided into 13 suborders. This introduction will focus on the suborders *Corynebacterineae*, containing the mycobacteria, Nocardiae and Rhodococci; and *Streptomycineae*, which contains the streptomycetes.

The taxonomy of the actinomycetes has historically been complex, but following its development in the 1980s 16S ribosomal RNA gene sequencing has been effectively used to clarify taxonomic groups. 16S rRNA sequencing typically involves the amplification of both conserved and variable regions of the 16S rRNA genomic or RNA sequences. Conserved regions can be used to identify higher taxa and also to infer phylogenetic relationships. Variable regions can be used to clarify taxonomy at the genus and species level. The *Streptomyces* 16S rRNA sequence has three

diagnostic variable regions designated α, β and γ (Mehling *et al.*, 1995; Stackebrandt *et al.*, 1991).

Sequencing of chosen housekeeping genes such as *atpD*, *recA*, *rpoB* and *trpB* (multilocus sequence typing or MLST) has also been used in order to overcome the problem of high 16S rRNA sequence similarity among closely related species (Labeda, 2010). Next generation sequencing technologies can now be used to generate huge datasets (for instance, 16S rRNA sequences of the human gut microbiota) and, combined with bioinformatic analysis, can provide detailed information on bacterial community structure (Sun Y, 2010).

Non-sequence-based methods can also be employed in the classification of actinomycetes. Notably chemotyping, in which features of the cell envelope such as fatty acid composition, mycolic acid, teichoic acid and phospholipid types are used to place a species within a taxonomic lineage (Anderson and Wellington, 2001; Naumova *et al.*, 2001). Phage-typing can also be used, in which bacterial species are screened for susceptibility to a range of bacteriophage, creating a profile which can be matched to other members of a taxonomic group (Anderson and Wellington, 2001).

The streptomycetes include the genera *Streptomyces*, *Intrasporangium*, *Sporichthya*, *Streptoverticillium* and *Kineosporia*. The genus *Streptomyces* comprises several hundred species and is divided into groups which are denoted alphabetically. *Streptomyces* A3(2) is a member of major group A (and within this, minor group 21) of the *Streptomyces* (Hodgson, 2000).

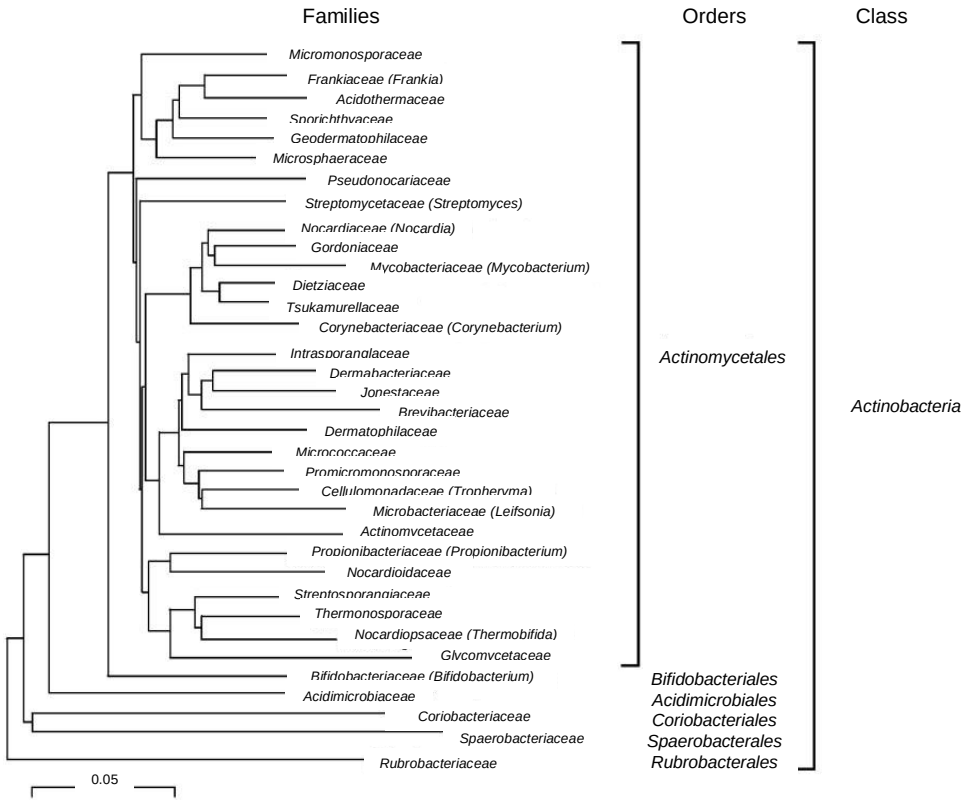

Figure 1.1: Phylogenetic tree of *Actinobacteria* constructed by comparison of 1,500 nucleotides of 16S rRNA. Scale bar: 5 nucleotides. (Figure adapted from Ventura *et al.* 2007).

Actinomycetes as pathogens

Mycobacterium is the most clinically important actinomycete genus of vertebrate pathogens and includes the human pathogen *Mycobacterium tuberculosis*, as well as other pathogens such as *Mycobacterium bovis*, *Mycobacterium avium*, *Mycobacterium ulcerans* and the fish pathogen *Mycobacterium marinum*. *M. tuberculosis* is the aetiological agent of tuberculosis (TB), a disease which affects a significant portion of the world population. WHO survey data estimate 14 million prevalent cases and 1.3 million deaths worldwide from TB in 2009. The mortality rate does not include deaths among HIV-positive people, who in parts of Africa make up more than 50% of new TB diagnoses (WHO, 2010).

Tubercular lung infections are generally contracted by inhalation of airborne droplets from an infected source. Once in the lung, *M. tuberculosis* infection may proceed in different ways. The host may develop active TB, in which the bacterium proliferates and spreads throughout the lungs, causing symptoms such as coughing and fever. Scarring of the lungs caused by an active infection may eventually result in death of the host (WHO, 2010).

Alternatively, the bacterium may be engulfed by a host macrophage which initiates a series of events resulting in the formation of a granuloma (also known as a tuberculoma), a nodule formed from host tissue, inside which the bacterium may survive in a low-level metabolic state for a protracted period of time. Latent TB may never progress beyond the formation of the granuloma and in these cases is generally asymptomatic. In some cases, however, latent TB may develop into an active infection, sometimes many years after the initial infection event (Bentrup and Russell, 2001; de Chastellier, 2009; Murray, 2005).

The cellular processes by which latent infection can develop involve both the host cell and the infecting bacterium. *M. tuberculosis* is phagocytosed by a mononuclear cell which subsequently migrates into tissue near the infection site and recruits additional macrophages. The immune cells aggregate and the macrophages

differentiate into epithelioid cells, creating a dense nodule in which the infectious agent is effectively "walled off" from the rest of the host (Volkman *et al.*, 2004). This prevents propagation of the infection through the lungs, but has the additional effect of protecting the sequestered bacteria from clearing by the host immune system.

Although granuloma formation itself appears to be primarily driven by host immune processes, it is thought that a number of bacterial products including mycolic acid glycolipids, Wax D, trehalose dimycolate (cord factor), ESAT-6 (early secretory antigenic target) and CFP-10 (culture filtrate protein) are necessary for the uptake of *M. tuberculosis* into host cells and its subsequent survival inside them (Riley, 1995; Volkman *et al.*, 2004). There is some evidence that "shedding" of mycobacterial cell envelope constituents and their subsequent trafficking by the host macrophage allows the bacterium to modulate immune responses in adjacent cells which do not contain bacteria (Bentrup and Russell, 2001).

Inhibition of lysosomal fusion

Phagocytic uptake and lysis of bacteria by macrophages follows a pathway in which the bacterium-containing phagosome fuses with early sorting and recycling endosomes containing proteins such as Rab5, Rab11, and SNARE (soluble N-ethylmaleimide-sensitive factor activating protein receptor) proteins such as VAMP3 (vesicle-associated membrane protein) and syntaxin-13 which mediate subsequent membrane fusions. The phagosome then fuses with late endosomes containing further Rab and SNARE proteins as well as a vacuolar ATPase. This vacuolar ATPase acts as a transmembrane proton importer and drives acidification of the phagosome to a pH of around 4.5 (Haas, 2007).

Fusion of the lysosome with the mature phagosome then forms the phagolysosome in which low pH resulting from proton import, lysosomal acid hydrolases such as β-glucuronidase, and superoxide and nitric oxide radicals combine to degrade the bacterial cell (Haas, 2007; Riley, 1995).

Various mycobacteria, notably *M. tuberculosis*, have developed mechanisms which prevent late-endosomal and lysosomal fusion with the bacterium-containing phagosome, thus avoiding degradation of the bacterium inside the macrophage. In *M. tuberculosis*-containing phagosomes pH typically stabilises at around 6.2 and the phagosomes do not mature but rather continue as part of the recycling endosome pathway (Bentrup and Russell, 2001).

Cord factor, and glycolipids such as lipoarabinomannan, have been identified as factors in prevention of lysosomal fusion. The mechanism by which they do this is unknown, but hypotheses include disruption of the biophysical properties of the phagosomal membrane by hydrophobic mycolic acid chains, or inhibition of host factors necessary for phagosomal maturation (Haas, 2007; Riley, 1995). It has been noted that cholesterol depletion in the host cell can lead to lifting of the inhibition of phagosome maturation (Brzostek *et al.*, 2009).

Cholesterol also appears to play an important role in the initial uptake of mycobacteria into the macrophage and it has been noted both that cholesterol is accumulated at sites of mycobacterial uptake and that cholesterol-depleted macrophages fail to phagocytose mycobacteria (Pieters, 2002). It is thus possible that sterol binding sites on the surface of the mycobacterial cell are involved in mediating uptake by macrophages. Further to this, it appears that uptake at cholesterol-rich sites in the macrophage membrane promotes the subsequent recruitment of degradation-preventing proteins to the phagosome (Gatfield and Pieters, 2000).

Cell envelope components of *Mycobacterium tuberculosis*

Sequestration inside granulomas is a key aspect of *M. tuberculosis* virulence and persistence, and one of the reasons why antibiotic treatment of the disease is problematic. For this reason there have been considerable efforts to identify virulence factors in *M. tuberculosis* which relate to this process. Cell envelope components are a likely candidate group as they are ideally placed to interact with

host cell factors. Although over 100 sequences encoding putative surface-exposed proteins have been identified in the *M. tuberculosis* genome, only a few have been characterised; these include channel-forming proteins which have been designated as outer membrane proteins (Niederweis *et al.*, 2010; Song *et al.*, 2008).

The mycobacterial cell envelope consists of an inner plasma membrane and an outer lipid barrier composed of mycolic acids (long fatty acids) linked to arabinogalactan and peptidoglycan (Niederweis *et al.*, 2010; Sutcliffe and Harrington, 2004). The cell envelope thus forms a pseudoperiplasmic compartment with an outer permeability barrier which allows the bacterium to survive in harsh conditions and contributes to antimicrobial resistance. However, while the presence of two concentric membranes has been broadly acknowledged, the precise structure of the cell envelope is unknown and the putative designation of *M. tuberculosis* as a diderm is debated (Desvaux *et al.*, 2009; Niederweis *et al.*, 2010).

Transport of hydrophilic solutes across the cell envelope occurs via a number of mechanisms; Porins such as MpsA allow non-specific uptake of nutrients along a diffusion gradient, while energy-dependent transport is required for large or less abundant molecules. As well as transport, proteins involved in other cellular processes such as membrane assembly and secretion are likely to be situated at the outer membrane (Niederweis *et al.*, 2010).

Putative surface-exposed proteins identified in *M. tuberculosis* include lipoprotein-containing substrate-binding proteins such as PstS-1 and PstS-2 (phosphate-binding proteins which also have a putative role in virulence), MBP83 (a putative adhesin) and the Mce lipoproteins (Sutcliffe and Harrington, 2004). In the course of host cell invasion these proteins are likely to be the first point of contact between pathogen and host.

Upregulation of proinflammatory cytokines such as TNFα (tumour necrosis factor), IRAK-1 (interleukin receptor) and TRAF-6 (TNF receptor-associated factor) inside macrophages in response to bacterial effectors is a key step in granuloma formation

and there is some evidence to suggest that Mce1A, and possibly other Mce proteins, play a role in stimulating this upregulation. In one study, RAW 264.7 murine macrophage-like cells that were treated with His-tagged *M. tuberculosis*-derived Mce1A showed a dose-dependent increase in levels of both IRAK-1 and TRAF-6 (Xue *et al.*, 2007). Additionally, both bioinformatic analysis (Casali and Riley, 2007; Song *et al.*, 2008) and immunoelectron microscopy (Chitale *et al.*, 2001) indicate that the *M. tuberculosis* Mce proteins are surface-exposed.

In addition to upregulation of murine immune response in response to Mce1A, it has been shown that infection of BALB/c mice with *M. tuberculosis mce2* or *mce3* mutants results in reduced host expression of IFNγ (interferon), IL-4 (interleukin) and TNFα during the period of infection. In contrast, an experiment that compared the immunoprotective effect of vaccination with the *mce2* or *mce3* mutant to vaccination with BCG (bacille Calmette-Guerin) showed that the *mce* mutants conferred better protection against H37Rv (a standard laboratory strain of *M. tuberculosis*) (Flesselles *et al.*, 1999). This was thought to be because *mce* mutants are attenuated but retain the ESAT-6 locus, a pathogenicity factor that is not present in BCG (Aguilar *et al.*, 2006).

Infection of RAW macrophage-like cells with a *mce2* mutant strain of *M. tuberculosis* results in reduction in the ability of the host cell to produce TNFα, IL-6 and MCP-1 (Marjanovic, 2009). The same *mce2* mutant is attenuated in C57BL/6 mouse infection, a finding which the authors attribute to the inability of the mutant to stimulate a typical immune response. Another study (Senaratne, 2008) found that *mce3* and *mce4* mutants were also attenuated in C57BL/6 mouse infections, and it has been suggested that the *mce4A* plays a role in invasion and intracellular survival of *M. tuberculosis* (Saini, 2008).

Studies in which latex beads were coated with the Mce1A or Mce3 proteins found that these beads could be internalised by non-phagocytic HeLa cells and were preferentially taken up by macrophages compared to beads coated in a control protein. However Mce2A did not induce uptake, leading to speculation that its

conformation may prevent the Mce domain from being exposed on the surface of the protein (El-Shazly *et al.*, 2007).

Additionally, a study using serum taken from human TB patients found that Mce3A, Mce3D and Mce3E are all expressed in pulmonary TB infection, supporting the designation of the Mce proteins as putative virulence factors.

The *Mycobacterium tuberculosis* genome sequence

The *Mycobacterium tuberculosis* H37Rv genome was published in 1998 (Cole *et al.*, 1998) and has been used as the basis for a number of virulence studies. Some researchers have used the genome sequence as the basis for systematic mutagenesis and subsequent phenotypic screening (Sassetti *et al.*, 2003). Others followed a shotgun cloning approach in which fragments of the *M. tuberculosis* genome were cloned into a non-pathogenic host to observe the effect on virulence (Arruda *et al.*, 1993). One virulence factor identified in this manner was the *mce* locus.

Identification of the *mce* locus in *Mycobacterium tuberculosis*

The *mce* operon was first identified in *M. tuberculosis* when it was found that a fragment of its genome, when cloned into a non-invasive strain of *Escherichia coli*, conferred the ability to invade HeLa cells. It was also noted that the transformed *E. coli* were preferentially taken up by macrophages, and able to persist inside macrophages for an extended period of time relative to a wild-type control. The fragment of *M. tuberculosis* genome responsible was found to carry an operon, which was named *mammalian cell entry* or *mce* (Arruda *et al.*, 1993).

Further investigation of the *M. tuberculosis mce* operon revealed that there were four *mce* loci, each with an apparently functional copy of the operon (Gioffre *et al.*, 2005).

Duplication of the operon in *Mycobacterium tuberculosis*

Gene duplication is an important evolutionary force that provides the opportunity for an organism to evolve new functions. One of the duplicated copies diverges and acquires differential regulation, or mutations occur, followed by evolution into a gene product with a new function. In the case of oligomeric proteins, duplicate copies sometimes evolve to function as hetero-oligomers (Dickson *et al.*, 2000). Duplication can also lead to the acquisition of a varied substrate spectrum. Thus, functional variations and differential regulation can be obtained as a result of gene duplication and provide an adaptive or fitness advantage in the natural environment. Indeed, data available for *E. coli* and *Saccharomyces cerevisiae* suggest that gene duplication plays a key role in the growth of gene networks (Teichmann and Babu, 2004).

Classically, gene duplication is thought to enable duplicates to become specialised in different tissues or developmental stages (Ohno, 1970). A central issue developing from these observations is why so many duplicate genes have been retained in genomes even though the most likely fate of a redundant duplicate is decay. The neofunctionalisation (Ohno, 1970) and subfunctionalisation (Lynch *et al.*, 2001) models are the most frequently quoted to explain the retention of duplicates.

The neofunctionalisation model postulates that the gain of new functions is the major selective factor for the retention of both duplicates in a genome. The subfunctionalisation model suggests that both duplicate genes undergo complementary degeneration, so that both copies are required to fully complement the ancestral gene: essentially a non-adaptive process. Studies of yeast paralogues suggest that both copies of duplicate genes become more specialised in their expression, and that neofunctionalisation is more common than subfunctionalisation (Huminiecki and Wolfe, 2004). However, it is also possible for both mechanisms to work in parallel, with a large proportion of genes undergoing rapid

subfunctionalisation following duplication, followed by a prolonged period of neofunctionalisation (He and Zhang, 2005).

Bacterial genomes with high levels of sequence duplication (which is not the result of large DNA-segment duplication) are being identified more frequently, and such duplication has been demonstrated in a range of organisms (Thomaides *et al.*, 2007). This appears to be the case in *S. coelicolor*, with 709 genes having at least one homologue within the genome (with at least 70% sequence similarity, and 70% coverage on both proteins; Hoskisson and Chandra, Unpublished). This accounts for 9% of the genome, corresponding well with the published figures from other bacterial genomes (Thomaides *et al.*, 2007).

Gene duplication is therefore an important prerequisite for gene innovation, facilitating adaptation, with paralogues comprising a significant proportion of bacterial genomes. This importance to biological innovation is likely to have contributed to the evolution of complex lifecycles in actinobacteria, given the large numbers of paralogous gene families associated with development and sporulation in complex actinobacteria (Chater and Chandra, 2006). Knowledge of these processes at the molecular level is fundamental to understanding the evolution of genome structure and bacterial populations, and is crucial to better understand the genetic traits behind industrially and biomedically relevant strains.

Why duplicate genes are maintained in genomes is a heavily debated issue in both prokaryotes and eukaryotes. It would, however, appear that duplication of certain genes within the chromosome of actinomycetes throughout evolution has contributed to pathogenicity, as with the *mce*, ESAT and WhiB-like gene clusters in mycobacteria and Nocardia (Chater and Chandra, 2006).

Expression of the *mce* operon in *Mycobacterium tuberculosis*

Mutational studies of the *mce1*, *2* and *3* operons showed that *mce* knockout mutants were attenuated in mouse infection models (Gioffre *et al.*, 2005). It has also been shown that the four *mce* operons in *M. tuberculosis* are differentially expressed at different stages of infection. The *mce1* operon is expressed early during infection while *mce4* is expressed more strongly after a number of weeks (Casali *et al.*, 2006). In spite of these differences it has been found that mutations in *mce1* and *mce4* interact negatively (i.e. an *mce1+4* mutant will display a phenotype that is more severely attenuated than the sum of the phenotype of two single-locus mutants), which has given rise to the suggestion that the two copies of the operon have "similar or even partially redundant" roles (Joshi *et al.*, 2006). It should however be noted that in this study phenotype was assessed by counting the number of viable bacteria of each strain recovered after inoculation of a mouse with a culture containing multiple mutant *M. tuberculosis* strains. As immunological conditions appear to be a significant factor in the outcome of *mce* mutant infections (Shimono *et al.*, 2003), the presence of competing strains may have influenced the results.

In *Nocardia farcinica* analysis of codon bias, which correlates positively with gene expression level, was used to predict highly expressed genes. These "PHX" genes included *mce1D*, *mce2C*, *mce6C* and *mce6F*, as well as a number of known virulence factors (Wu *et al.*, 2006). This would seem to indicate an important role for Mce proteins in *N. farcinica*. However, this analysis is predictive and does not take into account the possible effect of regulators on gene expression in vivo.

Regulation of the mycobacterial *mce* operons

All four *mce* operons in *M. tuberculosis* have putative or well-characterised regulators, two of which (Mce1R and Mce2R) are GntR-like while the remaining two (Mce3R and KstR) are TetR-like. GntR (for gluconate repressor) is a family of

largely self-regulatory proteins containing a C-terminal effector-binding or oligomerisation domain and a conserved DNA-binding helix-turn-helix motif at the N-terminus. GntR-like repressors inhibit transcription by binding to operator sites in the promoter regions of target genes. The GntR-like regulator DasR has been shown to play a role in primary metabolism and development in *S. coelicolor* (Hoskisson *et al.*, 2006; Santangelo *et al.*, 2009; Santangelo *et al.*, 2008).

The TetR (tetracycline resistance) regulator also contains an N-terminal helix-turn-helix motif, and belongs to a family of regulatory proteins that are often associated with resistance to compounds such as detergents and hydrophobic antibiotics (Reichheld *et al.*, 2009).

Mce1R (Rv0165c) is a GntR-like regulator belonging to the FadR (fatty acid degradation) subfamily. It lies adjacent to, but is transcribed divergently from, the *mce1* operon, and has been shown to negatively regulate this operon (Casali *et al.*, 2006). Mce2R (Rv0586) is the first ORF in the *mce2* operon and is transcribed in the same direction. Like Mce1R it is a GntR-like regulator, and has been shown to negatively regulate the *mce2* operon, although it is not a strong repressor. Mce2R is negatively self-regulated, and it is suggested that the regulation of *mce2* favours expression of the operon under most conditions (Santangelo *et al.*, 2009).

Mce3R (Rv1963c) is a TetR-like regulator, and like Mce2R it is negatively self-regulated. It is a repressor of *mce3* and has been shown to have no effect on the expression of the other *mce* operons. Unlike Mce2R it is a fairly strong repressor and appears to repress *mce3* expression under most circumstances (Santangelo *et al.*, 2008; Santangelo *et al.*, 2002).

Interestingly, the TetR-like *mce4* repressor KstR (ketosteroid regulator; Rv3574) additionally regulates a number of lipid metabolism genes that are induced by growth on cholesterol. The inclusion of *mce4* in this regulon suggests that it may be involved

in uptake of lipids which are subsequently metabolised by other members of the regulon (Kendall *et al.*, 2007). A similar role has been suggested for Mce3R which has been observed to regulate transcriptional units with putative roles in lipid metabolism (Santangelo, 2009).

The *mtrAB-lpqB* two-component response regulator

The two-component response regulator *mtrAB-lpqB* has been identified as a putative regulator of the *mce* clusters in *M. avium*. Two-component response regulators typically consist of a transmembrane sensor kinase (MtrB) and a cognate cytoplasmic response regulator (MtrA) which is phosphorylated by the sensor kinase in response to a chemical stimulus. The MtrAB two-component system also has an associated lipoprotein (LpqB) whose function is unknown, although it has been suggested that it modulates the sensor kinase (Hoskisson and Hutchings, 2006). Disruption of *mtrB* resulted in reduced expression of the *mce1*, *mce3* and *mce4* clusters, suggesting that MtrB is required for expression of *mce* in vivo. The *mtrB* mutant was also unable to persist intracellularly in a macrophage infection model (Cangelosi *et al.*, 2006).

Disruption of *mtrB* could not be performed in *M. tuberculosis* because *mtrB* is essential in this organism, however expression studies on *mtrA* show that it is expressed constitutively. In *M. bovis*, *mtrA* is upregulated tenfold during macrophage infection. Disruption of *mtrAB* in *Corynebacterium glutamicum* gave rise to a mutant that showed increased sensitivity to cell wall-targeting compounds (vancomycin, lysozyme), indicating that *mtrAB* may have a role in maintaining the stability of the cell envelope (Hoskisson and Hutchings, 2006).

The *mtrAB-lpq* operon is widely conserved in the actinomycetes including *Streptomyces*, and is present in *M. leprae* (which also has a copy of the *mce* operon) despite the widely decayed nature of its genome (Hoskisson and Hutchings, 2006).

Given the absence of any other identified regulators of *mce* outside of *M. tuberculosis*, the MtrAB response regulator is a good candidate for this role.

The *mce* locus encodes an ABC transporter assembly

Bioinformatic analysis of the *M. tuberculosis mce* operon (Casali and Riley, 2007) showed that the operon consisted of nine core genes (Fig. 1.3), putatively designated as encoding an ATPase, two transmembrane proteins, and six (Mce) proteins forming one or more substrate-binding domains. These features are characteristic of the ABC (ATP-binding cassette) class of transporters (Casali and Riley, 2007).

Phylogenetic analysis of the ATPase showed that it clustered with an "Mkl-like" clade of mycobacterial importer-associated ATPases, and taken together with the presence of a substrate-binding domain this indicates that the Mce ABC assembly is an importer (Casali and Riley, 2007). The Mkl subfamily has been postulated to have a role in maintaining cell surface integrity (Dassa and Bouige, 2001).

ABC transport in prokaryotes

ABC transporters are ubiquitous in living organisms, although ABC *importers* are unique to prokaryotes (Hollenstein *et al.*, 2007). The ABC superfamily is made up of more than 50 subfamilies which can be broadly divided into three classes: class 1 is made up of exporters, class 2 of assemblies without transmembrane domains, and class 3 of binding-protein-dependent systems. The Mce ABC assembly falls into the third class which includes the Mkl subfamily (Dassa and Bouige, 2001).

In Gram positive organisms ABC assemblies are situated across the plasma membrane and consist of two hydrophobic transmembrane permease domains coupled with a pair of hydrophilic nucleotide binding domains which bind and hydrolyse ATP on the cytoplasmic side of the membrane (Fig. 1.2) (Dawson *et al.*, 2007).

ABC-associated nucleotide binding proteins (NBPs) are characterised by several conserved domains – the Walker A (or P-loop) and Walker B motifs, located in a RecA-like subdomain, and a LSGGQ motif (or C-loop) found in an alpha-helical subdomain. It has been shown that the C-loop of each NBP monomer forms part of the binding site of the opposite monomer (Daus, 2007).

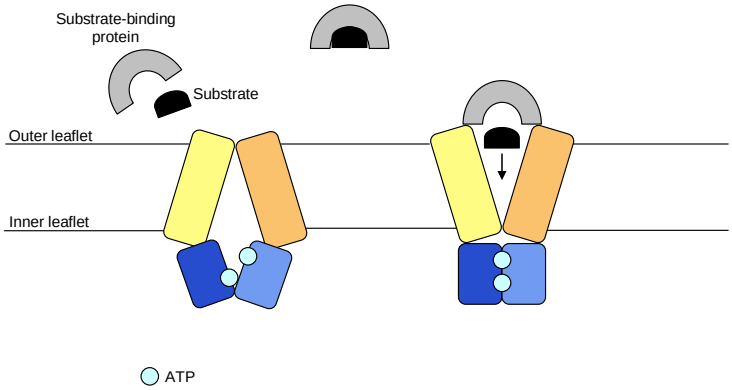

Figure 1.2: Import of a substrate molecule by an ABC transporter. In the inward-facing conformation (left) the transporter binds ATP at the nucleotide-binding domain (NBD, blue). Following binding of the substrate by the substrate-binding protein (SBP, grey) and ATP hydrolysis by the NBD the importer assembly changes to an outward-facing conformation (right) and the SBP releases the substrate into the transmembrane channel. ADP and P_i are released from the NBD, the ABC assembly reverts to an inward-facing conformation and the substrate is released into the cytoplasm. Adapted from Dawson *et al.* 2007.

Transmembrane domains of ABC importers typically consist of between 10 and 20 α-helices. Although there is little conservation at the sequence level, X-ray crystallography shows considerable similarity in the conformation of key regions, particularly the "coupling helices" which interact with the NBP (Hollenstein *et al.*, 2007).

Substrate binding proteins on the extracellular side of the membrane are also necessary in order to bind the relevant ligand prior to transport. The high specificity of the binding proteins (with K_d values typically ranging from 0.01 to 1μM) means that transport across the membrane will be unidirectional (Dawson *et al.*, 2007; Eitinger *et al.*). Substrate binding proteins are characterised by a bi-lobed conformation with a binding site situated between the two lobes, and in monoderms such as the *Firmicutes* and *Actinobacteria* are usually membrane-anchored via lipoproteins. In Gram-negative diderms the SBPs are periplasmic (Moussatova *et al.*, 2008).

In Gram-negative organisms it has been observed that "orphan" SBPs may compete to supply substrates to importer assemblies, with more than one type of substrate being imported by the same TMD-NBP assembly. Multiple orphan SBPs for the transport of sugars have been identified in *Streptomyces* (Thompson *et al.*, 2010; Widdick *et al.*, 2011). It is also possible that orphan SBPs could occur in the pseudoperiplasmic region in *M. tuberculosis* (Thomas, 2010).

When the transporter is in the ATP-bound state, the nucleotide is bound by the Walker A subdomain and is also in contact with the C-loop. The Walker B subdomain contains a conserved glutamate residue which facilitates nucleophilic attack of the bound ATP. The number of ATP molecules that can be bound by the NBP at one time has not been clearly established, but it is thought that two ATP molecules are required per molecule of substrate transported (Hollenstein *et al.*, 2007).

Binding of ATP triggers closing of the NBP, at which point coupling helices situated in a groove at the boundary of the RecA-like and α-helical subdomains transmit the conformational change from the NBP to the transmembrane domains. The TMDs then flip from an inward-facing to an outward-facing conformation (Fig. 1.2), allowing the substrate to be accepted from the substrate-binding protein. Hydrolysis of ATP and the subsequent release of ADP and P_i then triggers reversion to the inward-facing conformation, at which point the substrate is released into the cytoplasm (Hollenstein *et al.*, 2007; Oldham *et al.*, 2008).

The Mce ABC assembly in *Mycobacterium tuberculosis* is a cholesterol importer

The ligand transported by the putative Mce ABC assembly is of interest because of the light it could shed on the biological role of the transporter. A possible candidate, given the observed properties of the *mce* cluster, is cholesterol. Found in the membranes of eukaryotic cells such as macrophages, it would be a useful carbon source for bacteria sequestered in granulomas (Brzostek *et al.*, 2009). The potential membrane-membrane interaction implied could also give a clue as to the mechanism of induced uptake of bacteria by mononuclear cells, particularly as cholesterol is known to be a determinant of mycobacterial uptake (Gatfield and Pieters, 2000). An unusually high concentration of free mycolic acids has been observed in the outer lipid layer of an *mce1* mutant, supporting the hypothesis that the *mce* operon may be involved in cell envelope remodelling (Casali and Riley, 2007).

Uptake and metabolism of cholesterol has been identified as an important factor in the intracellular survival and persistence of *M. tuberculosis*. A number of genes and gene clusters have been identified, including *choD* (cholesterol oxidase), *HsaC* (iron-dependent extradiol dioxygenase) and a cluster including a Δ1 KTSD (3-keto-5α-steroid Δ4 dehydrogenase) (Brzostek *et al.*, 2007; Knol *et al.*, 2008; Yam, 2009).

It appears that cholesterol usage becomes essential for mycobacterial persistence in the secondary stage of macrophage infection, when macrophages have become activated by IFNγ. At this stage the intracellular environment is nutrient-poor, and it

has been shown that *M. tuberculosis* bacilli localise to areas of the cell that are rich in cholesterol (Pandey and Sassetti, 2008).

Cholesterol has been identified as a substrate molecule for the Mce assembly in both *M. tuberculosis* and *Rhodococcus sp* (Mohn *et al.*, 2008). However, it seems possible that the Mce assembly in *S. coelicolor* might have a different, although probably related, substrate. Cholesterol itself may be biologically available in the soil environment, and it is also likely that related molecules such as plant sterols are available (Dinel *et al.*, 2001). The *S. coelicolor* genome contains genes for sterol metabolism (putative cholesterol oxidase SCO4781 and cholesterol esterase SCO5420), suggesting that it is able to catabolise these compounds for use as a nutrient source (Aparicio and Martin, 2008; Xiang *et al.*, 2006).

Presence of the *mce* locus in other pathogenic actinomycetes

Although *M. tuberculosis* is the best known and most widespread human pathogen in the actinomycetes, there are other mycobacterial species which cause disease in higher eukaryotes. These include *M. bovis* (the cause of bovine TB), *M. avium*, *M. abscessus* and *Mycobacterium kansasii* which all cause TB-like lung infections (Goy *et al.*, 2007; Ripoll *et al.*, 2009; Tortoli, 2006).

The genus also includes the obligate intracellular pathogen *M. leprae*, which is the causative agent of leprosy (Hansen's disease), and *M. ulcerans* which is an emerging pathogen and the aetiological agent of Buruli ulcer (Eddyani *et al.*, 2008). All of these organisms contain one or more copies of the *mce* locus (Casali and Riley, 2007). The distributions of *mce* homologues are analysed in more detail in chapter 3.

The actinomycetes also contain several non-Mycobacterial mammalian pathogens. The *Nocardia* are a group of emerging pathogens which cause lung infections similar to TB. They can also cause localised infections which, if untreated, cause significant morbidity and may result in loss of limbs. Immunosuppression is a predisposing factor for *Nocardia* infection and the majority of nocardiosis cases occur in sub-

Saharan Africa which has a high prevalence of HIV infection (Ishikawa *et al.*, 2004; Murray, 2005).

In the same family as *Nocardia*, the genus *Rhodococcus* contains a number of mammalian and plant pathogens. *R. equi* is a common cause of equine pneumonia, but can also act as an opportunistic human pathogen in immunocompromised hosts (Letek *et al.*). *Gordonia* species such as *Gordonia bronchialis* are also opportunistic human pathogens (Brust *et al.*, 2009). These non-mycobacterial actinomycetes also possess homologues of the *mce* genes and will be discussed in detail in chapter 3 (Casali and Riley 2007).

As a general rule, organisms showing greater pathogenicity in mammalian infections have more copies of the operon. This is consistent with the designation of the *mce* cluster as a virulence factor, but raises the question of what the function of the operon is in non-pathogenic species. It also suggests that there might be a dosage effect as some organisms have so many apparently redundant copies (Fig. 3.1, chapter 3). This is explored further in the results chapters.

An exception to the rule is *M. leprae*, which is an obligate intracellular pathogen but only has a single copy of the operon. There are two hypotheses that might account for this. Firstly, that as an obligate intracellular bacterium *M. leprae* has a widely decayed genome: the fact that the single copy of the *mce* operon it does possess is apparently functional is an indication that it plays a role in the cell. Secondly, that the *mce* operon is involved, not only in intracellular survival of the bacterium but in mediating the transition from one environment to another (e.g. soil to macrophage). As it does not make such transitions, *M. leprae* may require fewer copies of the operon (Casali and Riley, 2007; Cole *et al.*, 2001).

Many actinomycetes are of interest to researchers primarily because of their role as aetiological agents of mammalian disease. However, species of the genus *Streptomyces* have attracted significant interest because of their ability to produce

bioactive secondary metabolites, some of which can be used to treat a broad range of bacterial infections including those caused by other actinomycetes.

The *Streptomycetes*

The actinomycete genus *Streptomyces* was defined by Waksman and Henrici in 1943 as "actinomycetes with branched slender mycelium, rarely or not septate, forming spores in chains on aerial hyphae". It currently contains almost 600 validly described species (Labeda, 2010). Although it contains several pathogenic species (*S. somaliensis, Streptomyces sudanensis*) and phytopathogens (*Streptomyces scabies, Streptomyces acidiscabies, Streptomyces europaeiscabiei, Streptomyces luridiscabiei, Streptomyces niveiscabiei, Streptomyces puniciscabiei, Streptomyces reticaliscabiei, Streptomyces stelliscabiei, Streptomyces turgidiscabiei, Streptomyces ipomoeae*), *Streptomyces* is largely made up of non-pathogens. Novel *Streptomyces* species are still being identified and sequenced; there are currently 26 completed *Streptomyces* genome sequences in the NCBI database (National Centre for Biotechnology Information; www.ncbi.nlm.nih.gov).

Streptomyces coelicolor

Streptomyces coelicolor is a soil-dwelling saprophytic bacterium. It has a complex lifecycle starting from a single spore which germinates and exhibits branching hyphal growth to produce a dense vegetative mycelium. On solid media aerial hyphae then grow upwards in a spiral conformation from the vegetative mycelium and subsequently septate to form spore chains (Chater and Chandra, 2006). The genus name *Streptomyces* reflects this fungus-like growth (from the Greek *streptos* [twisted] and *mykes* [fungus]). Dispersal of the spores allows the cycle to begin again. In liquid media aerial hyphae are not produced and the bacterium proliferates by growing into dense hyphal clumps. Fragments can be sheared off the outside of the clumps to produce new growth (Kieser *et al.*, 2000).

S. coelicolor produces a wide range of secondary metabolites, including the blue pigmented polyketide antibiotic actinorhodin from which the species takes its name (*coelicolor*, from the Latin "sky colour"), and geosmin which gives *S. coelicolor* its distinctive earthy smell. *Streptomyces* species also produce around a third of all medically used antibiotics and a number of anti-cancer and anti-helminth compounds (Kieser *et al.*, 2000).

The *S. coelicolor* genome sequence contains 20 gene clusters thought to be involved in secondary metabolite synthesis, including predicted siderophores coelichelin, coelibactin and desferrioxamine, as well as polyketide synthases, chalcone synthases, non-ribosomal peptide synthases and terpene cyclases (Bentley *et al.*, 2002). Most sequenced *Streptomyces* strains also produce cryptic antibiotics (Baltz, 2008).

Genetic features of *S. coelicolor* A3(2)

S. coelicolor A3(2) strain M145 is a laboratory strain that lacks both the SPC1 363 kb linear and the SPC2 31.4 kb circular fertility factor plasmids (Haug *et al.*, 2003; Yamasaki *et al.*, 2001). The M145 strain was used to produce both the transposon insertion library used in this work (Bishop *et al.*, 2004) and the genomic library used for sequencing of the *S. coelicolor* genome (Redenbach *et al.*, 1996), and is used throughout this thesis both as a wild-type control and as a background strain for genetic manipulation.

The *S. coelicolor* A3(2) M145 complete genome sequence was published in 2002. The genome is linear, approximately 8.66 mb and has a GC content of 72%. This high GC content produces a codon bias such that the third base position in approximately 90% of all codons is G or C (Chater and Chandra, 2006). The *S. coelicolor* genome contains 7825 predicted genes and more than 20 clusters encoding predicted secondary metabolites. There is a central origin of replication and inverted terminal repeats on the chromosome arms (Bentley *et al.*, 2002).

The *mce* operon is situated at 2.6 mb and thus falls within the designated "core" region of the genome which extends from 1.5 mb to 6.4 mb. The core region mainly contains genes responsible for essential cellular functions such as DNA replication, whereas genes encoding non-essential functions such as secondary metabolite production are typically situated on the chromosome arms. Comparisons between *S. coelicolor* and *M. tuberculosis* reveal that synteny is only conserved over the core region of the genome, suggesting that this portion of the chromosome is ancestral (Bentley *et al.*, 2002).

S. coelicolor has a restriction system which cuts DNA that has been methylated by the *E. coli* Dam ($GA^{*}TC$), Dcm (CC^{*}[A/T]GG) or Hsd ($A^{*}A^{*}C(N)_6GTGC$) modification systems (Gonzalez-Ceron *et al.*, 2009; MacNeil *et al.*, 1992). For this reason plasmids used for genetic manipulation of *S. coelicolor* must be passaged through a non-methylating *E. coli* strain prior to use (see results, chapter 4).

Development among the actinomycetes

The actinomycetes encompass a wide variety of lifestyles, from soil-dwelling saprophytes to obligate intracellular pathogens. Perhaps as a reflection of this, there is also broad diversity of morphological development. *Streptomyces* are arguably the most developmentally complex actinomycetes and possess a large and diverse collection of genes related to their distinctive morphology. Interestingly, however, many of the genes associated with development in *Streptomyces* are also present in other actinomycetes. Phylogenomic studies can thus be used to shed light on the evolution of this developmental complexity (Chater and Chandra, 2006).

In a scenario similar to that postulated in recapitulation theory (Dayrat, 2003), acquisition of developmental genes appears to have followed a timeline that is analogous to the progress of morphological differentiation itself; the first genes to emerge were those such as *bldH*, *G*, *C*, *D*, and the chaplins, responsible for stress responses and the development of an aerial mycelium, followed by genes such as

whiG, *H*, *I*, and *E* related to septation of the aerial hyphae and spore development (Chater and Chandra, 2006).

Morphological development of *Streptomyces coelicolor*

The formation of aerial hyphae in *S. coelicolor* is the result of a complex regulatory system. At least three separate pathways are involved in the regulation of growth, maturation and sporulation of aerial hyphae. Although these pathways were characterised separately, the pleiotropic nature of regulatory proteins such as BldD suggests that the pathways coordinate to form a complex network governing morphological differentiation (den Hengst *et al.*).

The formation of aerial hyphae from the substrate mycelium relies on the so-called bald genes (*bld*, from the bald appearance of colonies which are unable to form aerial hyphae). There are at least 12 classic *bld* genes which play essential roles in the formation of aerial hyphae. Some *bld* mutants are able to cross-complement when grown adjacent to one another and most *bld* phenotypes can be rescued to some extent by the exogenous application of SapB, a hydrophobic lantibiotic molecule (Kodani *et al.*, 2004; Nodwell *et al.*, 1999). Bld proteins characterised so far have been found to be antagonists of anti-σ-factors (Chater and Chandra, 2006).

The *bld* genes are postulated to act as a developmental checkpoint which allows morphological differentiation only if environmental conditions are suitable (Claessen *et al.*, 2006). SapB is a small hydrophobic peptide and it is probable that it acts by reducing the surface tension at the interface between the substrate and the air such that aerial hyphae are able to escape the surface and grow upwards (Nodwell *et al.*, 1999).

The *whi* genes are involved in control of outgrowth and maturation of the aerial hyphae to form mature spore chains. The term *whi* is used to describe colonies that are sporulation-deficient, as they have a white appearance due to the underproduction of the grey spore pigment WhiE. There are 8 loci which give rise to the *whi*

phenotype (*whiA, B, D, E, G, H, I, J*), six of which are deficient in the formation of septa in the aerial hyphae (Chater, 1998; Chater and Chandra, 2006; Ryding *et al.*, 1999).

Recently a third regulatory pathway has been identified, named the sky pathway. This pathway regulates the formation of the rodlet layer on the surface of the aerial hyphae. This layer plays a key part in the hydrophobicity of the spore chains that allows them to escape from the substrate. The rodlet layer on the spore surface is visible under atomic force or scanning electron microscopy (see results, chapter 4) (Claessen *et al.*, 2004).

Cell envelope components

S. coelicolor is a Gram positive monoderm and as such has a single thick cell wall composed primarily of peptidoglycan (Labeda, 2010). Peptidoglycan is made up of N-acetylglucosamine and N-acetylmuramic acid connected by glycosidic bonds to give a lattice-like structure. Peptidoglycan remodeling, which is necessary for apical growth of the hyphae, is controlled by cell wall hydrolases (Flardh, 2003; Heidrich *et al.*, 2002).

Secondary cell envelope components identified in *Streptomyces* include teichoic and (less commonly) lipoteichoic acids, lipoglycans, diacylglycerols, and phospholipids such as cardiolipin, phosphatidylinositol and phosphatidylethanolamine (Cascioferro *et al.*, 2007; Dramsi *et al.*, 2008; Guenin-Mace *et al.*, 2009; Rahman *et al.*, 2009). These secondary components allow anchoring of membrane proteins, help to determine cell shape, and play roles in cell division.

Outer envelope proteins in *S. coelicolor* may be secreted by the Sec general secretory pathway, a ubiquitous bacterial system which transports unfolded proteins through a membrane-embedded translocon (Chater *et al.*, 2010). Alternatively, proteins may be exported via the Tat (twin arginine translocase) pathway. The Tat pathway transports pre-folded proteins targeted by N-terminal signal peptides containing a twin arginine

motif (Chater *et al.*, 2010). The Tat pathway is only present in half of currently sequenced prokaryotes, and in most species appears to have relatively few substrates. However, in *Streptomyces* the Tat pathway is a major protein exporter, exporting around 30% of cell cell envelope secreted proteins (Widdick *et al.*, 2006).

Roughly 2.7% of the *S. coelicolor* proteome is composed of lipoproteins which are bound to the cell membrane by diacylglyceride lipid anchors. Studies demonstrate that the Tat system is a significant exporter of lipoproteins in *S. coelicolor* (Thompson *et al.*; Widdick *et al.*, 2006).

Lipoproteins are characterised by the presence of an N-terminal signal peptide which targets the protein to the cell envelope. The signal peptide contains a lipobox motif (see chapter 3) with the consensus sequence [LVI]-[ASTVI]-[GAS]-C. Following translocation of the protein via Sec or Tat, diacylglycerol transferase catalyses the thioether linkage of a lipid moiety to the sulphydryl group of the cysteine reside of the lipobox. The signal sequence is then cleaved on the N-terminal side of the lipidated cysteine by lipoprotein signal peptidase. Interestingly, neither the diacylglycerol transferase nor the signal peptidase is thought to be essential in Gram-positive organisms (Thompson *et al.*), although lipoprotein biosynthesis may be an essential pathway in *Streptomyces* (Thompson *et al.*, 2010; Widdick *et al.*, 2011).

Fatty acid biosynthesis and sterol metabolism

In order to maintain the integrity of its cell envelope under varying conditions, *Streptomyces* must regulate the concentration of lipids in the cell membrane. One of the mechanisms by which it does this is via the regulation of fatty acid metabolism genes by regulators such as FasR (Arabolaza *et al.*). FasR (for fatty acid synthesis regulator) regulates transcription of the *fab* (fatty acid biosynthesis) operon, which contains genes encoding a malonyl synthase (*fabD*) and two 3-ketoacyl-ACP synthases (*fabF, fabH*). It is thought that *fabD* is also involved in actinorhodin synthesis; this is not particularly surprising as fatty acid and polyketide biosynthesis

in *Streptomyces* share many of the same initial substrates (Banchio and Gramajo, 1997).

As well as biosynthesis, degradation of fatty acids is also necessary to maintain cell envelope homeostasis. Degradation of fatty acids takes place via β-oxidation, after which the resulting acetyl-CoA enters the TCA cycle and may be processed via the glyoxylate shunt (conversion of isocitrate to malate by isocitrate lyase and malate synthase) (Banchio and Gramajo, 1997; Hodgson, 2000).

It has been shown that *S. coelicolor* can utilise a wide range of fatty acids as sole carbon source (Banchio and Gramajo, 1997). Some actinomycetes such as *Streptomyces avermitilis* and *M. tuberculosis* have also been shown to metabolise sterols (McLean *et al.*, 2006; Yang *et al.*, 2007). Although the *S. coelicolor* genome includes genes putatively linked to sterol metabolism (SCO4781; SCO5420) and biosynthesis (SCO5223), it is probable that *S. coelicolor* does not synthesise sterols (a process which is rare in bacteria) but must rather obtain them from environmental sources (Lamb *et al.*, 2003; McLean *et al.*, 2006; Ogata *et al.*, 1999).

Uptake of carbon sources

S. coelicolor is a saprophytic organism; approximately 10% of its encoded proteins are secreted, many of which are hydrolytic enzymes that degrade complex organic molecules for use as nutrient sources (Chater *et al.*, 2010). The majority of mono- and disaccharides generated in this manner are likely to be imported via ABC assemblies (Bertram *et al.*, 2004; Thomas, 2010; Thompson *et al.*, 2010). Efficient import of complex nutrient sources is potentially key to the ability of *Streptomyces* to compete with other soil organisms, as inefficient uptake could allow competitors to "hijack" the hydrolysed organic matter (Hodgson, 2000).

Streptomyces coelicolor in the soil

The ability of *S. coelicolor* to form drought-resistant spores makes it perfectly adapted for life in the soil. It must contend with long periods of desiccation and low nutrient abundance and has developed a number of systems which allow it to respond to changing environmental conditions. Examples include signalling factors which inhibit germination if spore density is too high, and extracellular enzymes which allow degradation of a wide range of nutrient-containing detritus (Heuer *et al.*, 1997).

Another feature of life in the soil is the heterogeneous population of microorganisms that compete for its resources. *S. coelicolor* has a variety of dedicated systems which allow it to resist bacterial and viral pathogenesis and compete for nutrients in the soil.

The commonest microorganisms in the soil (and indeed on the planet) are bacteriophage; viruses which colonise bacteria (Kimura *et al.*, 2008). Bacteriophage occur in the order of 10^7 virions per gram of dry soil (Swanson *et al.*, 2009), and *Streptomyces* can be infected by a number of diverse phages. If bacteriophage infection is unchecked it can cause widespread lysis of bacterial cells in a colony. The *S. coelicolor* phage growth limitation (Pgl) system allows the bacterium to protect itself from re-infection by phage which has undergone a previous lytic cycle (Hoskisson and Smith, 2007).

Protection is also needed against bacterial, archaeal and fungal competitors. Although antibiotic secretion in *S. coelicolor* has not been definitively shown to occur in soil, it is postulated that its role in this environment is in the defence of the *Streptomyces* colony against invasive bacteria and fungi. *S. coelicolor* produces a number of secondary metabolites with demonstrated antimicrobial properties, such as actinorhodin and the recently-characterised yCPK (yellow *coelicolor* polyketide) (Gottelt *et al.*). Other compounds produced by *Streptomyces* include amphotericin B, which has antifungal and antiprotozoal effects; oxytetracycline, which is a broad-spectrum antibiotic; clavulanic acid, which is a β-lactamase inhibitor; and compounds such as daptomycin, streptomycin and viomycin which are effective

against Gram positive organisms (Baltz, 2008; Chakraburtty and Bibb, 1997; Kieser *et al.*, 2000; Ohnishi *et al.*, 2008).

Interestingly, the *Streptomyces* produce a number of compounds such as actinomycin D, mitomycin and tacrolimus (FK-506) that have been shown to have antitumour or immunomodulatory effects in eukaryotes (Kieser *et al.*, 2000). Given the non-pathogenic nature of most *Streptomyces* it seems likely that these compounds have evolved in response to selective pressure from eukaryotic competitors in the soil. It has been suggested that the frequent passage of soil through the earthworm gut lumen may also have a selective effect on soil bacteria, leading to the development of survival mechanisms appropriate to this environment (Chater and Chandra, 2006).

Streptomyces also produce several antihelminthic compounds (for instance avermectin produced by *Streptomyces avermitilis* and geldanamycin produced by *S. hygroscopicus*) which may protect against nematode predation in the environment (MacNeil *et al.*, 1992).

Secondary metabolite production is typically initiated at the start of morphological differentiation, when production of aerial hyphae begins (Kieser *et al.*, 2000). Secondary metabolite production may only become necessary at this stage because spores are protected from bacterial pathogenesis by their thick coats, and furthermore do not need to compete for nutrients, whereas this is not the case at later stages of development.

Although there is some evidence that unicellular protozoans have a (limited) sensitivity to some *S. coelicolor* secondary metabolites (see results, chapter 5), it is unclear how the bacterium protects itself against predation by these organisms. Unlike other forms of microbial pathogenesis (bacteriophage infection, secondary metabolites produced by other bacteria) against which *S. coelicolor* spores are protected by their coats, there is no obvious defence mechanism against phagocytosis by eukaryotic cells. The motility of these protozoans may well reduce the

effectiveness of antimicrobial metabolites, which rely on building up a high concentration of the metabolite in a localised area.

The *mce* operon in *Streptomyces coelicolor*

The *mce* operon in *S. coelicolor* is 13.4 kb long and consists of nine core conserved genes, with two conserved *mas* (*mce* associated) genes (Casali and Riley, 2007) in the downstream region, and a further three genes of unknown function (Fig. 1.3). On the StrepDB database (Bentley *et al.*, 2002; Bishop *et al.*, 2004) it is annotated as being on the minus or negatively-transcribed strand of the genome, and for this reason the SCO numbers (systematic numbers assigned according to the position of the gene in the genome) ascend from the distal to the proximal end of the operon (Bentley *et al.*, 2002). For ease of analysis the *mce* operon is depicted in this thesis with the upstream region on the left of the image.

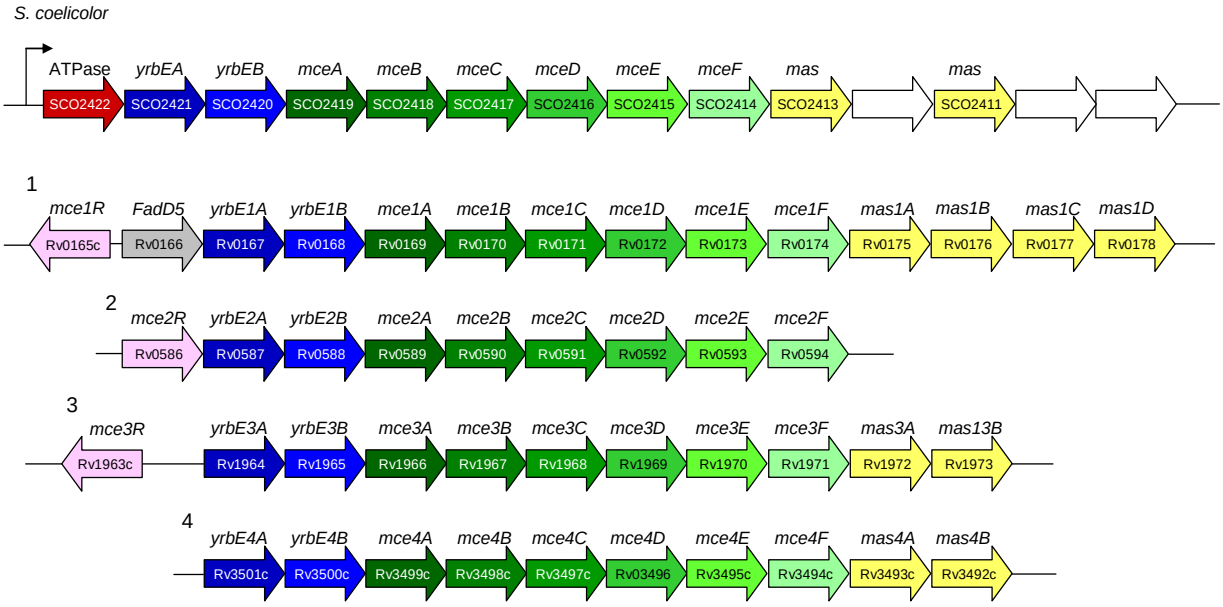

Figure 1.3: Top: The *S. coelicolor mce* operon. From left to right: putative upstream promoter region; nine core *mce* cluster genes consisting of putative APTase-encoding gene (red), two putative transmembrane domain-encoding genes (blue) and *mce* genes A-F (green); conserved *mas* gene (yellow); gene of unknown function (white); conserved *mas* gene; two genes of unknown function. Bottom (labelled 1-4): The *M. tuberculosis mce* operons: Regulator (pink); *FadD5* homologue; core *mce* cluster genes (as above); conserved *mas* genes.

The core cluster

The first gene in the operon is SCO2422, which is 1011 bp and has sequence homology to genes encoding ABC transporter ATP-binding domains (Casali and Riley, 2007). Although it is annotated in StrepDB as having the prokaryote start codon TTG, it seems more likely that the true start codon is the ATG 21 bases downstream of this (and therefore in the same reading frame). The presence of the Shine-Dalgarno consensus sequence GGAGG in the -8 position relative to this ATG would support this as the transcription initiation site. SCO2422 has a TGA stop codon which overlaps with the GTG start codon of the next gene in the operon, SCO2421.

SCO2421 is 765 bp and is annotated as a putative ABC transporter integral membrane protein. The corresponding gene in *M. tuberculosis* is annotated as a *yrbEA* homologue (Casali and Riley, 2007), and this annotation is also used in this thesis. SCO2421 has a TGA stop codon which is 6 bp upstream of the start codon for the next gene in the operon, SCO2420. SCO2420 is 807 bp and has an ATG start codon with a Shine-Dalgarno sequence (GGAGG) at the -11 position. SCO2420 has also been designated as a putative integral membrane protein with homology to *yrbEB* (Casali and Riley, 2007). SCO2420 has a TGA stop codon, with 1 bp between this and the start codon of the downstream gene.

The *mce* genes

The next gene in the operon is SCO2419, which is the first of the *mce* genes (i.e. genes in the *mce* operon which also contain the *mce* motif), annotated as *mceA*. SCO2419 has an ATG start codon and is 1257 bp long. The TGA stop codon overlaps with the ATG start codon of the next gene in the operon.

The *mce* genes are characterised by the presence of a region coding for a 98 amino acid “mce-like” subdomain (Pfam 02405) (Finn *et al.*).

The next five genes (SCO2418-SCO2414) also contain the *mce* motif and are annotated as *mceB, C, D, E* and *F*. Theses genes together with *mceA* encode a putative substrate binding domain. They are 1065, 1056, 1031, 1242 and 1302 bp respectively, and have overlapping stop/start codons.

The penultimate *mce* gene, *mceE*, also contains a lipobox motif which is discussed in greater detail in chapter 3.

The downstream region

The *S. coelicolor mce* operon contains five genes downstream of the core cluster. These genes are all of unknown function. Two of them (SCO2413 and SCO2411) are conserved as part of the *mce* cluster and are present in other actinomycetes such as *M. tuberculosis* (Casali and Riley, 2007). These genes were not included in mutational screening (see Results, chapter 4).

The homology suggests that this is a bona fide *mce* cluster, and that, as with *M. tuberculosis*, it encodes an ABC importer assembly.

Virulence factors in the actinomycetes

A diverse collection of genetic loci have been identified as virulence factors in the pathogenic actinomycetes. It is likely that the majority of these virulence factors started out as core genes for cellular functions selected outside of a host environment, but were subsequently co-opted as virulence determinants due to the selective advantage they provided in a host infection (Letek *et al.*).

The ESAT-6 gene cluster is unique to the actinomycetes. Five copies of the cluster have been identified in *M. tuberculosis* and the six most conserved genes in the cluster are also present in single copy in *S. coelicolor*. Deletion of part of the ESAT-6 region 1 cluster is one of the distinguishing characteristics of the attenuated vaccine

strain *M. bovis* BCG. Homologous regions have also been identified in *M. avium* and *M. leprae* (Gey Van Pittius *et al.*, 2001).

The ESAT-6 cluster includes genes encoding ABC transporters, the secreted T-cell antigens ESAT-6 and CFP-10 which are thought to be involved in granuloma development, cell wall-associated serine proteases, and various inner- and transmembrane proteins involved in transport including the ESX-1 secretory apparatus (Gey Van Pittius *et al.*, 2001; San Roman *et al.*). ESX-1 has been described as a Type VII secretion system, although there is some controversy in the literature regarding whether ESAT-6 systems constitute a separate secretory mechanism (Desvaux *et al.*, 2009; Sutcliffe, 2011).

Although a number of these genes have been identified as virulence factors in *M. tuberculosis* and other Gram positive pathogens, the presence of homologous genes in the non-pathogenic *S. coelicolor* indicates that they may have alternative functions. For instance, the *esxA* and *esxB* secreted proteins appear to have a role in virulence and persistent infection in *Staphylococcus aureus*, while in *S. coelicolor* they have been identified as having a role in morphological development and sporulation (San Roman *et al.*).

Persistence in the intracellular environment is one of the essential aspects of mycobacterial virulence, and many of the virulence factors identified in the mycobacteria are involved in this process. An example is the *whiB*-like family of putative DNA-binding proteins in *M. tuberculosis*. The genes encoding these proteins are upregulated under stress conditions similar to those that would be encountered inside macrophages (low pH, low abundance of iron and other nutrients) (Geiman *et al.*, 2006). *WhiB*-like proteins have been postulated to play a role in mycobacterial survival and persistence inside host cells, and in multidrug resistance (Crack *et al.*, 2009).

The *whiB* gene family in *S. coelicolor* is involved in maturation of spore chains. Although sporulation in *M. tuberculosis* is controversial (Ghosh *et al.*, 2009; Singh *et*

al., 2010; Traag *et al.*, 2010) it is possible that the functions in the two organisms are related; morphological development of *S. coelicolor* is at least partially dependent on environmental conditions such as nutrient availability. The *M. tuberculosis whiB*-like genes are predicted to encode DNA-binding proteins, largely due to the presence of a 2Fe-2S cluster, while the *S. coelicolor whiB* locus encodes a putative transcription factor (Chater, 1998; Geiman *et al.*, 2006).

The *nsrR* gene of *S. coelicolor* is a nitric oxide (NO)-sensitive regulator of the NO regulon. Like the *M. tuberculosis whiB*-like proteins, NsrR contains a 2Fe-2S cluster, which is sensitive to NO and which allows DNA binding. Nitric oxide production is a characteristic early defence mechanism in macrophages against bacterial pathogens, and thus resistance to NO is a likely virulence factor. NsrR is present in a number of Gram positive human pathogens such as *Salmonella enterica* and *Neisseria meningitidis* (Tucker *et al.*, 2008).

The *mce* cluster may share similarities with these loci, acting as a virulence factor during infection of mammalian cells by pathogenic organisms while fulfilling a different role in non-pathogenic organisms. Many virulence factors have adapted from their original functions under selection pressure from mammalian immune responses (Letek *et al.*) and it seems probable that homologues in non-pathogenic species where this selection pressure does not exist might retain the original function.

Aims of project

The aim of this project is to elucidate the function of the *mce* gene cluster in *Streptomyces coelicolor* at the genetic, cellular and community level.

At the genetic level the aims are to examine the regulation and transcription of the operon in order to establish the similarity or otherwise to the homologous operon in *M. tuberculosis*, identify any likely regulators, and establish a transcriptional profile of the *S. coelicolor mce* genes. At the cellular level the aims are to identify the

substrate of the Mce protein assembly and to establish a *mce* phenotype in *S. coelicolor*.

At the community level, the aim of the project is to establish what role (if any) the *mce* cluster plays in the soil environment and in the interactions of *S. coelicolor* with other organisms in the soil, particularly the free-living amoeba *Acanthamoeba polyphaga*. The wider aim of the project is to evaluate the *mce* operon of *S. coelicolor* in the broader context of the actinomycetes. The function of the *S. coelicolor mce* operon may illuminate the evolutionary origins of the cluster and its role as a virulence factor.

There are several specific hypotheses that will be addressed in this thesis. Firstly, that the *mce* operon is present in the majority of sequenced streptomycetes, as is the case among the mycobacteria. The recent sequencing of several *Streptomyces* species allows examination of *mce* distribution in non-pathogenic actinomycetes to investigate whether this follows the model of *S. coelicolor*.

Secondly, that the *mce* operon in *S. coelicolor* is functional and that the genes of the operon are expressed. The hypothesis that expression of the *mce* operon in *S. coelicolor* is regulated according to changes in the environment will also be tested. This hypothesis follows the observation that the *mce* operons of *M. tuberculosis* are differentially expressed depending on factors in the host cell environment.

Another hypothesis that will be tested in this thesis is that the *mce* operon of *S. coelicolor* contributes to survival of the bacterium in the soil environment, particularly by mediating its interactions with eukaryotic competitors. This hypothesis reflects the fact that several other actinomycete virulence factors are likely to have originated in this way.

Chapter 2: Materials and Methods

Strains, plasmids and cultivation

Plasmids and cosmids used in this study are listed in Tables 2.1 and 2.2. The *Escherichia coli* and *Streptomyces* strains used in this study are listed in Table 2.3. All *E. coli* strains were cultivated at 37^{o}C except where stated. All *Streptomyces* strains were cultivated at 30^{o}C except where stated. Media preparation is described below. Strains requiring antibiotic selection to maintain markers were grown with the appropriate antibiotic at the concentrations specified in Table 2.4.

Table 2.1: Cosmids used in experimental work

Cosmid	Gene with *Tn*5062 insertion	Antibiotic resistance marker(s)	Reference
8A2.1.G07	SCO2423	Apramycin, Kanamycin	(Bishop *et al.*, 2004)
8A2.1.B11	SCO2422 (ATPase)	Apramycin, Kanamycin	(Bishop *et al.*, 2004)
8A2.2.E04	SCO2421 (*yrbEA*)	Apramycin, Kanamycin	(Bishop *et al.*, 2004)
8A2.1.D12	SCO2420 (*yrbEB*)	Apramycin, Kanamycin	(Bishop *et al.*, 2004)
8A2.1.G06	SCO2419 (*mceA*)	Apramycin, Kanamycin	(Bishop *et al.*, 2004)
8A2.2.C07	SCO2418 (*mceB*)	Apramycin, Kanamycin	(Bishop *et al.*, 2004)
8A2.2.F02	SCO2416 (*mceD*)	Apramycin, Kanamycin	(Bishop *et al.*, 2004)
8A2.1.F04	SCO2415 (*mceE*)	Apramycin, Kanamycin	(Bishop *et al.*, 2004)
8A2.2.A09	SCO2408	Apramycin, Kanamycin	(Bishop *et al.*, 2004)

Table 2.2: Plasmids used in experimental work

Plasmid	Description	Antibiotic resistance markers	Reference
pLCS001	Supercos derivative 8A2.1.F04 with deletion between *BamH1* sites at 22505 and 13639bp	Apramycin	This work
pLCS002	Supercos derivative 8A2.1.G07 with deletion between *Eco*RI sites at 29452 and 43319 bp	Apramycin	This work
pLCS003	pLCS002 with deletion between *Kpn*I sites at 8130 and 22051 bp	Apramycin	This work
pLCS004	pLCS003 with 3372 bp section between cos sites replaced by 5247bp *Ssp*I fragment of pIJ10702	Apramycin, Ampicillin	This work
pLCS006	pLCS004 with ligation of pNRT4 at *Kpn*I site at 34231 bp	Apramycin, Ampicillin, Kanamycin	This work
pAR870	tep830, *luxAB*, Δ*TetRiS*		(Rodriguez-Garcia *et al.*, 2005)
pAR911b	tep830, *luxAB, SCO0253*, itep0252		(Rodriguez-Garcia *et al.*, 2005)
pAR913b	tep830, *luxAB*, itep0252		(Rodriguez-Garcia *et al.*, 2005)
pAR933a	tep830, *rbs*, *luxAB, TetRiS*		(Rodriguez-Garcia *et al.*, 2005)
pUZ8002		Kanamycin	(Paget)
pIJ790	λ-RED (*gam*, *bet*, *exo*), *cat*, *araC*, rep101^{ts}		(Gust *et al.*, 2004)
pSET152	ΦC31 pUC18, aac(3)IV, lacZα, oriT$_{RK2}$	Apramycin	(Bierman *et al.*, 1992)
pIJ8660	ΦC31 pUC18, aac(3)IV, lacZα, oriT$_{RK2}$ EGFP	Apramycin	(Sun *et al.*, 1999)
pMS82		Hygromycin	(Gregory *et al.*, 2003)
pNRT4		Kanamycin	Herron, P., personal communication
pIJ10702		Apramycin, Ampicillin	(Foulston and Bibb)

Table 2.3: Bacterial strains used in experimental work

Name	Description	Genotype	Reference
DH5α	*E. coli* K12 derivative	F^-, *endA1*, *hsdR17* (r_{K-} m_{K+}), *supE44*, *thi*-1 λ^-, *recA1*, *gyrA96*, *relA1*, *deoR*, Δ(*lacZYA*-*araF*)U169, Φ80d*lacZ* ΔM15	(Grant *et al.*, 1990)
JM109	*E. coli* K12 derivative	$e14^-$ ($McrA^-$), *recA1*, *endA1*, *gyrA96*, *thi*-1, *hsdR17* (r_{K-} m_{K+}), *supE44*, *relA1*, Δ(*lac-proAB*) [F' *traD36*, *proAB*, lac^qZ ΔM15]	(Vaillancourt *et al.*, 1994)
ET12567	*E. coli* K12 derivative	*dam13*::*Tn*9, *dcm6*, *hsdM*, *hsdR*, *recF143*, *zij201*::*Tn*10, *galK2*, *galT22*, *ara14*, *lacY1*, *xylS*, *leuB6*, *thi*-1, *tonA31*, *rpsL136*, *hisG4*, *tsx78*, *mtli*, *glnV44*, F^-	(MacNeil *et al.*, 1992)
BL21	*E. coli* K12 derivative	*dcm*, *ompT*, *hsdS* (r_{B-} m_{B-}), *gal*	(Vaillancourt *et al.*, 1994)
BW25113	*E. coli* K12 derivative	$lacI^+$, $rrnB_{T14}$, Δ$lacZ_{WJI6}$, *hsdR514*, Δ$araBAD_{AH33}$, Δ$rhaBAD_{LD78}$	(Datsenko and Wanner, 2000)
M600	*S. coelicolor*		(Kieser *et al.*, 2000)
J807	*S. coelicolor*		(Buttner *et al.*, 1987)
M145 A(3)2	*S. coelicolor*	$SCP1^-$ $SCP2^-$	(Kieser *et al.*, 2000)
J1929	*S. coelicolor*	Δ*pglY16*, $SCP1^-$ $SCP2^-$	(Kieser *et al.*, 2000)
ARS15	*S. coelicolor*	J1929 pAR870	(Rodriguez-Garcia *et al.*, 2005)
ARS117	*S. coelicolor*	J1929 pAR911b	(Rodriguez-Garcia *et al.*, 2005)
ARS121	*S. coelicolor*	J1929 pAR913b	(Rodriguez-Garcia *et al.*, 2005)
ARS130	*S. coelicolor*	J1929 pAR933a	(Rodriguez-Garcia *et al.*, 2005)
SLC101	*S. coelicolor*	M145 SCO2422::*Tn*5062	This work
SLC102	*S. coelicolor*	M145 SCO2421::*Tn*5062	This work
SLC103	*S. coelicolor*	M145 SCO2420::*Tn*5062	This work
SLC104	*S. coelicolor*	M145 SCO2418::*Tn*5062	This work
SLC105	*S. coelicolor*	M145 SCO2416::*Tn*5062	This work
SLC106	*S. coelicolor*	M145 SCO2415::*Tn*5062	This work
SLC201	*S. coelicolor*	M145 ΔSCO2422:SCO2415	This work

SLC202	*S. coelicolor*	SLC201 pLCS006	This work
SLC301	*S. coelicolor*	M145 pLCS006	This work
Δ*mtrA*	*S. coelicolor*		Seipke and Hutchings, unpublished
Δ*mtrA* complemented strain	*S. coelicolor*		Seipke and Hutchings, unpublished
eSXBA^{-}	*S. coelicolor*		(San Roman *et al.*, 2010)
DSC5734 (*eSXBA*$^{-}$ complemented strain)	*S. coelicolor*	SCO5734::*Tn*5062 / SC3C3.2.B11	(San Roman *et al.*, 2010)
DSC5722 (*eSXBA*$^{-}$ complemented strain)	*S. coelicolor*	SCO5722::*Tn*5062 / SC3C3.1.G11	(San Roman *et al.*, 2010)
Δ*relA*	*S. coelicolor*		(Sun *et al.*, 2001)
Δ*desD*	*S. coelicolor*		(Barona-Gomez *et al.*, 2004)
SD509	*S. sudanensis*		(Quintana *et al.*, 2008)
DSM41923	*S. sudanensis*		(Quintana *et al.*, 2008)
DSM40738	*S. somaliensis*		(Quintana *et al.*, 2008)
87-22	*S. scabies*		Gift from M. Hutchings

Table 2.4: Antibiotic concentrations

Antibiotic	Class	Stock concentration (mg/ml)	Working concentration (µg/ml)	Stock solution solvent
Kanamycin	Aminoglycoside	50	50	H_2O
Apramycin	Aminoglycoside	50	50	H_2O
Ampicillin	β-lactam	50	50	H_2O
Carbenicillin	β-lactam	100	100	H_2O
Chloramphenicol	N-dichloroacyl phenylpropanoid	25	25	100 % EtOH
Nalidixic acid	Gyrase inhibitor	25	25	H_2O
Tetracycline	Tetracycline	12.5	12.5	100 % EtOH
Hygromycin B	Substituted aminoglycoside	50	50 - 70	H_2O

Bacterial growth media

Recipes for bacterial growth media are listed in Table 2.5. All media were sterilised by autoclaving before use at 121^{o}C for 15 minutes.

Table 2.5: Bacterial growth media

LB (Sambrook *et al.*, 1989)	10 g tryptone 10 g NaCl 5 g yeast extract 20 g agar technical number 3* Make up to 1 litre with deionised water pH to 7.0 with NaOH
Mannitol soy flour (MS) (Hobbs *et al.*, 1989)	16 g soya bean flour 16 g d-mannitol 20 g agar technical number 3 Make up to 1 litre with tap water
Minimal medium (MM) (Hopwood, 1967)	0.5 g L-asparagine/ NH_2SO_4 0.5 g K_2HPO_4 0.2 g $MgSO_4.7H_2O$ 0.01 g $FeSO_4.7H_2O$ 10 g agar technical number 3* Make up to 1 litre with deionised water After autoclaving add 10 g glucose (or alternative carbon source)
R2/ R2YE (Hopwood and Wright, 1978; Okanishi *et al.*, 1974; Thompson *et al.*, 1980)	103 g sucrose 0.25 g K_2SO_4 10.12 g $MgCl_2.6H_2O$ 10 g glucose 0.1 g casamino acids 800 ml distilled water 2.2 g agar per 80 ml solution At time of use add: 1 ml KH_2PO_4 (0.5% w/v) 8 ml $CaCl_2.2H_2O$ (3.68% w/v) 1.5 ml L-proline (20% w/v) 10 ml TES buffer (5.73% w/v, pH7.2) 0.2 ml trace element solution** 0.5 ml NaOH (1N) To make R2YE add 5ml yeast extract (10% w/v)
Yeast extract malt extract (YEME) (Kieser *et al.*, 2000)	3 g yeast extract 5 g peptone 3 g malt extract 10 g glucose 340 g sucrose Make up to 1 litre with deionised water After autoclaving add 2 ml sterile 2.5 M $MgCl_2.6H_2O$
2x YT (Kieser *et al.*, 2000)	16 g tryptone 5 g NaCl 10 g yeast extract Make up to 1 litre with deionised water

Tryptone soy broth (TSB) (Oxoid)	30 g TSB powder 20 g agar technical number 3* Make up to 1 litre with deionised water
Nutrient agar (NA) (Oxoid)	13 g nutrient broth mix (Oxoid) 20 g agar technical number 3* Make up to 1 litre with deionised water
V8 medium (England, R. R., personal communication)	1 litre V8 vegetable juice 20 g agar technical number 3* Adjust to pH 7.0
Oatmeal agar (Shirling, 1966)	10 g oatmeal 20 g agar technical number 3* Make up to 1 litre with deionised water
SOC (Hanahan, 1983)	20 g Tryptone 5 g yeast extract 0.5 g NaCl 10 ml KCl (250 mM) Make up to 1 litre with deionised water pH to 7.0 with NaOH After autoclaving add 20 ml sterile glucose solution (1 M) Just before use add 5 ml sterile $MgCl_2$ (2 M)
GAE medium (Suarez *et al.*, 1980)	0.5 g K_2HPO_4 0.5 g $MgSO_4.7H_2O$ 0.01 g $FeSO_4.7H_2O$ 10 g glucose 1 g asparagine 0.5 g yeast extract 20 g agar technical number 3* Make up to 1 litre with deionised water

* To make liquid broth omit agar

** Trace element solution: 40 mg $ZnCl_2$, 200 mg $FeCl_3.2H_2O$, 10 mg $CuCl_2.2H_2O$, 10 mg $MnCl_2.4H_2O$, 10 mg $NaB_4O_7.10H_2O$, 10 mg $(NH_4)_6Mo_7O_{24}.4H_20$ in 1 litre deionised water.

Cultivation of *Streptomyces* strains

Streptomyces were routinely cultured on solid MS agar (see Table 2.5) for the preparation of spores, and the screening and selection of clones. Phenotypic testing was carried out on a range of media (see Table 2.5 and Results, chapter 4).
Liquid cultures, typically grown in YEME to promote dispersed growth, were inoculated with approximately 1 x 10^7 spores of each strain in 250 ml Erlenmeyer flasks containing springs. Flasks were incubated at 30ºC with shaking (250 rpm) for the required period.

Solid phase growth curves of *Streptomyces* (Rodriguez-Garcia *et al.*, 2005)

Agar plates were overlaid with sterile cellophane discs and inoculated with 3 x 10^6 pregerminated *S. coelicolor* spores. The plates were incubated at 30ºC. At 16, 24, 36 and 48 hours incubation a rectangular section of inoculated cellophane was removed and placed inside one wall of a 2 ml disposable cuvette. The cuvette was filled with deionised water and the OD_{600} measured.

Preparation of *Streptomyces* spore stocks (Kieser *et al.*, 2000)

MS plates were streaked for confluent growth of *Streptomyces* and incubated at 30°C for 4-5 days. When spore production was visible, as indicated by the formation of a grey spore pigment, plates were flooded with 9 ml sterile deionised water and spores detached from the surface of the mycelium using a sterile cotton bud. The resulting spore suspension was decanted, centrifuged at 1000 g for 10 min and the pellet resuspended in approx. 100 µl supernatant remaining in the tube. The pellet was vortexed to break up spore chains and diluted in 1 ml 20% glycerol. Spore stocks were stored at -20°C.

Coverslip cultures for microscopy (Kieser *et al.*, 2000)

Coverslips were placed diagonally into MS plates (45^{o} angle) and inoculated with 20 µl of a 1:1000 dilution of a dense spore suspension. The plates were incubated at 30ºC for the required length of time and the coverslips were then removed. Mycelium adhering to the coverslip was methanol fixed and coverslips mounted on slides.

Slides were examined microscopically on an inverted microscope (Nikon TE 2000 eclipse) using brightfield.

Dry weight growth curves (Kieser *et al.*, 2000)

Several 50 ml cultures of YEME broth were inoculated with approximately 1 x 10^{7} M145 spores and incubated at 30°C with shaking. At designated time points one culture was taken out and vacuum filtered through pre-weighed Whatman filter paper. The filter paper was dried for 15 minutes at low power in a microwave and then weighed again. The dry weight of the biomass in the culture was calculated by subtracting the weight of the filter paper from the final weight. This was repeated for all time points and the results plotted to produce a growth curve.

Cultivation of *E. coli*

Aliquots (5-10 ml) of LB broth with appropriate antibiotics were inoculated with the relevant strain of *E. coli* and grown at 37ºC with shaking at 220 rpm for 16-18 hours. Broth cultures were inoculated with either a single colony picked from a fresh overnight culture of the strain from a plate or a small amount of material removed from a frozen glycerol stock.

To inoculate large cultures (e.g. a 50 ml culture for protein overexpression), an aliquot from a 5 ml overnight culture as described above was diluted 1:100 in fresh LB broth with appropriate antibiotics in a 250 ml Erlenmeyer flask. This was

incubated at 37ºC with shaking at 220 rpm until the required OD_{600} (typically 0.4 – 0.6) was reached.

Storage of *E. coli* stocks

Glycerol stocks of *E. coli* were made by diluting an aliquot of a fresh overnight culture 1:1 with 50% glycerol (25% final glycerol concentration). Stocks were stored at -80ºC.

Preparation of electrocompetent cells (Sambrook *et al.*, 1989)

Aliquots (5 ml) of LB with appropriate antibiotics were inoculated with *E. coli* and grown overnight at 37ºC with shaking. The overnight cultures were used to inoculate fresh 50 ml LB cultures in 250 ml Erlenmeyer flasks and these were grown at 37ºC with shaking at 220 rpm until an OD_{600} of approximately 0.6 was reached. Cells were harvested by centrifugation for 5 minutes at 5000 rpm and resuspended in 20 ml ice cold 10% glycerol. This was repeated and cells were left on ice for 30 minutes. The cell suspension was aliquoted in 50 µl volumes and either flash frozen in liquid nitrogen or used immediately for electroporation.

Electroporation of *E. coli* (Dower *et al.*, 1988)

A 50 µl aliquot of electrocompetent cells was incubated on ice with 1 µl of the appropriate cosmid (0.01 µg-1 µg of DNA). The mixture was transferred to a 1 µm electroporation cuvette and electroporated using a Biorad electroporator set at 10 kV cm^{-1}. Immediately, 1 ml ice cold super-optimal broth with catabolite repression (SOC) medium was added and the cells incubated at 37ºC with shaking at 220 rpm for 60 to 180 minutes. The cells were then spread on LB agar containing appropriate antibiotics and incubated overnight at 37ºC.

The resulting colonies were picked and used to inoculate 10 ml LB overnight cultures with appropriate antibiotics. These cultures were used for conjugation (Kieser *et al.*, 2000) or stored as glycerol stocks.

Preparation of chemically competent *E. coli* cells (Sambrook *et al.*, 1989)

Aliquots (5 ml) of LB containing the correct antibiotics for marker selection were inoculated with the appropriate *E. coli* strain and grown overnight at 37ºC (or 30ºC for strains with a temperature-sensitive plasmid) with shaking at 220 rpm. The overnight culture was then used to inoculate fresh LB media at a dilution of 1:100 in 250 ml Erlenmeyer flasks. These were grown at the relevant temperature with shaking at 220 rpm until an OD_{600} of approximately 0.6 was reached. Cells were harvested by centrifugation for 5 minutes at 5000 rpm and resuspended in 20 ml ice cold 75 mM $CaCl_2$. This was repeated and cells were then recentrifuged and resuspended in 4 ml TFB2 (100 mM MOPS pH7, 1 M $CaCl_2$, 1 M RbCl, 50% glycerol). The cells were left on ice for 30 minutes. The cell suspension was then aliquoted in 50 µl volumes and either flash frozen in liquid nitrogen or used immediately for transformation.

Transformation of *E. coli* (Sambrook *et al.*, 1989)

A 50 µl aliquot of chemically competent cells was incubated on ice with 1-5 µl of the appropriate plasmid (1 µg-10 µg DNA) for 30 minutes. The cells were heat shocked at 42ºC for 50 seconds and placed on ice for 2 minutes. Immediately, 1 ml room-temperature LB or SOC was added and the cells incubated at 37ºC with shaking for 60 to 180 minutes. The cells were then spread onto LB agar with appropriate antibiotics and incubated overnight at 37ºC.

Intergenic conjugation of plasmids and cosmids from *E. coli* to *Streptomyces* (Kieser *et al.*, 2000)

An overnight culture of *E. coli* strain ET12567/pUZ8002 transformed with the relevant plasmid or cosmid was diluted 1:100, grown to an OD_{600} of between 0.4 and 0.6 and the cells harvested by centrifugation for 5 minutes at 10000 rpm. The cells were washed twice with LB containing no antibiotics. A suspension of *Streptomyces* spores was centrifuged and the spores resuspended in 2x YT to a concentration of 2 x 10^8 spores/ml. This mixture was heat shocked for 10 minutes at 50ºC and left to cool. An aliquot (500 µl) of this suspension was mixed with 500 µl ET12567/pUZ8002 containing the conjugative vector. The mixture was spread onto MS agar and incubated at 30ºC for 14-18 hours, after which time the plates were overlaid with nalidixic acid (25 µg/ml) and the relevant selective antibiotic. The plates were incubated for a further two days and colonies were patched on to fresh MS containing the appropriate antibiotics to screen for double crossovers.

Screening for double crossovers in *Streptomyces*

Primary exconjugant colonies were patched onto two nutrient agar plates containing kanamycin or apramycin respectively (or other appropriate selective antibiotics as required). The plates were incubated at 30ºC for two days. Colonies which grew on apramycin (selective marker in the insertion cassette) but not on kanamycin (selective marker on the cosmid backbone) were deemed to be double crossovers. These colonies were subsequently streaked on MS agar for the preparation of spores stocks for further characterisation.

Isolation of plasmid and cosmid DNA from *E. coli* cultures using the alkaline lysis method

Adapted from Birnboim and Doly; Ishhorrowicz and Burke
(Birnboim and Doly, 1979; Ishhorowicz and Burke, 1981)

Aliquots (5 ml) of LB containing the appropriate antibiotics were inoculated with an *E. coli* strain containing the relevant cosmid or plasmid and grown overnight at 37ºC with shaking at 220 rpm. Cells were harvested by centrifugation at 13000 rpm and resuspended in 100 µl ice cold solution 1 (see Table 2.6) in a 1.5 ml microcentrifuge

tube. An aliquot (200 µl) of solution 2 was added to each tube and the contents of the tube mixed by inverting. Finally, 150 µl of ice cold solution 3 was added to each tube. The mixture was vortexed until completely mixed and then the tubes were stored on ice for 5 minutes. The mixture was then centrifuged for 5 minutes at 13000 rpm and the supernatant transferred to a fresh microcentrifuge tube. Two volumes of ethanol were added and the contents of the tube were mixed by inversion and then allowed to stand for 2 minutes at room temperature. The tube was centrifuged for 5 minutes at 13000 rpm and the supernatant removed. The pellet was rinsed with 1 ml 70% ethanol and allowed to air dry at room temperature for 10 minutes. Pellets of DNA were resuspended in 50 µl of TE buffer (10 mM Tris-HCl, 1 mM EDTA, pH 8.0).

Table 2.6: Alkaline lysis plasmid preparation solutions
Adapted from Birnboim and Doly (1979) and Ishhorrowicz and Burke (1981)

Solution 1 – Resuspension Solution	50mM glucose 25mM Tris.Cl (pH 8.0) 10mM EDTA (pH 8.0)
Solution 2 – Lysis Solution	0.2N NaOH 1% SDS
Solution 3 – Neutralisation solution	60ml 5M potassium acetate 11.5ml glacial acetic acid 28.5ml deionised water

Small-scale plasmid DNA isolations using commercial kits (Promega, Qiagen) were performed according to the manufacturers' instructions.

Isolation of genomic DNA from *Streptomyces* (Kieser *et al.*, 2000)

Small scale DNA isolation

Cultures (10 ml) of 1:1 TSB and YEME in 250 ml Erlenmeyer flasks with springs were inoculated with approximately 1 x 10^6 *S. coelicolor* spores and incubated at 30ºC with shaking at 220 rpm for two days. Cells were harvested by centrifugation

for 5 minutes at 10000 rpm, resuspended in 500 µl Solution 1 of the alkaline lysis method and transferred to a 1.5 ml microcentrifuge tube. Aliquots (10 µl of each) of 30 mg/ml lysozyme and 5 mg/ml RNaseA were added and the cells incubated at 37ºC for 60 minutes. Thereafter, 10 µl of 10 % SDS solution was added and mixed gently. Phenol solution (250 µl) was then added, followed by gentle shaking for 5 minutes. The mixture was centrifuged at 13000 rpm for 5 minutes. The aqueous layer (upper phase) was removed to a fresh tube and 1 ml of ethanol or isopropanol added to precipitate the nucleic acid. The nucleic acid was pelleted by centrifugation at 13000 rpm for 2 minutes, the supernatant removed and the pellet rinsed in 1 ml 70% ethanol. The pellet was air dried and resuspended in 50 µl TE buffer.

Large scale DNA isolation

Cultures (80 ml) of 1:1 TSB and YEME in 250 ml Erlenmeyer flasks with springs were inoculated with approximately 1 x 10^7 *S. coelicolor* spores and incubated at 30ºC with shaking at 220 rpm for two days. Cells were harvested by centrifugation for 5 minutes at 10000 rpm, resuspended in 20 ml Solution 1 of the alkaline lysis method and transferred to a 50 ml centrifuge tube. Aliquots (400µl each) of 30 mg/ml lysozyme and 5 mg/ml RNaseA were added and the cells incubated at 37ºC for 60 minutes. 1 ml of 10 % SDS was added and mixed gently. 10 ml phenol solution was added and shaken gently for 10 minutes and the mixture was centrifuged at 13000 rpm for 5 minutes. The aqueous layer was decanted to a fresh tube and phenol treatment repeated as necessary. Once a clean preparation was obtained, 20 ml of ethanol or isopropanol was added to it and mixed. Precipitated DNA was spooled onto a sealed pipette, washed with 70 % ethanol, allowed to dry, and resuspended in 1.5 ml TE buffer.

Agarose gel electrophoresis

Gel electrophoresis was carried out using Biorad electrophoresis tanks according to the manufacturer's instructions. Except where otherwise stated, gels were prepared at 0.8% in 1x TAE buffer (40 mM Tris-acetate, 1 mM EDTA) from a 50 x stock

solution. Ethidium bromide was added to gels to a final concentration of 100 μg ml^{-1}. Gels were electrophoresed at 80 V for 80 – 120 minutes in 1x TAE buffer and visualised by UV transillumination at 100% using the Syngene GelDoc system. Molecular size markers were included on each gel as standard and were appropriate for the size of the fragments to be resolved (see individual gels).

Gel extraction was performed using the UV transilluminator (UVP) on a low setting for ethidium bromide-stained gels, or, where UV irradiation was undesirable, the DarkReader (Clare Chemical Research) for gels post-stained with SYBR Gold (Invitrogen).

Southern blotting (Sambrook *et al.*, 1989)

Probe preparation and labelling

Probe DNA (1 μg) was diluted to 15 μl with deionised water, incubated for 15 minutes at 95°C and then cooled in ice water for approximately 10 minutes. The denatured DNA was then mixed with 2 μl of hexanucleotide mix (Roche), 2 μl digoxigenin (DIG) DNA labelling mix (Roche) and 1 μl Klenow fragment (Promega). The mixture was incubated overnight at 37°C. The reaction was stopped by the addition of 2 μl 0.2 M EDTA.

Sample DNA digest and transfer

Samples of test DNA were digested using relevant restriction enzymes according to manufacturers' instructions and electrophoresed as described previously. Unless otherwise stated, 2 μg of digested genomic DNA or 3 ng of digested cosmid DNA was used per lane of the gel. VacuGene equipment was used to transfer DNA from the gel to Hybond N nitrocellulose membrane (Amersham) according to the manufacturer's instructions. Following transfer membranes were exposed to UV irradiation (Syngene transilluminator at 100%) for 2 minutes and then washed in 2 x SSC (see Table 2.7) for a further 2 minutes.

Hybridisation and washes

The membrane was wrapped in mesh and inserted into a Hybaid tube containing 20 ml standard hybridisation buffer (SHB; preheated to 65ºC), and placed in a rotating Hybaid oven at 65ºC for 60 minutes. The probe was melted at 100ºC for 15 minutes and placed on ice for 10 minutes, then added to 20 ml SHB at room temperature. The SHB was removed from the tube containing the membrane and replaced with the fresh SHB containing the probe. The tube was replaced in the Hybaid oven and left to hybridise, with rotation at 65ºC overnight.

Subsequently, the SHB and probe was decanted off, replaced with 150 ml stringency buffer A (see Table 2.7) and incubated for 15 minutes at 65ºC. This wash was repeated. The same procedure was then performed using stringency buffer B (see Table 2.7). All subsequent steps were performed at room temperature. The membrane was removed from the Hybaid tube and rinsed in washing buffer (see Table 2.7) for 30 seconds, then washed in blocking solution (Roche) for 30 minutes with gentle shaking. This was followed by washing with 100 ml washing buffer for two periods of 15 minutes each. The membrane was equilibrated in 20 ml detection buffer for 2 minutes and then incubated with 20 ml colour substrate solution in the dark. When colour was sufficiently developed the membrane was rinsed in distilled water to stop the reaction.

Table 2.7: Reagents used in Southern blotting

Buffer	Composition
20x SSC	175.3 g NaCl 388.2 g Sodium citrate Make up to 1 litre with deionised water Adjust to pH 7.0 with HCl
Maleic acid buffer	22.2 g Maleic acid 17.6 g NaCl Make up to 1 litre with deionised water Adjust to pH 7.5 with NaOH
10% blocking solution	10 g blocking reagent 100 ml maleic acid buffer Microwave to dissolve
Detection buffer	3.63 g Tris-HCl 1.753 g NaCl Make up to 300 ml with deionised water Adjust to pH 9.5
Standard hybridisation buffer (SHB)	5x SSC 0.1% w/v N-laurylsarcosine 0.02% w/v SDS 1% v/v blocking solution
Washing buffer	1x Maleic acid buffer 0.3% w/v Tween 20
Antibody solution	Dilute anti-DIG-AP 1:5000 in 1% blocking solution
Colour substrate solution	One NBT/BCIP tablet in 10 ml deionised water
Stringency buffer A	2x SSC 0.1% SDS
Stringency buffer B	0.2x SSC 0.1% w/v SDS

Acanthamoeba co-culture

(personal communication, Maria Sanchez-Contreras, University of Bath, UK) (Waterfield *et al.*, 2009)

Growth and culture conditions

Acanthamoeba polyphaga was grown as a monolayer in 5 ml PYG (peptone yeast glucose) medium (see Table 2.8) in 25 cm^2 tissue culture flasks incubated at room temperature (approx. 22ºC). Amoebae were sub-cultured once a week by tapping the flask to detach the cells, removing a 500 µl aliquot and adding it to 5 ml fresh PYG.

Harvesting amoeba cells

After 3 days of growth, stationary phase cells were harvested by tapping the flask, centrifuging the culture for 1 minute at 6000 rpm and resuspending the cells in PAS (Page's amoebal saline). A small sample was mixed with an equal volume of trypan blue and a haemocytometer was used to calculate the live/ dead cell concentrations.

Co-culture and microscopy

Live cell concentration of *A. polyphaga* was adjusted to 1 x 10^5 cells/ml by dilution with Page's amoebal saline (PAS). *S. coelicolor* spore stocks were adjusted to either 1 x 10^5 or 1 x 10^6 spores/ml. 1 ml each of *A. polyphaga* and *S. coelicolor* were aliquoted into one well of a 24-well plate and incubated at 22ºC. The plates were examined under a light microscope at various time points and assessed for signs of bacterial growth. Wet-mount slides were made and observed under bright-field x1000 magnification in order to more closely examine the interaction between bacteria and amoebae.

Plaque assay (Froquet, 2009)

S. coelicolor spores (50 µl) at a concentration of 1 x 10^8 spores/ml were used to inoculate nutrient agar (at a concentration of between 100% and 10%) in each well of a 24-well plate. The plate was allowed to dry for approximately 1 hour. Exponential phase *A. polyphaga* cells were harvested by centrifugation at 500 g for 3 minutes and the cell concentration adjusted to 200 x 10^4, 20 x 10^4, 2 x 10^4 or 0.2 x 10^4 cells/ml. 5 µl of the 200 x 10^4 cell/ml *A. polyphaga* suspension was added to the centre of a well, on top of the dried bacterial spores. This was repeated with all cell suspensions, adding each to a different well. The plates were dried for a few minutes and incubated at 22ºC. The plates were examined at various time points and assessed for the formation of plaques in the bacterial lawn.

Table 2.8: Media used in *A. polyphaga* culture

All media was sterilised by autoclaving before use at 121°C for 15 minutes.

Medium	Composition
Page's Amoebal Saline (PAS)	Stock solution 1 12 g NaCl 0.4 g MgSO4.7H2O 0.6 g CaCl2.6H2O Make up to 500 ml with deionised water Stock solution 2 14.2 g Na2HPO4 13.6 g KH2PO4 Make up to 500 ml with deionised water Add 5ml of each stock solution to 990 ml deionised water
Peptone Yeast Glucose (PYG)	15 g proteose peptone 18 g D-glucose 2.5 g yeast extract Make up to 1 litre with PAS
Encystment medium (Campbell *et al.*, 2008)	20 mM Tris-HCl, pH8.8 100 mM KCl 8 mM $MgSO_4$ 0.4 mM $CaCl_2$ 1 mM $NaHCO_3$ 40% glycerol if storing at -80ºC

RNA isolation from *Streptomyces* cultures (Bucca *et al.*, 2009; Mersinias, 2003)

All RNA work was carried out using triple-autoclaved plasticware, glassware, water and reagents.

Pregermination of S. coelicolor *spores*

A dense suspension of *S. coelicolor* spores was suspended in 2x YT and incubated at 30ºC with shaking for 8 hours. Spores were pelleted at 3000 rpm for 10 minutes and resuspended in 10 ml sterile water. The suspension was vortexed briefly to disrupt clumped mycelia and the OD_{450} measured. The equation below was used to calculate

the volume (V) of spore suspension required to inoculate 3 x 10^6 spores for subsequent studies.

$V= (3x10^6/[OD_{450} \times 10^8]) \times 1000$ µl

Harvesting biomass

MS plates were overlaid with sterile cellophane discs and inoculated with 3 x 10^6 pregerminated *S. coelicolor* spores. The plates were incubated at 30ºC. Plates were removed at 16, 24, 36 and 48 hours incubation and the biomass harvested using a razor blade. The volume of biomass was then estimated, it was suspended in the appropriate volume of RNAprotect bacterial reagent (Qiagen) according to the manufacturers' instructions (usually 2 x the volume of biomass), the mixture was vortexed and incubated at room temperature for 5 minutes. It was then centrifuged at 5000 g, the supernatant removed, and the biomass stored at -20ºC.

RNA isolation

(Adapted from Qiagen protocol and Mersinias V., University of Surrey *Streptomyces* microarray group online protocol (Bucca *et al.*, 2009; Mersinias, 2003))

The frozen biomass was thawed on ice and resuspended in 1 x TE buffer containing 3 mg/ml lysozyme. The tubes were vortexed for 10 seconds and incubated at room temperature for 45 minutes with shaking. The appropriate volume of buffer RLT was added and the tube vortexed. A phenol/ chloroform extraction was carried out to remove particulate material, and the appropriate volume of ethanol added to the aqueous phase. Subsequent steps were performed according to the Qiagen RNeasy mini handbook.

DNA contamination of purified RNA was removed by DNase digestion and the RNA re-purified according to the Qiagen RNeasy mini handbook.

RNA yield was quantified using the Qubit RNA quantification kit (Invitrogen) or the nanodrop2000c (Thermo) according to the manufacturers' instructions. RNA quality was assessed by gel electrophoresis, using electrophoresis equipment soaked in 0.1 M NaOH overnight to prevent RNA degradation.

RT-PCR (Sambrook *et al.*, 1989)

Reverse transcription

An aliquot of RNA (2 µg) was mixed with 1 µg of random hexamers (Roche) in a total volume of 10 µl. The mixture was heated to 70ºC for 5 minutes and then chilled on ice for 5 minutes. Avian Myxovirus RT 5x reaction buffer (5 µl, Promega), 2.5 µl of 10 mM dNTP mix, 2.5 µl of 40 mM sodium pyrophosphate, 1 µl of AMV reverse transcriptase (Promega) and 5 µl distilled water were added to each tube in that order. The reaction was incubated at 37ºC for 60 minutes and then placed on ice.

RT-PCR

PCR was performed using GoTaq DNA Polymerase (Promega) in 50 µl reactions. Between 1 and 5 µl of reverse-transcribed DNA mixture (approximately 0.1µg – 0.5 µg DNA) was used as template. See Tables 2.9 and 2.11 for primer sequences and thermocycling conditions respectively.

One-step kit protocol

The Qiagen one-step RT-PCR kit was used according to the manufacturer's instructions, following the Q-solution protocol for the amplification of GC rich DNA. See Tables 2.9 and 2.10 for primer sequences and thermocycling conditions respectively.

PCR primers and their design

PCR primers were designed using GeneFisher software (Giegerich *et al.*, 1996) and manufactured by Eurofins. Standard 10 µl or 50 µl PCR reactions were performed using GoTaq Flexi DNA polymerase (Promega) according to manufacturer's instructions. See Tables 2.9 and 2.10 for primer sequences and thermocycling conditions respectively.

Table 2.9: PCR primer sequences

Primer	Sequence	Melting temperature (ºC)
SCO2422RTF	ATCTGGCGGGACGTGTCACTCA	64.0
SCO2422RTR	CACGGTGGCCGCGATGTCGA	65.5
SCO2421RTF	GCTCCAGGTCGGCTCCCTGA	65.5
SCO2421RTR	ATCTGGAGGTAGACGGCCGTCA	64.0
SCO2420RTF	CCGTCGTCGGAATCCAGGGCTA	65.8
SCO2420RTR	CCACAGGGCCAGCGACAGGA	65.5
SCO2419RTF	TCCGACCCGGTGGTCGTCGAGA	67.7
SCO2419RTR	GTGAAGTCGGTGAGCGCCGTGA	65.8
SCO2418RTF	AAGGCCCTGTTCACCGACGTCA	64.0
SCO2418RTR	AAGCCGGTGACGAGCTTCTGGA	64.0
SCO2417RTF	ACCACCTCCCCCTACGACGTGA	65.8
SCO2417RTR	CAGGTAGTCGCGGGGCACGA	65.5
SCO2416RTF	AGCGTCGTCGCCGACCGCTA	65.5
SCO2416RTR	CAGCGAGGCGCGTTGCTCGA	65.5
SCO2415RTF	GGCCGGATCACCGGCATCGAA	65.7
SCO2415RTR	GACGCCGGACAGCGTGTCGA	65.5
SCO2414RTF	CGCATCCCCGCCGACACCAA	65.5
SCO2414RTR	GTGGTCAGGAGGTTGGCGAGGA	65.8
HrdBRTF	GAGGCGACCGAGGAGCCGAA	65.5
HrdBRTR	GCGGAGGTTGGCCTCCAGCA	65.5
SCO2422GFPNEWF	GCGAACAATGCGGCCGTCCA	63.5
SCO2422GFPNEWR	GCCCTCGACCACCACTTCGA	63.5
MtrARTF	GACACCGCACTGGCCGAGA	63.1
MtrARTR	GTAGCCCCAGACCTGCTCGA	63.5
2415OEF	CACCATGAAGCGCGCAACGCTCC	67.8
2415OER	CAGCCGTACGGCAGAGGTGATCA	67.8
2418OEF	CACCATGACCGGCGCCGA	62.8
2418OER	GGCGCTTCATCCGCGGCA	62.8
2422OEF	CACCATGGGAATCGAAGTGGTGG	64.2
2422OER	GGCGCCGGTGATCACGCGCCG	71.5

Table 2.10: Generalised PCR conditions

No. cycles	Temperature (ºC)	Time (minutes: seconds)
1 - Denaturation	98	2:00
26 - Denaturation	98	0:15
- Annealing	T_a	1:00
- Extension	72	1:00
1 -Final extension	72	10:00

These conditions used for all standard PCR reactions unless otherwise stated.

Table 2.11: RT PCR conditions

No. cycles	Temperature (°C)	Time (minutes: seconds)
1 -Reverse transcription	50	30:00
1 -Denaturation	95	15:00
30 -Denaturation	94	1:00
-Annealing	T_a	1:00
-Extension	72	1:00
1 -Final extension	72	10:00

These conditions used for all RT PCR reactions unless otherwise stated.

Catalase assay of vacuole catalase activity (Durchschlag *et al.*, 2004)

Acanthamoeba cells were suspended in PAS and lysed by passaging three times through a French press. Approximately 5 μg protein (determined by Bradford assay – see below) was added to 1.5 ml catalase buffer (50 mM Na_2HPO_4 pH7, 0.1 % Triton X-100) containing 25 mM H_2O_2, in a quartz cuvette. Absorbance was measured at 240 nm for 3 minutes.

Bradford assay for protein concentration (Bradford, 1976)

A series of protein standards were created by diluting bovine serum albumin (BSA, Promega, 10 mg/ml) with deionised water to a concentration of 0.2 – 0.8 mg/ml (the

linear range of the assay). Dye reagent (Biorad) was prepared according to manufacturer's instructions and 50 µl of standard or sample was added to 2.5 ml dye reagent. Colour was developed by incubation at room temperature for 5 minutes and absorbance at 595 nm was measured against the standard to determine the protein concentration of the sample.

Spore sensitivity assays

Lysozyme, SDS and DMSO sensitivity

An MS agar plate was inoculated with approximately 6 x 10^7 spores in a volume of 50 µl which was spread evenly across the surface of the plate. The plate was dried for 10 minutes. A number of dilutions of the desired reagent (lysozyme, SDS, DMSO) were prepared, and spotted onto the surface of the plate in 10 µl aliquots. The plate was incubated at 30ºC and examined daily for signs of growth inhibition.

Toluene sensitivity

A 10 ml aliquot of 2xYT was inoculated with approximately 6x10^7 spores and incubated at 37 ºC for 5 hours with shaking at 220 rpm. A 2.5 ml aliquot of 100% toluene was added to half of the tubes, and 2.5 ml 2xYT added to the remaining tubes, and incubation continued for a further 20 minutes. Aliquots from each sample were diluted 1/10 or 1/100 with 2xYT, and 1ml of each dilution was spread onto MS agar and incubated at 30 ºC for 3 days. The number of colonies was counted and the toluene-treated samples compared to the untreated controls.

Bioinformatics

See Chapter 3 for methodologies. *S. coelicolor* nucleotide sequences were taken from the StrepDB database (Bentley *et al.*, 2002; Bishop *et al.*, 2004).

Cloning

Cloning reactions were performed using DNA modification enzymes (Promega, New England Biolabs) according to manufacturers' instructions. See Results chapter 4 for individual cloning strategies.

Unless otherwise stated, *E. coli* strains DH5α and JM109 were used as hosts for all intermediate cloning products.

Overexpression of *mce* cluster genes

Invitrogen Champion pET Directional TOPO Expression Kit

Selected genes (SCO2422 and SCO2415) were amplified by PCR and cloned into the pET100/D-TOPO vector according to the manufacturer's instructions, using primers (specified in Table 2.9) which contained a CACC overhang to facilitate directional cloning. Cloning products were transformed into One Shot TOPO 10 chemically competent *E. coli* and plated on LB containing ampicillin. Plasmid DNA was isolated from transformants and screened by restriction digest. Plasmids apparently containing the correct insert were confirmed by sequencing (GATC).

SCO2422 and 2415 expression vectors were transformed into BL21 chemically competent *E. coli* and expression was optimised according to the manufacturer's instructions.

FTIR

Plates were inoculated and biomass was harvested as for RNA isolation. Biomass was suspended in 0.1 M Tris-HCl pH7 and vortexed to disperse clumps. The cell suspension was then spotted onto $CaCl_2$ windows and dried. Absorption was measured using IR spectroscopy and analysed using Opus software (Bruker Optics).

Germination assay (Suarez *et al.*, 1980)

Spore stocks were diluted to an OD_{450} of 0.4 – 0.5 in GAE medium and incubated at 30°C. Aliquots of 1 ml were taken at various time-points and the OD_{450} measured.

Plant cultivation

Colonisation assays were performed using tobacco (*Nicotiana tabacum*; a gift from Mr Michael Ambrose, John Innes Centre, UK), *Arabidopsis thaliana* (Ecovar Columbia CL295; a gift from Mr Michael Ambrose, John Innes Centre, UK), alfalfa (*Medicago salvia* cultivar Sabilt; a gift from Dr Ian Thomas, Institute of Grassland and Environmental Research, University of Aberystwyth, UK) and radish (*Raphanus sativus* Cultivar Saxa; a gift from Dr Charlotte Allender, Horticultural Research Institute, University of Warwick). Seeds were surface sterilized by bleaching (15% sodium hypochlorite solution for 15 minutes), washed in sterile distilled water and germinated on Murashige and Skoog agar medium with 2% sucrose (Murashige, 1962) in Petri dishes. Plants were grown at 21 ^{o}C with a 16-h day length. Plants for colonization experiments were transferred to Magenta boxes (Sigma) or 6-well plates and allowed to equilibrate for 24 hrs before inoculation with *Streptomyces* spores, wild-type and mutant strains, by adding to the surface of the Murashige and Skoog agar in the vicinity of the seedling roots. After 3 days and 7 days, plants were removed from the boxes, washed in sterile distilled water and the roots examined for colonisation.

To enumerate bacterial colonization, 1 cm sections of root were removed under sterile conditions and homogenized, using disposable micro-tube pestles (Starlabs) in 500 µl of distilled water. Samples were serially diluted and counted by plating on to Nutrient agar. Given the large amount of plant material when compared to the bacterial load, bacterial counts were normalized by optical density of plant tissue/bacteria using a Nanodrop spectrophotometer.

Root samples were also removed and added directly to 500 µl of RNAprotect (Qiagen) for the isolation of plant/*Streptomyces* RNA. Samples were homogenized with disposable micro-tube pestles (Starlabs) and frozen at -80 ^{o}C prior to harvest of the RNA using the methods described previously.

Microscopy of plant roots.

Plant roots (1 cm samples) and colonizing *Streptomyces* were visualized by confocal microscopy (Leica SP5 Confocal) after mounting in distilled water. GFP signals were visualised following excitation at 488 nm.

Western blot (Sambrook *et al.*, 1989)

Protein time-courses

Streptomyces strains were grown on solid YEME overlaid with cellophane as for RNA isolation (see above). Biomass was harvested at 16, 24, 36 and 48 hour time-points using a razor blade and suspended in 0.1 M Tris pH7 in microcentrifuge tubes. Biomass was stored at -20ºC until required.

Frozen samples were thawed on ice and sonicated using a probe sonicator (Branson Sonifier 250) with a stepped microtip for 2 x 20 second cycles on setting 4 followed by 4 x 20 second cycles on setting 6. The resulting lysate was treated with protease inhibitor (Roche) and assayed for protein concentration by Bradford assay (see above).

SDS PAGE

An aliquot of cell lysate containing 15 µg protein was diluted to a total volume of 10 µl in 0.1 M Tris pH7 in a microcentrifuge tube. An equal volume of Laemmli loading dye (60 mM Tris-HCl pH6.8, 2% SDS, 10% glycerol, 5% β-mercaptoethanol, 0.01%

bromophenol blue) was added and the sample boiled at 90ºC for 5 minutes. Broad range protein marker (NEB) was heat treated in the same way.

After heat treatment, marker and samples were loaded onto NuPAGE Bis-Tris acrylamide gels (Invitrogen) and electrophoresed at 150 V for 90 minutes using the XCell *SureLock* Mini-Cell according to manufacturer's instructions.

Gels which were not required for western transfer were stained in Coomassie (45% methanol, 10% acetic acid, 0.25% Coomassie blue) for 40 minutes with gentle shaking and then transferred to destain solution (5% methanol, 10% acetic acid) with gentle shaking until the required level of destaining was achieved.

Transfer

Following electrophoresis, protein was transferred from the gel to 0.45 μm PVDF membrane (Millipore imobilin-P) using Invitrogen XCell II Blot Module with NuPAGE transfer buffer according to the manufacturer's instructions. Following transfer the membrane was air-dried, sealed in a plastic bag and stored at 4ºC until required.

Table 2.12: Solutions used in western blotting

Solution	Composition
Tris-buffered saline (TBS)	1.2 g Tris Base 8.7 g NaCl Make up to 1 litre with distilled water Adjust to pH 7.4 with conc. HCl
Blocking solution	TBS + 5% Marvel
Chemiluminescence solution I	10 ml 1 M Tris pH 8.5 1 ml 250 mM Luminol (in DMSO) 0.46 ml 250 mM P-Coumaric acid (in DMSO) Make up to 100 ml with distilled water
Chemiluminescence solution II	10 ml 1 M Tris pH 8.5 64 µl H_2O_2 Make up to 100 ml with distilled water
Stripping buffer	15 g Glycine 1 g SDS 10 ml Tween 20 Make up to 1 litre with distilled water Adjust to pH 2.2 with conc. HCl

Blotting

Stored post-transfer PVDF membrane was re-wetted by brief rinsing with methanol, followed by thorough rinsing with distilled water to remove methanol. This and all subsequent steps were performed at room temperature. The membrane was placed in a shallow tray with approximately 100 ml TBS containing 5% Marvel and left overnight with gentle shaking.

The blocking solution was decanted and replaced with 20 ml TBS containing 2.5% Marvel and the primary antibody (rabbit polyclonal antibody raised against *M. tuberculosis* Mce1A) at a dilution of 1:1000. This solution was left for 2 hours with gentle shaking, following which the antibody solution was decanted and the membrane washed for 3 periods of 15 minutes with TBS. The TBS was decanted and replaced by 20 ml TBS containing 2.5% Marvel and the secondary antibody (anti-Rabbit HRP conjugate) at a dilution of 1:1000. This solution was left for 1 hour with

gentle shaking, following which the antibody solution was decanted and the membrane washed for a further 3 periods of 15 minutes with TBS.

Development

The membrane was removed from the TBS and placed in another shallow tray. Chemiluminescence Solution I (4ml) was added to one corner of the tray and Chemiluminescence Solution II (4ml) was added to the opposite corner. The tray was shaken vigorously for 90 seconds, following which the membrane was removed, blotted on paper towel to remove excess solution, and placed in an autoradiography cassette. In the dark, the membrane was overlaid with clingfilm and a sheet of enhanced chemiluminescence (ECL) detection film (Amersham) placed over the top. The cassette was closed and left for 2 minutes, following which the film was removed and developed using an X-omat (Kodak). Depending on the level of detection obtained from the initial 2 minute exposure, further exposures were performed in which exposure time was varied from 10 seconds to 5 minutes.

Re-probing

Membranes to be re-probed were placed in a shallow tray and covered with approximately 100 ml stripping buffer. The membrane was washed with stripping buffer for 2 periods of 10 minutes, followed by washing with TBS for 2 periods of 10 minutes. The membrane was then placed in blocking solution overnight and the western blotting protocol followed as normal (see above).

Chapter 3: Detailed analysis of the *mce* gene cluster in *Streptomyces*

Bioinformatic analysis of the *mce* gene cluster

Currently there are 26 fully sequenced *Streptomyces* genomes in the NCBI database, with a further 138 non-streptomycete *Actinobacteria*. Many of these are newly-sequenced actinomycetes which have not been included in the previous bioinformatic analysis of the *mce* operon (Casali & Riley 2007).

Utilising bioinformatic techniques is a key part of the analysis of the *mce* cluster. The crystal structure of the Mce assembly has not yet been determined and thus in silico analysis is the major source of information regarding the structures, evolutionary relationships and putative functions of these proteins.

Phylogenomic analysis of the cluster is also particularly useful in the actinomycetes, as their taxonomy is complex. The bioinformatic analysis of the *mce* operon had three primary purposes: to investigate the distribution of the operon in newly-sequenced actinomycetes; to infer phylogenetic relationships within the *Streptomyces* and whether this is reflected by the *mce* cluster; and to gather information on the probable structures of the *S. coelicolor* Mce proteins with a view to clarifying their functions.

The *mce* promoter region

Structural features of the *mce* operon, for example the fact that it is transcribed in the opposite direction from the operon upstream of it, and that the genes of the operon overlap, suggest that there is most likely a single upstream promoter region. However, *Streptomyces* promoters are difficult to identify due to the high GC content of the genome, and the *mce* promoter sequence has not yet been identified. Comparisons with known *Streptomyces* σ-factor promoter sequences such as *hrdB* and *ermE* show no homology, but there are many diverse σ-factors in *Streptomyces* whose cognate promoter sequences have yet to be characterised (Seghezzi, 2010).

Alternatively, there may be internal promoters upstream of one or more genes in the operon. The *S. coelicolor* consensus Shine-Dalgarno sequence GGAGG is present in the -10 region of all the core *mce* genes, and this might support the hypothesis that internal promoter regions are also present. If there is only a single upstream promoter, the genes of the operon are likely to be expressed as a single polycistronic transcript. This possibility is investigated further in chapter 6.

Distribution of the *mce* operon

Prior to this work bioinformatic analysis of the *mce* operon had been undertaken, the most recent review being Casali and Riley (2007) in which analysis was based on *M. tuberculosis* query sequences. Analysis of the distribution of *mce* homologues within the actinomycetes showed copy number varying from zero to twelve homologous operons (Fig. 3.1).

Conservation of the *mce* operon in newly-sequenced actinomycetes

Analysis of the distribution of the *mce* cluster was performed in order to include the many newly-sequenced actinomycetes genomes that have become available since the last published survey. Previous analyses have focused on the *mce* operons in *M. tuberculosis* and for this reason the database(s) was queried using sequences from the *M. tuberculosis* genome. In this case, the starting point is the *S. coelicolor mce* operon which had been identified previously as homologous to *mce* in *M. tuberculosis* (Sutcliffe and Harrington, 2004). Using this rationale *S. coelicolor*-derived query sequences were used query the non-redundant NCBI database. Query sequences were obtained from the StrepDB database (Bentley *et al.*, 2002; Bishop *et al.*, 2004).

Analysis was carried out initially by blastx (Altschul *et al.*, 1990), a translated nucleotide query of the NCBI protein database (Fig. 3.2). This method was used in order to find the widest possible distribution of the Mce proteins and to eliminate the

effects of synonymous substitutions on a nucleotide-nucleotide alignment. One of the drawbacks of this approach is that it can difficult to infer synteny, but this can be clarified by subsequent blastn analysis of sequences showing hits with blastx.

There is also some sequence homology between different genes of the *mce* cluster such that a blastx query using the sequence of one gene may produce hits from the gene product of another. This problem can be largely solved by the application of strict criteria (an e value of $4e^{-50}$ or lower; homology across the entire query sequence) to the matches.

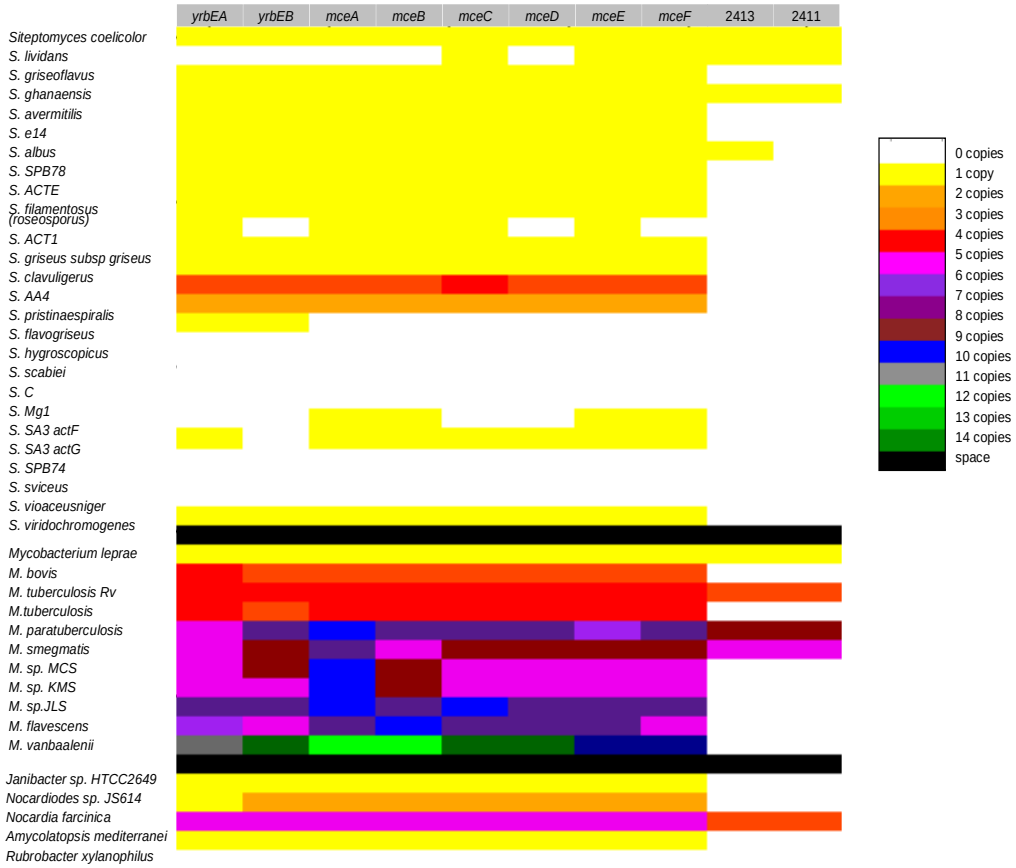

Figure 3.1: Distribution of *mce* homologues among the *Actinobacteria*. Date of analysis February 2011.

Of the 26 complete streptomycete genomes in the NCBI database, 18 show homology to one or more genes in the *mce* cluster (Fig. 3.1). Most (14 species) have a single copy of the entire core operon, with sequences showing relatively little divergence between species (86% - 54% identity). Synteny is also conserved. Three *Streptomyces* species (*S. coelicolor*, *S. ghanaensis* and *S. lividans*) show conservation of the *mas* genes in the downstream region of the operon.

Presence of the ATPase (SCO2422) is not shown due to the wide conservation of ATPases throughout the prokaryotes. This made it difficult to distinguish between Mce assembly ATPases and those belonging to different assemblies, especially in organisms which did not have the other *mce* core genes.

Rubrobacter xylanophilus, thought to be the basal species of the actinomycetes (Kunisawa, 2007), does not have any sequence showing significant homology to the *mce* core cluster genes. This suggests that the cluster was a more recent aquisition.

The recently sequenced species *Streptomyces AA4* contains three copies of the complete *mce* core operon, possibly as the result of a duplication event. *S. pristinaespiralis* contains two complete copies of the operon. Phylogenetic analysis was performed in order to investigate whether this was the result of a duplication event or of horizontal gene transfer.

Constructing phylogenetic trees for the *mce* cluster

Having established the distribution of Mce-like proteins in the actinomycetes, the phylogenetic properties of the *mce* operon were examined. Multiple alignments were constructed using selected sequences and used to construct phylogenetic trees for members of the *mce* operon (Fig. 3.2-3.3B).

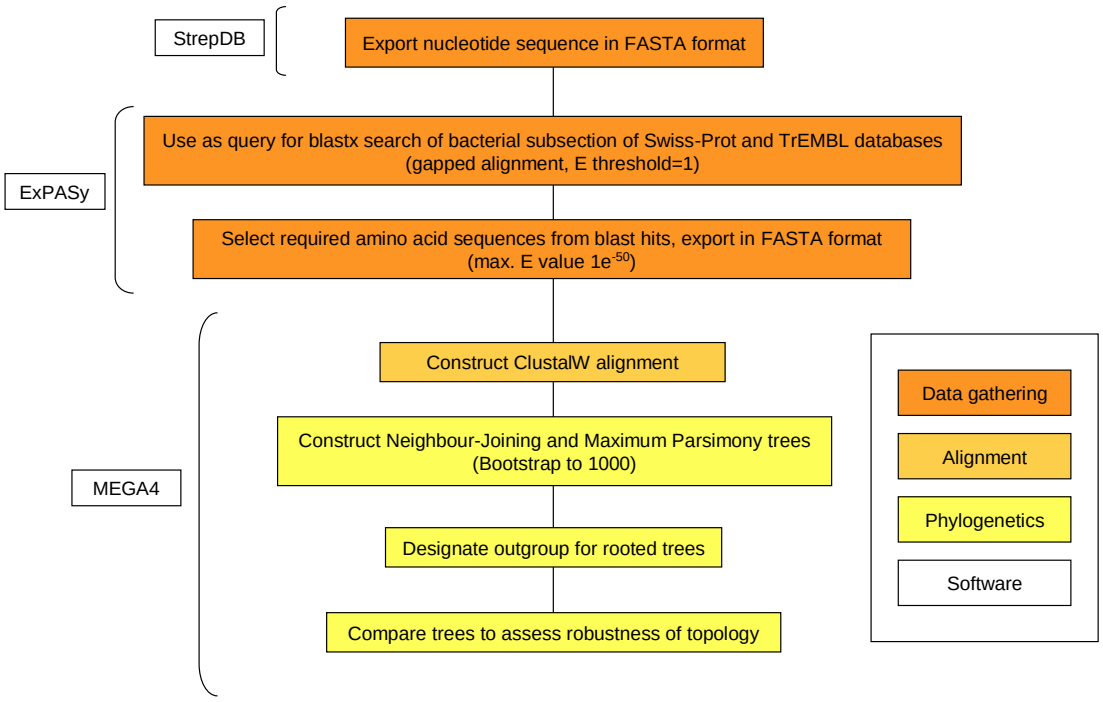

Figure 3.2: Pipeline of bioinformatic analysis in the construction of phylogenetic trees from sequence data.

Amino acid sequences were exported from ExPASy in FastA format and aligned using the clustalW function of the MEGA4 software (Tamura *et al.*, 2007).

The alignments were subsequently used to construct phylogenetic trees, also using MEGA (Tamura *et al.*, 2007). For each data set two trees were constructed, using the neighbour-joining and maximum parsimony algorithms, and compared to assess the robustness of the tree topology. Bootstrap values of 1000 were applied and (where a rooted tree was required) the trees were rooted using an appropriate outgroup (see figure legends for the specific outgroup used in each tree) (Saitou and Nei, 1987).

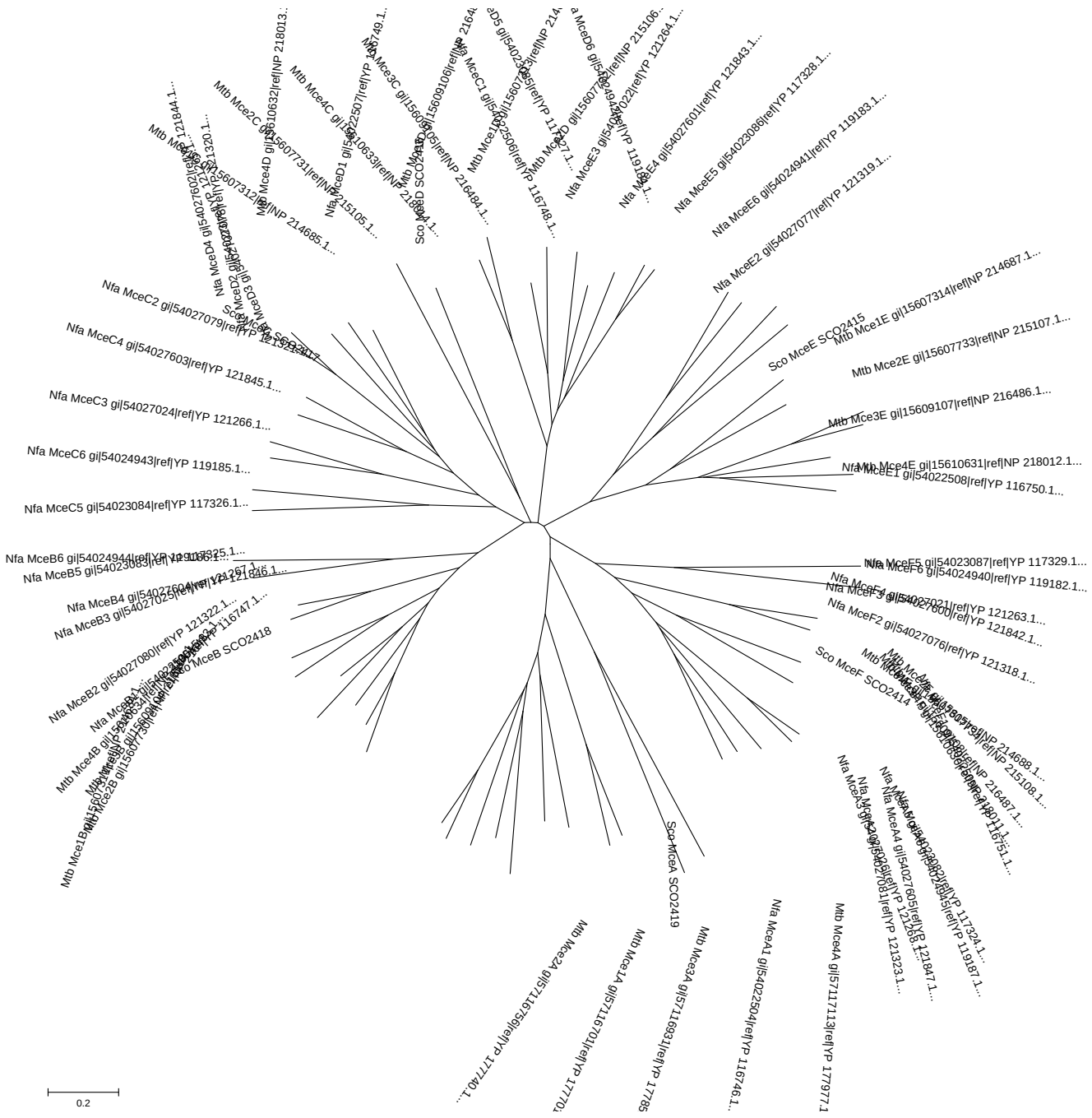

Figure 3.3A: Evolutionary relationships of the Mce proteins in *M. tuberculosis*, *N. farcinica* and *S. coelicolor* inferred using the Neighbor-Joining method. The optimal tree with the sum of branch length = 31.97 is shown to scale. Evolutionary distances are in the units of the number of amino acid substitutions per site.

An unrooted Neighbour-Joining tree (Fig. 3.3A) of the *mce* homologues in *M. tuberculosis*, *N. farcinica* and *S. coelicolor* shows that, rather than clustering by species, the genes cluster by their position in the operon (i.e. the *mceA* genes cluster together, as do the *mceB* genes and so on). This indicates that the ancestral core operon also consisted of six *mce* genes and that the synteny has been conserved (Saitou and Nei, 1987).

One implication of this is that, for the purposes of constructing a phylogenetic tree of multiple actinomycete species, the *mce* core genes can essentially be treated as a single ORF, i.e. a tree generated using sequences from MceA homologues will have identical topology to one constructed using sequences from MceF homologues.

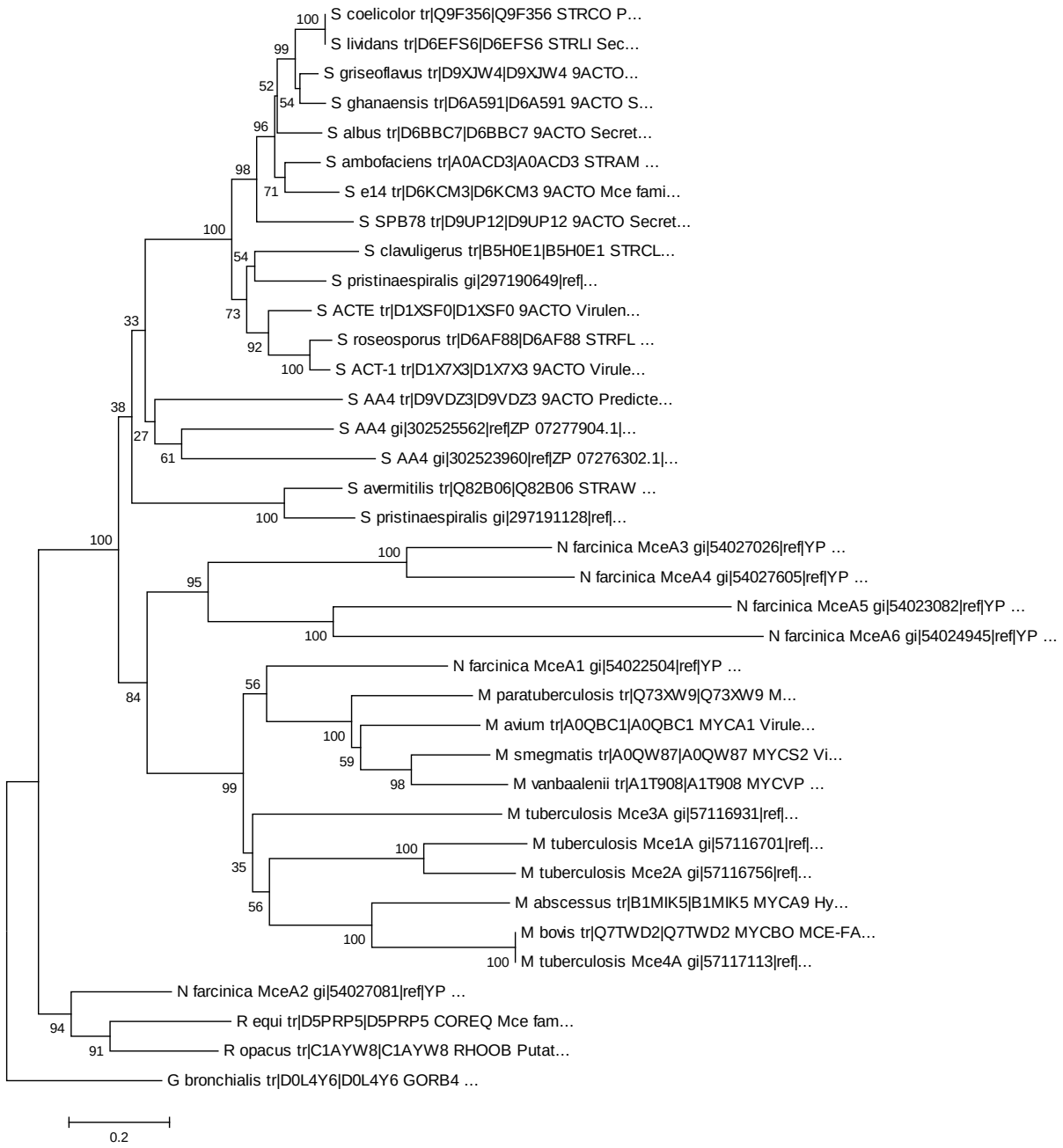

Figure 3.3B: Evolutionary relationships of the MceA proteins in 26 taxa inferred using the Neighbor-Joining method. The optimal tree with the sum of branch length = 11.48 is shown to scale. The percentage of replicate trees in which the associated taxa clustered together in the bootstrap test (1000 replicates) are shown next to the branches. The evolutionary distances are in units of the number of amino acid substitutions per site. The tree is rooted using *Gordonia bronchialis* as the outgroup.

A Neighbour-Joining tree of MceA homologues across the *Actinomycetales* (Fig. 3.3B) shows that the *Streptomyces* cluster together, as do the mycobacteria. Interestingly, the two copies in *S. pristinaespiralis* are distant on the tree, suggesting either an ancient duplication event or the horizontal acquisition of at least one of its two *mce* clusters. The three copies in *S. AA4* are clustered closely on the tree, suggesting a recent duplication event. *S. AA4* has three complete copies of the entire operon which supports this hypothesis, as there has been no gene loss from the duplicated copies of the operon.

Of the six copies of the *mce* operon present in *N. farcinica*, four are clustered closely together suggesting that they have arisen from duplication events. Two other copies of the operon cluster with the Mycobacteria and *Rhodococcus* respectively, suggesting a possible horizontal gene transfer event.

Regulation of the *mce* operon

M. tuberculosis, as well as a number of other actinomycetes, appears to regulate transcription of its *mce* operons using GntR-like and TetR-like repressors. It is thought that this regulation may allow for the temporal expression of the *mce1, 2, 3* and *4* operons (Santangelo *et al.*, 2009; Santangelo *et al.*, 2008).

A Blast search using the *M. tuberculosis* Mce1R amino acid sequence as the query reveals homologues in *Mycobacterium, Nocardia* and *Rhodococcus*. Interestingly, *Streptomyces* species *e14* and *AA4* also have predicted proteins showing some homology (41% and 39% identity respectively). A search using the Mce2R sequence yields similar results, but includes a *S. coelicolor* transcriptional regulator (SCO0582) with 38% identity. Queries using sequences from the two TetR-like regulators Mce3R and Mce4R yield similar results as for the GntR-like regulators, but with slightly increased scores from *Streptomyces* species (including *S. coelicolor* SCO2319, 44% identity), possibly because TetR-like repressors are more common than GntR-like repressors in *Streptomyces* (Bentley *et al.*, 2002).

Homologues of the *M. tuberculosis mce* regulators appear to be present mainly in species which possess multiple copies of the *mce* operon. This is perhaps a reflection of the putative role of these regulators in controlling temporal expression of the different operons. Although homologues of all MceR proteins are present in *Streptomyces*, the homology is not particularly strong and there is no evidence that these proteins play a role in *mce* regulation. The distance between the MceR homolgues and the *mce* cluster in the *Streptomyces* also argues against their involvement in *mce* regulation.

No other plausible candidate regulators have so far been identified in the region of the *mce* operon in *S. coelicolor*; the operons on either side of *mce* are transcribed in the opposite direction and there are no genes with sequence similarity to the mycobacterial regulators in the region. A putative regulator (SCO2426; designated on the basis of a possible helix-turn-helix motif) is present in an adjoining gene cluster. However, an orthologue of this putative regulator is present in unknown *Streptomyces* species *s4* (Bentley *et al.*, 2002) and comparison between this species and *S. coelicolor* shows that synteny with the *mce* cluster is not conserved. It therefore seems unlikely that SCO2426 regulates the *mce* cluster.

The absence of a local regulator does not preclude the possibility that the regulator is located elsewhere in the *S. coelicolor* genome. It is not known whether the *mce* operon has a dedicated regulatory system or if it is part of a broad regulon and is regulated in parallel with other cellular functions, but the presence of a non-local regulator might support the latter hypothesis.

The *mtrAB-lpqB* two-component system has been proposed as a possible regulator of the *S. coelicolor mce* operon. This is investigated further in chapter 6.

The *mce* operon encodes an ABC importer

Analysis of the *M. tuberculosis* Mce cluster predicted amino acid sequences shows several features characteristic of ABC transporters (Casali and Riley, 2007; Mohn *et*

al., 2008). Structural predictions were performed using *S. coelicolor* amino acid sequences to investigate whether or not they were also consistent with this role.

Substrate-binding proteins and the MceE lipobox motif

Substrate-binding proteins associated with ABC importers are situated on the outside of the plasma membrane, and are typically anchored to the membrane via a lipoprotein. Lipoproteins are characterised by a conserved sequence [LVI][ASTVI][GAS][C] called the lipobox. This sequence includes an invariant cysteine residue which is lipidated following protein translocation through the Sec or Tat pathway (Thompson *et al.*).

An alignment (Fig 3.4) of the *M. tuberculosis* and *Streptomyces* lipobox motifs from the *mceE* gene show that, while the *M. tuberculosis* sequences contain the invariant cysteine, *S. coelicolor* does not. This is the result of a single-nucleotide polymorphism which changes the first base in the codon from U to A, resulting in a change of encoded amino acid from cysteine to serine. The strong likelihood is that this mutation renders the lipobox in the *S. coelicolor mceE* gene non-functional.

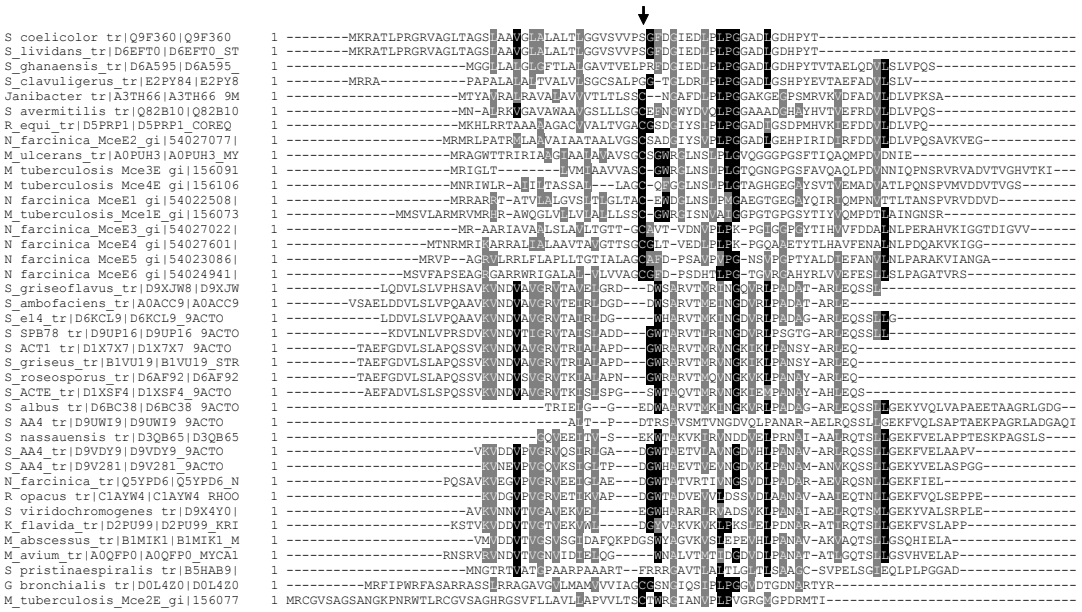

Figure 3.4: Alignment of the lipobox region of MceE in 26 taxa. Arrow shows position of conserved cysteine residue.

Predicted structure of the Mce assembly

The crystal structure of the Mce assembly has not yet been determined. Predictions have been made using the *M. tuberculosis* Mce1A amino acid sequence by mapping it onto a structurally solved *E. coli* protein of similar size (Das *et al.*, 2003). These showed that the epitope responsible for mediating uptake was on the surface of Mce1A, but likely to be hidden in Mce2A.

S. coelicolor predicted amino acid sequences were analysed using TMpred (www.ch.embnet.org/software/TMPRED_form) (Hofmann, 1993) to predict the presence and orientation of any transmembrane domains.

Analysis of the *yrbEA* and *yrbEB* homologues SCO2421 and SCO2420 using TMpred show a predicted 11 transmembrane helices (5 for SCO2421 and 6 for SCO2420), with the N-terminal on the cytoplasmic side of the membrane (Fig. 3.5). This is consistent with the putative role of YrbEAB as a transmembrane domain in an ABC transporter assembly. It is also consistent with previous observations that importer-associated TMDs have between 10 and 20 membrane-spanning helices (Hollenstein *et al.*, 2007).

In a typical ABC importer there are one or two substrate-binding proteins associated with each membrane permease domain (Dawson *et al.*, 2007). In the Mce assembly there are a predicted six SBPs (MceA-F). The localisation of the Mce proteins was predicted using SignalP (Bendtsen *et al.*, 2004) which predicts the location of signal peptide cleavage sites, and TMpred. The results of this analysis indicated that three of the Mce proteins (MceA, B, E) are signal anchored, and 3 (MceC, D, E) are secreted. It is possible that the unusually high number of SBPs associated with the Mce complex reflects the substrate or substrates that are imported; large hydrophobic molecules such as sterols may require a large substrate-binding domain.

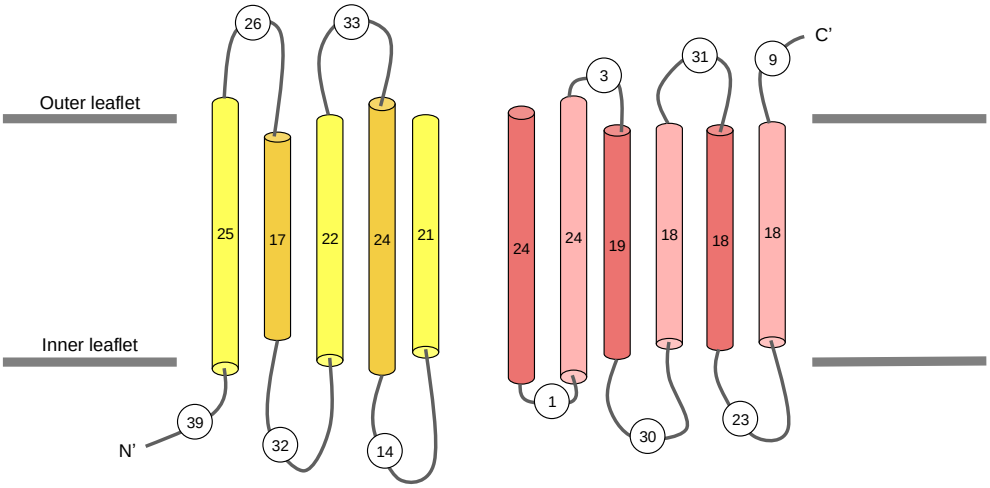

Figure 3.5: Predicted organisation of the transmembrane domains of the YrbEA (yellow) and YrbEB (red) homologues in *S. coelicolor*. Numbers denote number of amino acid residues present in each region. The N-terminal is predicted to be on the inside of the membrane, with the C-terminal on the outside and 11 transmembrane helices.

Chapter 3 summary

The *mce* operon is present in the majority of fully-sequenced *Streptomyces*. Among the organisms which have homologous sequences, most have a complete copy of the core operon in which synteny is conserved. Exceptions are *S. AA4* in which the operon has undergone a duplication event and *S. pristinaespiralis* in which there appears to be a horizontal gene transfer. This has implications for the designation of the *mce* operon as a virulence factor as it is also well conserved in many non-pathogenic streptomycetes.

Amongst the wider actinomycete group, copy number is highly variable. Regulation of the operon also appears to be related to copy number, with GntR homologues predominantly present in species with multiple copies of the *mce* operon. This may be related to the reported temporal expression of the *mce* operons in *M. tuberculosis*.

Investigation of secondary protein structure shows that the Mce cluster proteins in *S. coelicolor* are consistent with those of an ABC importer assembly. However, the lipobox motif in the predicted substrate-binding protein MceE has undergone a point mutation which is likely to result in severely reduced or non-secretion of the lipoprotein. Of the six Mce proteins, it appears likely that three (MceA, B and E) are anchored while the remaining three (MceC, D and F) are secreted. The presence of six predicted substrate-binding proteins is unusual in ABC importers and may reflect the nature of the substrate transported by the Mce assembly.

Bioinformatic analysis can shed light on phylogenetic relationships, and point to the structure and function of an operon at both the genetic and the protein level. However, it is also important to confirm these conclusions by direct experimentation. This will be addressed in the following results chapters (Chapters 4-6).

Chapter 4: Construction of *mce* mutants and phenotypic screening

Introduction

In order to elucidate the function of the *mce* operon in *Streptomyces coelicolor* a number of techniques were employed. Initially, single gene disruption mutants were created within the *mce* core cluster. Following this a multiple-gene knockout was created which spanned the first 8 genes of the operon. Finally, a complementation vector was created to demonstrate linkage of the mutant phenotype to the disruption/deletion. All mutant strains were confirmed using molecular techniques and subsequently screened under a variety of conditions to characterise their phenotype.

The construction of mutant strains, their confirmation and verification, and subsequent screening of these strains, is dealt with in this chapter. The following two results chapters will describe the optimisation and implementation of a virulence screen, and examination of the *mce* operon at the level of expression.

Construction of single gene disruption mutants

Single gene disruption mutants of the *mce* cluster were constructed by conjugal transformation of the wild-type *S. coelicolor* strain M145 using cosmids from the *S. coelicolor* transposon insertion library at the University of Wales Swansea (Herron *et al.*, 2004). These cosmids are derived from the ordered *S. coelicolor* cosmid library (Redenbach et al., 1996) and contain fragments of the *S. coelicolor* genome, which had been randomly mutagenised by insertion of the transposon *Tn*5062, which is based on EZ-Tn (Epicentre).

E. coli is transformed with an *in vitro Tn*5062 mutagenised cosmid from the ordered cosmid library and colonies containing a successful transposition event are selected with apramycin. These cosmids are subsequently sequenced using oligonucleotides specific to the *Tn*5062 terminal inverted repeats to determine the site and orientation

of transposon insertion. The insertion site corresponding to each cosmid used in this study is shown in Fig. 4.1 and Table 4.1.

Table 4.1: Position of *tn*5062 insertions in the *mce* operon

Cosmid name	Insertion in gene	Position of gene in genome	*Tn*5062 position
8A2.1.B11	SCO2422	2595123 – 2596154	2596093
8A2.2.E04	SCO2421	2594362 – 2595126	2594484
8A2.1.D12	SCO2420	2593549 – 2594355	2593929
8A2.2.C07	SCO2418	2591230 – 2592294	2591457
8A2.2.F02	SCO2416	2589168 – 2590181	2589333
8A2.1.F04	SCO2415	2587930 – 2589171	2588290
8A2.1.G07	SCO2423	2596787 – 2597419	2596921

Transposon *Tn*5062 (Fig. 4.2) contains EGFP - GFP that has been optimised for use in *Streptomyces* by modifying its codon usage to mirror that of GC-rich organisms (Sun *et al.*, 1999) - and an antibiotic marker (aac(3)IV - apramycin) that allows for selection for colonies containing the transposon. The EGFP does not have its own promoter but if the transposon insertion is in the correct orientation transcription may be driven by the promoter of the disrupted gene (Herron *et al.*, 2004).

*Tn*5062 also contains transcriptional terminators which prevent read-through from the EGFP or apramycin genes. In the absence of additional promoter sequences, a transposon insertion in an upstream region of an operon is therefore likely to disrupt not only the gene in which it has inserted, but also the genes downstream of the insertion site.

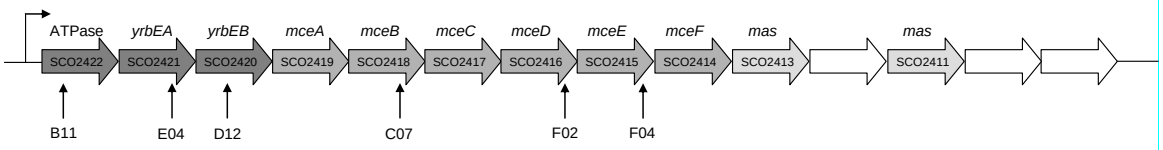

Figure 4.1: The *S. coelicolor* A3(2) *mce* operon (10686 bp), showing putative upstream promoter region, nine core genes including putative ATPase and *yrbE* homologues (SCO2422-SCO2420; dark grey) and *mce* genes *A-F* (SCO2419-SCO2414; grey), two conserved *mce-associated* genes (SCO2413, SCO2411; light grey) and three genes of unknown function (white). Black arrows show the positions of *Tn*5062 insertions in cosmids 8A2.1.B11, 8A2.2.E04, 8A2.1.D12, 8A2.2.C07, 8A2.2.F02, 8A2.1.F04 (see Table 4.1 for exact insertion sites).

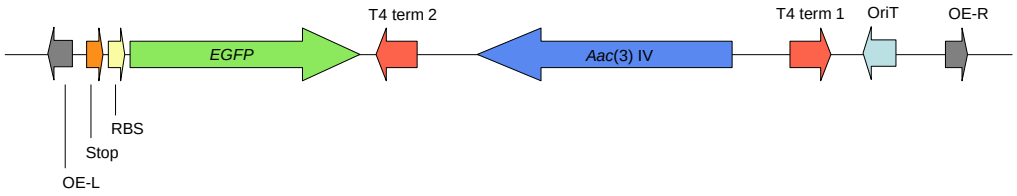

Figure 4.2: Transposon *Tn*5062 (3442 bp) showing positions of EGFP (green), *Aac*(3)IV (apramycin resistance; dark blue), T4 terminators (red), translational stop codon (orange), RK2 origin of transfer (OriT; light blue), streptomycete consensus ribosome binding site (RBS; yellow) and inverted repeats (OE-L and OE-R; grey).

Bioinformatic analysis of the *mce* operon indicates that the *mce* operon has a single upstream promoter region (see chapter 3). The core genes in the operon also have the classical ATGA overlapping stop/start codon which suggests a single polycistronic transcript. This raises the possibility that mutations in the operon will have a polar effect on downstream genes, in which disruptions in the upstream region of the operon produce a more severe phenotype than disruptions in the downstream region, due to truncation of the polycistronic message.

All cosmids have a Supercos-1 backbone containing a kanamycin resistance marker (Redenbach *et al.*, 1996). Sequence data was exported from StrepDB (Bentley *et al.*, 2002) into the CloneManager programme (Scientific & Educational Software) and used to construct cosmid maps (Fig. 4.3B-D), allowing in silico restriction digests and concomitant prediction of fragment sizes. Orientation of the *S. coelicolor* genomic fragment within the Supercos-1 backbone was subsequently established by restriction digest (Fig. 4.3A; Table 4.2).

Table 4.2: Band sizes for *Sph*I and *Mlu*I digest of cosmids 8A2.1.B11, 8A2.2.E04, 8A2.1.D12, 8A2.2.C07, 8A2.2.F02 and 8A2.1.F04. Bands diagnostic for genomic fragment orientation are shown in bold.

	8A2.1.B11	8A2.2.E04	8A2.1.D12	8A2.2.C07	8A2.2.F02	8A2.1.F04
*Sph*I	13402	12230	11666	10595	10595	10817
	10595	10595	10595	9194	9774	10595
	10367	8055	8055	8055	8055	8055
	8055	7353	7353	7650	7353	7353
	2608	4623	5178	7353	7070	6027
	2442	2608	2608	2608	2608	2608
	1085	**2442**	**2442**	**2442**	**2442**	**2442**
	480	1085	1085	1085	1085	1085
	437	480	480	480	840	480
	342	342	342	342	342	342
	240	240	240	240	240	240
	72	72	72	72	72	72
	27	27	27	27	27	27
*Mlu*I	22783	22783	22783	24073	21949	20906
	11389	11389	11389	11389	11389	11389
	8194	**8194**	**8194**	**8194**	**8194**	**8194**
	5935	4326	4015	4335	4335	5319
	1851	3460	3762	2152	4276	4335

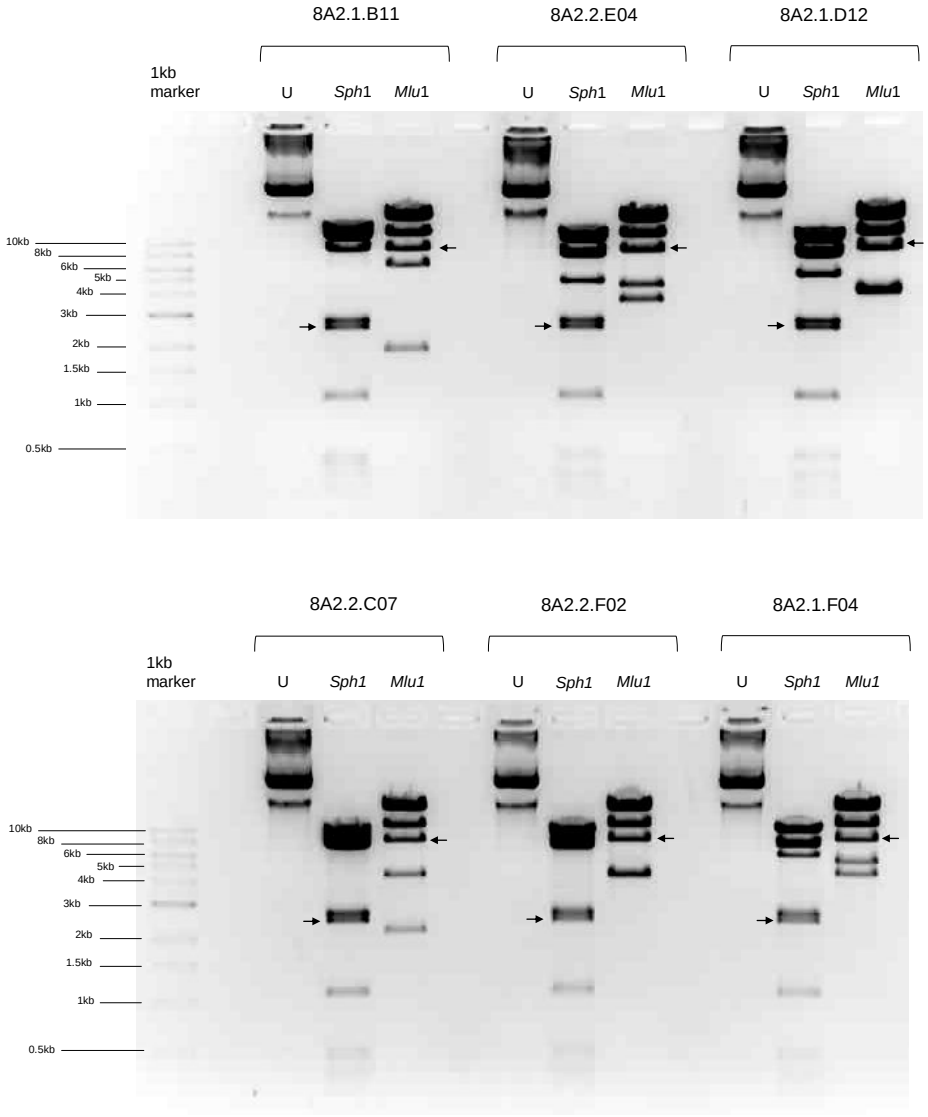

Figure 4.3A: Restriction digests of cosmid DNA with enzymes *Sph*1, *Mlu*1, showing orientation of supercos backbone in *Tn*5062-insertion cosmids 8A2.1.B11, 8A2.2.E04, 8A2.1.D12, 8A2.2.C07, 8A2.2.F02, 8A2.1.F04. U=uncut cosmid DNA. Arrows indicate diagnostic bands (see Table 4.2 for exact band sizes). Gel: 0.8% agarose, 80 V, approximately 10 µg DNA per lane.

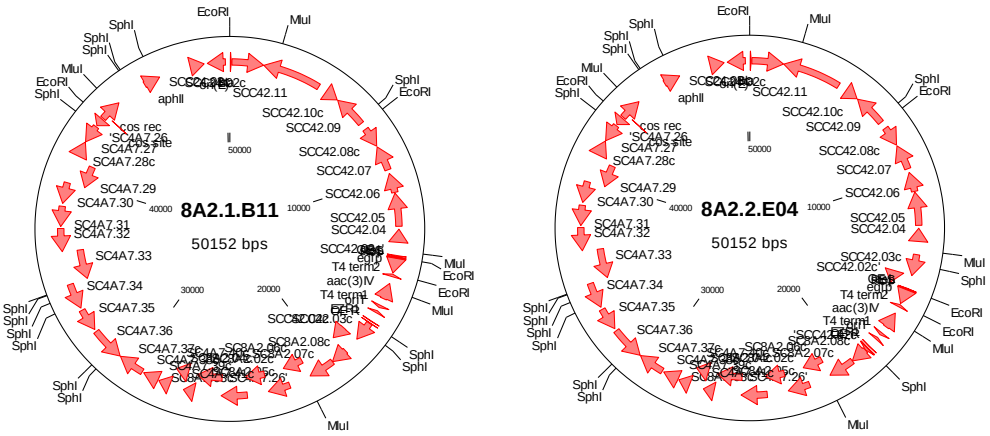

Figure 4.3B: Maps of cosmids 8A2.1.B11, 8A2.2.E04 showing orientation of genomic fragment as confirmed by restriction digest (Fig. 4.3A). Maps constructed in Clonemanager using sequences from StrepDB.

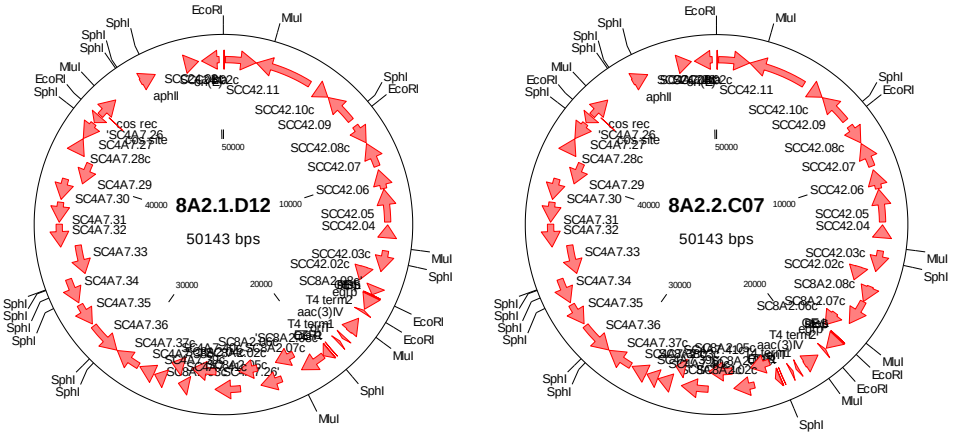

Figure 4.3C: Maps of cosmids 8A2.1.D12, 8A2.2.C07 showing orientation of genomic fragment as confirmed by restriction digest (Fig. 4.3A). Maps constructed in Clonemanager using sequences from StrepDB.

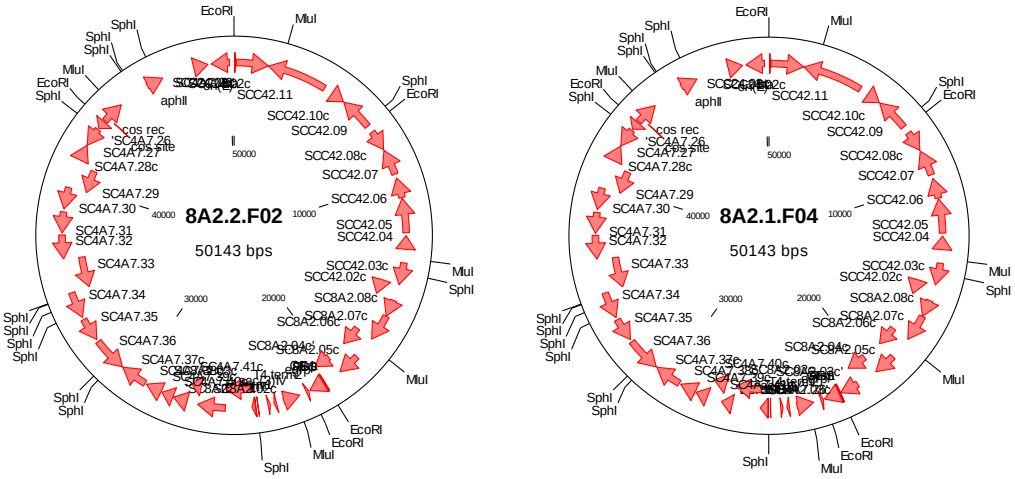

Figure 4.3D: Maps of cosmids 8A2.2.F02, 8A2.1.F04 showing orientation of genomic fragment as confirmed by restriction digest (Fig. 4.3A). Maps constructed in Clonemanager using sequences from StrepDB.

Mutation via homologous recombination

The non-methylating conjugative *E. coli* strain ET12567/pUZ8002 was transformed with the *Tn*5062 mutagenised cosmid vector and subsequently conjugated with the wild-type *S. coelicolor* M145 in order to effect transfer of the cosmid (MacNeil *et al.*, 1992; Paget).

Following conjugative transfer of the cosmid, *S. coelicolor* genomic mutants are generated via homologous recombination (crossing over; Fig. 4.4) of the genomic regions flanking the transposon insertion. Single crossovers indicate integration of the entire cosmid into the *S. coelicolor* chromosome, resulting in one disrupted and one wild-type copy of the gene of interest. Double crossovers indicate allelic replacement of the gene of interest resulting in only a single, disrupted copy of the gene.

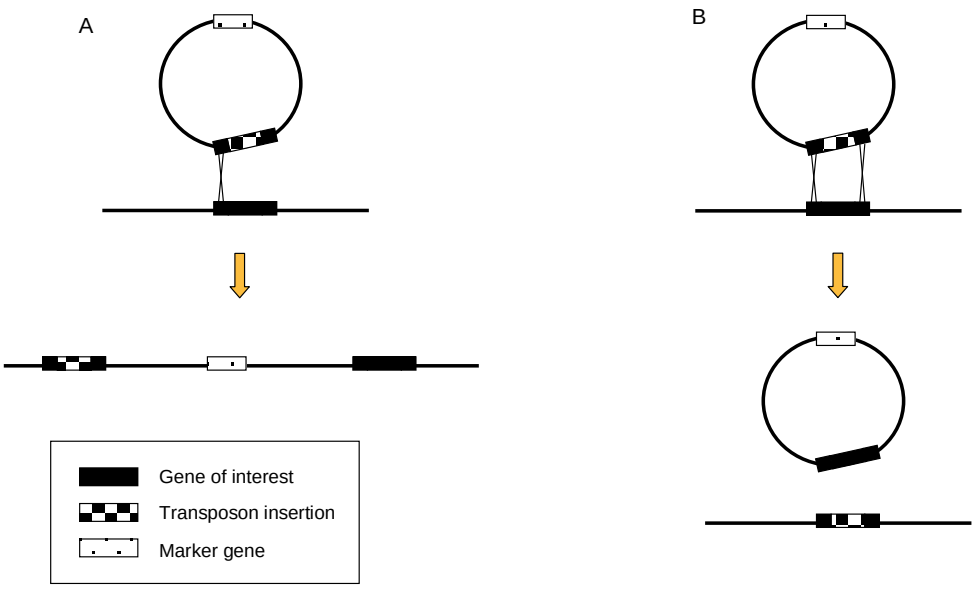

Figure 4.4: Allelic replacement by homologous recombination. A: Single crossover. Crossover at one homologous site results in integration of entire plasmid leaving one functional and one disrupted copy of the gene of interest. B: Double crossover. Crossover at two homologous sites flanking the gene of interest results in replacement of the native gene with a disrupted copy.

Double crossovers were selected by replica plating of exconjugants on kanamycin and apramycin, where growth on apramycin but not kanamycin indicates loss of the cosmid backbone due to double crossover (see Materials and Methods).

All mutant strains were confirmed by Southern blot analysis using whole-cosmid probes, described in detail for all strains below (Fig. 4.7) and in the Materials and Methods chapter.

Construction of a *mce* multiple knockout

In addition to the single-gene disruption mutants, a strain was created in which the first eight genes of the *mce* cluster (SCO2422 – SCO2415) were deleted.

A *mce* multiple knockout was constructed by modifying cosmid 8A2.1.F04 using partial digest with *Bam*HI (Fig. 4.5A) followed by self-ligation of the 50.136 kb fragment. The ligation product was used to transform *E. coli* host strain DH5α, and was then re-isolated from the host and screened for loss of the 6.539 kb fragment by digestion with *Bam*HI (Fig. 4.5B). The plasmids identified as knockouts using this screen were then confirmed by restriction digest with *Kpn*I.

Table 4.3: Band sizes (bp) for *Bam*HI and *Kpn*I digest of cosmids 8A2.1.F04 and pLCS001. Diagnostic bands are shown in bold.

	8A2.1.F04	pLCS001
*Bam*HI	34392	34392
	6539	
	2602	2602
	2520	2520
	1763	1763
	1540	
	787	
*Kpn*I	12477	12477
	10095	10095
	9973	
	7961	7961
	5600	**6707**
	2056	2056
	1444	1444
	537	537

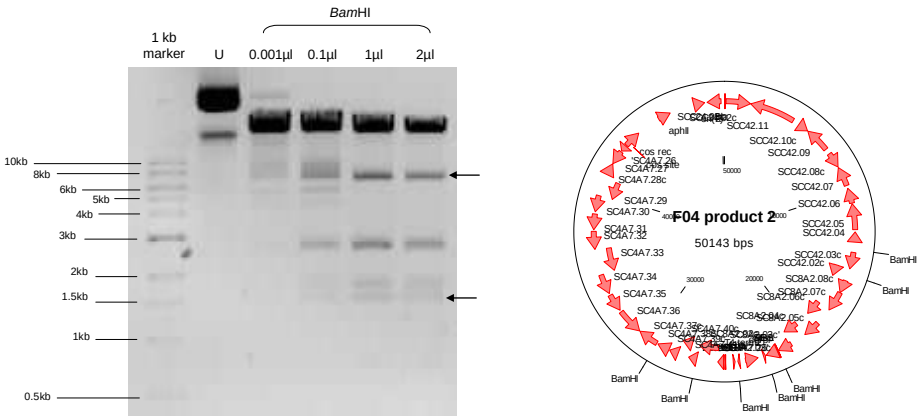

Figure 4.5A: Restriction digest and map of cosmid 8A2.1.F04, showing loss of *mce* cluster genes SCO2422-SCO2415. Gel: Partial digest of parental cosmid 8A2.1.F04 with *Bam*HI. 0.8% w/v agarose, 80V, ~10 µg DNA per lane. See Table 4.3 for exact band sizes.

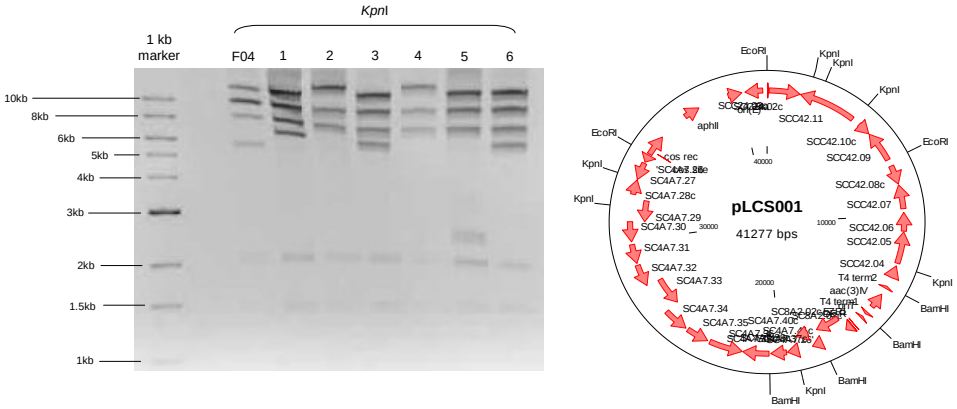

Figure 4.5B: Restriction digests and map of cosmid pLCS001, showing loss of *mce* cluster genes SCO2422-SCO2415. Gel: Partial digest of parental cosmid 8A2.1.F04 and religated cosmids (cosmid isolates from several different transformant colonies, numbered 1-6) with *Kpn*I. 0.8% w/v agarose, 80V, approximately 10 µg DNA per lane. See Table 4.3 for exact band sizes.

The resulting construct was then used to transform M145 by conjugation and primary exconjugants were selected as with the single gene disruption mutants. Due to the positions of the antibiotic markers and regions of homology, double crossovers must necessarily have lost the region of the genome between SCO2415 and SCO2422. This deletion was also confirmed by Southern blot analysis using a whole-cosmid probe (Fig. 4.7).

Construction of a *mce* complementation vector

To validate experimental results from the phenotypic analysis of the mutant strains and demonstrate linkage of the phenotype to the genetic lesion, a complementation vector was constructed. The vector was derived from cosmid 8A2.1.G07 (Fig. 4.6A) which contains a *Tn*5062 insertion in SCO2423, a gene adjacent to the *mce* cluster (see Table 4.1). This allowed selection for the cosmid using apramycin whilst not disrupting the *mce* operon itself. Another advantage of this approach is that transcription of the *mce* cluster remained under the control of its native promoter.

A partial digest approach was used to reduce the size of the cosmid 8A2.1.G07, removing much of the non-*mce* cluster DNA. These sections of the cosmid backbone and the genomic regions flanking the *mce* operon were excised by partial digest with *Kpn*I, *Eco*RI and subsequent self-ligation. Using this method the cosmid was reduced from 50.1 kb to 22.3 kb while maintaining origin of replication and antibiotic selection. This results in a 12.9 kb fragment of *S. coelicolor* genomic DNA containing the first 11 genes of the *mce* cluster.

The cosmid was then co-electrotransformed into hyper-recombinant *E. coli* strain BW25113 containing the λRed recombination plasmid (pIJ790; Gust et al., 2002) with a 5247 bp *Ssp*I fragment from plasmid pIJ10702 (Fig. 4.6A) which has an approximately 450 bp region of homology to the Supercos backbone at each end. This homology facilitates recombination and exchange of the Supercos cosmid backbone with a backbone containing an origin of transfer, ϕC31 integrase, and an

attP site from bacteriophage ϕC31, enabling ectopic integration in to the ϕC31 *attB* site in the *S. coelicolor* genome (Foulston and Bibb).

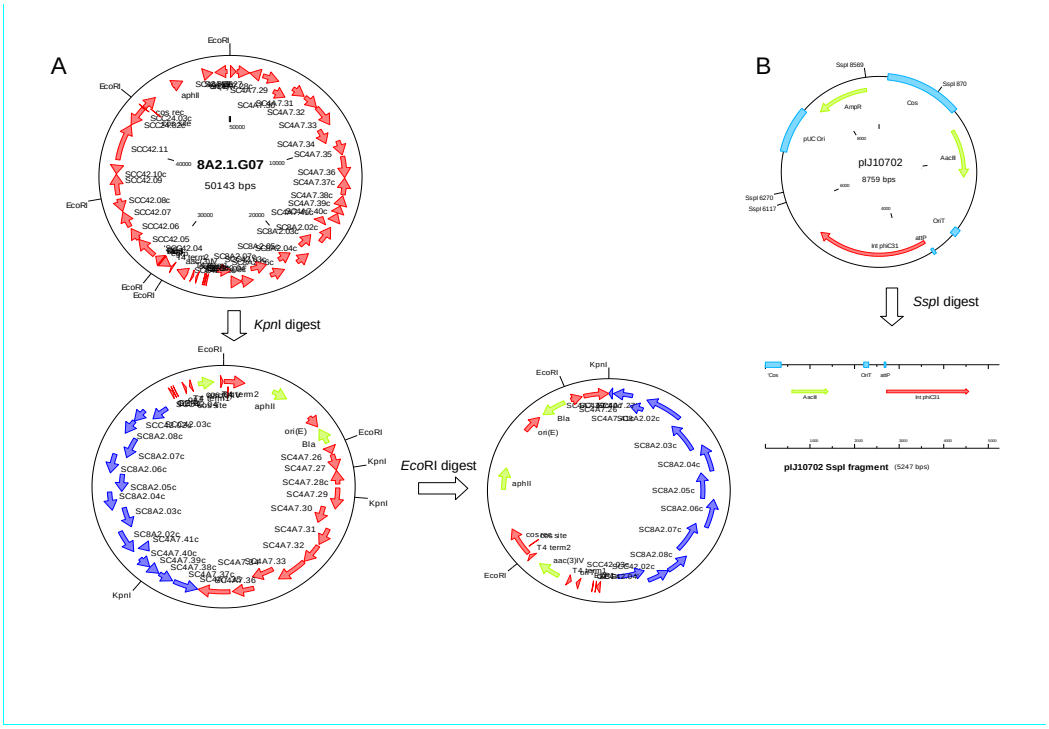

Figure 4.6A: Complementation vector cloning strategy. A: Parental cosmid 8A2.1.G07, and intermediate cosmids pLCS002 and pLCS003 which have lost sections of the supercos backbone and genomic DNA insert. B: 5.2 kb *Ssp*I fragment of plasmid pIJ10702 containing regions of homology to supercos, as well as *aac*(3)IV and ΦC31 integrase.

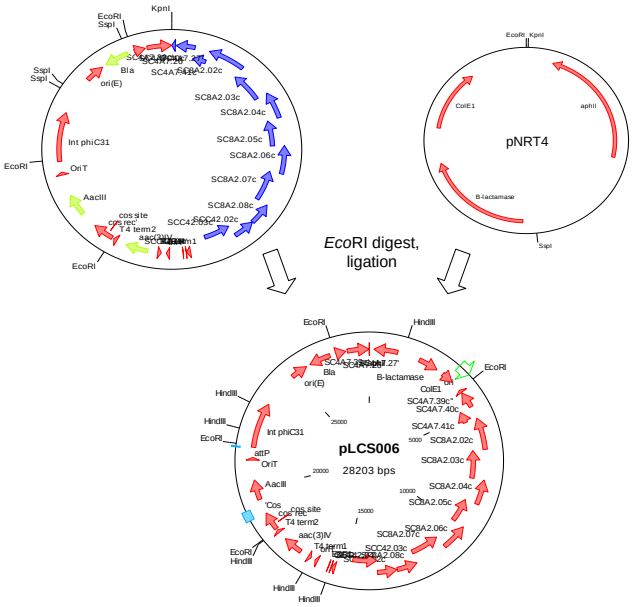

Figure 4.6B: pLCS004 in which the supercos backbone has been exchanged for the *Ssp*I fragment of pIJ10702, and plasmid pNRT4. Also shown is cosmid pLCS006 in which pNRT4 has been ligated into pLCS004 to create the final complementation vector.

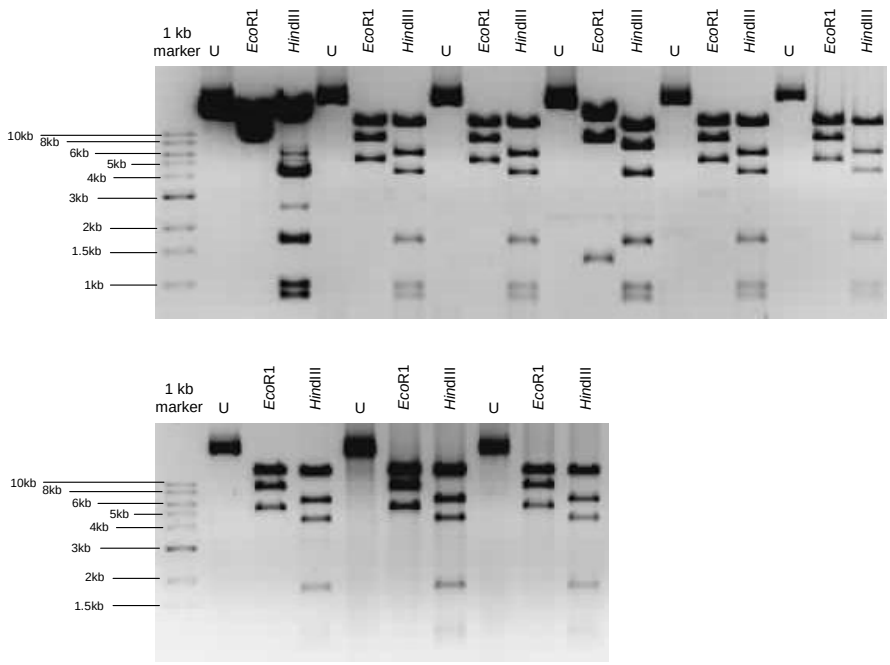

Figure 4.6C: Restriction digest confirming cosmid pLCS006 with enzymes *Eco*R1, *Hin*DIII. DNA isolates from 9 separate colonies are shown. U=uncut cosmid DNA. See Table 4.4 for exact band sizes. Gel: 0.8% agarose, 80 V, approximately 10 µg DNA per lane.

Recombinant cosmids were selected by growth on apramycin and ampicillin. Finally, plasmid pNTR4 (Herron, P. personal communication) in its entirety was ligated into the cosmid in order to restore kanamycin resistance and allow selection for the complementation vector in mutant strains already resistant to apramycin.

Table 4.4: Band sizes (bp) for *Eco*RI and *Hin*dIII digest of plasmid pLCS006

	pLCS006
*Eco*RI	14237 8669 5297
*Hin*dIII	14278 6250 4144 1721 969 841

Applications of the complementation vector

The complementation vector was used to complement the multiple knockout strain, as well as complemented single gene disruption mutants. It is possible that gene dosage effects might result from the introduction of the complete *mce* operon to complement a single-gene disruption, but this may be mitigated by polar effects of the disruption.

The complementation vector was also introduced into the wild-type strain in order to produce a strain (SLC301) containing two undisrupted copies of the entire *mce* operon.

Analysis of genomic mutations by Southern blot

The CloneManager programme was used to produce virtual digests of all cosmids (Table 4.5). This was to allow selection of appropriate restriction enzymes for digestion of genomic DNA prior to Southern blot analysis, and also to predict the

band sizes that would be detected in wild-type and mutant strains. On this basis, *Sac*I was selected to digest the sample DNA.

A whole cosmid probe was constructed for each transposon mutant and the *mce* cluster knockout, using digoxigenin (DIG) labelling of the *Tn*5062-containing cosmid that was used to create the strain. This meant that the specific site of transposon insertion could be confirmed (as opposed to just the presence or absence of the transposon), and accordingly the mutants could be differentiated by the band pattern observed on each blot.

All mutants conformed to the expected band pattern, confirming the modifications made to the genomic DNA sequence. Bands highlighted in Fig. 4.7A-D are diagnostic of transposon insertion in the expected region of the genome. In the case of the *mce* cluster knockout strain, the highlighted band is diagnostic of a deletion in the expected region.

Table 4.5: Band sizes (bp) for *Sac*I digest of wild-type and *mce* mutant genomic DNA followed by Southern hybridisation of labelled probe

Diagnostic bands are shown in bold. There is also a 12069 bp band which appears in the cosmid-only control and corresponds to the supercos backbone. This band will not be present in the genomic DNA sample.

	M145	B11	E04	D12	C07	F02	F04	pLCS001
*Sac*I fragment sizes (bp)	12434		12394	**12949**	12434	12434	12434	
		10792						
	10778	10778	10778	10778	10778	10778	10778	10778
								9722
	5216					**5111**		
	4508	4508	4508	4508			4508	
		4348			**4211**			
	4098	4098	4098	4098	4098	4098	4098	4098
			2739	**2175**	**2987**	**2087**	**2179**	**2179**
							1646	
	1217	1217	1217	1217	1217	1217	1217	1217
	1135	1135	1135	1135	1135	1135		
		752	**752**	**752**	**752**	**752**	**752**	**752**
	462	462	462	462	462	462	462	462

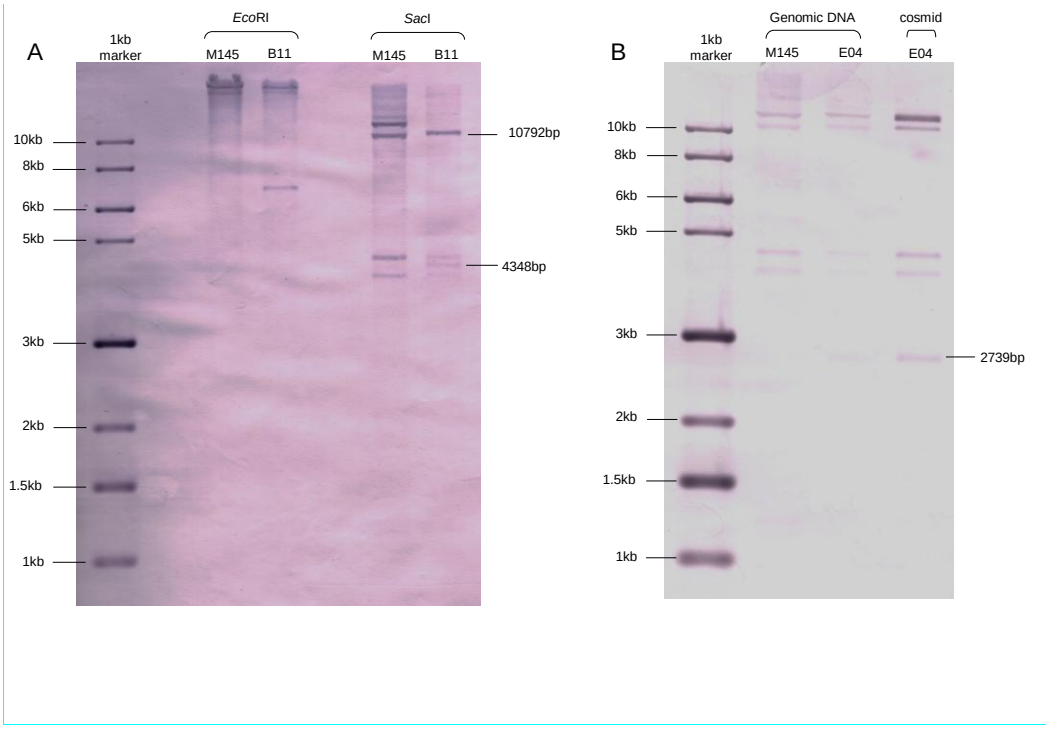

Fig 4.7A: Southern blot analysis of *Tn*5062 insertion mutants. A: strain SCL101 (insertion in SCO2422) and wild-type genomic DNA digested with *Eco*RI, *Sac*I and probed with cosmid 8A2.1.B11. It was determined that *Sac*I provides the best digest and thus *Eco*RI is not used in subsequent blots. B: strain SLC102 (insertion in SCO2421) and wild-type genomic DNA, and positive control cosmid 8A2.2.E04, digested with *Sac*I and probed with cosmid 8A2.2.E04. Diagnostic bands are highlighted (see Table 4.5 for exact band sizes).

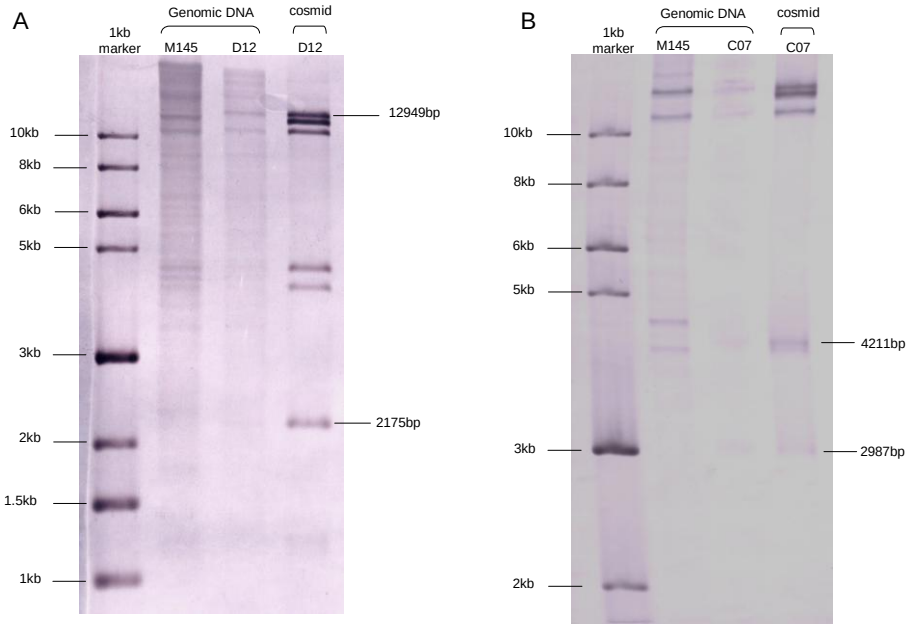

Figure 4.7B: Southern blot analysis of *Tn*5062 insertion mutants. A: strain SLC103 (insertion in SCO2420) and wild-type genomic DNA, and positive control cosmid 8A2.2.D12, digested with *Sac*I and probed with cosmid 8A2.2.D12. B: strain SLC104 (insertion in SCO2418) and wild-type genomic DNA, and positive control cosmid 8A2.1.C07, digested with *Sac*I and probed with cosmid 8A2.1.C07. Diagnostic bands are highlighted (see Table 4.5 for exact band sizes).

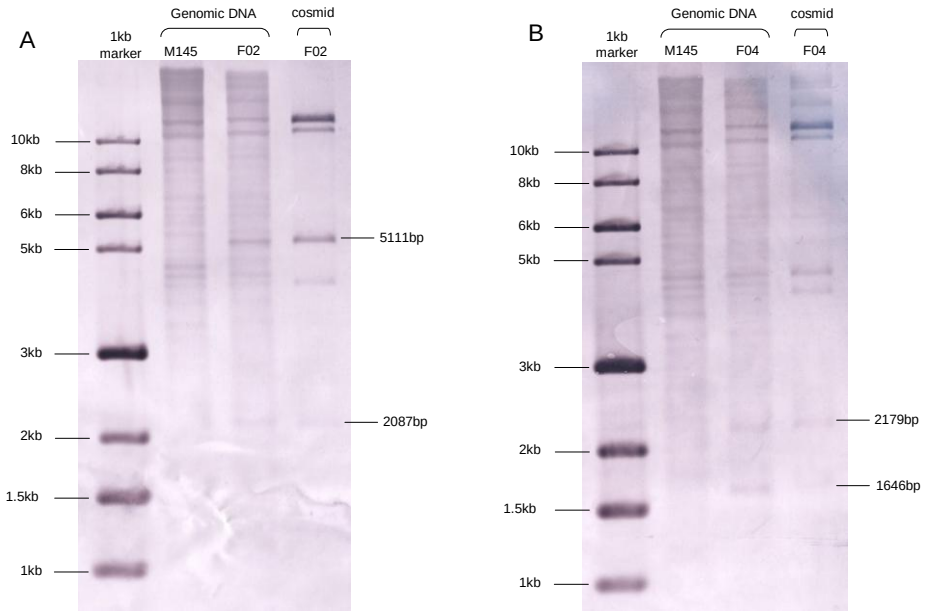

Figure 4.7C: Southern blot analysis of *Tn*5062 insertion mutants. A: strain SLC105 (insertion in SCO2416) and wild-type genomic DNA, and positive control cosmid 8A2.2.F02, digested with *Sac*I and probed with cosmid 8A2.2.F02. B: strain SLC106 (insertion in SCO2415) and wild-type genomic DNA, and positive control cosmid 8A2.1.F04, digested with *Sac*I and probed with cosmid 8A2.1.F04. Diagnostic bands are highlighted (see Table 4.5 for exact band sizes).

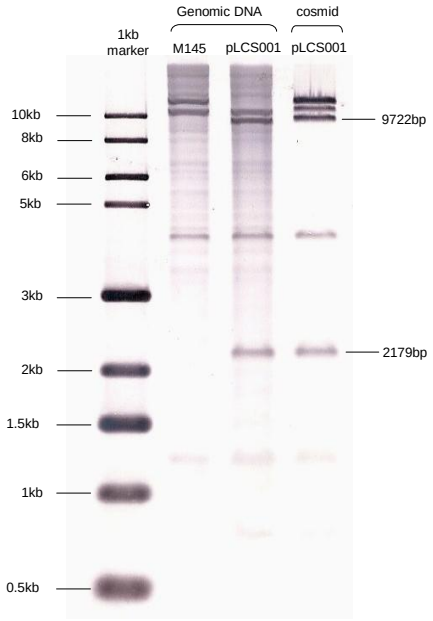

Figure 4.7D: Southern blot analysis of *Tn*5062 insertion mutants. Strain SLC201 (*mce* multiple knockout) and wild-type genomic DNA, and positive control cosmid pLCS001 digested with *Sac*I and probed with cosmid pLCS001. Diagnostic bands are highlighted (see Table 4.5 for exact band sizes).

Screening for mutant phenotypes

The *mce* operon is not essential in *Streptomyces coelicolor*

Essential genes typically yield an extremely low ratio of double crossovers to single crossovers when disruption by allelic replacement is carried out (1:1000 or fewer – double crossovers in this situation are usually the result of a compensatory mutation elsewhere in the chromosome (Kieser *et al.*, 2000)). The frequency of double crossovers among exconjugants in the case of the core *mce* genes was approximately one in ten, indicating that the *mce* genes are not essential in *S. coelicolor*. This is consistent with observations made in other actinomycetes (Casali and Riley, 2007).

Having established that the *S. coelicolor mce* operon is non-essential and confirmed the mutants by Southern blotting, the mutant strains were screened under a range of conditions to establish the phenotype associated with mutation of the *mce* gene cluster.

Phenotypic screening on carbon sources

The *mce* cluster has been shown to encode a cholesterol uptake importer in *M. tuberculosis* and *Rhodococcus* (Mohn *et al.*, 2008). Given that *mce* homologues in related actinomycetes encode carbon source uptake systems, initial screening for mutant phenotypes in *S. coelicolor* was performed by screening the mutant strains on a number of different carbon sources in order to assay for defects in growth, antibiotic production and development.

Screening was performed on minimal medium agar (Kieser et al., 2000), using ammonium sulphate as the nitrogen source to avoid introducing additional carbon sources to the medium (Fig. 4.8A-D). Carbon source screening presents a challenge when working with *S. coelicolor* as the wild-type strain is able to metabolise agar due to the presence of the agarase gene *dagA* (Buttner *et al.*, 1987). The use of liquid culture for screening was not practical in this case due to the insoluble nature of

many of the carbon sources used in the study, and also the inability of *S. coelicolor* to sporulate in liquid culture.

In an effort to overcome this problem the *mce* multiple knockout was also constructed in J807, a *dag*$^{-}$ *S. coelicolor* strain which is incapable of metabolising agar (Buttner *et al.*, 1987). However, the phenotype observed in this background did not differ from that observed in an M145 background (data not shown). It is possible that this may be as a result of agar hydrolysis which takes place during autoclaving and its subsequent use by the J807 strain (Buttner, M. personal communication).

Table 4.6: Carbon sources used in screening all transposon insertion mutants, *mce* multiple knockout and complemented strain.

Carbon source	**Incubation temperature**	**Mutant phenotype**
EtOH 1.4% v/v	30ºC	Not different from wild type
Glycerol 0.5% w/v	30ºC	Not different from wild type
Pyruvic acid 1mM	30ºC	Not different from wild type
Oleic acid 1mM	30ºC	Not different from wild type
Palmitic acid 1mM	30ºC	Not different from wild type
Stearic acid 1mM	30ºC	Not different from wild type
Galactose 0.5% w/v	30ºC	Not different from wild type
Arabinose 0.5% w/v	30ºC	Not different from wild type
Lactose 0.5% w/v	30ºC	Not different from wild type
Sucrose 0.5% w/v	30ºC	Not different from wild type
None	30ºC	Not different from wild type
None	37ºC	Not different from wild type
None	40ºC	Not different from wild type
Glucose 0.5% w/v	30ºC	Not different from wild type
Glucose 0.5% w/v	37ºC	Not different from wild type
Glucose 0.5% w/v	40ºC	Not different from wild type
Glucose 0.5% w/v (+ NaCl 1M)	30ºC	Not different from wild type
Glucose 0.5% w/v (+ NaCl 1M)	37ºC	Not different from wild type
Glucose 0.5% w/v (+ NaCl 1M)	40ºC	Not different from wild type
Sorbitol 0.5% w/v	30ºC	Not different from wild type
Sorbitol 0.5% w/v	37ºC	Not different from wild type
Sorbitol 0.5% w/v	40ºC	Not different from wild type
Cholic acid 1mM + EtOH 1.4% v/v	30ºC	Not different from wild type
Cholic acid 1mM + EtOH 1.4% v/v	37ºC	Not different from wild type
Cholic acid 1mM + EtOH 1.4% v/v	40ºC	Not different from wild type
Mannitol 0.5% w/v	30ºC	Mutants showed increased growth compared to w/t after 2 days of incubation.
Mannitol 0.5% w/v	37ºC	Not different from wild type
Mannitol 0.5% w/v	40ºC	Not different from wild type
Tween 20 4% w/v	30ºC	Not different from wild type
Tween 20 4% w/v	37ºC	Not different from wild type
Tween 20 4% w/v	40ºC	Not different from wild type
Tween 20 4% + mannitol 0.05% w/v	30ºC	Not different from wild type
Tween 20 4% + mannitol 0.05% w/v	37ºC	Not different from wild type
Tween 20 4% + mannitol 0.05% w/v	40ºC	Not different from wild type
Tween 20 4% + mannitol 0.05% w/v + cholesterol 0.1% w/v	30ºC	Mutants appeared to produce more actinorhodin than w/t after 7 days of incubation.
Tween 20 4% w/v + mannitol 0.05% w/v + cholesterol 0.1% w/v	37ºC	Not different from wild type
Tween 20 4% w/v + mannitol 0.05%	40ºC	Not different from wild type

w/v + cholesterol 0.1% w/v		
Tween 20 4% w/v + cholesterol 0.1% w/v	30ºC	Not different from wild type
Tween 20 4% w/v + cholesterol 0.1% w/v	37ºC	Not different from wild type
Tween 20 4% w/v + cholesterol 0.1% w/v	40ºC	Not different from wild type
Betaine	30ºC	Not different from wild type
V8	30ºC	Not different from wild type
β-sitosterol 0.1% w/v	30ºC	Not different from wild type

The carbon sources used for screening fall into a number of categories. The initial screen consisted of sugars which are commonly used in bacterial culture: the hexose sugars glucose and galactose, the pentose sugar arabinose and disaccharides lactose and sucrose. Also included in the initial screen was the polyol mannitol, as it is commonly used as a carbon source that permits abundant sporulation in *S. coelicolor* (Kieser *et al.*, 2000). These sugars were chosen to provide a wide initial screen covering a number of different chemical properties. Glucose, which did not result in a discernibly different phenotype from the wild-type, was used as a control in subsequent screens (Fig. 4.8A-D). The complemented strain SLC202 was screened under all conditions (data not shown) and displayed a phenotype identical to that of the wild-type.

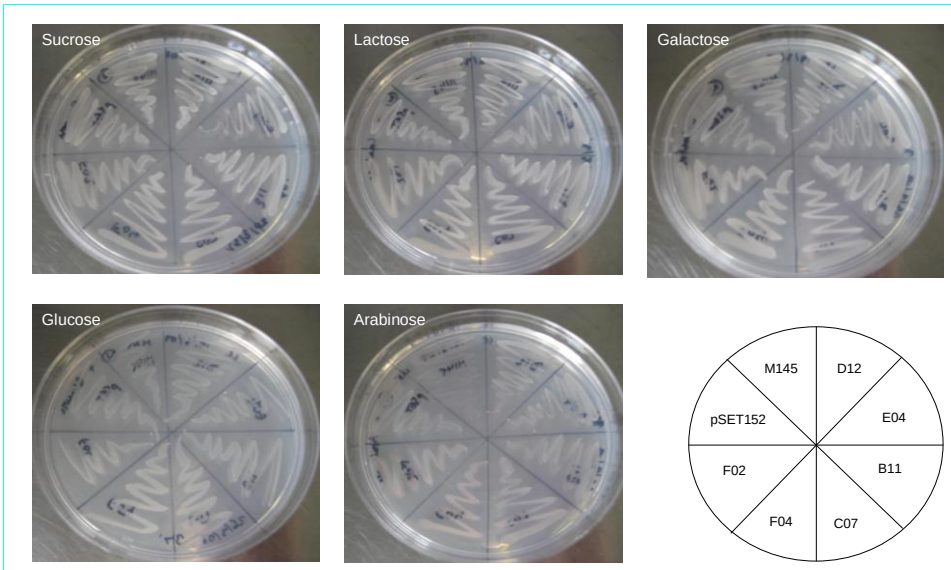

Figure 4.8A: Carbon source screening of *mce* mutants. Minimal medium agar using ammonium sulphate as the nitrogen source; carbon source as specified above. Plates shown after 2 days incubation. Map shows order of strains on plates (clockwise from top left: M145, wild-type; 8A2.2.D12, insertion in SCO2420; 8A2.2.E04, insertion in SCO2421; 8A2.1.B11, insertion in SCO2422; 8A2.1.F04, insertion in SCO2415; 8A2.2.F02, insertion in SCO2416; pSET152, plasmid control for apramycin resistance).

Growth of the mutant strains and the wild-type controls was the same on all sugars with the exception of mannitol. When grown on mannitol, the *mce* mutant strains showed more rapid growth than the controls (Fig. 4.8B). This was most obvious after two days of incubation, with denser colonies being observed. Apart from the enhanced growth, there were no other apparent differences between the strains when grown on mannitol.

This phenotype differed from what was expected; generally a gene disruption would be expected to cause loss of function rather than gain. In order to investigate this phenotype further the mutant strains were screened on media containing the polyols glycerol and sorbitol, due to their chemical similarities to mannitol. However, the phenotype was not reproduced on these carbon sources.

Other carbon sources used in the screen were selected on the basis of their chemical similarity to cholesterol. This group includes cholesterol itself, β-sitosterol (a phytosterol) and cholic acid. Also screened was pyruvic acid, due to its role in many metabolic pathways, and oleic, palmitic and stearic acids which are common fatty acids in plants and thus may be available to *Streptomyces* in the soil (Dinel *et al.*, 2001) (Fig. 4.8C).

Various solvents (tween-20, ethyl acetate, ethanol, brij-58, triton X-100) were used to overcome the difficulty of dissolving cholesterol and other immiscible compounds in an aqueous medium, and controls were also performed using these solvents in the absence of the solute. This was important because *S. coelicolor* is able to use some solvents, for example tween-20, as carbon sources via activation of the glyoxylate shunt (Hodgson, 2000; Kieser *et al.*, 2000).

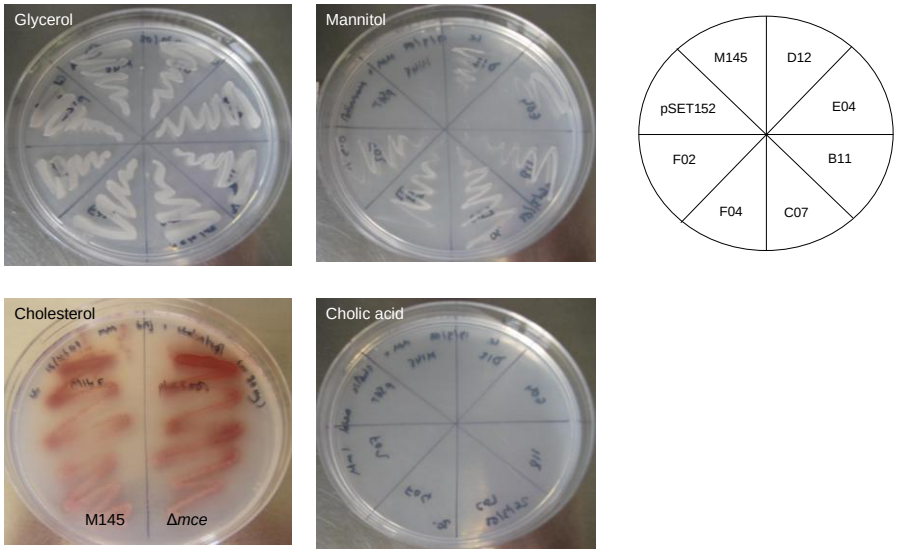

Figure 4.8B: Carbon source screening of *mce* mutants. Minimal medium agar using ammonium sulphate as the nitrogen source; carbon source as specified above. Plates shown after 2 days incubation. Map shows order of strains on plates. Cholesterol plate (bottom left) shows only M145 wild-type (left) and *mce* multiple knockout strain (right).

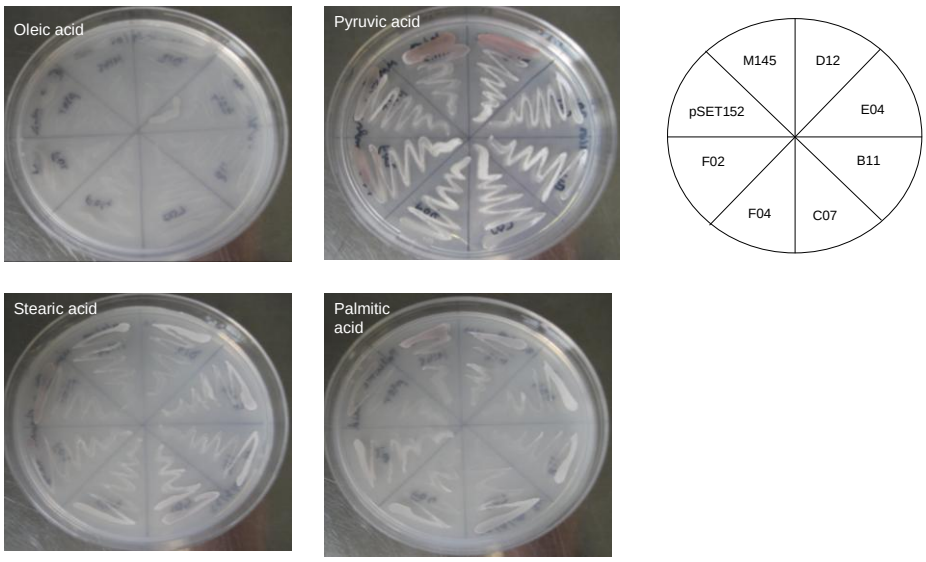

Figure 4.8C: Carbon source screening of *mce* mutants. Minimal medium agar using ammonium sulphate as the nitrogen source; carbon source as specified above. Plates shown after 2 days incubation. Map shows order of strains on plates.

Interestingly, none of the carbon sources in this group produced a visible difference in growth, antibiotic production or development. The exception to this is cholesterol which appeared to induce slight overproduction of actinorhodin in the mutant strains. It is difficult to ascribe changes in antibiotic production to a specific mechanism of the mutation, but it may be a result of additional supply of acetyl-CoA units to primary metabolism which can be incorporated in to polyketide antibiotics (Hodgson, 2000).

The mutants were also screened under stress conditions such as increased incubation temperature and osmotic stress (created by varying NaCl concentrations in the plates). This was conducted in order to investigate possible changes in membrane structure as the result of the *mce* mutations, which might result in a phenotype under these conditions. Glucose was used as a carbon source for these experiments.

In addition to carbon source screening on minimal medium, several specialised media were also used (Fig. 4.8D). Examples of these are V8 medium, used to examine the effects of vegetable-derived nutrients (e.g. phytosterols), and R2YE which is commonly used in phenotypic screening of *Streptomyces* strains. The strains were also screened for their tolerance to the antibiotics chloramphenicol and kanamycin, representing the N-dichloroacyl phenylpropanoid and aminoglycoside classes of antibiotic. Antibiotic screening was limited in scope due to the natural resistance of *S. coelicolor* to many antibiotics, and the additional resistance cassettes present in the mutant strains.

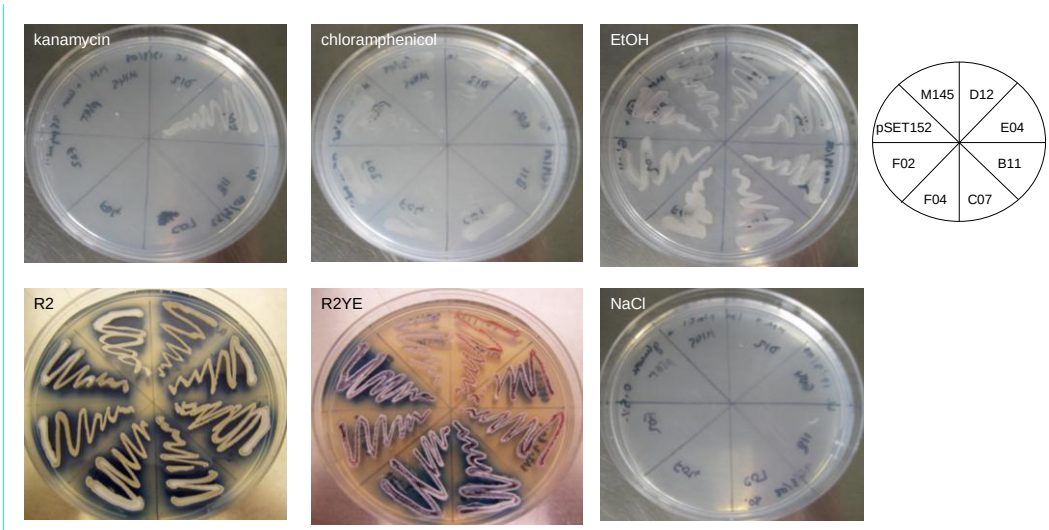

Figure 4.8D: Carbon source screening of *mce* mutants. Minimal medium agar using ammonium sulphate as the nitrogen source; carbon source as specified above. Plates shown after 2 days incubation. Map shows order of strains on plates.

Even these extreme changes in conditions did not induce a noticeable phenotype in the mutant strains when compared to wild-type *S. coelicolor*. This is perhaps not surprising; previous studies of *M. tuberculosis mce* mutants screened for phenotypes solely through virulence assays and did not indicate any developmental or phenotypic changes. Additionally, the creation of viable *mce* mutants had already demonstrated in this study that the *mce* cluster is not essential for growth, survival and development in *S. coelicolor*.

Dry weight growth curves (Fig. 4.9) showing growth of M145 and the transposon insertion mutants in liquid culture show no significant difference in growth rate between the strains (calculated from gradient of slope in exponential phase when plotted logarithmically; equal to 38.3mg/l/h). This indicates that any phenotypes observed in mutant strains are due to primary effects of the *mce* mutations and not to secondary effects resulting from changes in growth rate.

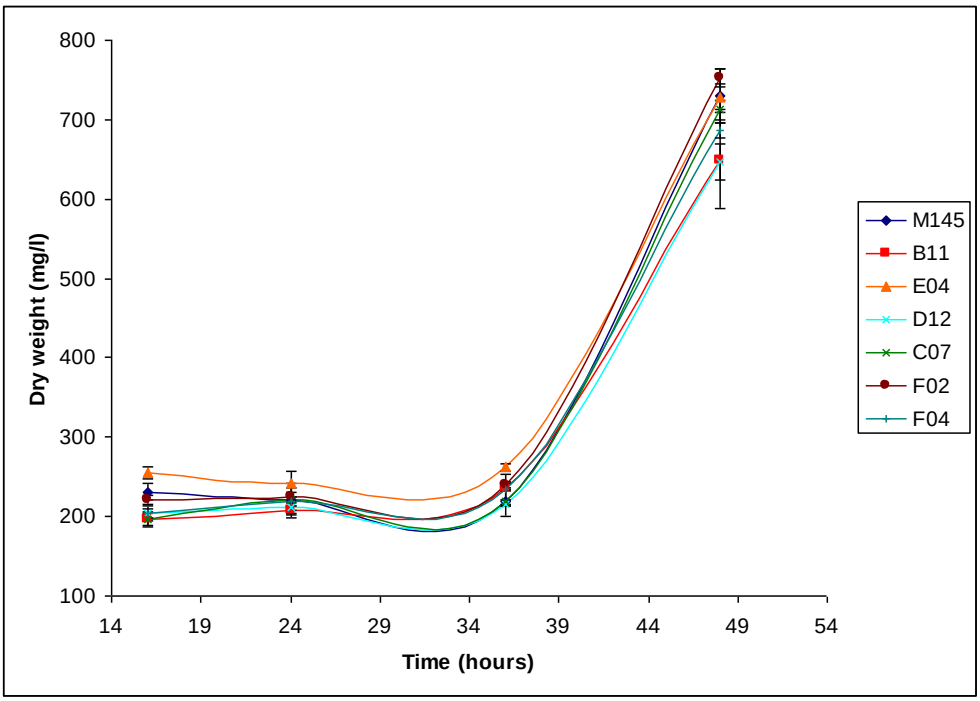

Figure 4.9: Dry weight growth curves of wild-type and *mce* transposon insertion mutants grown in liquid YEME at 30ºC. Time-points at 16, 24, 36 and 48 hours. Data points are mean of 3 measurements, error bars are standard deviation. Mutant strains show no difference in growth rate relative to wild-type.

Morphological screening of mutant strains

Scanning electron microscopy

Selected *mce* mutant strains were imaged using Cryo-scanning Electron Microscopy (SEM) in order to examine their morphology in detail. Strains were grown on solid MS medium for 5 days, after which time blocks of agar containing colonies of *S. coelicolor* were removed and frozen in liquid nitrogen before being transferred to the electron microscope, sputter-coated in gold and examined by Cryo-SEM.

The four strains examined by SEM were SCO2422::*Tn*5062, SCO2418::*Tn*5062 and SCO2415::*Tn*5062, which contained transposon insertions in the putative ATPase-encoding gene at the start of the operon, *mceB* which is the first *mce* gene to contain a transposon insertion, and *mceE* which contains a putative lipobox motif; and the *mce* cluster knockout which spans all of these genes. These strains were chosen to represent the entire *mce* operon, and also for consistency with later experiments.

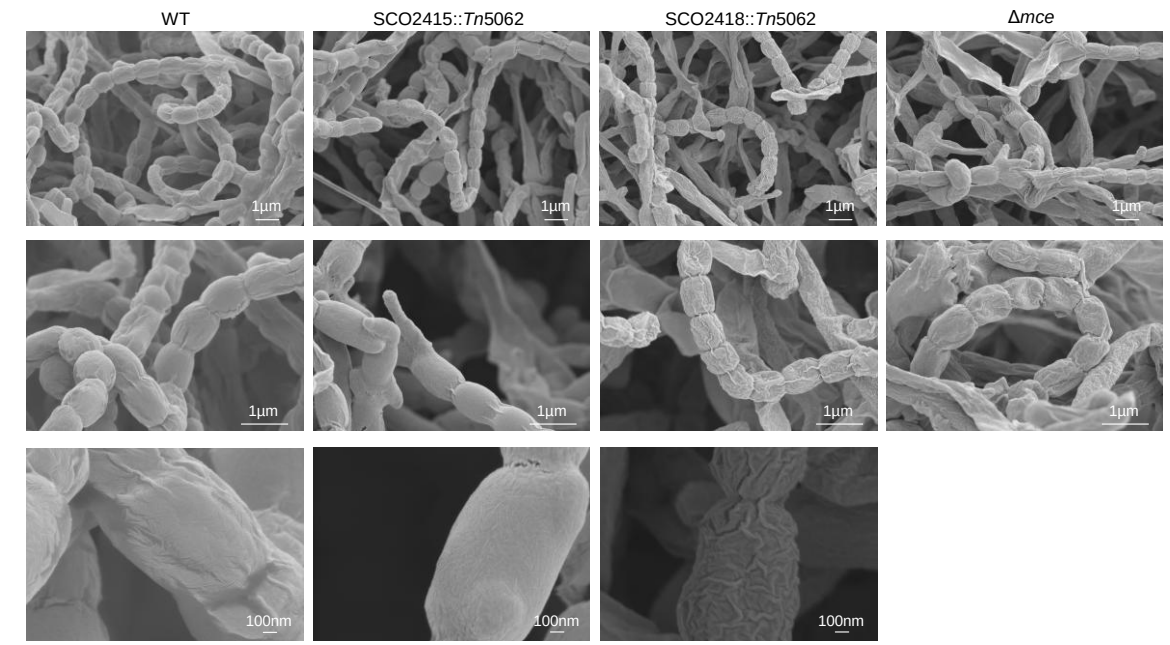

Figure 10: Cryo-electron microscopy of wild-type and *mce* mutants. Aerial hyphae at x10 000 magnification (top row), x20 000 magnification (middle row) and x60 000 magnification (bottom row). The wild-type strain (far left) shows smooth elliptical spores, with the rodlet layer visible on the spore surface at the highest magnification. SCO2415::*Tn*5062 (left) shows no apparent alteration to spore coat morphology, but aberrant growth is visible at x20 000 magnification. At the highest magnification a bulge is visible in the spore surface, caused by germination of the spore. SCO2418::*Tn*5062 (right) shows truncation of spores and wrinkling of the spore coat. Δ*mce* (far right) shows both aberrant growth resulting from premature germination, and wrinkling of the spore coat.

Wild-type *S. coelicolor* (Fig. 4.10) typically displays curled aerial hyphae containing smooth elliptical spores. The spore surface displays a regular array of rodlets (Claessen *et al.*, 2004) which can be seen at x60,000 magnification. There is no evidence of germination of spores on the spore chains in M145.

The electron micrographs of the mutant strains show unusual spore chain morphology. In the SCO2418::*Tn*5062 strain the spores appear to be shorter and squarer than the wild-type, and also display a marked wrinkling of the spore coat. Similar phenotypes have been observed in *S. coelicolor* developmental mutants such as *mreBCD* and *mbl* (Mazza *et al.*, 2006).

In the SCO2415::*Tn*5062 disruption the spore coat appears normal, but there are unusual bulges in the spores which appear to be premature germination while spores are still attached to the spore chains. This premature germination phenotype is extremely unusual, although it has also been seen in a Δ*nepA* strain. NepA is a structural cell wall protein that is thought to play a role in maintenance of spore dormancy (de Jong *et al.*, 2009).

The observation of rapid germination in the SCO2415::*Tn*5062 strains but not in the SCO2418::*Tn*5062 strain suggests that the effects of mutations in the *mce* operon are not polar, given that SCO2415 is downstream of SCO2418. However, given the extremely unusual morphology of the SCO2418::*Tn*5062 spore coat it is possible that this phenotype is masked by the coat morphology.

The *mce* cluster knockout strain displays both the premature germination and the wrinkled spore coat phenotypes observed in the individual gene disruption mutants. This is as expected since the cluster knockout spans the genes disrupted by transposon insertions.

The SCO2422::*Tn*5062 mutant (not shown in Fig. 4.10) also showed some wrinkling of the spore coat in comparison to the wild-type, but to a lesser degree than that seen in other mutant strains.

Spores of each of the four mutant strains and the wild-type were measured (35 spores per strain), and the results plotted as histograms (Fig. 4.11). Both the *mce* multiple knockout and the *mceB*::*tn*5062 strain show a decrease in spore size relative to the wild-type. The 2422::*Tn*5062 and *mceE*::*Tn*5062 strains show no significant change in spore size relative to the wild-type. It appears that the reduction in spore size may be correlated with the severity of the wrinkling of the spore coat, possibly reflecting the role of cell envelope constituents in the positioning of division septa.

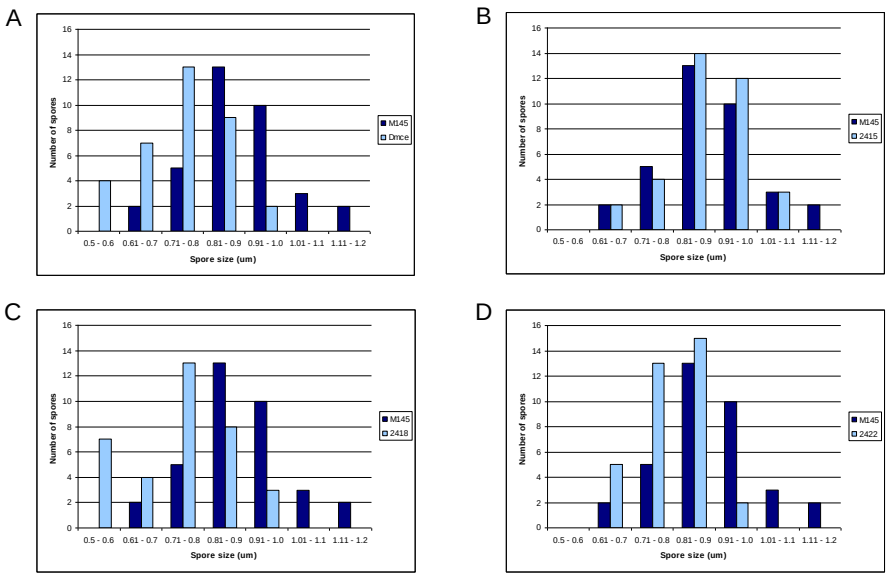

Figure 4.11: Comparison of spore sizes between wild-type (M145) and *mce* mutant strains. A: M145 (dark blue) and Δ*mce* (Dmce; light blue). B: M145 (dark blue) and *mceE*::*Tn*5062 (2415; light blue). C: M145 (dark blue) and *mceB*::*Tn*5062 (2418; light blue. D: M145 (dark blue) and SCO2422::*Tn*5062 (2422; light blue). 35 spores from each strain were measured. Median and mode spore sizes show significant difference between M145 and Δ*mce* and between M145 and *mceB*::*Tn*5062.

Germination assay

Because of the premature spore germination, whilst still attached to the spore chains, of the *mce* mutants observed using SEM, a germination assay was conducted to attempt to quantify the phenotype and any differences in germination. Spores were incubated in GAE liquid medium and germination was assayed using absorbance at 600 nm (Suarez *et al.*, 1980). As *Streptomyces* spores germinate they undergo changes such as swelling, germ tube emergence and a change from phase light to phase dark which can be measured specrophotometrically.

As shown in Fig. 4.12, germination rate of all strains (Δ*mce*, Δ*mce* pLCS006, SLC301) in liquid was identical to that of wild-type *S. coelicolor*. This may indicate that the presence of germ tubes in spores still attached to spore chains may occur in the presence of specific nutrients e.g. mannitol, or alternatively it may be that the sensitivity of the assay is not sufficient to pick up a subtle change in germination rate.

FTIR

FTIR (Fourier transform infra-red spectroscopy) was performed on the wild-type and Δ*mce* strains to look for any differences in the spectra that could be attributable to the loss of the *mce* cluster; for instance changes in cell envelope composition. No difference was observed (data not shown), however it is possible that differences in the spectra may have been masked by the presence of a large water peak.

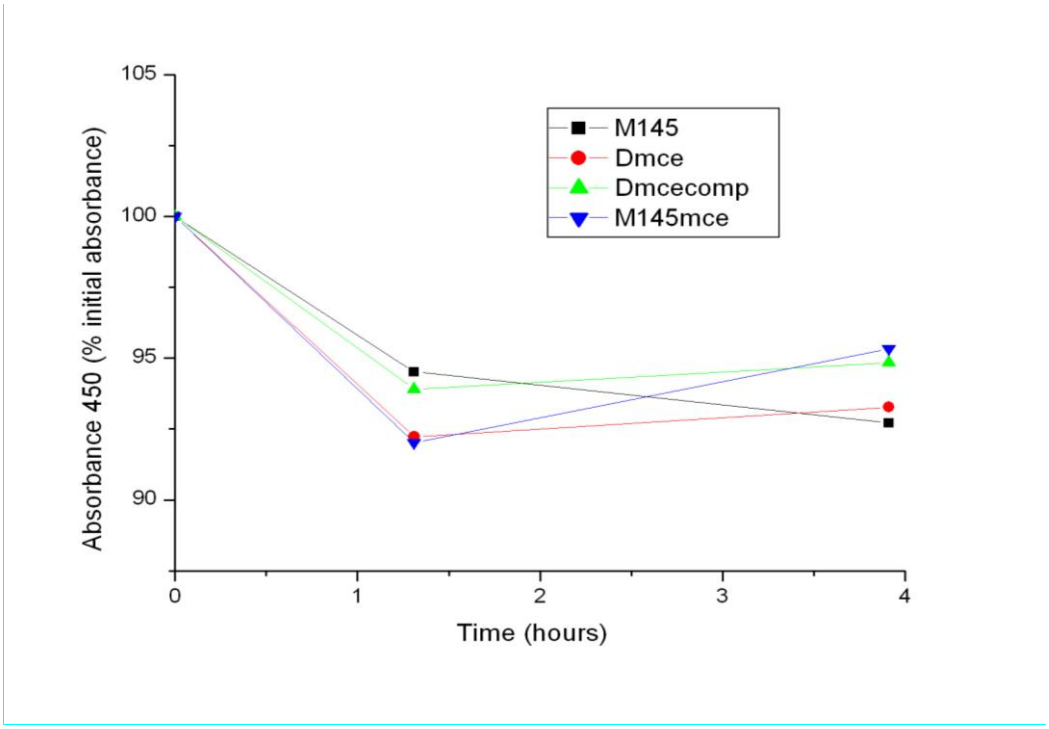

Figure 4.12: Spore germination assay showing absorbance at 450 nm (as a percentage of the initial absorbance) over time for the wild-type strain (M145), Δ*mce* (Dmce), complemented Δ*mce* (Dmcecomp) and M145 containing an extra copy of the *mce* operon (M145mce). No difference in germination rate was observed between mutant and wild-type strains.

Spore sensitivity assay

The unusual morphology of the *mce* mutant spore chains suggested that the spores may also be altered in their ability to withstand chemical or enzymatic stresses. This was tested by conducting spore sensitivity assays in which test compounds at various dilutions were spotted on to a lawn of freshly plated spores.

Compounds selected for this assay were SDS, lysozyme and DMSO. SDS is an anionic surfactant that is commonly used to disrupt bacterial cells. Lysozyme is a peptidoglycan hydrolase and disrupts the cell wall, thus cells with thinner walls or those with altered composition may respond differently to lysozyme treatment. Lysozyme is also a constituent of the amoebal lysosome (Khan, 2009) and is thus biologically relevant to the role of the Mce proteins. DMSO is involved in altering membrane fluidity and may reveal phenotypes in which the cell membrane composition is altered (Gurtovenko and Anwar, 2007).

No difference could be observed between the strains when treated with DMSO; however the *mce* multiple knockout showed a surprising increase in resistance to both SDS and lysozyme in comparison to wild-type *S. coelicolor* and to the complemented knockout strain (Fig. 4.13A-B). These increased resistances are likely to be the result of the effect of the reagents upon the spores prior to germination, however it is possible that they could affect freshly emerged germ tubes.

A

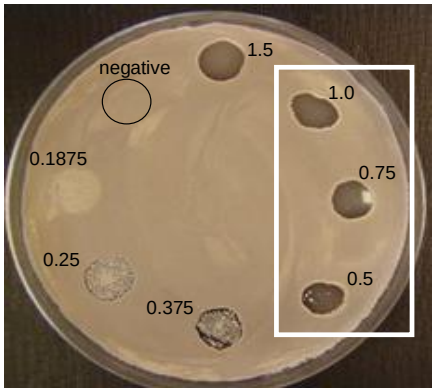

B

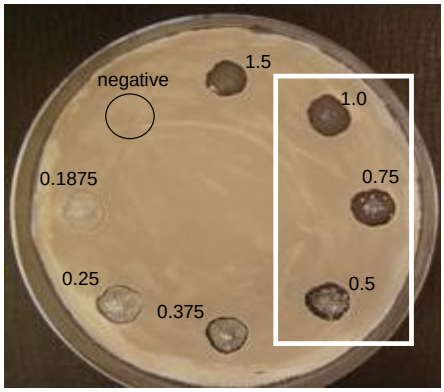

Figure 4.13A: Lysozyme sensitivity assay. Lysozyme concentration in mg.ml^{-1}, approximately 6.25x10^{7} viable spores per plate. A: M145 (wild-type) spores. There is little or no growth between 1.0 and 0.5 mg.ml^{-1} lysozyme. B: Δ*mce*. There is growth at 1.0, 0.75 and 0.5 mg.ml^{-1} lysozyme, indicating an increased resistance in this strain.

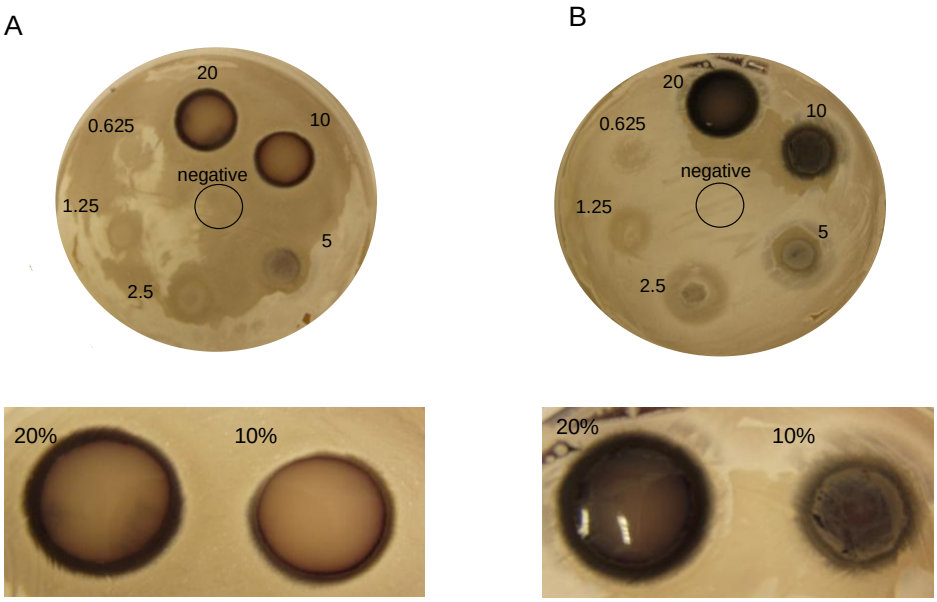

Figure 4.13B: SDS sensitivity assay. SDS concentration in %, approximately $6.25x10^7$ viable spores per plate. Images below are enlargements of the 20% and 10% SDS spots. A: M145 (wild-type) spores. There is no growth at 10% or 20% SDS. B: Δ*mce*. There is no growth at 20% SDS, but growth is apparent at 10% SDS, indicating increased resistance in this strain. There also appears to be some overproduction of actinorhodin in this strain.

A study conducted on *Pseudomonas putida* concluded that *mce* homologues in that organism play a role in tolerance to organic solvents such as toluene (Kim *et al.*, 1998). In order to investigate whether they also have this role in *S. coelicolor*, both the wild-type and the *mce* multiple knockout were screened for resistance to toluene (see Materials and Methods).

Toluene sensitivity was measured by comparing the colony forming units (CFUs) derived from a known spore titre after incubation with and without toluene. Both the wild-type and the *mce* multiple knockout showed the same percentage reduction in CFU count following incubation with toluene (approximately 25%). The reduction in CFU was small, indicating that *S. coelicolor* has a high level of resistance to toluene. This hypothesis is supported by the presence in the *S. coelicolor* genome of a number of genes such as SCO7436 (aldehyde dehydrogenase) and SCO7359 (carboxymethylenbutanolidase) which are likely to be involved in the degradation of organic solvents (Ogata *et al.*, 1999). In light of this, it seems unlikely that the *mce* genes in *S. coelicolor* play any significant role in toluene tolerance.

Chapter 4 summary

Mutations in the *mce* gene cluster, both as single gene transposon insertions and as a multiple gene knockout, were successfully constructed and confirmed by Southern blotting. A complementation vector was constructed to demonstrate linkage and the complementation vector used to create a strain containing two copies of the *mce* operon (see Chapter 5). Mutants were screened using a variety of techniques and under a range of conditions and a preliminary phenotype identified; a morphological phenotype in which aerial hyphae have a wrinkled appearance and spores are truncated and may prematurely germinate, and increased resistance of spores to lysozyme and SDS. These phenotypes were complemented by pLCS006 demonstrating linkage of the phenotype with the genetic lesions in the strains.

Of the more than 50 conditions under which the *mce* mutants were screened, a phenotype was only detected when the strains were grown on mannitol or 0.1% cholesterol. However, the results of morphological study using SEM show that there are significant morphological changes to the mutant strains. Although these changes do not appear to affect growth or development to any great degree it seems likely, given their severity, that phenotypic effects will be present under some circumstances. The results of the spore sensitivity assay in which the *mce* cluster knockout displays increased resistance to chemical and enzymatic lysis seem to support this.

Previous studies of *mce* mutants in *M. tuberculosis* and *Rhodococcus* concentrated on the virulence effects of the mutation, using cell culture infection assays and whole-animal studies. *S. coelicolor* is not pathogenic to mammalian cells, but analogous systems exist in order to assay virulence of non-pathogens. These are explored in detail in chapter 5.

Chapter 5: Role of the *mce* operon in Streptomycete virulence and interactions

Introduction to *Acanthamoeba* biology

In recent years amoebae have emerged as a useful tool for assaying bacterial virulence, often as an alternative to macrophages which are much more difficult to culture, requiring specialised media, temperature and gaseous environments for optimal growth (Froquet, 2009; Harb *et al.*, 2000; Waterfield *et al.*, 2009). Although *Dictyostelium discoideum* has previously been the predominant model organism for the amoebae it has been suggested that *Acanthamoeba polyphaga* is a more appropriate model for macrophage infections as it is able to grow at a higher temperature range, thus more closely mimicking conditions in mammalian infection (Goy *et al.*, 2007). *A. polyphaga* also has a simpler lifecycle, not exhibiting the multicellular behaviour characteristic of *D. discoideum* (Khan, 2009).

A significant advantage to using amoebae as an alternative to macrophages is that, while persistence inside macrophages is characteristic of only a few bacterial pathogens (O'Riordan and Portnoy, 2002), the ability to persist inside amoebal cells may be much more widespread due to the ubiquity of amoebae in the environment (Adiba *et al.*; Harb *et al.*, 2000; Khan, 2009). Use of amoebae allows virulence assays to be performed on bacterial species such as *S. coelicolor* which are typically considered to be avirulent and would not survive in a macrophage assay (Froquet, 2009; Kieser *et al.*, 2000).

Acanthamoeba polyphaga in the environment

A. polyphaga is a free-living unicellular protozoan found in soil, fresh water and a number of engineered environments such as air conditioning systems (Garcia *et al.*, 2007). It is also a relatively uncommon opportunistic pathogen in humans (Kilvington *et al.*, 2004). Under favourable conditions (abundance of nutrients, no extremes of temperature or pH) *A. polyphaga* exists as a trophozoite, a motile

phagocytic state in which it forms the acanthopodia (spike-like projections) from which it takes its name in order to roam in search of prey (Khan, 2009).

In the trophozoite phase *A. polyphaga* divides by fission, producing two daughter cells per division event (Fig. 5.1). When conditions become less favourable *A. polyphaga* is able to adapt by suspending the normal cell cycle and forming a cyst, a tough coat made from proteins and polysaccharides which enables the amoeba to remain dormant for long periods of time (Lemgruber *et al.*). When conditions improve the amoeba undergoes a process of excystation and resumes life as a trophozoite.

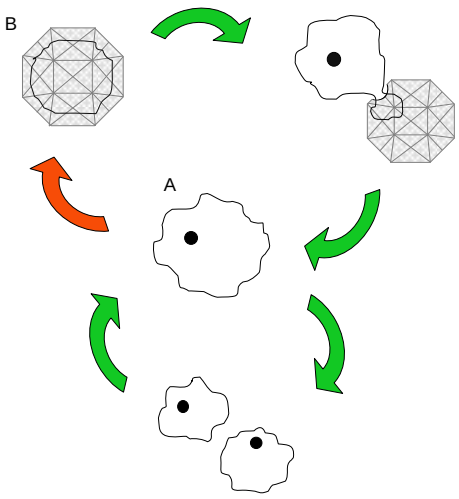

Figure 5.1: The lifecycle of *Acanthamoeba polyphaga* showing A: Trophozoite phase, B: Cyst. Green arrows represent favourable growth conditions; red arrow represents unfavourable growth conditions.

In the trophozoite stage the amoeba gains the majority of its nutrients by grazing on bacteria, yeasts and organic particles by a process of pinocytosis (uptake of solutes in a non-specific manner) or phagocytosis (specific uptake of particles 0.5 μm in diameter or larger). Both processes require invagination of the plasma membrane in order to form vesicles known as phagosomes (Khan, 2009; Salah *et al.*, 2009).

The phagosomes thus formed then fuse with lysosomes (vesicles containing lytic enzymes such as lysozyme) to form phagolysosomes, also known as acid vacuoles, where enzymatic degradation occurs (Fig. 5.2) (Salah *et al.*, 2009). This is similar to the process of phagocytic uptake and lysis of pathogens in macrophages, indicative of a shared evolutionary origin (Boulais *et al.*; O'Riordan and Portnoy, 2002).

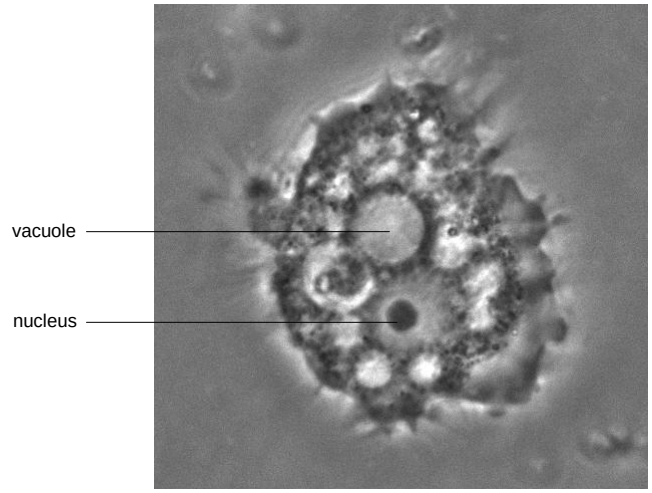

Figure 5.2: *Acanthamoeba polyphaga* trophozoite showing nucleus and multiple vacuoles. Acanthapodia (spike-like projections) are faintly visible around the edges of the cell.

Interaction of *Acanthamoeba* and bacteria

In addition to grazing on bacteria, *A. polyphaga* in the environment is known to form associations with various species of bacteria, most notably *Legionella pneumophila* which are able to persist inside the protozoan cell for long periods of time, even surviving where the host cell has undergone encystment (Greub and Raoult, 2004).

Recent research has investigated what benefits the bacteria might derive from this interaction. One hypothesis is that the extended intracellular survival enables the bacteria to withstand harsh environments that would otherwise prove lethal. For instance, it has been shown that bacteria within an amoebal host are able to withstand chemical stress such as high chlorine concentration, allowing them to colonise previously uninhabitable environmental niches such as water cooling systems (Adekambi *et al.*, 2006; Garcia *et al.*, 2007).

Another hypothesis is that of the 'microbial gymnasium', which suggests that as a consequence of intracellular association with protozoa, bacteria express genes which enhance intracellular survival in an environment that is similar to a mammalian cell, but which lacks a developed immune response. These bacteria are subsequently fitter if they go on to infect a mammalian host (Harb *et al.*, 2000; Huws *et al.*, 2008). This hypothesis was proposed primarily as the result of experiments on *L. pneumophila* which is pathogenic in mammals even without association with amoebae (Newton *et al.*), but it is possible that a similar effect may be observed even in non-pathogenic bacteria.

It is currently unclear whether the amoeba itself benefits from these interactions with bacteria, but one study has shown that endosymbiont-containing *Acanthamoeba* exhibits enhanced cytopathic effects, suggesting that in some cases it is a mutualistic relationship (Fritsche *et al.*, 1998). Other sources have suggested that the bacterial role within the amoebae is parasitic or pathogenic (Schmitz-Esser *et al.*, 2008) : in some cases the bacteria are actively invasive, however in many cases the association may simply be a consequence of the feeding behaviour of the *Acanthamoeba* which leads it to ingest bacteria more-or-less indiscriminately (Khan, 2009).

Acanthamoeba and the actinomycetes

Associations have been documented between *A. polyphaga* and various actinomycetes such as *Mycobacterium avium*, a pathogenic bacterium similar to *M. tuberculosis*, and *M. ulcerans*, an emerging pathogen that is the causative agent of Buruli ulcer (Adekambi *et al.*, 2006; Eddyani *et al.*, 2008).

Buruli ulcer is a disease affecting bone and soft tissue and is endemic to parts of Africa. *M. ulcerans* is thought to be unable to persist in the environment without a host, and freshwater amoebae have been suggested as a possible environmental reservoir. It has been found that still or slow-flowing bodies of water are more likely to contain amoebae in areas where Buruli ulcer is highly endemic (Eddyani *et al.*, 2008).

The relationship between *M. avium* and *A. polyphaga* is much like that of *M. tuberculosis* inside macrophages; the bacterium inhibits the fusion of lysosomes with the phagosome and is thus able to persist and replicate within the phagocytic vacuoles. In addition to replication inside the amoebal cell, *M. avium* has been shown to exhibit enhanced virulence when cultured with *Acanthamoeba* prior to inoculation in mice (Cirillo *et al.*, 1997), a finding that is consistent with the 'microbial gymnasium' hypothesis.

Given these previously documented associations of amoebae and actinomycetes, it seemed likely that there might be a similar association between *Acanthamoebae* and streptomycetes in the soil environment, and that strategies may have evolved for survival in these organisms. It is likely that *Acanthamoebae* would routinely encounter streptomycetes in the soil environment; one study estimated the number of protozoa in 1g of surface soil as 9.7×10^4, with bacteria present at $1.1 \times 10^9 g^{-1}$ (Ekelund *et al.*, 2001).

Investigating the relationship between *S. coelicolor* and a free-living protozoan

The relationship between *A. polyphaga* and *S. coelicolor* was investigated using a simple co-culture experiment. *S. coelicolor* spores were diluted to the required titre (see Materials and Methods) and incubated with trophozoite-phase *A. polyphaga* at a multiplicity of infection of 1:1. Co-culture was performed in a saline solution (PAS) to eliminate extraneous carbon sources. Samples were harvested at various time-points and examined microscopically to assess the progress of the co-culture (Fig. 5.3).

Uptake of wild-type *S. coelicolor* spores leads to lysis of amoebal cells

During the early stages of the co-culture (between 8 and 12 hours), wild-type *S. coelicolor* spores are taken up by phagocytosis and sequestered in the phagocytic vacuoles. The spores remain in the vacuoles for a period of around 12 hours, after which they begin to germinate. Hyphal growth is apparent approximately six hours after germination, eventually leading to lysis of the amoebal cell. This lysis appears to be mechanical rather than chemical in nature, in contrast to previously documented examples of bacterial escape from protozoan cells (Gao and Kwaik).

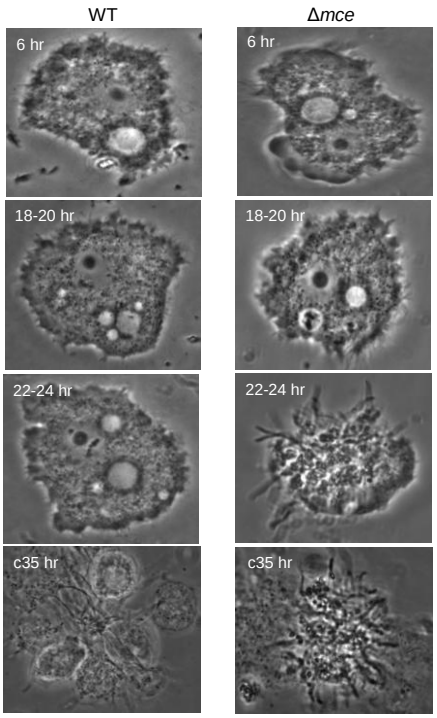

Figure 5.3: *A. polyphaga* in co-culture with M145 and Δ*mce* strains at 6, 20, 24 and 35 hours. Multiplicity of infection 1:1.

If the cultures are left for an extended period of time (48 hours or longer) the *Streptomyces* will form dense mycelial clumps focused around the dead amoebae, suggesting that the *Streptomyces* microcolonies are using the lysed amoebal cells as a nutrient source. The *Acanthamoeba* in turn cluster around these mycelial clumps, perhaps because of the grazing opportunity they provide. However, once *S. coelicolor* secondary metabolite production is established (between 48 and 72 hours, as evidenced by a slight pink colour in the medium indicative of undecylprodigiosin production) the *Acanthamoeba* throughout the culture are rapidly killed.

The observed interaction of *A. polyphaga* and *S. coelicolor* in co-culture was surprising because in this situation wild-type *S. coelicolor* appears not only to persist inside the amoebal cell but to be actively pathogenic. It is particularly intriguing because, although *S. coelicolor* produces a range of antimicrobial and antihelminth compounds, it is not considered to be an intracellular pathogen (Kieser *et al.*, 2000).

Virulence of *Streptomyces coelicolor* is enhanced by disruption of the *mce* genes

In order to investigate the role of the *mce* cluster in mediating the interaction between *S. coelicolor* and *A. polyphaga* the co-culture was repeated using the single-gene *mce* disruption mutants, the *mce* multiple knockout strain and the wild-type M145 strain. The co-culture was assessed microscopically as before to identify any difference in behaviour between the different strains (Fig. 5.3).

At the earliest time-point (6 hours) there was no uptake of spores of any strain, although the *Acanthamoeba* showed proliferation of lytic vesicles indicating the presence of a food source (Khan, 2009). After 18 hours there was phagocytic uptake of both wild-type and *mce* mutant spores, with between one and ten spores being visible in the phagocytic vacuoles of a single amoeba. The wild-type spores showed no change, however some of the *mce* mutant strains (SCO2422::*Tn*5062, SCO2421::*Tn*5062, SCO2415::*Tn*5062 and the *mce* multiple knockout) showed signs of swelling indicative of germination.

After 24 hours of co-culture the wild-type spores began to show signs of germination; at the same time-point the *mce* mutant strains (SCO2422::*Tn*5062, SCO2421::*Tn*5062, SCO2415::*Tn*5062 and the *mce* multiple knockout) had germinated and exhibited hyphal growth to an extent that caused lysis of the amoebal cells. The same level of hyphal growth in the wild-type was reached after a further six hours of co-culture (Fig. 5.3).

The increase in streptomycete virulence when the *mce* genes were disrupted or deleted is supported by the results of previous experiments (growth on mannitol; resistance to SDS and lysozyme) but was nonetheless unexpected as it represents an apparent gain of function as the result of a gene knockout. While this is not unprecedented (ten Bokum *et al.*, 2008) it is extremely unusual.

This hypervirulence appears to stem from rapid spore germination following uptake by the amoebal cell, rather than from the preferential uptake of mutant spores in the first instance. One study of the *M. tuberculosis mce3* operon reported that latex beads coated with Mce3 proteins were preferentially taken up by macrophages (El-Shazly *et al.*, 2007), however there is no evidence that the *S. coelicolor* Mce proteins are present on the spore surface.

It is possible that the changes to spore coat morphology in the *mce* mutants may alter the interaction of the spore with the amoeba, but it is difficult to envisage the mechanism by which this might lead to preferential uptake of mutants and such a preference was not observed experimentally.

A rapid germination phenotype would be consistent with the results observed from morphological screening of the *mce* mutants. Although the phenotype appears to represent a gain of function in the context of this assay, it is entirely possible that in the complex soil environment it would prove to be disadvantageous.

The extent of the phenotype displayed by each single-gene disruption mutant was assessed to see if polar effects might be present. However, there was no indication

that mutants with transposon insertions at the proximal end of the operon had a more severe phenotype than those with the transposon insertion at the distal end. The *mce* multiple knockout did appear to have a more severe phenotype than the single-gene mutants, indicating that the *mce* operon retains some function when individual genes are disrupted.

A. polyphaga does not encyst in co-culture with *S. coelicolor*

It is interesting to note that, although typically resistant to antimicrobials (Khan, 2009), the *Acanthamoeba* were apparently unable to withstand them in the aqueous co-culture experiments. The predominant mechanism of Acanthamoebic resistance to antimicrobials is encystment (Lemgruber *et al.*, 2010) and in this case the susceptibility may be linked to the failure of the *A. polyphaga* to encyst when *S. coelicolor* secondary metabolite production was initiated.

This failure may have been due to the particular secondary metabolites produced by *S. coelicolor* (e.g. actinomycin D which can induce amoebal apoptosis (Gao and Abu Kwaik, 2000)), the conditions of the assay (saline suspension with no additional nutrient source), or a combination of several factors.

Acanthamoeba has demonstrated its ability to encyst in liquid culture when nutrients become limiting, indicating that the maintenance of the trophozoite phase seen in this case was the result of experimental factors. A previous study using a number of bacterial species has shown that amoebal encystment can be delayed when bacteria are present in the medium (de Moraes and Alfieri, 2008).

Further development of the co-culture assay

Some studies involving *Acanthamoeba* use colorimetric assays to assess amoebal survival. Such assays typically use a substrate such as alamar blue which undergoes a colour change as a result of the metabolic processes of the amoebae (McBride *et al.*, 2005). This approach was applied to the co-culture assay but was unsuccessful due to

the presence of a second organism (i.e. *S. coelicolor*) which was also capable of driving the colour change (results not shown). Alamar blue is reduced by NADPH as well as a number of other cellular compounds such as cytochromes which are present in bacteria, and has in fact been used previously to assay for bacterial proliferation (McBride *et al.*, 2005).

A simple live/dead stain (trypan blue, which is excluded by live cells but absorbed by dead ones) was used to generate live cell counts both before and after co-culture, but again proved problematic due to the difficulty of removing adherent cells from the wells. Failure to detach all adherent cells produces a bias towards dead cells in the sample, as they do not adhere but rather float freely in the medium and are thus easily harvested. Cells must be harvested in order to perform the assay because the optical density of the trypan blue stain is such that when added directly to the wells in the required quantity it is opaque.

It was possible to separate the two organisms using mechanical means (scraping of the wells to dislodge adherent amoebae, followed by short centrifugation) but this technique introduced significant error due to the number of cells lysed by the separation process. The association between *A. polyphaga* and *S. coelicolor* in co-culture was also such that after a certain point (approximately 30 hours) it was impossible to separate them fully.

The results of the live/dead assay indicate that *A. polyphaga* alone has a high survival rate after 24 hours (approximately 78%). When in co-culture with M145 the survival rate is lower (65%), and is lowest in co-culture with the Δ*mce* strain (52%). Although the percentage values can be compared to one another, they likely do not reflect the absolute numbers of live cells in the co-cultures prior to cell harvesting.

Optimisation of an amoebal plaque assay for use with streptomycetes

The aqueous co-culture experiments detailed previously provided some useful qualitative results but were difficult to quantify and time-consuming to set up. Once

the experiment had been started it was difficult to monitor its progress without harvesting the sample, and the virulence of *S. coelicolor* contributed to this problem by shortening the window in which useful data could be gathered.

In order to circumvent some of these problems a plaque assay developed by Froquet et al (2009) using *D. discoideum* was adapted and optimised for use with *A. polyphaga* and *S. coelicolor*. This allowed a more quantitative approach and provided a convenient way to screen a large number of strains comparatively quickly. The nature of the experimental setup also eliminated the need for extensive optimisation of spore titre beforehand (Fig. 5.4; Materials and Methods).

The graduation of nutrient content of the agar, and the use of four different concentrations of *Acanthamoeba* per plate, allow a range of conditions to be tested in parallel which would require multiple experiments if optimised singly. These factors also compensate for slight fluctuations in incubation temperature by allowing selection of a higher or lower nutrient percentage in response to temperature-dependent changes in bacterial growth rate. Although there is not likely to be a significant difference in conditions between different plates, controls have been included on each plate to reduce the necessity of comparing between them.

The optimal number of amoebae per well was found to be between 1000 and 10000, and for this reason both dilutions were included on each plate. Plaques were visible at all media concentrations (nutrient agar; concentration from 100% - 10% nutrient broth), but were larger at lower concentrations. At room temperature (approximately 25ºC) growth of bacteria and plaque formation were both visible at 3 days post-inoculation. Plaques are formed by amoebal grazing on the bacterial spores creating a clear zone where no bacterial growth occurs, and the size of the plaque is inversely proportional to the virulence of the bacterium.

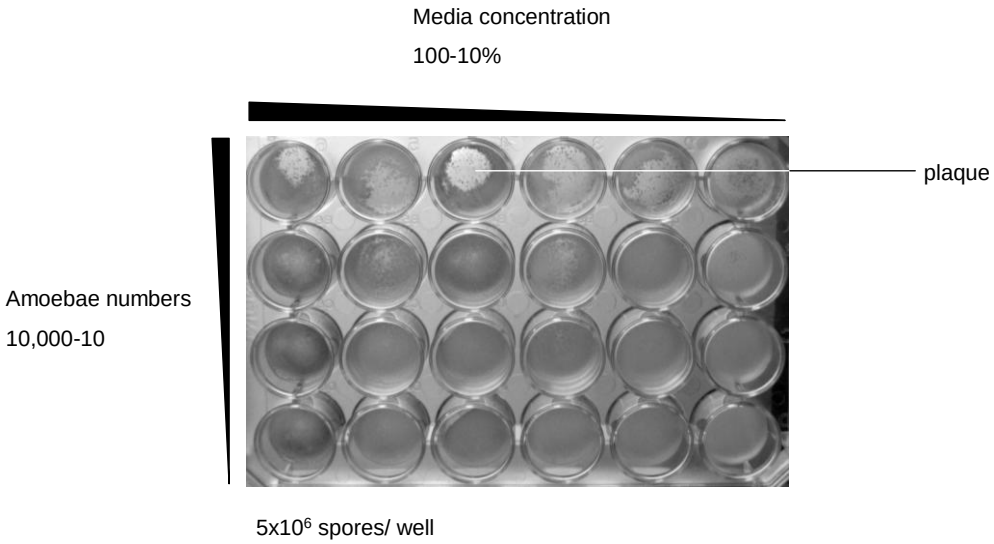

Figure 5.4: Experimental setup for plaque assays. Amoebae are spotted onto a lawn of *Streptomyces* spores. Media concentration (percentage v/v nutrient broth) and number of amoebae are varied in order to obtain a number of different bacterial growth rates.

mce mutants display hypervirulence in plaque assay

The *mce* cluster knockout was compared with the wild-type strain and the complemented cluster knockout (Fig. 5.5A). The results of the aqueous co-culture were replicated, with the *mce* mutant strains proving comparatively resistant to predation by *Acanthamoeba*. The most striking difference was between M145 and the *mce* multiple knockout. The *mce* knockout shows enhanced resistance to plaquing relative to M145 at all nutrient concentrations and with all four different amoeba concentrations. The mutant phenotype is fully complemented in strains containing the pLCS006 plasmid, which contains the full *mce* operon.

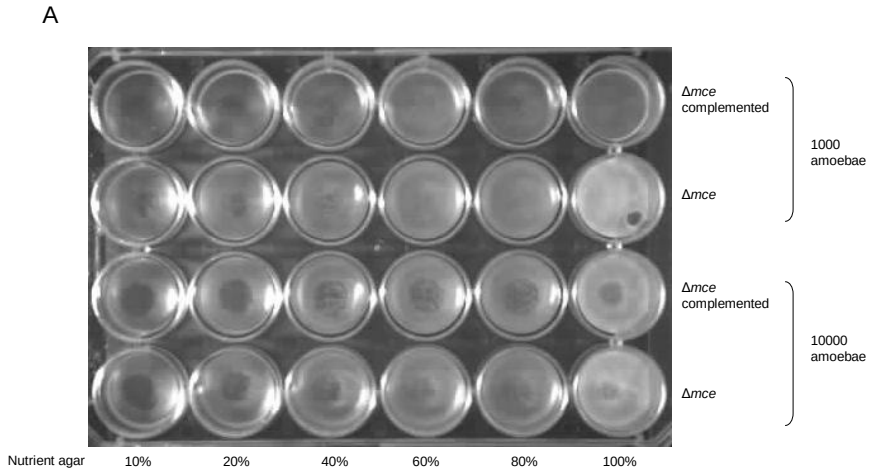

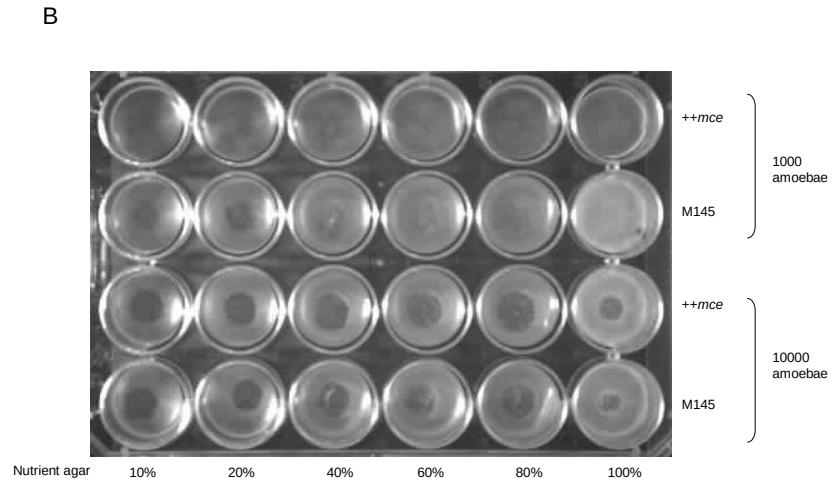

Figure 5.5A: A: Plaque assay comparing Δ*mce* and Δ*mce* complemented strains. Plaques formed on the complemented strain are larger than those on the multiple knockout. B: Plaque assay comparing M145 and SLC301 (++*mce*) strains. Plaques are larger on the SLC301 strain than the wild-type.

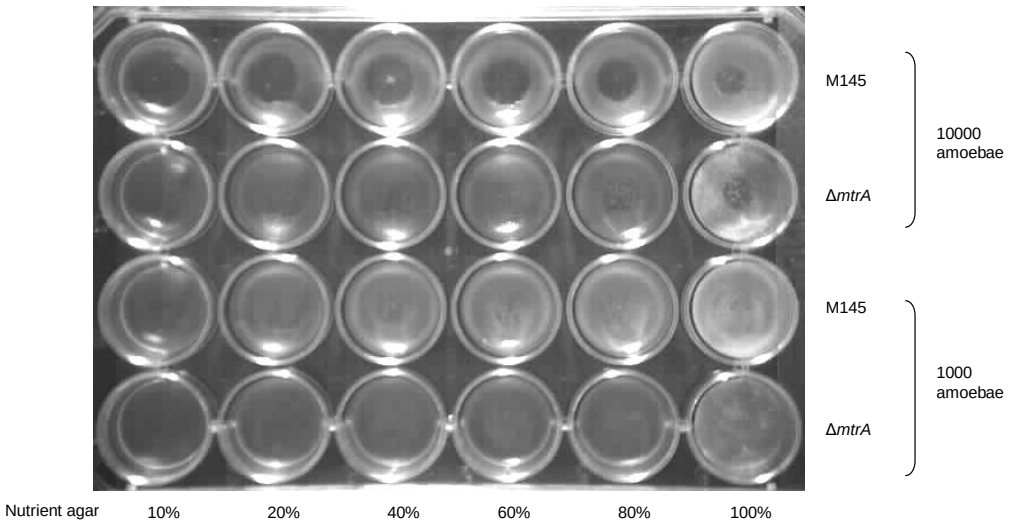

Figure 5.5B: Plaque assay comparing Δ*mtrA* and M145 strains. Plaques are smaller on the Δ*mtrA* strain, as was observed with the Δ*mce* strain.

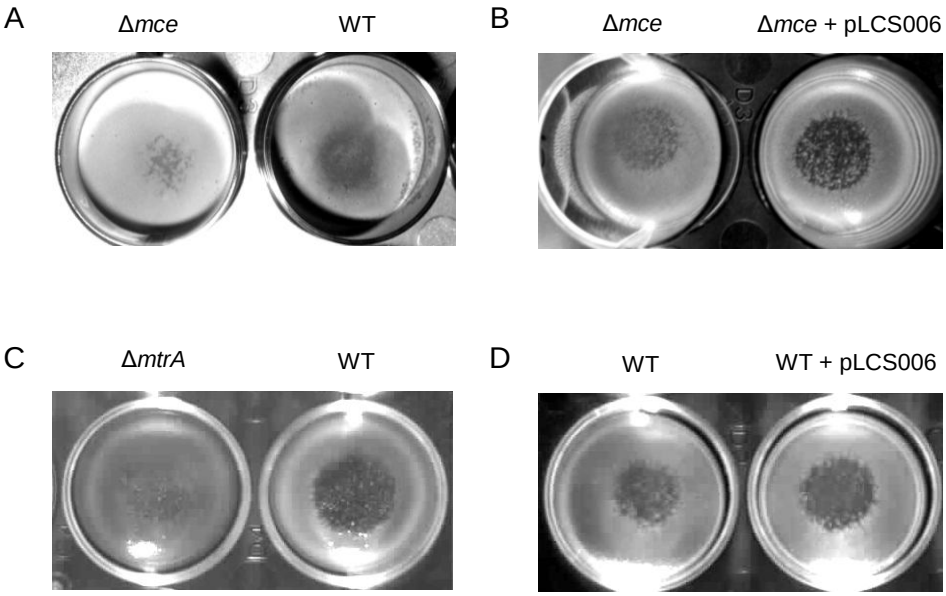

Figure 5.5C: Enlargements of figures 5.5A-B to more clearly show the differences in plaque size between *S. coelicolor* strains. A: Δ*mce* and M145 wild-type (WT). B: Δ*mce* and complemented knockout (Δ*mce* + pLCS006). C: Δ*mtrA* and M145. D: M145 and M145 + pLCS006. Plaque size appears to correlate positively with the number of copies of the *mce* operon present in the strain (when plaque size is measured at 20% v/v nutrient concentration with 10000 amoebae the plaque sizes are: M145 5.1mm; Δ*mce* + pLCS006 5.3mm; Δ*mce* 4.0mm; Δ*mtrA* 4.3mm; M145 + pLCS006 5.7mm). Additionally, the *mtrA* mutant displays a similar phenotype to the *mce* multiple knockout.

Repetition of the assay using strain SLC301, which is M145 containing an additional copy of the *mce* gene cluster though conjugation of plasmid pLCS006, shows enhanced plaque formation relative to that of M145. This indicates that the phenotype is *mce* gene-dose-dependent. This finding is consistent with the distribution of *mce* homologues in the actinomycetes, where increased copy number appears to correlate with increased pathogenicity.

The *mce* overexpression strain also shows reduced resistance to lysozyme compared to the wild-type (see chapter 4) and it is possible that the reduced resistance to plaquing seen in the *Acanthamoeba* co-cultures is in fact a function of this lysozyme sensitivity. Lysozyme is a key component in amoebal lysosomes, and increased lysozyme sensitivity might thus be expected to impair intracellular survival of the bacterium.

A *mtrA* knockout is also resistant to plaquing

MtrA is a response regulator in *S. coelicolor* that has been identified as a possible regulator of the *mce* operon (see chapter 1). A Δ*mtrA* strain (Hutchings and Seipke, unpublished) was assayed for sensitivity to plaquing (Fig. 5.5B). The Δ*mtrA* mutant displayed increased resistance to plaquing, the same phenotype as the *mce* multiple knockout. The mutant phenotype is fully complemented by restoration of *mtrA*. This result supports the hypothesis that MtrA may regulate the *mce* operon.

Δ*relA*, Δ*desD* and an *esxBA* mutant show no difference in plaque assay

A *S. coelicolor esxBA* mutant, a Δ*relA* and a Δ*desD* strain were screened for sensitivity to plaquing. The *esxBA*, *relA* and *desD* loci are involved in various aspects of development, sporulation and secondary metabolite production (Barona-Gomez *et al.*, 2004; Chakraburtty and Bibb, 1997; San Roman *et al.*; Sun *et al.*, 2001).

The *relA* gene encodes the RelA (p)ppGpp sythetase which is necessary for the production of actinorhodin and undecylprodigiosin and which appears to play a role in morphological differentiation (Sun *et al.*, 2001).

The *esx-1* locus in *S. coelicolor* is an operon which includes the *bldB* regulatory gene, various genes encoding components of the ESX-1 secretory apparatus, and *esxA* and *esxB* which encode small secreted proteins. Deletion of the locus results in attenuation and is one of the features of the *M. bovis* BCG vaccination strain. EsxBA forms a dimer which has a role in the correct septation of aerial hyphae. A transposon mutant of *esxBA* produces a wrinkled spore morphology similar to that of the *mce* mutants (San Roman *et al.*).

DesD is a siderophore synthetase, playing an essential role in the biosynthesis of desferrioxamine. Siderophores have been mooted as possible virulence factors due to their role in transporting iron, which is typically limited in eukaryotic intracellular infection due to sequestration by the host cell (Barona-Gomez *et al.*, 2004).

None of these strains displayed a noticeable phenotype when screened using the plaque assay (Fig. 5.6). This would suggest that the phenotype seen in the *mce* and *mtrA* mutants is specific to those loci and not the result of a more generalised developmental phenotype. The *esxBA* mutant is particularly interesting in this regard as it displays a similar spore morphology phenotype to the *mce* mutants but does not show hypervirulence in the amoeba assay.

A

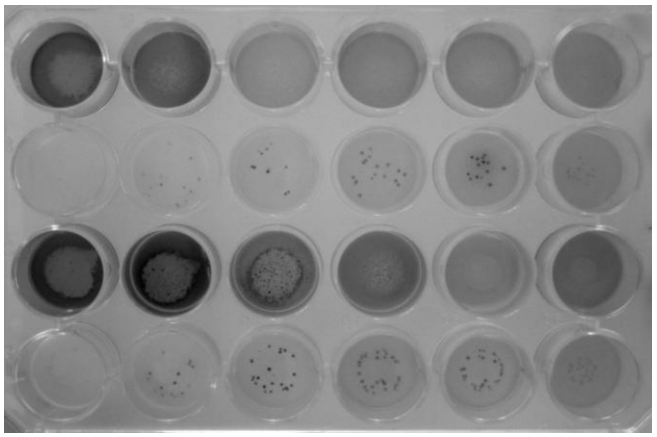

B

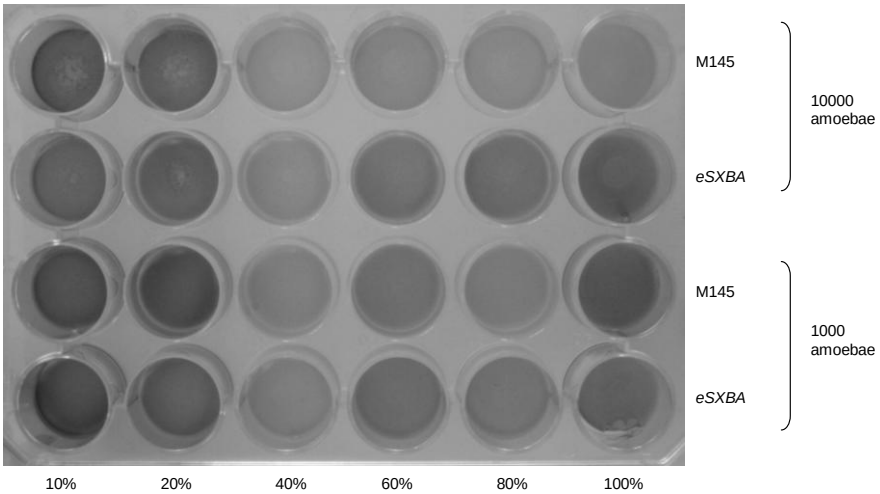

Figure 5.6A: A: Plaque assay comparing *S. scabies* and M145. *S. scabies* is more susceptible to plaquing than *S. coelicolor*. B: Plaque assay comparing *eSXBA* and M145 strains. No difference was observed in plaque formation.

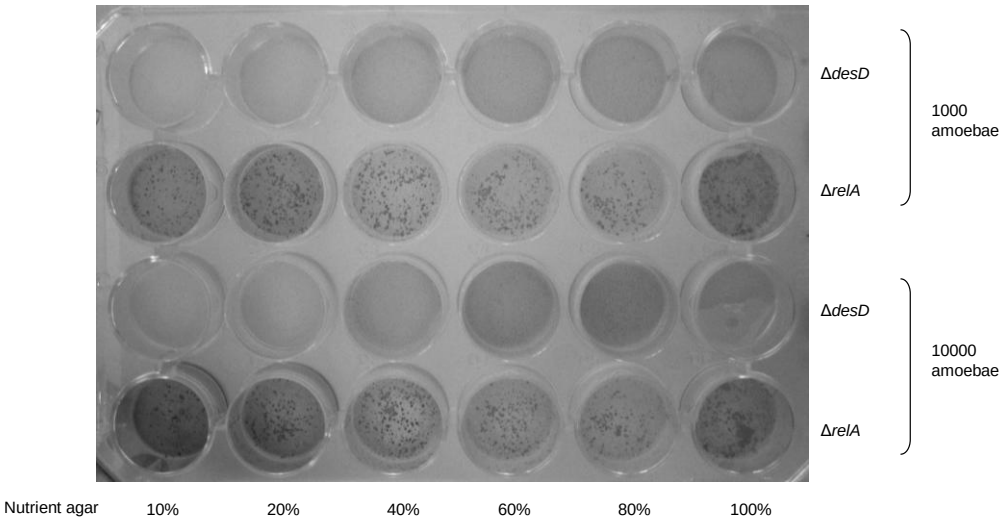

Figure 5.6B: Plaque assay comparing Δ*relA* and Δ*desD* strains. No difference was observed in plaque formation between these strains and the wild-type.

Streptomyces scabies is less resistant to plaquing than *S. coelicolor*

Streptomyces scabies is a plant pathogen, the causative agent of potato scab disease. Its genome does not have the *mce* operon and was screened for sensitivity to amoebal plaquing in order to compare it to the non-pathogenic strains screened previously (Fig. 5.6A). Interestingly, *S. scabies* showed significantly more plaquing than wild-type *S. coelicolor*. This is the opposite result from what might have been expected on the basis of the putative role of the *mce* operon, however there are a number of genetic and physiological differences between the species which may account for the difference (Lerat *et al.*, 2009). *S. scabies* does not grow optimally on nutrient agar and this may be a factor which reduces its resistance to amoebal plaquing on this medium.

A. polyphaga behaves differently in solid and liquid medium

An interesting feature of the plaque assay is that, although it replicates the findings of the co-culture, the progression of the experiment is slightly different in each case. In the aqueous co-culture there is initial predation of *S. coelicolor* spores by a proportion of the amoeba. However, after approximately 24 hours the ingested *Streptomyces* begins to act as a pathogen. This is followed by mycelial growth of the *Streptomyces*, mechanical lysis of the amoebal cells (Fig. 5.3) and grazing of the Streptomycete mycelium by surviving amoebae which migrate towards it.

S. coelicolor then begins production of secondary metabolites which rapidly kills the remaining viable amoebae. After approximately 72 hours of co-culture there are no surviving amoebae in the trophozoite phase and, interestingly, no evidence of encystment. *S. coelicolor* continues to grow into dense hyphal clumps, apparently using the amoebal remains as a nutrient source.

In contrast to this, on the plaque assay plates *A. polyphaga* appears to be a more successful predator of *S. coelicolor*, perhaps because this assay is more

representative of the soil environment. The amoebae produce zones in which there is no bacterial growth, even after prolonged incubation (72 hours +).

There may be a number of factors which account for this. One possibility is that in the presence of an alternative nutrient source (i.e. the nutrient agar), *S. coelicolor* delays secondary metabolite production (Rigali *et al.*, 2008) and is thus less effective at killing amoebae in the early stages of the assay. Where secondary metabolite production occurs, the metabolites are likely not able to diffuse as rapidly as in an aqueous culture and this may also favour amoebal growth.

Growth on solid media also appears to induce amoebal encystment to a degree that is not seen in aqueous co-culture, possibly as a response to desiccation. This encystment may prevent germination and/or growth of ingested *Streptomyces* spores via changes in the intracellular environment of the amoebae (Lemgruber *et al.*). Finally, the amoebae may be able to proliferate more effectively in the presence of an alternative nutrient source (i.e. nutrient agar) than they can in saline solution. This could allow more effective recovery of the population from streptomycete pathogenicity.

Catalase assay

In order to examine the amoeba-bacteria interaction on a cellular level, an experiment was performed to determine the activity of *A. polyphaga* lysosomes and whether this activity was differentially induced by the *S. coelicolor mce* mutants. Lysosomal activity was measured by assaying for catalase activity in cell lysate from co-cultures of *A. polyphaga* with the *mce* cluster knockout and wild-type strains (Fig. 5.7). *A. polyphaga* without bacteria was used as a control.

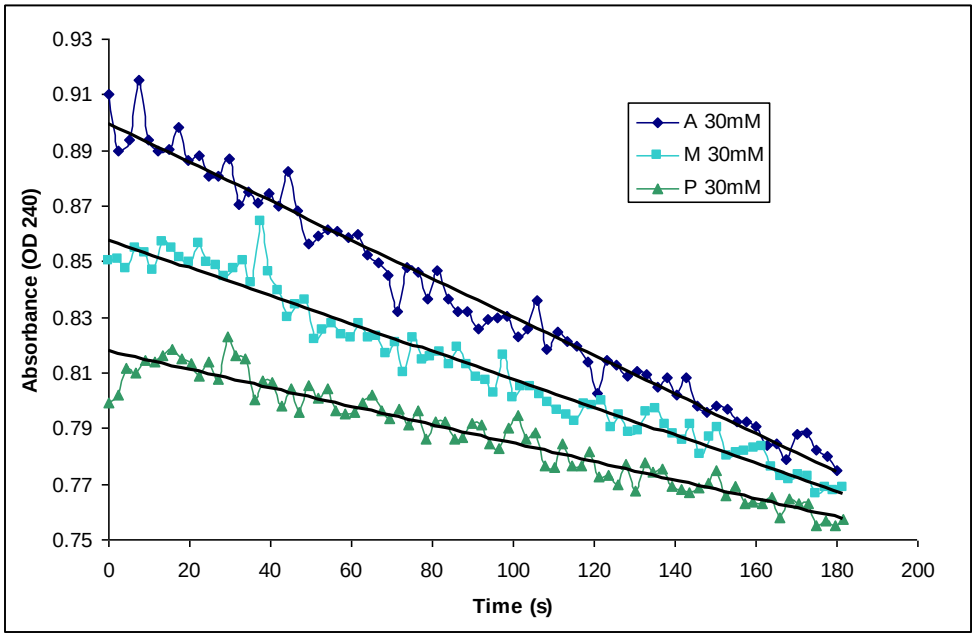

Figure 5.7: Graph showing results of catalase assay using 5µg protein and 30mM H_2O_2. Catalase activity is greatest in the amoeba-only control (A; 0.016 mmol/s H_2O_2 consumed). There is approximately 30% reduction of activity following co-culture with M145 (M; 0.012 mmol/s H_2O_2 consumed), and approximately 60% reduction of activity following co-culture with the *mce* multiple knockout strain (P; 0.007 mmol/s H_2O_2 consumed). Data represent one experiment but rates are reproduced in experiments using 20, 25 and 35mM concentrations of H_2O_2 (data not shown).

The assay shows a reduction in catalase activity when *A. polyphaga* is co-cultured with the *mce* multiple knockout compared to the wild-type. This could be a consequence of reduced lysosomal activity in the amoebae, which has also been observed in macrophages infected with *M. tuberculosis* (Haas, 2007). Alternatively, the reduced catalase activity could be a consequence of increased amoebal mortality when in co-culture with the *mce* multiple knockout in comparison to the wild-type.

Although *S. coelicolor* itself produces catalase, the bacteria-only control (not shown) showed that its activity was not sufficient to be detected in this assay.

The role of the *mce* gene cluster in the Rhizosphere

It has recently been shown in *M. tuberculosis* that the *mce* loci encode ABC-like cholesterol importer systems, which are likely to be involved in carbon uptake during growth in the host macrophage (Casali and Riley, 2007; Mohn *et al.*, 2008). Using the amoeba model, often used as a surrogate macrophage model, it was shown that mutations in the *mce* gene cluster in *S. coelicolor* have a hyper-virulent phenotype in the amoebae. This reinforces the hypothesis that these genes somehow mediate interactions of *Streptomyces* with other soil organisms. The likely substrate imported by the mycobacterial Mce proteins is cholesterol (Mohn *et al.*, 2008).

The substrate for the *Streptomyces* importer is unknown, but we hypothesise that it is likely to be sterols and/or sterol-like molecules. It is known that plants are a rich source of sterols in the rhizosphere, with leaves, roots and stem membranes comprising of phytosterols such as sitosterol, stigmasterol and campersterol (Pavlik *et al.*, 2010). Given the rich source of nutrients these may provide, and that streptomycetes are abundant in the rhizosphere (Tokala *et al.*, 2002) it is likely that these genes may aid survival of these organisms in the rhizosphere.

Using the *mce* gene cluster mutants created in this study, a plant-*Streptomyces* model was established to investigate the role of *mce* genes in plant root colonisation. The

plant colonisation and microscopy work was carried out in the Instituto de Agricultura Sostenible (CSIC), Cordoba, Spain in the summer of 2010 by Dr Paul A Hoskisson and Dr Pilar Prieto-Aranda. Subsequent analysis of the samples was carried out by Laura Clark at the University of Strathclyde and is presented in this thesis as a collaborative piece of work.

Establishment of a model plant species

Many different plant species have been used as models for interaction with *Streptomyces*, including tobacco (*Nicotiana tabacum*), *Arabidopsis thaliana*, alfalfa (*Medicago salvia*), potato (*Solanum tuberosum*) and radish (*Raphanus sativus*), with each model being suitable for differing infection/pathogen processes (Bignell *et al.*, 2010). To establish a plant species suitable for investigating the role of *mce* genes from *Streptomyces* four species were tried, based on previous use in *Streptomyces*-plant assays: tobacco (*Nicotiana tabacum*; a gift from Mr Michael Ambrose, John Innes Centre, UK), *Arabidopsis thaliana*, (a gift from Mr Michael Ambrose, John Innes Centre, UK) Alfalfa (*Medicago salvia*; a gift from Dr Ian Thomas, Institute of Grassland and Environmental Research, University of Aberystwyth, UK) and radish (*Raphanus sativus*; a gift from Dr Charlotte Allender, Horticultural Research Institute, University of Warwick).

Each of these plant species were germinated on agar plates of Murashige and Skoog medium following bleaching of the seeds (see materials and methods). The seeds showed variation in the speed of germination with *Arabidopsis* germinating in 4 days, *Medicago* in 3 days, *Raphanus* in 3 days, and *Nicotiana* in 4 days. Subsequent out-growth and leaf formation meant that whole plants could be moved to Magenta pots (larger plant cultivation vessels) or 6 well plates (*Nicotiana* and *Arabidopsis*) containing fresh Murashige and Skoog medium in approximately 10 days for all species. Following transfer all plants were allowed to acclimatise to their new environment for 24 hrs before inoculation. Inoculated and mock inoculated (distilled water) plants were allowed to grow for up to 2 weeks.

Following 2 weeks of growth the plants were qualitatively assessed for their ease of handling (size, vigour, ease of transfer, reproducibility of germination, auto-fluorescence under the microscope, colonisation by *Streptomyces* and dissection of roots for further study e.g. colony counts and RT-PCR) and two species were chosen for investigation of the *mce* genes. These were *Nicotiana* and *Arabidopsis* largely due to the managable plant size, developmental differences observed and ease of tissue handling for microscopy and disruption.

Impact of *Streptomyces* colonisiation of plant growth and development.

Nicotiana and *Arabidopsis* seedlings were inoculated with 1 x 10^6 spores of each *Streptomyces* strain (M145, Δ*mce*, Δ*mce* pLCS006, SLC301) and the plants were allowed to grow for 3 and 7 days at 21 ^oC with a 16-h day length. Following the required incubation period plants were removed for microscopic examination of root colonization, the bacterial colonization load was determined, the effect on plant growth and development assessed and samples harvested for examination of transcription of *hrdB* and *mce* genes (see chapter 6).

Following inoculation of *Nicotiana* with *Streptomyces* the plants grew and developed normally. There was no discernable difference between inoculated and uninoculated *Nicotiana* plants at 7 days (Fig. 5.8, 1-A-D). Microscopic examination of the plant roots (Fig. 5.8, 3-A-D) indicated that the colonisation patterns differ between strains. Wild-type *Streptomyces coelicolor* M145 colonises the roots of *Nicotiana* heavily, forming a layer of mycelium along the root surface (Fig. 5.8, 3-A). The *S. coelicolor* Δ*mce* cluster strain colonisted the roots of *Nicotiana* to a much lesser degree (Fig. 5.8, 3-C) suggesting that *mce* genes may play a role in plant root colonisation. The phenotype was restored when the mutation was complemented by the integrating vector pLCS006, containing the *mce* cluster (Fig. 5.8, 1-B). Remarkably the plants respond very differently to the presence of the bacteria, with the *Streptomyces*-

inoculated plants forming many fewer root hairs than in the uninoculated control plants (Fig. 5.8, 1-D).

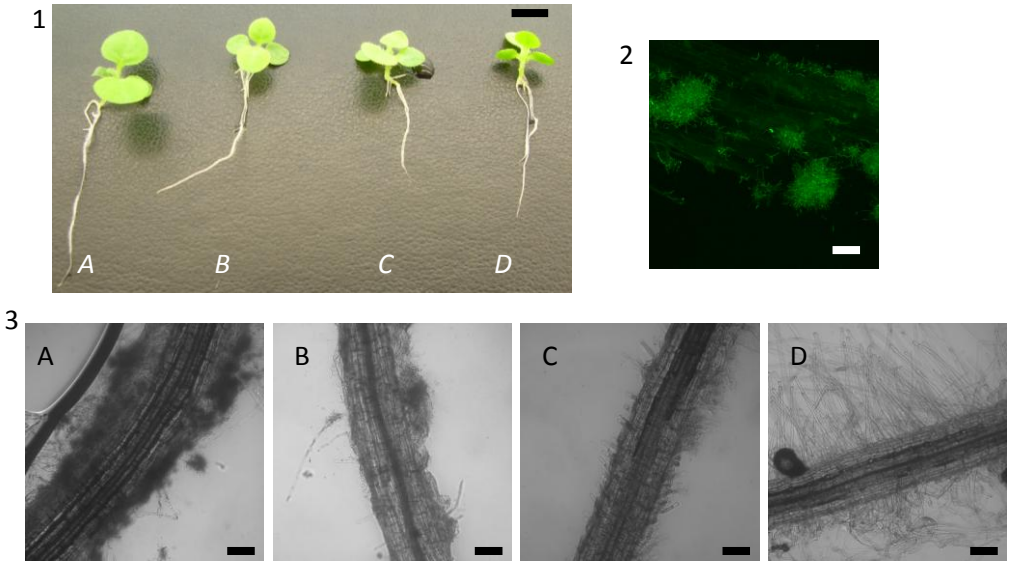

Figure 5.8: Tobacco (*Nicotiana tabacum*) root colonisation by *Streptomyces coelicolor* Wild type and mutants at 3 and 7 days post-inoculation. Representative of 4 experiments. 1: Effect of colonisation on plant growth and development at 7 days (A: M145 –WT; B: Δ*mce* + comp; C: Δ*mce*; D: uninoculated control). Bar = 1cm 2: Root Colonisation at 3 days M145 *+ egfp.* Bar = 500 µm 3: Root Colonisation at 3 days (A: M145 –WT; B: Δ*mce* + comp; C: Δ*mce*; D - uninoculated control). Bar = 500 µm.

Quantitative assessement of the *Streptomyces* colonisation of *Nicotiana* roots (Fig. 5.9) shows that the *S. coelicolor* Δ*mce* cluster strain colonises the roots of *Nicotiana*

much more poorly than the wild type strains, and that the mutant phenotype is restored by the integrating vector pLCS006, containing the *mce* cluster. Interestingly, provision of an additional copy of the *mce* cluster to wild-type *S. coelicolor* results in a reduction in colonisation when compared to wild-type *S. coelicolor* alone.

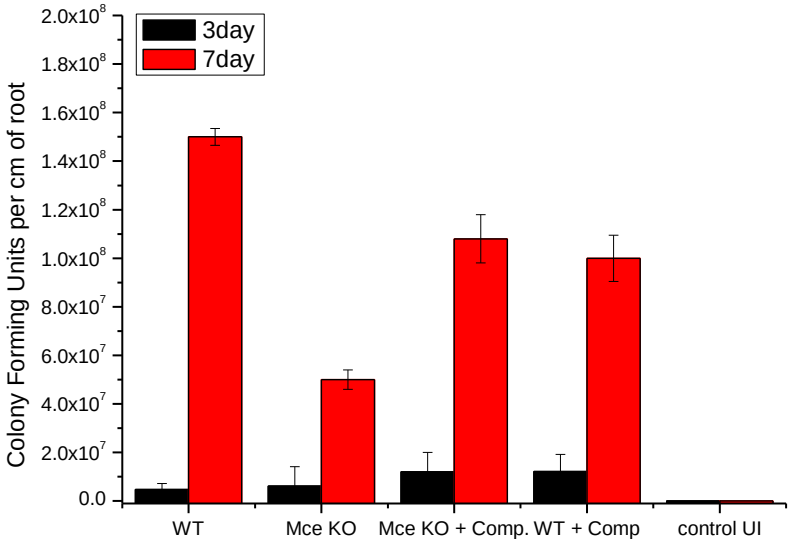

Figure 5.9: Tobacco (*Nicotiana tabacum*) root colonisation by *Streptomyces coelicolor* wild-type and mutants at 3 and 7 days post-inoculation. Error bars indicate the Standard Deviation of 3 replicates. Difference indicated is statistically significant.

Inoculation of *Arabidopsis* with *Streptomyces* again resulted in normal plant growth and development (Fig. 5.10, 1-A-D). The *S. coelicolor* Δ*mce* cluster strain did result in slightly smaller plants with less developed roots, however without significant further work on the plant aspects of colonisation it is difficult to ascertain the reasons for this. Microscopic analysis of *Arabidopsis* roots colonised with *Streptomyces*, as for *Nicotiana*, showed a reduction in colonisation by the Δ*mce* cluster strain when compared to the wild type *S. coelicolor*, which could be complemented with the provision of the *mce* cluster on the integrating pLCS006 plasmid (Fig. 5.10, 3-A-C). It is also notable that the uninoculated plants formed many more root hairs when compared to the inoculated plants.

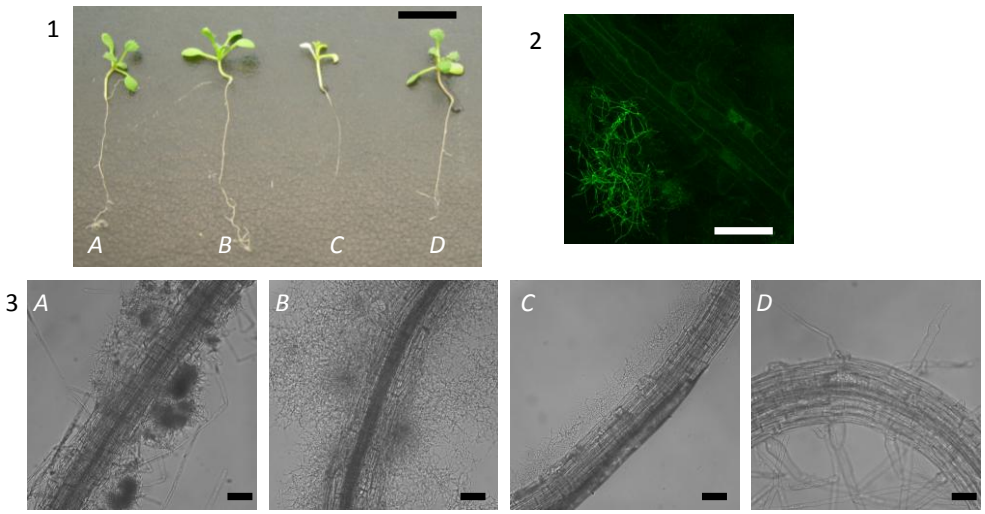

Figure 5.10: *Arabidopsis thaliana* root colonisation by *Streptomyces coelicolor* wild-type and mutants at 3 and 7 days post-inoculation. Representative of 4 experiments. 1: Effect of colonisation on plant growth and development (A: M145 – WT; B: Δ*mce* + comp; C: Δ*mce*; D: uninoculated control). Bar = 1 cm. 2: Root colonisation at 3 days M145 *+ egfp.* Bar = 500 µm. 3: Root colonisation at 3 days **(**A: M145 –WT; B - Δ*mce* + comp; C: Δ*mce*; D: uninoculated control). Bar = 500 µm.

Quantitative assessment of the *Streptomyces* colonisation of *Arabidopsis* roots (Fig. 5.11) shows that the *S. coelicolor* Δ*mce* cluster strain colonises the roots of *Nicotiana* much less than the wild type strains, and that the mutant phenotype is restored by the integrating vector pLCS006, containing the *mce* cluster. Interestingly provision of an additional copy of the *mce* cluster to wild-type *S. coelicolor* does not affect the level of colonisation unlike in *Nicotiana*.

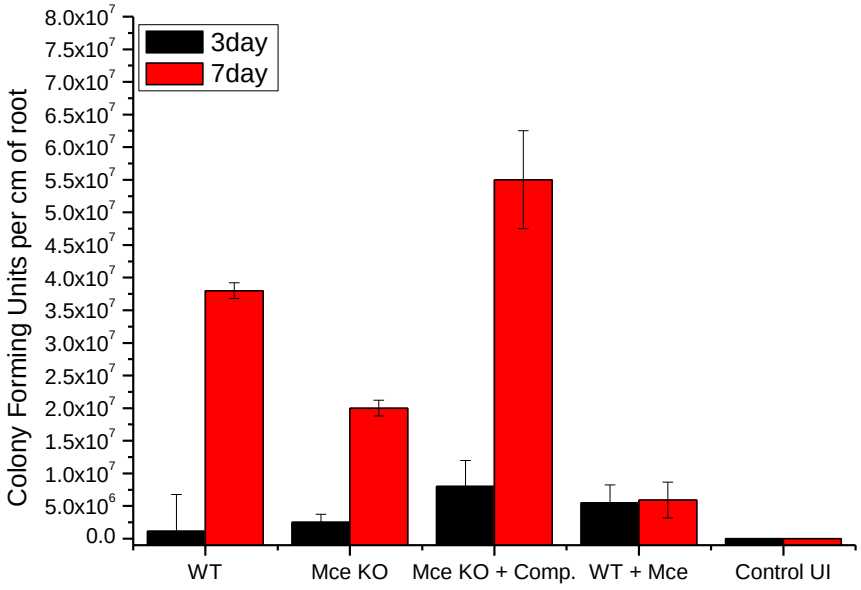

Figure 5.11: *Arabidopsis thaliana* root colonisation by *Streptomyces coelicolor* Wild type and mutants at 3 and 7 days post-inoculation. Error bars indicate the Standard Deviation of 3 replicates. Difference indicated is statistically significant.

Examination of wild-type *Streptomyces* expressing eGFP constitutively (M600/ pIJ8655) in the plant root colonisation assay indicated that *S. coelicolor* does not penetrate the plant tissue during colonisation of *Arabidopsis* and *Nicotiana*, with *Streptomyces* forming micro-colonies on the surface of the root, suggesting that close association may be a result of nutrient usage from the plant roots. The reduction in colonisation observed in the Δ*mce* cluster strain maybe a result of reduced nutrient availability due to the absence of the transporter. It is attractive to hypothesise that the *mce* cluster may facilitate this close interaction in the rhizosphere.

Chapter 5 summary

There is an interesting parallel between the interactions of *M. tuberculosis* and macrophages in a lung infection, and those of Streptomycetes and *Acanthamoebae* in the soil. *M. tuberculosis* is able to persist inside the macrophage partly due to its ability to prevent lysosome-phagosome fusion. Whilst it is not clear whether *S. coelicolor* is able to do the same in macrophages, the increased resistance of the *mce* multiple knockout strain to lysozyme, and the decreased catalase activity displayed by *A. polyphaga* when in co-culture with it, suggest that interaction with the lysosome may play a part in *S. coelicolor* pathogenicity towards *A. polyphaga*.

That the *mce* cluster plays a role in *S. coelicolor* virulence has been demonstrated in both the aqueous co-culture experiments and the plaque assays. Deletion of the *mce* cluster results in increased virulence, and this phenotype can be complemented by reintroduction of the *mce* operon. Additionally, a strain with two copies of the *mce* operon displays the reverse phenotype to the *mce* cluster knockout, indicating a dosage effect.

These observations are consistent with the hypothesis that the role of the *mce* cluster is to mediate the interactions of the actinomycetes with eukaryotic cells such as macrophages or unicellular protozoans. It is interesting that although there are well-understood mechanisms by which *S. coelicolor* is able to deal with other soil competitor organisms (for instance the phage growth limitation [Pgl] system; the production of antibacterial and antifungal metabolites to cope with microbial competition; and antihelminth compounds for nematode predators (Baltz, 2008; Hoskisson and Smith, 2007)), a dedicated system which mediates interactions with protozoans has not previously been documented.

The phenotype observed in the amoebal experiments raises the question of what is happening at the transcriptional level. The next chapter will examine regulation and transcription of the *mce* operon, and expression of the Mce proteins.

Chapter 6: Expression and regulation of the *mce* operon

Introduction

The role of the *mce* operon was explored in the previous chapters through mutation and phenotypic screening. However, to get a full picture of its activity it is also important to examine expression of the operon.

This chapter will explore the expression of the *S. coelicolor mce* operon under a number of different conditions, examining the effects of growth media, stage of morphological development and co-culture with *Acanthamoeba polyphaga*, *Arabidopsis thaliana* and *Nicotiana tabacum*. The effect on *mce* expression of a putative regulator, *mtrA*, will also be considered. The presence of the *mce* operon in pathogenic *Streptomyces* species will be examined using PCR analysis.

In addition to transcriptional studies, Mce protein expression will be investigated through western blot analysis using antibodies developed against the *Mycobacterium* proteins, and by overexpression of selected proteins.

mce expression during development

The first step towards characterising *mce* expression in *S. coelicolor* was to examine transcription of the operon during growth on solid medium, at a number of time-points. These time-points (16, 24, 36 and 48 hours) were selected in order to show the phases of morphological development from production of vegetative hyphae, through growth of aerial hyphae to the production of differentiated spores. In this way the role of the *mce* operon in *S. coelicolor* development could be addressed.

Following harvest of biomass and RNA isolation, samples were processed using a one-step reverse transcription (RT) PCR reaction. Two pairs of primers were used in each reaction; one for amplification of the gene of interest and another for amplification of the *S. coelicolor* housekeeping gene *hrdB* which is expressed at a

consistent level throughout exponential growth (Kang *et al.*, 1997). In this way it was possible to normalise the expression level of the gene of interest using the analysis function in GeneTools (Syngene), providing a semi-quantitative measure of transcription activity.

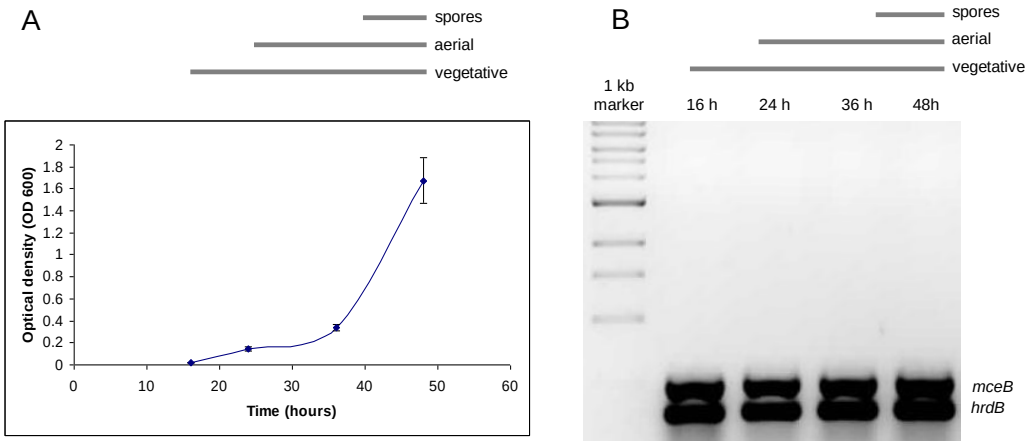

Figure 6.1: Expression of *hrdB* and *mceB* in wild-type *S. coelicolor* grown on MS medium. A: Solid-phase growth curve showing 16, 24, 36 and 48 hour timepoints. B: RTPCR analysis of gene expression at the same timepoints using primers for *hrdB* and *mceB*. Expression of *mceB* is consistent at all stages of morphological development, and brightness of the *mceB* band is approximately 30% that of *hrdB*. Data is representative of 2 experiments (growth curve) and 6 experiments (RT reaction). Comparable expression data are obtained using primers for other *mce* genes (data not shown). Gel: 0.8% agarose, 10 µl reaction initially containing 200 ng RNA per lane.

The results of the solid-phase growth curve show that expression of the *mce* cluster genes is consistent at a low level throughout all phases of development (Fig. 6.1). The level of *mceB* expression was approximately 30% of that of *hrdB*, and comparable results were obtained when assaying expression of the other *mce* cluster genes. There was no difference in expression level between the different genes in the *mce* cluster, which is the expected result if the genes in the cluster are co-transcribed.

It is interesting that the *mce* genes are not expressed at a higher level during production of aerial hyphae or spore differentiation as the wrinkled spore phenotype described in chapter 4 would indicate that the *mce* genes may play a role in morphological differentiation. It is possible that they do this at the post-transcriptional/post-translational level without a corresponding increase in expression, or that the *mce* gene products interact with another factor that is specific to morphological differentiation.

The relatively low level of *mce* expression in *S. coelicolor* is consistent with predictions made on the basis of codon usage (Wu *et al.*, 2006), although it is interesting that *mce* expression generally appears to be stronger in pathogenic actinomycetes, where expression levels are consistent with those of housekeeping genes. However, where more than one *mce* operon is present in the genome, temporal expression appears to be a feature of *mce* expression (Kumar *et al.*, 2003; Kumar *et al.*, 2005). These differences may be due to the different mechanisms of *mce* regulation between species, and/or the presence of multiple copies of the *mce* operon in pathogenic species. Regulation of the *S. coelicolor mce* operon is addressed later in this chapter.

mce expression in the presence of cholesterol

As discussed in chapter 1, the *mce* operon in *M. tuberculosis* has been identified as a cholesterol importer (Mohn *et al.*, 2008). For this reason the effect of cholesterol on *mce* expression in *S. coelicolor* was also investigated by adding cholesterol to the growth medium to a concentration of 0.01%. Due to the slower growth and lower

biomass of *S. coelicolor* on this medium, only the last (48 hour) time-point was harvested for RNA isolation.

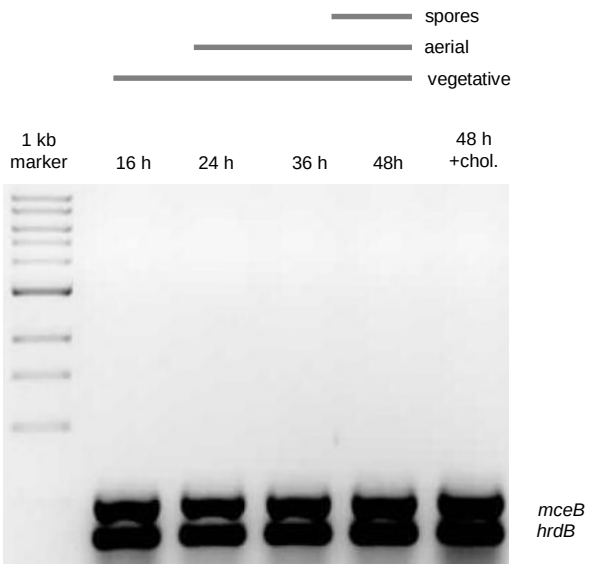

Figure 6.2: Expression of *hrdB* and *mceB* in M145 grown on minimal medium in the presence and absence of 0.01% cholesterol. The presence of 0.01% cholesterol does not appear to affect expression of *hrdB* or *mceB*.

At this low concentration of cholesterol there appeared to be no significant effect on *mce* expression (Fig. 6.2). Although the *mceB* band appears to be slightly brighter (approximately 5%) relative to *hrdB* (brightness measured using GeneTools), this difference falls within the variation seen in the time-course without cholesterol. It is also possible that any effect on transcription may in fact be due to the slower growth of *S. coelicolor* on cholesterol and not a direct effect of the cholesterol itself. This result was replicated using primers for other *mce* genes (*mceE*, *mceF*; results not shown).

The bacterial strains from which RNA was harvested were grown on solid minimal medium supplemented with 0.01% cholesterol in order to eliminate the possibility of cholesterol analogues (e.g. phytosterols from soy flour) being present in the medium. However, the combination of a nutrient-poor medium and growth on cellophane significantly slowed the growth of the bacterium. Growth rate can have a profound effect on gene expression (McMahon *et al.*, 1997), so to eliminate this factor the experiment was repeated using solid YEME (containing glucose) which is a richer nutrient source. The concentration of cholesterol in the medium was also doubled to 0.02% in an effort to enhance any transcriptional effects (Fig. 6.3).

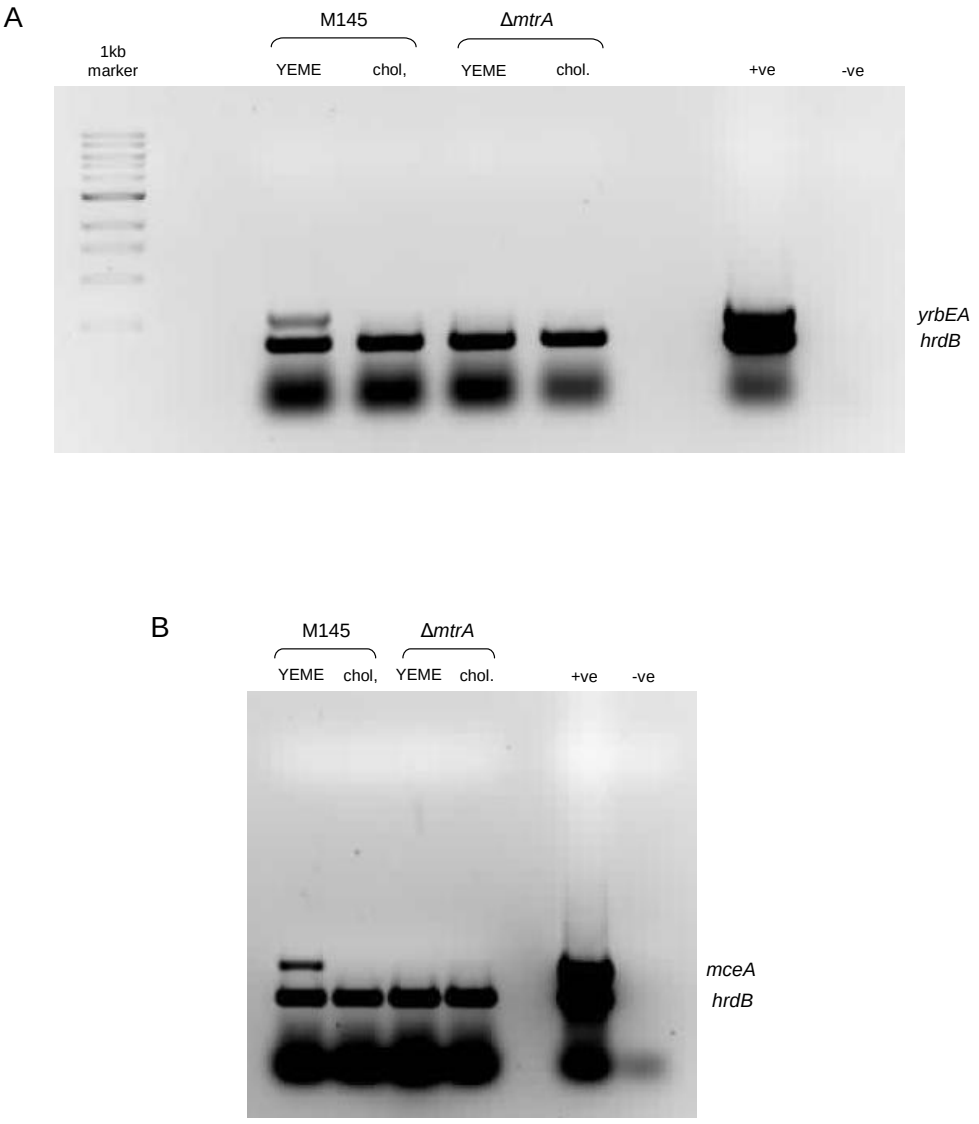

Figure 6.3A: A: Expression of *hrdB* and *yrbEA* in wild-type and Δ*mtrA* strains grown on YEME in the presence and absence of 0.02% cholesterol. Positive control: M145 genomic DNA template. Gel: 0.8% agarose, 10 µl reaction initially containing 200 ng RNA per lane. B: Expression of *hrdB* and *mceA* in wild-type and Δ*mtrA* strains grown on YEME in the presence and absence of 0.02% cholesterol. Positive control: M145 genomic DNA template. Gel: 0.8% agarose, 10 µl reaction initially containing 200 ng RNA per lane.

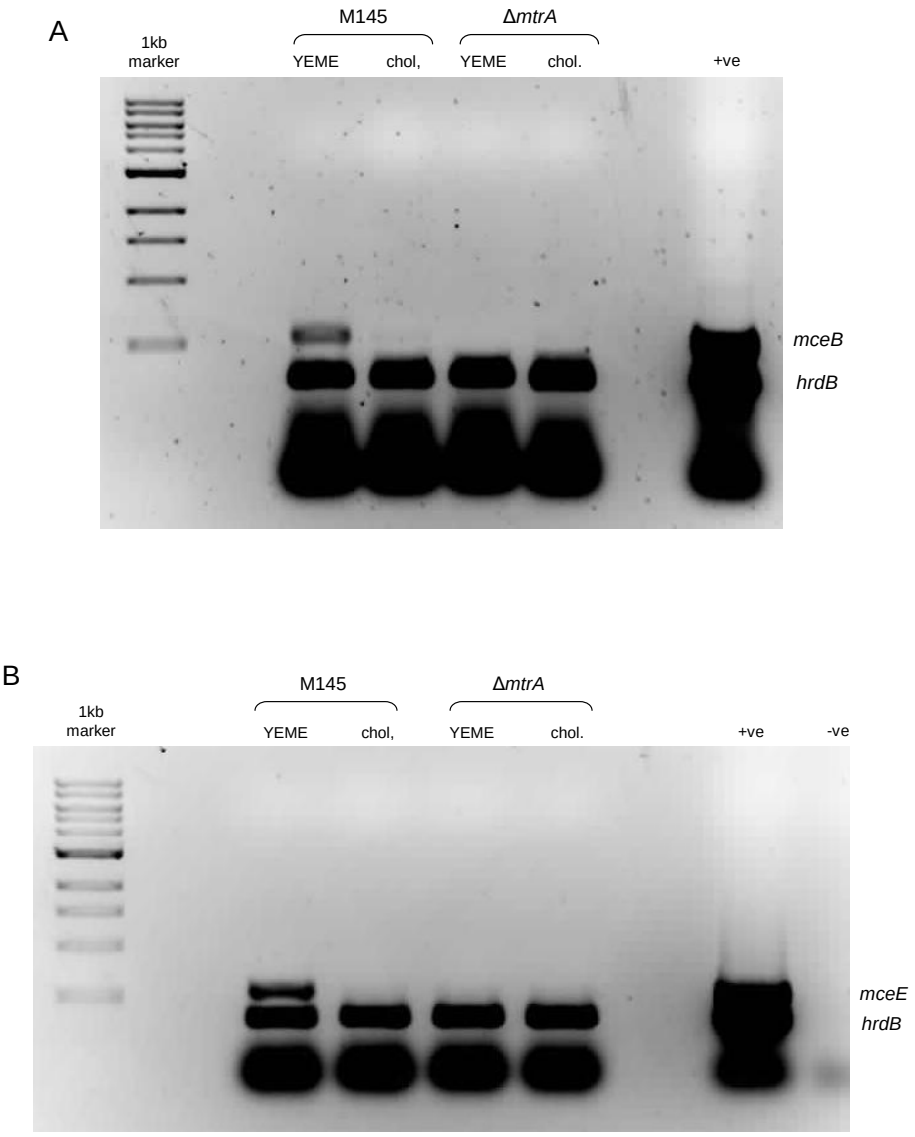

Figure 6.3B: A: Expression of *hrdB* and *mceB* in wild-type and Δ*mtrA* strains grown on YEME in the presence and absence of 0.02% cholesterol. Positive control: M145 genomic DNA template. Gel: 0.8% agarose, 10 µl reaction initially containing 200 ng RNA per lane. B: Expression of *hrdB* and *mceE* in wild-type and Δ*mtrA* strains grown on YEME in the presence and absence of 0.02% cholesterol. Positive control: M145 genomic DNA template. Gel: 0.8% agarose, 10 µl reaction initially containing 200 ng RNA per lane.

On changing the medium used and doubling the cholesterol concentration it was observed that *mce* expression on this medium appears to be repressed (Fig. 6.3). An extremely low level of *mceB* expression was observed (less than 5% of that of *hrdB*), but no other screened *mce* genes (*yrbEA*, *mceA*, *mceE*) were detected, even at a low level. The *hrdB* controls appeared normal which suggest that this result was not due to degradation of the RNA sample.

This result suggests that *mce* expression is downregulated in the presence of cholesterol, either directly (repression of *mce* expression in response to the presence of its own substrate) or indirectly (cholesterol is imported via another mechanism and subsequently results in repression of the *mce* operon).

Repression of the *mce* operon in the presence of cholesterol could explain the phenotype which is observed in co-culture with amoebae, in which the *mce* mutants appear to germinate and grow more rapidly than the wild-type in the intracellular environment. If the *mce* operon is repressed under these conditions, the *mce* multiple knockout has a "head start" over the wild-type. This corresponds with the observed results in which the wild-type strain displays the same behaviour as the multiple knockout but with a delay of several hours.

Downregulation of the *mce* cluster in the presence of cholesterol is inconsistent with results observed in pathogenic actinomycetes (Mohn *et al.*, 2008; Pandey and Sassetti, 2008), perhaps reflecting the differences in the regulatory systems governing *mce* expression in these organisms. It is possible that in *S. coelicolor* the Mce assembly is involved in low-abundance scavenging of sterols, and that at high abundance a different mechanism is used (Hodgson, 2000). Alternatively, *mce* expression in *S. coelicolor* may be induced by a sterol other than cholesterol.

Regulation of the *mce* operon

Bioinformatic analysis, mutational and expression studies (Casali *et al.*, 2006) have shown that in *M. tuberculosis* the *mce1* operon is negatively regulated by a GntR-like

regulator homologous to the FadR subfamily, Mce1R. Additionally, the *mce2* operon is negatively regulated by Mce2R, and the *mce3* operon is negatively regulated by a TetR family regulator Mce3R (Santangelo *et al.*, 2009; Santangelo *et al.*, 2008).

S. coelicolor does not have any genes that show significant homology to these regulators, and analysis of the region surrounding the *mce* operon does not reveal any other likely candidates for *mce* regulation (see chapter 3). This raises the question of whether the *S. coelicolor mce* operon has a specific regulator, and if so, what is the nature of the regulation?

The *mtrAB-lpqB* gene cluster encodes a two-component response regulator (MtrAB) and the associated lipoprotein LpqB (Fig. 6.4). The operon was initially identified in *M. tuberculosis* where it is essential, but homologues are present in *S. coelicolor*, *M. avium* and, interestingly, *M. leprae*, an organism which has lost most of its two-component regulators. The operon has been shown to be upregulated in *M. tuberculosis* during macrophage infection, and overexpression of MtrA inhibits cell division under the same conditions (Hoskisson and Hutchings, 2006; Nguyen *et al.*).

Microarray analysis of gene expression in a *M. avium mtrB* disruption mutant showed reduced expression of a number of genes including three of the nine *mce* genes. The mutant phenotype included increased sensitivity to β-lactam antibiotics, thought to be due to cell wall defects possibly as a result of reduced *mce* expression. Thus, the *mtrAB* two-component system was identified as a putative regulator of the *mce* operon in the actinomycetes (Hoskisson and Hutchings, 2006; Nguyen *et al.*). Increased antibiotic sensitivity is difficult to assay in *S. coelicolor* due to its intrinsic resistance to many antibiotics, and this problem is compounded when antibiotic resistance markers are used in the construction of mutant strains.

Figure 6.4: The *mtrAB-lpqB* operon (5741 bp) in *S. coelicolor*. SCO3014 (white) is a putative translation initiation factor. Also shown are SCO3013 (*mtrA*, cytoplasmic response regulator), SCO3012 (*mtrB*, transmembrane sensor kinase) and SCO3011 (*lpqB*, lipoprotein).

An experiment was conducted to examine the putative role of *mtrA* as a regulator of *mce*. Wild-type and *mce* multiple knockout strains were assayed for expression of *mtrA* at a 48 hour time-point in the presence and the absence of cholesterol. It was observed that *mtrA* is expressed at a high level (97% *hrdB*) under all conditions in both strains (Fig. 6.5). It is difficult to draw conclusions about the role of *mtrA* in *mce* regulation from these data, but they do not rule out *mtrA* as the regulator.

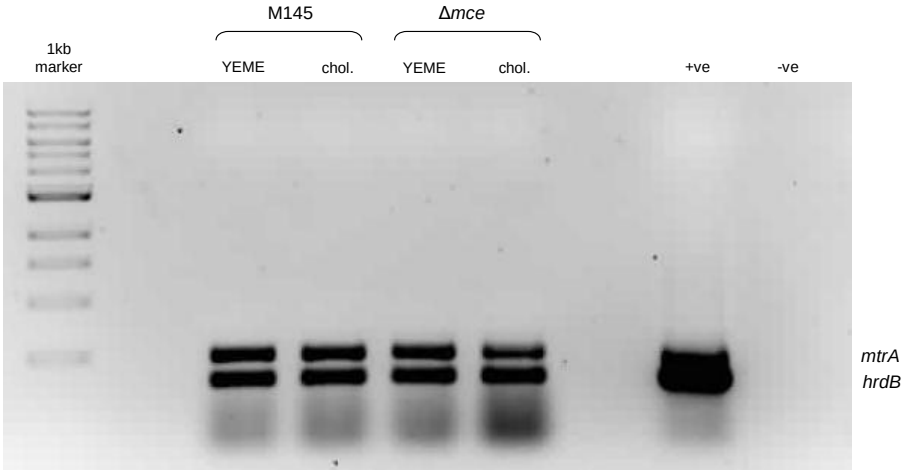

Figure 6.5: Expression of *hrdB* and *mtrA* in wild-type and Δ*mce* strains grown on YEME in the presence and absence of 0.02% cholesterol. Positive control: M145 genomic DNA template. Gel: 0.8% w/v agarose, 5 µl reaction initially containing 100 ng RNA per lane.

In order to clarify the role of *mtrA*, the inverse experiment was carried out to examine *mce* expression in an *mtrA* knockout. An *mtrA* mutant (Seipke and Hutchings, unpublished) was grown on solid YEME medium with and without cholesterol (0.02%) and harvested as for the *mce* mutant and wild-type strains. The *mtrA* mutant was examined using RT-PCR with primers for *hrdB* and *mce* genes *yrbEA*, *mceA*, *mceB* and *mceE* (Fig. 6.3).

This experiment showed that *mce* expression is abolished in the *mtrA* knockout in both the presence and absence of cholesterol. Not only does this support the hypothesis that *mtrA* has a regulatory role in *mce* expression, but it also supports the results of the *Acanthamoeba* plaque assay in which the *mtrA* mutant displayed a similar phenotype to the *mce* multiple knockout.

The fact that *mce* expression is abolished and not upregulated in the *mtrA* knockout implies that *mtrA* has a positive role in *mce* regulation; either by directly promoting *mce* transcription or by derepressing it. The reduction in *mce* expression in the *mtrA* mutant is consistent with the findings in *M. avium* in which expression of *mce* genes was reduced in an *mtrB* disruption mutant (Hoskisson and Hutchings, 2006).

It is interesting that the effect of *mtrA* deletion is the same as that of growing the wild-type strain on medium containing cholesterol. Without further experimentation it is not possible to say whether the *mtrAB* two-component system responds to the presence of cholesterol but this is one possible explanation of the experimental results.

Transcriptional coupling

An experiment was conducted to examine whether or not the genes of the *mce* operon are transcriptionally coupled. RT-PCR reactions were performed using primers situated in adjacent genes of the operon, with wild-type RNA as the template and genomic DNA as a positive control. Although the positive controls showed bands of the expected size (data not shown), there was no amplification from the

RNA samples. A control reaction using an RNA template with primers situated in the same gene showed amplification at the expected band size, indicating that lack of amplification in other reactions was not likely to be due to complete degradation of the RNA sample.

It is possible that there are internal promoters in the *mce* operon and that each gene of the operon is individually transcribed. However, it seems unlikely given the overlapping stop/start codons of many of the genes (see chapter 3). Alternatively, the RNA used in the experiment may not have been of sufficient quality to provide a reliable template over long stretches (upwards of 1 kb). Further experiments such as nuclear run-off and 5' RACE (rapid amplification of cDNA ends) would be necessary to clarify the lengths of the transcripts and the location of the transcriptional start point(s).

mce expression in amoebal co-culture

Having seen differential *mce* expression in the presence and absence of cholesterol, a RT-PCR experiment was done using RNA isolated from bacterial co-culture with *A. polyphaga* to see if the differential expression was replicated. Given the phenotype observed when *mce* mutants were co-cultured with *A. polyphaga* (see chapter 5) it seemed probable that a change in *mce* expression might be observed in co-cultured bacteria.

RNA was isolated from *A. polyphaga* alone, and from co-cultures of *A. polyphaga* with the wild-type M145 and the *mce* cluster knockout strains. RT-PCR was performed using primers for *hrdB* and *mceB*.

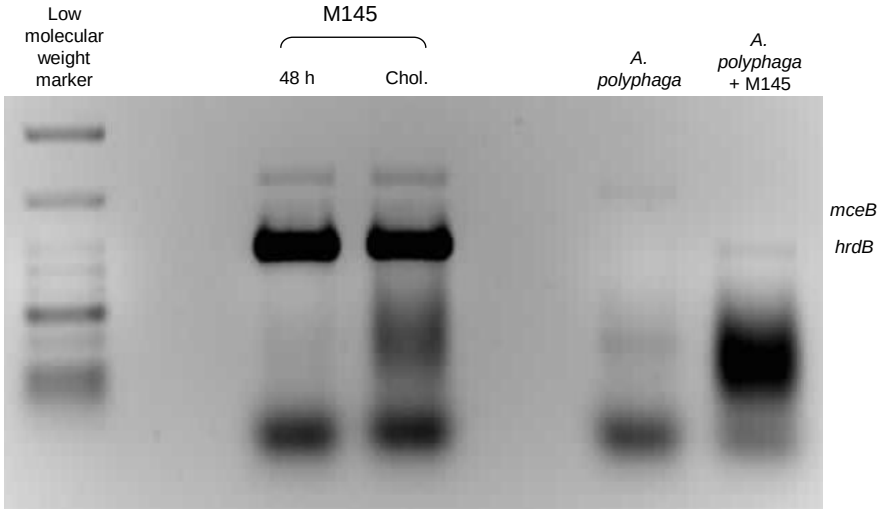

Figure 6.6: Expression of *hrdB* and *mceB* in M145 grown on MS in the presence and absence of 0.01% w/v cholesterol and M145 co-cultured with *A. polyphaga*. Gel: 0.8% w/v agarose.

The presence of bands in the *Acanthamoeba*-only lane that did not correspond to *hrdB* or *mceB* indicates non-specific amplification from one of the two primer pairs. The presence of a band corresponding to *hrdB* in the bacterial co-culture samples indicates the successful purification of bacterial RNA from the co-culture. However, the *hrdB* band is extremely faint, probably due to the comparatively low bacterial component in the sample, and it is likely that *mce* expression - if present - is at too low a level to be detected in this assay.

As with the live/dead assays described in chapter 5, it is difficult to separate the bacteria and the amoebae following co-culture. Amoebal RNA is purified extremely efficiently even when following a bacterial protocol, and the RNA-binding limit of the extraction columns (100 µg total RNA) is such that simply increasing the size of the co-culture will not lead to enrichment of the bacterial sample. A bacterial enrichment step prior to RNA isolation would be necessary in order to purify sufficient bacterial RNA for the RT-PCR reaction.

S. coelicolor mce expression in plant root-associated bacteria

Having observed a *mce* mutant phenotype in bacteria associated with plant roots (see chapter 5), an experiment was conducted in order to observe the effect of root association on the expression of the *mce* operon.

RNA was isolated from *A. thaliana* and *N. tabacum* alone, and from co-cultures of each plant species with the wild-type M145 strain and the *mce* cluster knockout strain. RT-PCR was performed using primers for *hrdB* and *mceB*. RNA isolation was performed using a bacterial protocol to minimise the amount of plant RNA that was isolated.

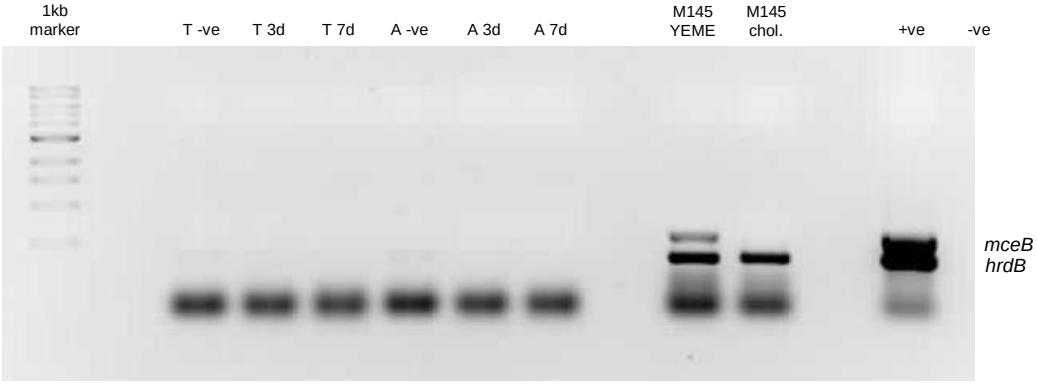

Figure 6.7: Expression of *hrdB* and *mceB* in plant samples at 3 and 7 days post-inoculation. T=*Nicotiana tabacum*, A=*Arabidopsis thaliana*. Positive control: M145 genomic DNA template. Gel: 0.8% w/v agarose, 10 µl RTPCR reaction per lane.

As with the *A. polyphaga* co-culture samples, the bacterial titre was very low following co-culture. Unfortunately there was no observed amplification of *hrdB* or the selected *mce* gene in any of the samples, suggesting that the bacterial RNA concentration was too low for effective reverse transcription.

Presence of *mce* genes in pathogenic *Streptomyces*

The putative role of the *mce* operon in *Streptomyces* pathogenesis suggests that one or more copies of the operon may be present in species such as *S. sudanensis* and *S. somaliensis*, which are pathogenic to humans and are endemic in tropical and sub-tropical areas such as Sudan (Quintana *et al.*, 2008). At the time of writing there was no genomic sequence data available for either of these strains, so the experiment was conducted using primers for selected *S. coelicolor mce* cluster genes (see Table 2.9, Materials and Methods).

Genomic DNA from three pathogenic *Streptomyces* species (two strains of *S. sudanensis*, SD509 and DSM41923, and one strain of *S. somaliensis*, DSM40738) was screened using PCR to see if any of the *mce* cluster genes could be amplified (Fig. 6.8). The PCR was performed three times using primers for the *S. coelicolor mce* cluster genes SCO2422, SCO2418 and SCO2415 (ATPase, *mceB*, *mceE*).

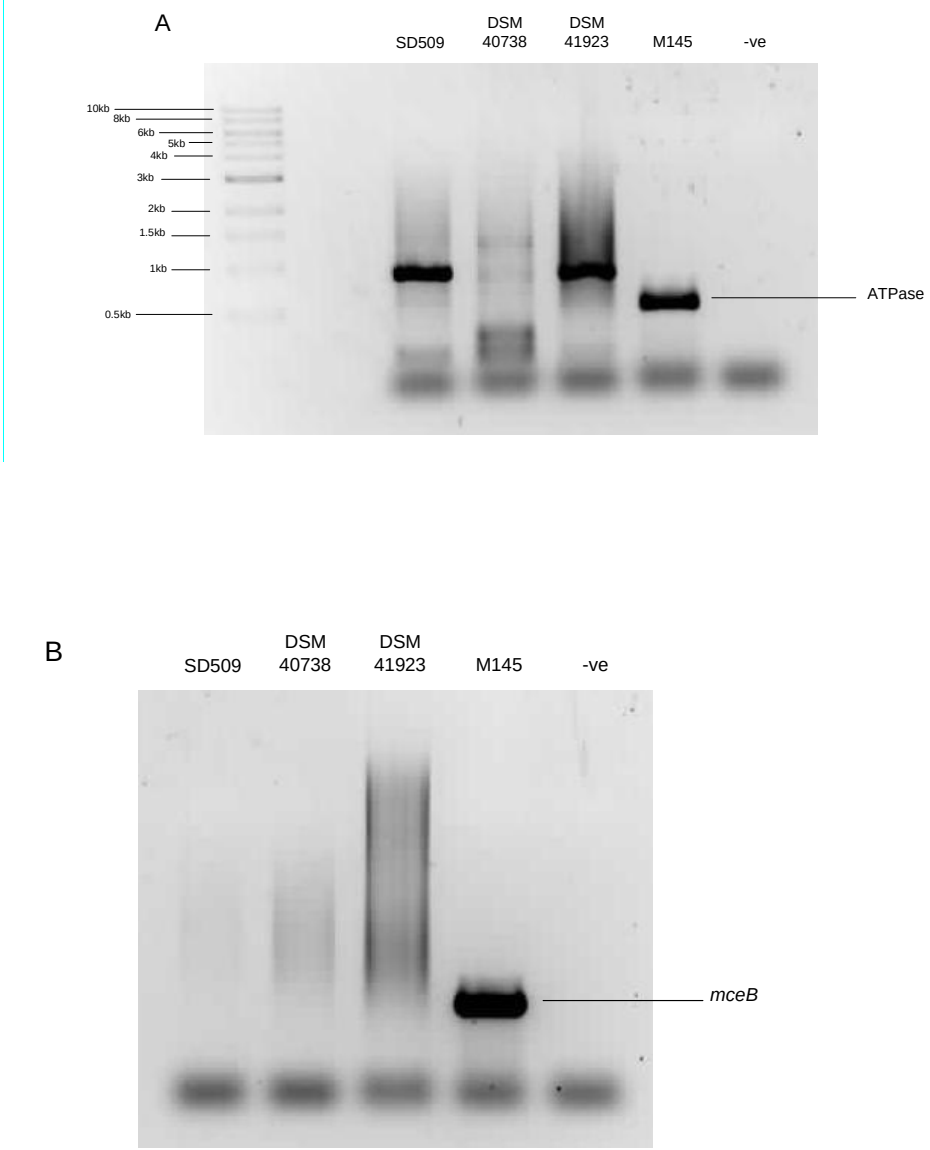

Figure 6.8A: A: PCR analysis of the SCO2422 (ATPase) gene in M145, *S. somaliensis* (DSM40738) and *S. sudanensis* (SD509 and DSM41923). B: PCR analysis of the *mceB* gene in M145, *S. somaliensis* (DSM40738) and *S. sudanensis* (SD509 and DSM41923).

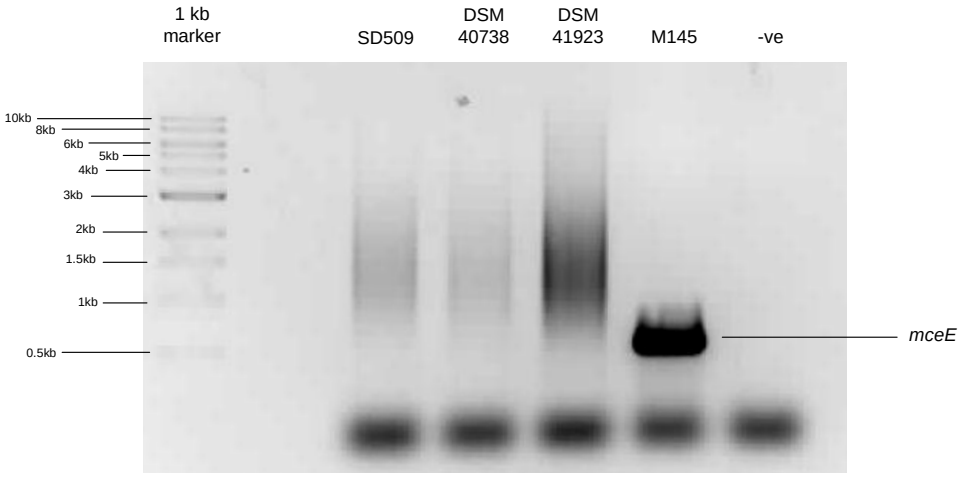

Figure 6.8B: PCR analysis of the *mceE* gene in M145, *S. somaliensis* (DSM40738) and *S. sudanensis* (SD509 and DSM41923).

Gel electrophoresis of the PCR product shows no amplification of either SCO2418 or SCO2415 when using DNA from the pathogenic species as a template. Both SD509 and DSM41923 show amplification of a product with primers designed against SCO2422, but the band size is approximately 375 bp larger that of the M145 control. This suggests that the amplification is non-specific, possibly the result of sequence similarity between SCO2422 and other ATPase-encoding genes in *S. sudanensis*.

The absence of amplification may be because the *S. coelicolor*-derived primers did not have sufficient sequence similarity with the other *Streptomyces* species to enable amplification of their target genes. Alternatively, the *mce* genes may not be present in these strains.

Expression of the Mce proteins

Following characterisation of gene expression in wild-type and two mutant strains a series of experiments were performed to investigate expression at the level of protein. A protein time-course similar to that used for RNA isolation was performed using the wild-type and *mce* cluster knockout strains, with samples taken at 16, 24, 36 and 48 hours (Fig. 6.9).

Following production of a crude lysate from the various time-points, growth conditions and strains, SDS PAGE and western blot were carried out to examine Mce expression. The primary antibody used for blotting was a rabbit polyclonal antibody raised against the *M. tuberculosis* Mce1A protein (a kind gift from Dr Lee Riley, University of California at Berkeley, USA), a modified protein of about 27 kDa in which 105 amino acids at the N-terminus were missing (Chitale *et al.*, 2001).

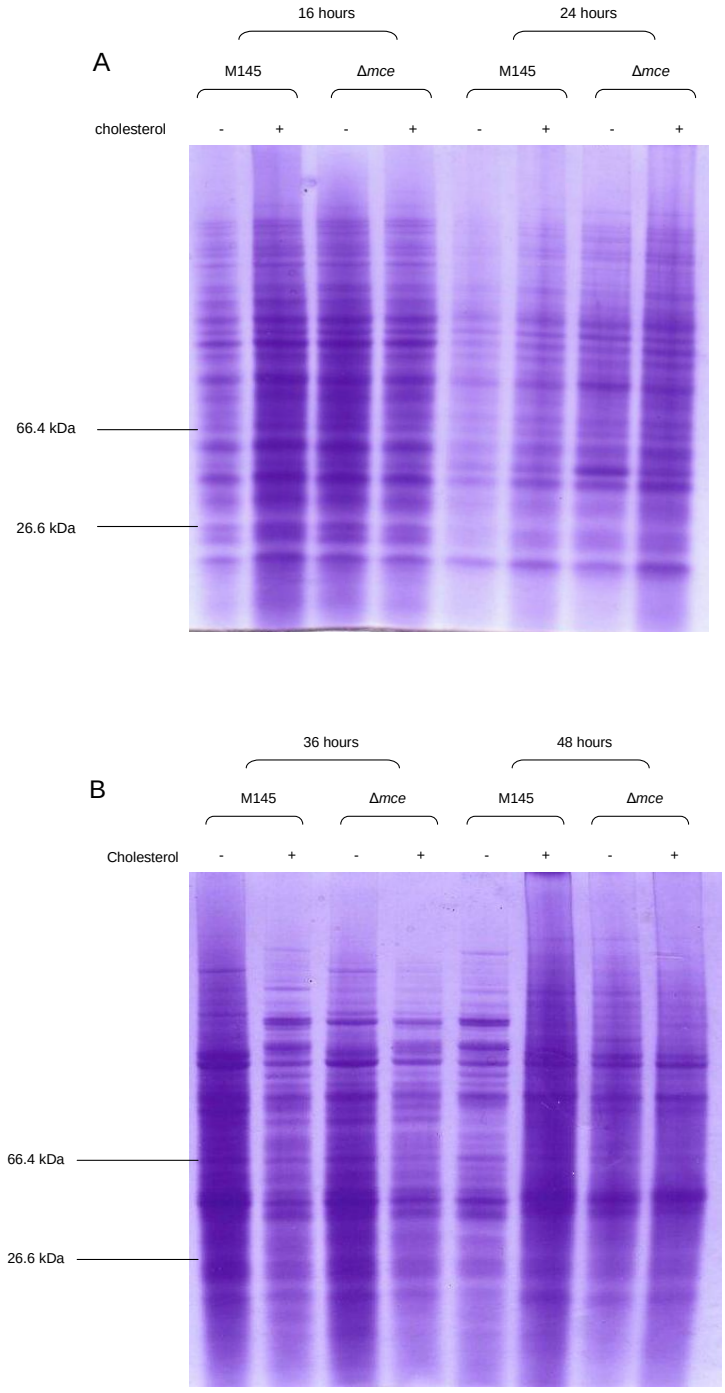

Figure 6.9: A: SDS-PAGE analysis of M145 and Δ*mce* strains at 16 and 24 hour time-points in the presence and absence of cholesterol. B: SDS-PAGE analysis of M145 and Δ*mce* strains at 36 and 48 hour time-points in the presence and absence of cholesterol.

On development of the blot a number of bands were visible (Fig. 6.10). However, none of these bands corresponded to the expected size of the Mce proteins, either singly (between 35.4 and 44.0 kDa) or as a hexamer (approximately 240 kDa). The most probable explanation for the bands is that they are due to non-specific binding of the antibody.

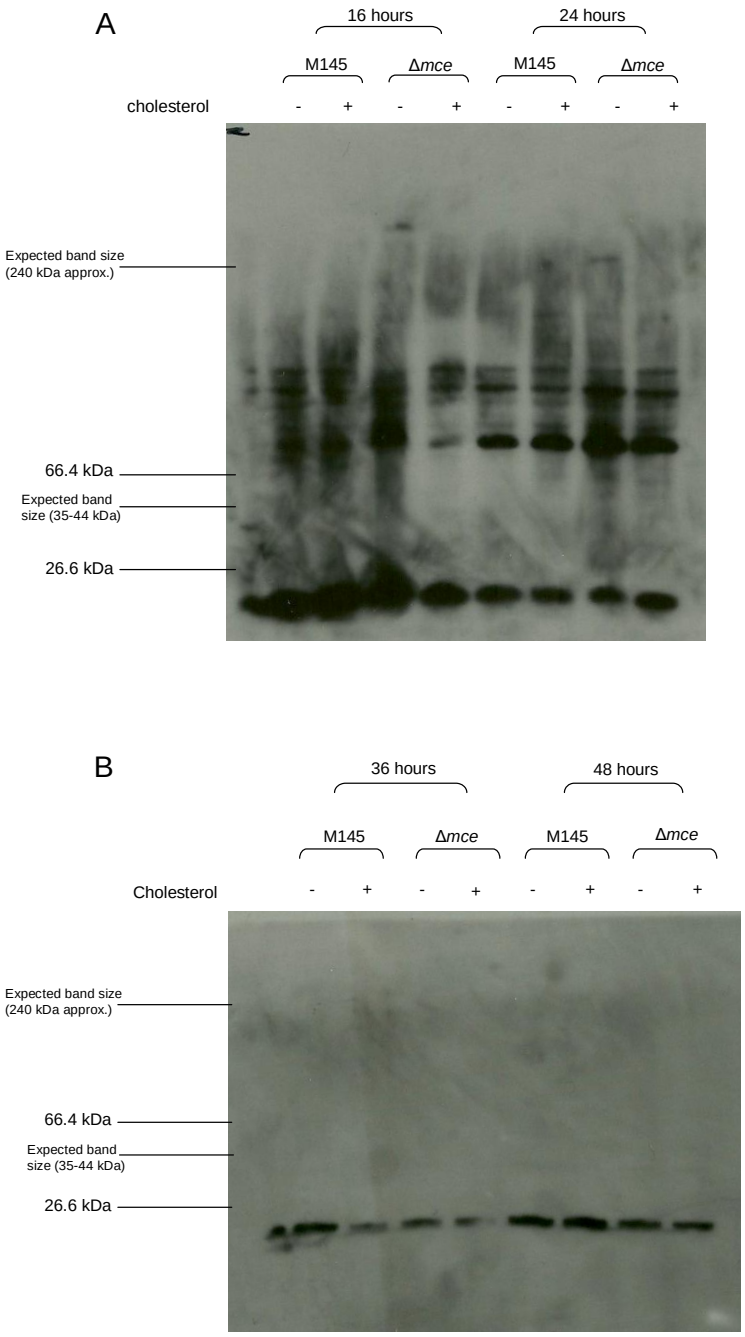

Figure 6.10: A: Western blot analysis of MceA expression. 16-24 hour time-points, M145 and Δ*mce* in the presence and absence of cholesterol, 5 minute exposure. B: Western blot analysis of MceA expression. 36-48 hour time-points, M145 and Δ*mce* in the presence and absence of cholesterol, 10 second exposure.

This hypothesis is supported by the fact that when the western blot was performed using a monoclonal antibody raised against the *M. tuberculosis* Mce1F protein (a kind gift from Dr Lee Riley, University of California at Berkeley, USA) (Chitale *et al.*, 2001) no bands were visible, suggesting that specific binding to the *S. coelicolor* Mce epitope does not occur using antibodies raised against *M. tuberculosis* proteins. It is also supported by the presence of identical bands in all lanes when using the Mce1A-derived probe, even where the sample was from the *mce* multiple knockout. Southern blot analysis (chapter 4 Fig. 4.7) and RT-PCR experiments (data not shown) confirm that there is no gene product from the *mce* operon in this strain, making it extremely unlikely that the bands correspond to Mce proteins.

The low level of amino acid sequence homology between *M. tuberculosis* and *S. coelicolor* MceA (31% identity) and MceF (30% identity) seen using BlastP analysis provides a likely explanation for the lack of cross-reaction between *M. tuberculosis*-derived antibodies and *S. coelicolor* Mce proteins (Sutcliffe, personal communication).

Overexpression of *mce* cluster genes

The *S. coelicolor* Mce proteins have not previously been purified. Selected Mce proteins from *M. tuberculosis* have been purified as recombinant proteins (Chitale *et al.*, 2001; El-Shazly *et al.*, 2007), however structural predictions are based largely on bioinformatic analysis (Das *et al.*, 2003).

An attempt was made to purify the *S. coelicolor* ATPase and MceE. SCO2422 and SCO2415 were amplified by PCR and ligated into the pET-100 Dtopo vector which contains a hexa-histidine sequence adjacent to the insertion site. The vector was sequenced to confirm the presence and orientation of the insert and subsequently used to transform the *E. coli* overexpression strain BL21 (see Materials and Methods).

Overexpression of the cloned *mce* genes was induced at 30ºC and 37ºC. The cells were harvested and lysed, and the crude lysate was analysed by SDS PAGE to assess the extent of overexpression (Fig. 6.11).

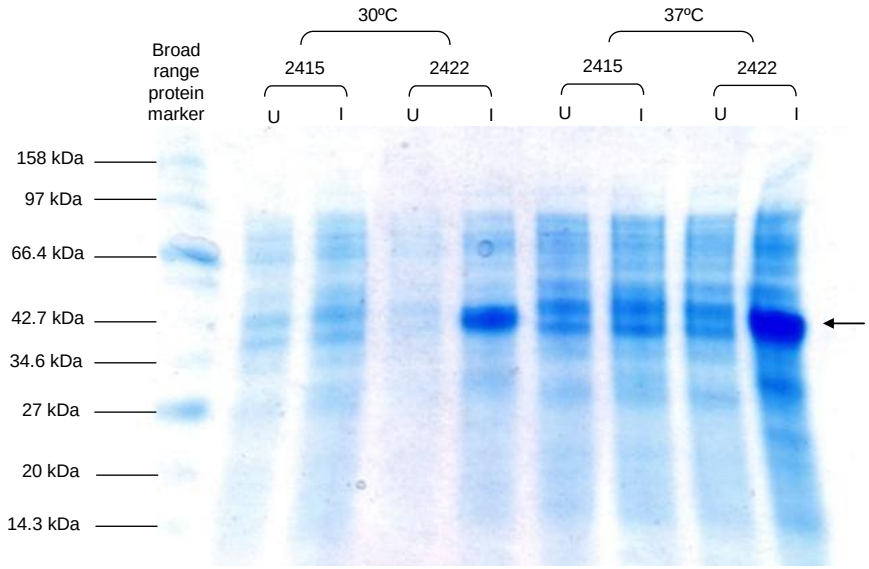

Figure 6.11A: Overexpression of Mce proteins MceE (2415) and ATPase (2422). A: SDS-PAGE showing induced (I) and uninduced (U) samples at 30ºC and 37ºC. Arrow indicates 44 kDa band corresponding to overexpression of the ATPase.

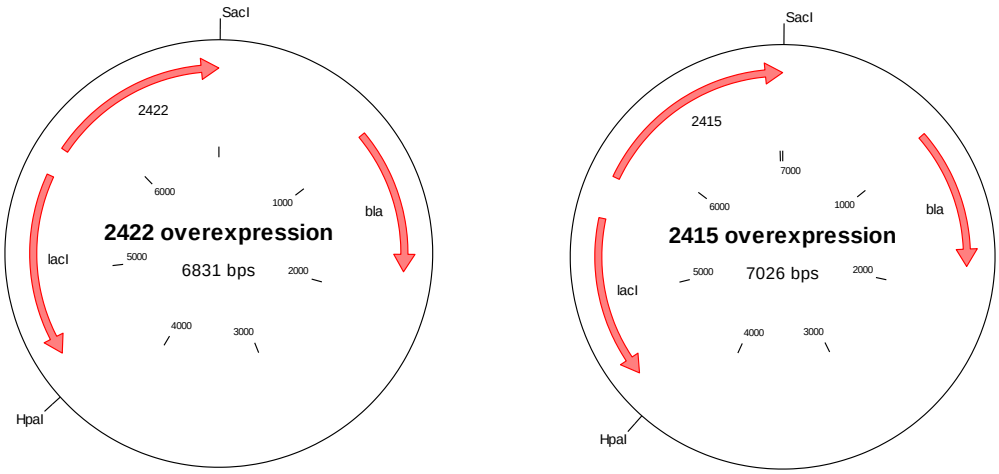

Figure 6.11B: overexpression vector maps showing insertion sites (2415/2422) in pET100D-topo vector.

The gels show overexpression at the predicted size for the Mce proteins (36.6 kDa; 42.7 kDa). The cell lysate was subsequently passed through a NiNTA column using an AKTA protein purification system in order to purify the polyhistidine-tagged Mce proteins.

The use of the AKTA allowed elution across a gradient of imidazole concentration. Unfortunately the protein purification was unsuccessful. The readout from the AKTA software did not show a peak corresponding to protein elution even at high concentrations of imidazole, indicating that the tagged protein may not have bound to the column. The induction was repeated but due to time constraints purification of the Mce proteins could not be completed.

GFP expression from the *mce* cluster

The transposon *Tn*5062 used to create the *mce* disruption mutants used in this study contains a promoterless EGFP gene. The transposon in each mutant is inserted in the correct orientation to (hypothetically) allow GFP expression; however, when examined microscopically, GFP expression was not detected in any of the transposon insertion mutants. This is probably due to two factors: a low level of expression of the *mce* cluster (as seen in the RT-PCR experiments) and thus of the EGFP, and the high level of autofluorescence generated by *S. coelicolor* under normal conditions, due to the prolific production of secondary metabolites which fluoresce under illumination at 530 nm.

Chapter 6 summary

The *mce* operon is expressed at a consistent, low level throughout all phases of morphological development on solid minimal medium and YEME. The addition of 0.02% cholesterol to the medium results in severely reduced or abolished expression of the *mce* genes, while having no effect on the expression of the housekeeping gene *hrdB*, or on the response regulator *mtrA*.

Deletion of the *mtrA* gene abolishes expression of the *S. coelicolor mce* genes, which is consistent with a previous study in *M. avium*. It also supports the putative role of the *mtrAB* cluster as a regulator of the *mce* operon.

Attempts to investigate *mce* expression in *S. coelicolor* when in co-culture with *A. polyphaga*, *A. thaliana* or *N. tabacum* were unsuccessful. An attempt to amplify the *mceB* and *mceE* genes in *S. sudanensis* and *S. somaliensis* did not produce amplification products, indicating that the *mce* cluster genes may not be present in these organisms, or that the sequence variation is great enough to preclude amplification using *S. coelicolor*-specific primers. Amplification using primers for the *mce* cluster ATPase produced amplification products in *S. sudanensis*, although these were not of the expected size and were likely due to the presence of similar ATPase-encoding domains in the genome, given the high level of conservation exhibited by this family.

Analysis of promoter activity using the EGFP contained in the *Tn*5062 insertion cassette was not successful.

Western blot analysis of a protein time course yielded non-specific binding of the Mce1A probe and a lack of binding specificity for Mce1F. This is probably due to lack of specificity of the *M. tuberculosis*-derived antibody for the *S. coelicolor* Mce proteins. Preliminary cloning and overexpression of His-tagged MceE and ATPase proteins from *S. coelicolor* at both 30ºC and 37ºC was successful, allowing for future work to purify and characterise the proteins at the functional level.

Chapter 7: Discussion

The major habitat of *Streptomyces coelicolor* is soil. In order to survive in this environment *S. coelicolor* must compete with other soil-dwelling organisms, and a number of mechanisms have been identified for defence against viral, bacterial, fungal and helminthic competitors. However, no dedicated mechanism has been identified in *S. coelicolor* for resistance to protozoal predation and little is known about the interaction of *S. coelicolor* with other features of the soil environment such as plant roots.

The *mce* gene cluster was identified as a virulence factor in *M. tuberculosis*, involved in entry to and survival within macrophages. The *mce* cluster is also present in *S. coelicolor* where its function is unknown. The widespread distribution of the *mce* cluster among the actinomycetes raises interesting questions about the evolutionary origins of the operon.

The *mce* operon is present in many newly-sequenced streptomycetes

The *mce* operon is widely distributed throughout the actinomycetes, and multiple sequence alignments demonstrate that it is well conserved at both the sequence and syntenic level. BLAST analysis using *S. coelicolor mce* nucleotide sequences shows that *mce* cluster genes are present in many newly-sequenced *Streptomyces* species which have not been included in previous bioinformatic analysis of the cluster.

Multiple copies of the *mce* operon are present in *S. AA4* and *S. pristinaespiralis*, probably as the result of a duplication event in the case of *S. AA4* and of horizontal gene transfer in *S. pristinaespiralis*.

Amplification of *mce* cluster genes in *S. somaliensis* and *S. sudanensis* using primers based on the sequences of SCO2422, SCO2418 and SCO2415 was unsuccessful, indicating that the *mce* cluster may not be present in these pathogenic streptomycetes, as with species such as *S. scabies*. Alternatively, there may be

insufficient sequence similarity between the species to allow amplification from primers based on the *S. coelicolor* sequence.

The highly conserved nature of the *mce* operon in both pathogenic and non-pathogenic species suggests that, although the operon has previously been identified as a virulence factor, it may have arisen as a result of selection pressures in the soil environment. It seems possible that the operon fulfils some function which, while allowing survival in the soil, also provides a selective advantage in the intracellular environment.

Streptomyces coelicolor mce mutants have unusual morphology

The hypothesis that the *mce* cluster may have a function distinct from its role as a virulence factor is supported by the detection of *mce* core-gene transcription at all stages of *S. coelicolor* morphological development. Disruption of all or part of the *mce* operon results in a morphological phenotype in which spore chains have a wrinkled appearance, and aberrant growth and premature germination is observed. This is similar to phenotypes which have been observed in *S. coelicolor* developmental mutants *mreBCD* and *mbl* (Mazza *et al.*, 2006).

In addition to changes in the appearance of the spores, their resistance to chemical and enzymatic lysis is increased when the *mce* operon is knocked out, with the *mce* multiple knockout displaying increased resistance to both lysozyme and SDS compared to the wild-type strain.

The mechanism by which these changes occur may be regulatory (the substrate imported by the Mce assembly plays a role in regulation of morphological development, perhaps as the ligand for a receptor) or mechanical (the substrate and/or the Mce assembly itself forms part of the cell envelope, with disruption resulting in physical changes to the envelope).

The *Streptomyces coelicolor* Mce assembly may be a cholesterol importer

RT-PCR analysis of *mce* expression shows that, when grown on 0.02% cholesterol, *mce* expression is abolished. Although this does not conclusively prove that cholesterol is the substrate for the Mce assembly, it suggests that this might be the case. One possibility is that the *mce* operon encodes a high-affinity, low-capacity transporter for cholesterol. In times of low cholesterol abundance the transporter acts as a scavenger, while in times of high abundance an alternative cholesterol import mechanism is active and the *mce* operon is downregulated. Another possibility is that the Mce assembly is able to import a number of different substrates, for instance different sterols such as ergosterol (found in *A. polyphaga*) or β-sitosterol (found in plants) (Dinel *et al.*, 2001; Khan, 2009).

The presence of cholesterol oxidase (SCO4781) and esterase (SCO5420) genes in the *S. coelicolor* genome indicate that this organism is capable of metabolising cholesterol. Fatty acid biosynthesis and degradation have been shown to occur, and play an important role in maintaining the cell envelope (Arabolaza *et al.*, 2010; Banchio and Gramajo, 1997; Hodgson, 2000).

Disruption of the *mce* cluster causes hypervirulence in co-culture with amoebae

The phenotypic difference between the *mce* multiple knockout and the wild-type M145 strain are most apparent when the bacteria are co-cultured with eukaryotic organisms. The *mce* multiple knockout displays hypervirulence in co-culture with the protozoan *A. polyphaga* and decreased colonisation in plant species *A. thaliana* and *N. tabacum*.

This phenotype has parallels with those observed in *M. tuberculosis mce* knockout experiments. Although these mutants are typically characterised as being attenuated, this refers to the phenotype that is observed in a whole-organism infection model. Where single-cell assays were used, a hypervirulent phenotype was observed in some cases (Lima *et al.*, 2007; Shimono *et al.*, 2003). It was also noted that the route of

infection in a mouse model had an effect on the outcome of the infection, leading to the conclusion that the prevailing immunological conditions played a large role in infection outcome (Casali and Riley, 2007).

Again there are a number of possible mechanisms by which the hypervirulent *mce* knockout phenotype may occur. One possibility is that the presence of cholesterol analogues (e.g. ergosterol in *A. polyphaga*) which are imported into the bacterial cell is an indication to the bacterium that it is in an intracellular environment, as these substances are not typically available at high concentration in soil (Dinel *et al.*, 2001). The imported sterol may then interact with a response regulator leading to modification of gene expression in the bacterium.

Although this hypervirulence may appear to be a gain of function in the context of a controlled laboratory environment, it is possible that in the more complex soil environment it would prove to be disadvantageous. It is also possible that the morphological phenotype observed in the *mce* mutants may prove to be disadvantageous to an extent that outweighs the apparent advantages of the mutation in co-culture.

Rather than arising from alteration in gene or protein expression, it is also possible that the hypervirulent phenotype of the *mce* mutants is the result of chemical and biophysical alterations in the bacterial cell envelope as a direct result of either loss of the membrane-associated Mce assembly, or loss of cholesterol (or its analogues) from the membrane. This hypothesis is probably the simplest way to account for the phenotype. However, an *esxBA* mutant which displays morphological alteration of the cell membrane (San Roman *et al.*, 2010) did not display hypervirulence in co-culture with *Acanthamoeba*. This suggests that the hypervirulent phenotype of the *mce* mutants is specific to loss of the *mce* operon and not a general feature of altered cell envelope morphology.

The observed increase in spore resistance to SDS and lysozyme may be relevant to the hypervirulence observed in co-culture, in that avoiding lysis by the amoebal

lysosome is a key factor in intracellular survival of bacteria in co-culture. Lysozyme is a chief component of the lysosome (Haas, 2007; Khan, 2009) and resistance to it may therefore prove to be advantageous.

The *mce* phenotype is dose-dependent and rescued by complementation

There is no evidence of polar effects resulting from the disruption of genes near the start of the operon. The phenotype resulting from the *mce* multiple knockout was more severe than those of the single-gene disruption mutants, indicating that the Mce assembly retains some of its function when single components are disrupted.

It is possible that the Mce substrate-binding domain does not require a specific ABC assembly to function but rather can operate as an "orphan" receptor (Thomas, 2010). It is also possible that, if the Mce substrate-binding domain functions as a hexamer, it is also able to bind its substrate if one of its monomers is missing.

The *mce* multiple knockout phenotype can be complemented by reintroduction of the complete *mce* operon into the genome. Interestingly, introduction of an additional copy of the *mce* locus into the wild-type strain results in a phenotype that is opposite to that of the *mce* knockout mutant; reduced virulence in co-culture with *A. polyphaga*.

The implication of this result is that the effect of the *mce* operon is dose-dependent. This conclusion is supported by the variation in *mce* copy number seen throughout the actinomycetes. It also highlights the potential importance of *mce* regulation, as the level of transcription is likely to have a profound effect on phenotype.

The *mtrA* locus encodes a putative regulator of *mce*

A regulator has been identified for each of the four *mce* operons in *M. tuberculosis*, and there is evidence to suggest that expression of the operons is temporally differentiated (Santangelo *et al.*, 2009; Santangelo *et al.*, 2008). Bioinformatic

analysis shows homologues of the *M. tuberculosis* regulators in several other actinomycetes with multiple copies of the *mce* operon, including several Mycobacterial species, *Rhodococcus* and *Nocardia*.

This may reflect a need for temporal expression where multiple copies of the operon are present, suggesting that each copy of the operon may perform a slightly different function. However, it is not clear whether temporal expression is a feature of organisms other than *M. tuberculosis*.

Streptomyces species *e14* and *AA4* also have predicted proteins showing some homology to the Mce1R regulator, and *S. coelicolor* has putative homologues of both Mce2R and Mce4R, although not associated with the *mce* cluster. However, the low percentage identities of the *Streptomyces* homologues, and the presence of a number of GntR-like and TetR-like repressors in *Streptomyces*, suggest that these repressors may have no specific affinity for the *mce* operon.

The *S. coelicolor mtrA* locus had previously been identified as a putative regulator of the *mce* operon (Hoskisson and Hutchings, 2006), and no other likely candidate regulators have yet been identified in the *S. coelicolor* genome. Experiments using an *mtrA* mutant showed that it displayed the same phenotype in co-culture as the *mce* multiple knockout.

The results of these experiments suggest that *mtrA* acts as a regulator of the *mce* operon in *S. coelicolor*. Disruption of *mtrA* results in loss of *mce* expression, indicating that the regulation is positive. This is in contrast to *M. tuberculosis* in which regulation of all four *mce* operons is negative.

The *mce* operon is involved in the colonisation of plant roots

Experiments with *N. tabacum* and *A. thaliana* showed that the *S. coelicolor* Δ*mce* strain had a reduced ability to colonise the plant roots, a phenotype that could be restored by replacing the *mce* operon. This suggests that the *mce* operon plays a role

in root colonisation. However, it was noted that the bacteria do not penetrate the plant cells, suggesting that the mechanism of colonisation may be different from the behaviour exhibited in co-culture with *Acanthamoeba*. Interestingly, there was no difference between the wild-type strain and one which contained an additional copy of the *mce* operon.

The *mce* operon may have originated as a survival mechanism in soil

Taken together, the results of these experiments show that the *mce* cluster has a role beyond that of virulence factor. The operon plays a part, probably indirectly, in morphological development and spore maturation. It also seems probable that the Mce assembly in *S. coelicolor* is a cholesterol importer.

Of particular interest is the role of the operon in intracellular survival of bacteria in co-culture with eukaryotes. Although *S. coelicolor* is typically considered to be non-pathogenic, it is able to act as a pathogen in the context of the co-culture assay. This is analogous to the behaviour of *M. tuberculosis* in association with macrophages.

The hypervirulence of the *mce* multiple knockout suggests that a possible role of the Mce assembly is transport of a substrate that is specific to the eukaryotic intracellular milieu. In this way it might be possible for the bacterial cell to sense whether it is in an intracellular environment by the presence or absence of the substrate.

More broadly, these results raise the possibility that the *mce* operon evolved initially as a survival mechanism in the soil environment. Like many other proteins with a specific cellular function (for instance siderophores, DNA-binding proteins (Crack *et al.*, 2009)), the Mce assembly may have been subject to the selection pressures of the eukaryotic intracellular environment in actinomycetes which had adapted to become mammalian pathogens. Subsequent duplication of the operon and the development of regulatory systems allowed adaptation of the operon to become a key virulence factor in species such as *M. tuberculosis*.

Future work

The deletion of the *mce* genes results in a phenotype that appears to represent a gain of function when screened using standard laboratory techniques. Although such gain of function mutations have been described before (ten Bokum *et al.*, 2008), they are unusual, especially when they are the result of a large deletion. An interesting experiment would therefore be to assay the *mce* multiple knockout for survival in the soil, relative to the wild-type strain. In this way it might be possible to identify a loss of function phenotype resulting from the mutation.

It is interesting to note that the species with the highest copy number of the *mce* operon are mainly facultative intracellular pathogens. *M. leprae*, which is an obligate intracellular pathogen, has a single copy and *S. scabies*, which is not a mammalian pathogen, lacks the *mce* operon altogether.

One possibility is that the *mce* operon is involved in the transition from one environment to another; from soil to cell. If the operon encodes a cholesterol (or cholesterol analogue) importer, it is possible that the presence or absence of cholesterol is one way in which the bacterial cell is able to sense its environment. Free cholesterol is not commonly found in high concentrations in the soil and so its availability would indicate that the bacterium is in an intracellular environment.

This ability to sense environment is important; *M. tuberculosis* is able to survive in macrophages during latent infection by altering the behaviour of the host cell, and requires infection-specific pathways that allow it to do this. Failure to modify its own behaviour once inside a macrophage would result in rapid clearing of the infection by the host immune system.

Further to the phylogenetic studies presented here, it may be possible to gain a clearer insight into the evolutionary history of the *mce* operon by extending the analysis to include comparisons of synonymous and non-synonymous substitutions across species. The ongoing discovery and genomic sequencing of novel

actinomycetes will add to the available data and provide a broader picture of *mce* distribution, particularly in non-pathogenic and non-industrial species.

Structural knowledge about the Mce proteins is still largely based on bioinformatic analysis. The *S. coelicolor* MceE and ATPase were overexpressed, and successful purification of these proteins would allow a range of studies to be conducted. These could include ATP cycling experiments to identify a possible substrate, pull-down experiments and mass spectrometry to clarify the conformation of the Mce proteins. This could clarify whether the proteins encoded by the six *mce* genes exist as monomers or multimers.

Another interesting question is that of *mce* regulation. The *mtrA* region was identified as encoding a putative regulator and experiments such as S1 mapping, DNase1 footprinting and EMSA could clarify whether there is a binding site for MtrA in the upstream region of the *mce* cluster.

The fate of cholesterol in the *S. coelicolor* cell is poorly understood; experiments using labelled cholesterol could elucidate the uptake and subsequent metabolism of this molecule by *S. coelicolor*. Thin-layer chromatography (TLC) could also be used to compare the lipid profiles of wild-type and *mce* mutant *S. coelicolor*.

Conclusion

There is much work still to be done before the role of the *mce* operon in *S. coelicolor* and the *Actinobacteria* can be fully understood. However, the data presented here provide a possible explanation for the presence of a virulence factor in a non-pathogenic organism and suggest an evolutionary origin for the operon as a mechanism of survival in the soil.

The bioinformatic analysis presented in chapter 3 updates and expands on previous reviews of the subject and includes a novel analysis of the predicted structure of the *S. coelicolor* Mce assembly. Phenotypic screening of *mce* mutants has allowed

identification of a Δ*mce* phenotype, and expression studies have shown the possible role of cholesterol in determining *mce* expression and confirmed the *mtrA* gene cluster a putative *mce* regulator.

This work also elucidates the interactions of *S. coelicolor* with its fellow soil inhabitants, both protozoa and plants, and the role of the *mce* operon in mediating these. The optimisation of an *Acanthamoeba*-based protocol for assaying the virulence of non-pathogenic mycelial bacteria will hopefully prove to be a useful addition to the microbiological toolkit.

The continuing discovery and genomic sequencing of novel actinomycetes, the possibility of obtaining the crystal structure of the Mce assembly, and the increased understanding of the complex interactions of microbial life in the environment will all contribute to the understanding of the *mce* cluster and the complicated and fascinating role it plays in the actinomycetes.

References

Adekambi, T., S. Ben Salah, M. Khlif, D. Raoult, and M. Drancourt. 2006. Survival of environmental mycobacteria in Acanthamoeba polyphaga. *Applied and Environmental Microbiology*. 72:5974-5981.

Adiba, S., C. Nizak, M. van Baalen, E. Denamur, and F. Depaulis. 2010. From Grazing Resistance to Pathogenesis: The Coincidental Evolution of Virulence Factors. *PLoS One*. 5:10.

Aguilar, L.D., E. Infante, M.V. Bianco, A. Cataldi, F. Bigi, and R.H. Pando. 2006. Immunogenicity and protection induced by Mycobacterium tuberculosis mce-2 and mce-3 mutants in a Balb/c mouse model of progressive pulmonary tuberculosis. *Vaccine*. 24:2333-2342.

Altschul, S.F., W. Gish, W. Miller, E.W. Myers, and D.J. Lipman. 1990. Basic Local Alignment Search Tool. *Journal of Molecular Biology*. 215:403-410.

Anderson, A.S., and E.M.H. Wellington. 2001. The taxonomy of Streptomyces and related genera. *International Journal of Systematic and Evolutionary Microbiology*. 51:797-814.

Aparicio, J.F., and J.F. Martin. 2008. Microbial cholesterol oxidases: bioconversion enzymes or signal proteins? *Mol. Biosyst.* 4:804-809.

Arabolaza, A., M. D'Angelo, S. Comba, and H. Gramajo. 2010. FasR, a novel class of transcriptional regulator, governs the activation of fatty acid biosynthesis genes in Streptomyces coelicolor. *Molecular Microbiology*. 78:47-63.

Arruda, S., G. Bomfim, R. Knights, T. Huimabyron, and L.W. Riley. 1993. Cloning of an Mycobacterium-Tuberculosis DNA Fragment Associated with Entry and Survival inside Cells. *Science*. 261:1454-1457.

Baltz, R.H. 2008. Renaissance in antibacterial discovery from actinomycetes. *Curr. Opin. Pharmacol.* 8:557-563.

Banchio, C., and H.C. Gramajo. 1997. Medium- and long-chain fatty acid uptake and utilization by Streptomyces coelicolor A3(2): First characterization of a Gram-positive bacterial system. *Microbiology-Uk*. 143:2439-2447.

Barona-Gomez, F., U. Wong, A.E. Giannakopulos, P.J. Derrick, and G.L. Challis. 2004. Identification of a cluster of genes that directs desferrioxamine biosynthesis in Streptomyces coelicolor M145. *J. Am. Chem. Soc.* 126:16282-16283.

Bendtsen, J.D., H. Nielsen, G. von Heijne, and S. Brunak. 2004. Improved prediction of signal peptides: SignalP 3.0. *Journal of Molecular Biology*. 340:783-795.

Bentley, S.D., K.F. Chater, A.M. Cerdeno-Tarraga, G.L. Challis, N.R. Thomson, K.D. James, D.E. Harris, M.A. Quail, H. Kieser, D. Harper, A. Bateman, S. Brown, G. Chandra, C.W. Chen, M. Collins, A. Cronin, A. Fraser, A. Goble, J. Hidalgo, T. Hornsby, S. Howarth, C.H. Huang, T. Kieser, L. Larke, L. Murphy, K. Oliver, S. O'Neil, E. Rabbinowitsch, M.A. Rajandream, K. Rutherford, S. Rutter, K. Seeger, D. Saunders, S. Sharp, R. Squares, S. Squares, K. Taylor, T. Warren, A. Wietzorrek, J. Woodward, B.G. Barrell, J. Parkhill, and D.A. Hopwood. 2002. Complete genome sequence of the model actinomycete Streptomyces coelicolor A3(2). *Nature*. 417:141-147.

Bentrup, K.H.Z., and D.G. Russell. 2001. Mycobacterial persistence: adaptation to a changing environment. *Trends in Microbiology*. 9:597-605.

Bertram, R., M. Schlicht, K. Mahr, H. Nothaft, M.H. Saier, and F. Titgemeyer. 2004. In silico and transcriptional analysis of carbohydrate uptake systems of Streptomyces coelicolor A3(2). *Journal of Bacteriology*. 186:1362-1373.

Bierman, M., R. Logan, K. Obrien, E.T. Seno, R.N. Rao, and B.E. Schoner. 1992. Plasmid Cloning Vectors for the Conjugal Transfer of DNA from Escherichia-Coli to Streptomyces Spp. *Gene*. 116:43-49.

Bignell, D.R.D., J.C. Huguet-Tapia, M.V. Joshi, G.S. Pettis, and R. Loria. 2010. What does it take to be a plant pathogen: genomic insights from Streptomyces species. *Antonie Van Leeuwenhoek*. 98.

Birnboim, H.C., and J. Doly. 1979. Rapid Alkaline Extraction Procedure for Screening Recombinant Plasmid DNA. *Nucleic Acids Research*. 7:1513-1523.

Bishop, A., S. Fielding, P. Dyson, and P. Herron. 2004. Systematic insertional mutagenesis of a streptomycete genome: A link between osmoadaptation and antibiotic production. *Genome Research*. 14:893-900.

Boulais, J., M. Trost, C.R. Landry, R. Dieckmann, E.D. Levy, T. Soldati, S.W. Michnick, P. Thibault, and M. Desjardins. 2010. Molecular characterization of the evolution of phagosomes. *Molecular Systems Biology*. 6.

Bradford, M.M. 1976. Rapid and Sensitive Method for Quantitation of Microgram Quantities of Protein Utilizing Principle of Protein-Dye Binding. *Analytical Biochemistry*. 72:248-254.

Brust, J.C.M., S. Whittier, B.E. Scully, C.C. McGregor, and M.T. Yin. 2009. Five cases of bacteraemia due to Gordonia species. *Journal of Medical Microbiology*. 58:1376-1378.

Brzostek, A., B. Dziadek, A. Rumijowska-Galewicz, J. Pawelczyk, and J. Dziadek. 2007. Cholesterol oxidase is required for virulence of Mycobacterium tuberculosis. *Fems Microbiology Letters*. 275:106-112.

Brzostek, A., J. Pawelczyk, A. Rumijowska-Galewicz, B. Dziadek, and J. Dziadek. 2009. Mycobacterium tuberculosis Is Able To Accumulate and Utilize Cholesterol. *Journal of Bacteriology*. 191:6584-6591.

Bucca, G., E. Laing, V. Mersinias, N. Allenby, D. Hurd, J. Holdstock, V. Brenner, M. Harrison, and C.P. Smith. 2009. Development and application of versatile high density microarrays for genome-wide analysis of Streptomyces coelicolor: characterization of the HspR regulon. *Genome Biol.* 10:14.

Buttner, M.J., I.M. Fearnley, and M.J. Bibb. 1987. The Agarase Gene (*dagA*) of *Streptomyces coelicolor* A3(2) - Nucleotide Sequence and Transcriptional Analysis. *Molecular & General Genetics*. 209:101-109.

Campbell, S.J., P.R. Ingram, C.W. Roberts, and F.L. Henriquez. 2008. Induced encystment improves resistance to preservation and storage of Acanthamoeba castellanii. *Parasitology*. 135:1401-1405.

Cangelosi, G.A., J.S. Do, R. Freeman, J.G. Bennett, M. Semret, and M.A. Behr. 2006. The two-component regulatory system mtrAB is required for morphotypic multidrug resistance in Mycobacterium avium. *Antimicrob. Agents Chemother.* 50:461-468.

Casali, N., and L.W. Riley. 2007. A phylogenomic analysis of the Actinomycetales mce operons. *Bmc Genomics*. 8.

Casali, N., A.M. White, and L.W. Riley. 2006. Regulation of the Mycobacterium tuberculosis mce1 operon. *Journal of Bacteriology*. 188:441-449.

Cascioferro, A., G. Delogu, M. Colone, M. Sali, A. Stringaro, G. Arancia, G. Fadda, G. Palu, and R. Manganelli. 2007. PE is a functional domain responsible for protein translocation and localization on mycobacterial cell wall. *Molecular Microbiology*. 66:1536-1547.

Chakraburtty, R., and M. Bibb. 1997. The ppGpp synthetase gene (relA) of Streptomyces coelicolor A3(2) play's a conditional role in antibiotic production and morphological differentiation. *Journal of Bacteriology*. 179:5854-5861.

Chater, K.F. 1998. Taking a genetic scalpel to the Streptomyces colony. *Microbiology-(UK)*. 144:1465-1478.

Chater, K.F., S. Biro, K.J. Lee, T. Palmer, and H. Schrempf. 2010. The complex extracellular biology of Streptomyces. *FEMS Microbiology Reviews*. 34:171-198.

Chater, K.F., and G. Chandra. 2006. The evolution of development in Streptomyces analysed by genome comparisons. *FEMS Microbiology Reviews*. 30:651-672.

Chitale, S., S. Ehrt, I. Kawamura, T. Fujimura, N. Shimono, N. Anand, S.W. Lu, L. Cohen-Gould, and L.W. Riley. 2001. Recombinant Mycobacterium tuberculosis protein associated with mammalian cell entry. *Cellular Microbiology*. 3:247-254.

Cirillo, J.D., S. Falkow, L.S. Tompkins, and L.E. Bermudez. 1997. Interaction of Mycobacterium avium with environmental amoebae enhances virulence. *Infection and Immunity*. 65:3759-3767.

Claessen, D., W. de Jong, L. Dijkhuizen, and H.A.B. Wosten. 2006. Regulation of Streptomyces development: reach for the sky! *Trends in Microbiology*. 14:313-319.

Claessen, D., I. Stokroos, H.J. Deelstra, N.A. Penninga, C. Bormann, J.A. Salas, L. Dijkhuizen, and H.A.B. Wosten. 2004. The formation of the rodlet layer of streptomycetes is the result of the interplay between rodlins and chaplins. *Molecular Microbiology*. 53:433-443.

Cole, S.T., R. Brosch, J. Parkhill, T. Garnier, C. Churcher, D. Harris, S.V. Gordon, K. Eiglmeier, S. Gas, C.E. Barry, F. Tekaia, K. Badcock, D. Basham, D. Brown, T. Chillingworth, R. Connor, R. Davies, K. Devlin, T. Feltwell, S. Gentles, N. Hamlin, S. Holroyd, T. Hornby, K. Jagels, A. Krogh, J. McLean, S. Moule, L. Murphy, K. Oliver, J. Osborne, M.A. Quail, M.A. Rajandream, J. Rogers, S. Rutter, K. Seeger, J. Skelton, R. Squares, S. Squares, J.E. Sulston, K. Taylor, S. Whitehead, and B.G. Barrell. 1998. Deciphering the biology of Mycobacterium tuberculosis from the complete genome sequence. *Nature*. 393:537-+.

Cole, S.T., K. Eiglmeier, J. Parkhill, K.D. James, N.R. Thomson, P.R. Wheeler, N. Honore, T. Garnier, C. Churcher, D. Harris, K. Mungall, D. Basham, D. Brown, T. Chillingworth, R. Connor, R.M. Davies, K. Devlin, S. Duthoy, T. Feltwell, A. Fraser, N. Hamlin, S. Holroyd, T. Hornsby, K. Jagels, C. Lacroix, J. Maclean, S. Moule, L. Murphy, K. Oliver, M.A. Quail, M.A. Rajandream, K.M. Rutherford, S. Rutter, K. Seeger, S. Simon, M. Simmonds, J. Skelton, R. Squares, S. Squares, K. Stevens, K. Taylor, S. Whitehead, J.R. Woodward, and B.G. Barrell. 2001. Massive gene decay in the leprosy bacillus. *Nature*. 409:1007-1011.

Crack, J.C., C.D. den Hengst, P. Jakimowicz, S. Subramanian, M.K. Johnson, M.J. Buttner, A.J. Thomson, and N.E. Le Brun. 2009. Characterization of [4Fe-4S]-Containing and Cluster-Free Forms of Streptomyces WhiD. *Biochemistry*. 48:12252-12264.

Das, A.K., D. Mitra, M. Harboe, B. Nandi, R.E. Harkness, D. Das, and H.G. Wiker. 2003. Predicted molecular structure of the mammalian cell entry protein Mce1A of Mycobacterium tuberculosis. *Biochemical and Biophysical Research Communications*. 302:442-447.

Dassa, E., and P. Bouige. 2001. The ABC of ABCs: a phylogenetic and functional classification of ABC systems in living organisms. *Research in Microbiology*. 152:211-229.

Datsenko, K.A., and B.L. Wanner. 2000. One-step inactivation of chromosomal genes in Escherichia coli K-12 using PCR products. *Proceedings of the National Academy of Sciences of the United States of America*. 97:6640-6645.

Daus, M.L., Berendts, S., Wuttge, S., Schneider, E. 2007. (*Postprint*) Maltose binding protein (MalE) interacts with periplasmic loops P2 and P1, respectively, of the MalFG subunits of the maltose ATP-binding cassette transporter (MalFGK2) from Escherichia coli/Salmonella during the transport cycle. *Molecular Microbiology*.

Dawson, R.J.P., K. Hollenstein, and K.P. Locher. 2007. Uptake or extrusion: crystal structures of full ABC transporters suggest a common mechanism. *Molecular Microbiology*. 65:250-257.

Dayrat, B. 2003. The roots of phylogeny: How did Haeckel build his trees? *Syst. Biol.* 52:515-527.

de Chastellier, C. 2009. The many niches and strategies used by pathogenic mycobacteria for survival within host macrophages. *Immunobiology*. 214:526-542.

de Jong, W., A. Manteca, J. Sanchez, G. Bucca, C.P. Smith, L. Dijkhuizen, D. Claessen, and H.A.B. Wosten. 2009. NepA is a structural cell wall protein involved in maintenance of spore dormancy in Streptomyces coelicolor. *Molecular Microbiology*. 71:1591-1603.

de Moraes, J., and S.C. Alfieri. 2008. Growth, encystment and survival of Acanthamoeba castellanii grazing on different bacteria. *FEMS Microbiol. Ecol.* 66:221-229.

den Hengst, C.D., N.T. Tran, M.J. Bibb, G. Chandra, B.K. Leskiw, and M.J. Buttner. 2010. Genes essential for morphological development and antibiotic

production in Streptomyces coelicolor are targets of BldD during vegetative growth. *Molecular Microbiology*. 78:361-379.

Desvaux, M., M. Hebraud, R. Talon, and I.R. Henderson. 2009. Outer membrane translocation: numerical protein secretion nomenclature in question in mycobacteria. *Trends in Microbiology*. 17:338-340.

Dickson, R., C. Weiss, R.J. Howard, S.P. Alldrick, R.J. Ellis, G. Lorimer, A. Azem, and P.V. Viitanen. 2000. Reconstitution of higher plant chloroplast chaperonin 60 tetradecamers active in protein folding. *Journal of Biological Chemistry*. 275:11829-11835.

Dinel, H., M. Schnitzer, T. Pare, L. Lemee, A. Ambles, and S. Lafond. 2001. Changes in lipids and sterols during composting. *J. Environ. Sci. Health Part B-Pestic. Contam. Agric. Wastes*. 36:651-665.

Dower, W.J., J.F. Miller, and C.W. Ragsdale. 1988. High-Efficiency Transformation of *Escherichia coli* by High-Voltage Electroporation. *Nucleic Acids Research*. 16:6127-6145.

Dramsi, S., S. Magnet, S. Davison, and M. Arthur. 2008. Covalent attachment of proteins to peptidoglycan. *FEMS Microbiology Reviews*. 32:307-320.

Durchschlag, E., W. Reiter, G. Ammerer, and C. Schuller. 2004. Nuclear localization destabilizes the stress-regulated transcription factor Msn2. *Journal of Biological Chemistry*. 279:55425-55432.

Eddyani, M., J.F. De Jonckheere, L. Durnez, P. Suykerbuyk, H. Leirs, and F. Portaels. 2008. Occurrence of Free-Living Amoebae in Communities of Low and High Endemicity for Buruli Ulcer in Southern Benin. *Applied and Environmental Microbiology*. 74:6547-6553.

Eitinger, T., D.A. Rodionov, M. Grote, and E. Schneider. 2010. Canonical and ECF-type ATP-binding cassette importers in prokaryotes: diversity in modular organization and cellular functions. *FEMS Microbiol Rev*. 35:3-67.

Ekelund, F., R. Ronn, and S. Christensen. 2001. Distribution with depth of protozoa, bacteria and fungi in soil profiles from three Danish forest sites. *Soil Biology & Biochemistry*. 33:475-481.

El-Shazly, S., S. Ahmad, A.S. Mustafa, R. Al-Attiyah, and D. Krajci. 2007. Internalization by HeLa cells of latex beads coated with mammalian cell entry (Mce) proteins encoded by the mce3 operon of Mycobacterium tuberculosis. *Journal of Medical Microbiology*. 56:1145-1151.

Embley, T.M., and E. Stackebrandt. 1994. The Molecular Phylogeny and Systematics of the Actinomycetes. *Annual Review of Microbiology*. 48:257-289.

Finn, R.D., J. Mistry, J. Tate, P. Coggill, A. Heger, J.E. Pollington, O.L. Gavin, P. Gunasekaran, G. Ceric, K. Forslund, L. Holm, E.L.L. Sonnhammer, S.R. Eddy, and A. Bateman. 2010. The Pfam protein families database. *Nucleic Acids Research*. 38:D211-D222.

Flardh, K. 2003. Essential role of DivIVA in polar growth and morphogenesis in Streptomyces coelicolor A3(2). *Molecular Microbiology*. 49:1523-1536.

Flesselles, B., N.N. Anand, J. Remani, S.M. Loosmore, and M.H. Klein. 1999. Disruption of the mycobacterial cell entry gene of Mycobacterium bovis BCG results in a mutant that exhibits a reduced invasiveness for epithelial cells. *Fems Microbiology Letters*. 177:237-242.

Foulston, L.C., and M.J. Bibb. 2010. Microbisporicin gene cluster reveals unusual features of lantibiotic biosynthesis in actinomycetes. *Proceedings of the National Academy of Sciences of the United States of America*. 107:13461-13466.

Fritsche, T.R., D. Sobek, and R.K. Gautom. 1998. Enhancement of in vitro cytopathogenicity by Acanthamoeba spp. following acquisition of bacterial endosymbionts. *Fems Microbiology Letters*. 166:231-236.

Froquet, R., Lelong, E., Marchetti, A., Cosson, P. 2009. *Dictyostelium discoideum*: a model host to measure bacterial virulence. *Nature protocols*. 4:5.

Gao, L.Y., and Y. Abu Kwaik. 2000. The mechanism of killing and exiting the protozoan host Acanthamoeba polyphaga by Legionella pneumophila. *Environmental Microbiology*. 2:79-90.

Garcia, M.T., S. Jones, C. Pelaz, R.D. Millar, and Y. Abu Kwaik. 2007. Acanthamoeba polyphaga resuscitates viable non-culturable Legionella pneumophila after disinfection. *Environmental Microbiology*. 9:1267-1277.

Gatfield, J., and J. Pieters. 2000. Essential role for cholesterol in entry of mycobacteria into macrophages. *Science*. 288:1647-1650.

Geiman, D.E., T.R. Raghunand, N. Agarwal, and W.R. Bishai. 2006. Differential gene expression in response to exposure to antimycobacterial agents and other stress conditions among seven Mycobacterium tuberculosis whiB-like genes. *Antimicrob. Agents Chemother.* 50:2836-2841.

Gey Van Pittius, N.C., J. Gamieldien, W. Hide, G.D. Brown, R.J. Siezen, and A.D. Beyers. 2001. The ESAT-6 gene cluster of Mycobacterium tuberculosis and other high G+C Gram-positive bacteria. *Genome Biol*. 2:RESEARCH0044.

Ghosh, J., P. Larsson, B. Singh, B.M.F. Pettersson, N.M. Islam, S.N. Sarkar, S. Dasgupta, and L.A. Kirsebom. 2009. Sporulation in mycobacteria. *Proceedings of the National Academy of Sciences of the United States of America*. 106:10781-10786.

Giegerich, R., F. Meyer, and C. Schleiermacher. 1996. GeneFisher--software support for the detection of postulated genes. *Proc Int Conf Intell Syst Mol Biol*. 4:68-77.

Gioffre, A., E. Infante, D. Aguilar, M. Santangelo, L. Klepp, A. Amadio, V. Meikle, I. Etchechoury, M.I. Romano, A. Cataldi, R.P. Hernandez, and F. Bigi. 2005. Mutation in mce operons attenuates Mycobacterium tuberculosis virulence. *Microbes and Infection*. 7:325-334.

Gonzalez-Ceron, G., O.J. Miranda-Olivares, and L. Servin-Gonzalez. 2009. Characterization of the methyl-specific restriction system of Streptomyces coelicolor A3(2) and of the role played by laterally acquired nucleases. *FEMS Microbiol Lett*. 301:35-43.

Gottelt, M., S. Kol, J.P. Gomez-Escribano, M. Bibb, and E. Takano. 2010. Deletion of a regulatory gene within the cpk gene cluster reveals novel antibacterial activity in Streptomyces coelicolor A3(2). *Microbiology-(UK)*. 156:2343-2353.

Goy, G., V. Thomas, K. Rimann, K. Jaton, G. Prod'hom, and G. Greub. 2007. The Neff strain of Acanthamoeba castellanii, a tool for testing the virulence of Mycobacterium kansasii. *Research in Microbiology*. 158:393-397.

Grant, S.G.N., J. Jessee, F.R. Bloom, and D. Hanahan. 1990. Differential Plasmid Rescue form Transgenic Mouse DNAs into *Escherichia coli* Methylation-Restriction Mutants. *Proceedings of the National Academy of Sciences of the United States of America*. 87:4645-4649.

Gregory, M.A., R. Till, and M.C.M. Smith. 2003. Integration site for streptomyces phage phi BT1 and development of site-specific integrating vectors. *Journal of Bacteriology*. 185:5320-5323.

Greub, G., and D. Raoult. 2004. Microorganisms resistant to free-living amoebae. *Clinical Microbiology Reviews*. 17:413-+.

Guenin-Mace, L., R. Simeone, and C. Demangel. 2009. Lipids of Pathogenic Mycobacteria: Contributions to Virulence and Host Immune Suppression. *Transboundary and Emerging Diseases*. 56:255-268.

Gurtovenko, A.A., and J. Anwar. 2007. Modulating the structure and properties of cell membranes: The molecular mechanism of action of dimethyl sulfoxide. *J. Phys. Chem. B*. 111:10453-10460.

Gust, B., G. Chandra, D. Jakimowicz, Y.Q. Tian, C.J. Bruton, and K.F. Chater. 2004. lambda red-mediated genetic manipulation of antibiotic-producing Streptomyces. *Advances in Applied Microbiology, Vol 54*. 54:107-128.

Haas, A. 2007. The phagosome: Compartment with a license to kill. *Traffic*. 8:311-330.

Hanahan, D. 1983. Studies on Transformation of *Escherichia coli* with Plasmids. *Journal of Molecular Biology*. 166:557-580.

Harb, O.S., L.Y. Gao, and Y. Abu Kwaik. 2000. From protozoa to mammalian cells: a new paradigm in the life cycle of intracellular bacterial pathogens. *Environmental Microbiology*. 2:251-265.

Hartmann, M., S. Lee, S.J. Hallam, and W.W. Mohn. 2009. Bacterial, archaeal and eukaryal community structures throughout soil horizons of harvested and

naturally disturbed forest stands. *Environmental Microbiology*. 11:3045-3062.

Haug, I., A. Weissenborn, D. Brolle, S. Bentley, T. Kieser, and J. Altenbuchner. 2003. Streptomyces coelicolor A3(2) plasmid SCP2*: deductions from the complete sequence. *Microbiology-(UK)*. 149:505-513.

He, X.L., and J.Z. Zhang. 2005. Gene complexity and gene duplicability. *Current Biology*. 15:1016-1021.

Heidrich, C., A. Ursinus, J. Berger, H. Schwarz, and J.V. Holtje. 2002. Effects of multiple deletions of murein hydrolases on viability, septum cleavage, and sensitivity to large toxic molecules in Escherichia coli. *Journal of Bacteriology*. 184:6093-6099.

Herron, P.R., G. Hughes, G. Chandra, S. Fielding, and P.J. Dyson. 2004. Transposon Express, a software application to report the identity of insertions obtained by comprehensive transposon mutagenesis of sequenced genomes: analysis of the preference for in vitro Tn5 transposition into GC-rich DNA. *Nucleic Acids Research*. 32.

Heuer, H., M. Krsek, P. Baker, K. Smalla, and E.M.H. Wellington. 1997. Analysis of actinomycete communities by specific amplification of genes encoding 16S rRNA and gel-electrophoretic separation in denaturing gradients. *Applied and Environmental Microbiology*. 63:3233-3241.

Hobbs, G., C.M. Frazer, D.C.J. Gardner, J.A. Cullum, and S.G. Oliver. 1989. Dispersed Growth of Streptomyces in Liquid Culture. *Applied Microbiology and Biotechnology*. 31:272-277.

Hodgson, D.A. 2000. Primary metabolism and its control in streptomycetes: A most unusual group of bacteria. *Advances in Microbial Physiology, Vol 42*. 42:47-238.

Hofmann, K., & Stoffel, W. 1993. TMbase - A database of membrane spanning protein segments. *Biological Chemistry Hoppe-Seyler*. 374.

Hollenstein, K., R.J.P. Dawson, and K.P. Locher. 2007. Structure and mechanism of ABC transporter proteins. *Current Opinion in Structural Biology*. 17:412-418.

Hopwood, D.A. 1967. Genetic analysis and genome structure in *Streptomyces coelicolor*. *Bacteriology Review*. 31:373-403.

Hopwood, D.A., and H.M. Wright. 1978. Bacterial protoplast fusion: recombination in fused protoplasts of *Streptomyces coelicolor Mol. Gen. Genet.* 162:307-317.

Hoskisson, P.A., and M.I. Hutchings. 2006. MtrAB-LpqB: a conserved threecomponent system in actinobacteria? *Trends in Microbiology*. 14:444-449.

Hoskisson, P.A., S. Rigali, K. Fowler, K.C. Findlay, and M.J. Buttner. 2006. DevA, a GntR-like transcriptional regulator required for development in Streptomyces coelicolor. *Journal of Bacteriology*. 188:5014-5023.

Hoskisson, P.A., and M.C.M. Smith. 2007. Hypervariation and phase variation in the bacteriophage 'resistome'. *Curr. Opin. Microbiol.* 10:396-400.

Huminiecki, L., and K.H. Wolfe. 2004. Divergence of spatial gene expression profiles following species-specific gene duplications in human and mouse. *Genome Research*. 14:1870-1879.

Huws, S.A., R.J. Morley, M.V. Jones, M.R.W. Brown, and A.W. Smith. 2008. Interactions of some common pathogenic bacteria with Acanthamoeba polyphaga. *Fems Microbiology Letters*. 282:258-265.

Ishhorowicz, D., and J.F. Burke. 1981. Rapid and Efficient Cosmid Cloning. *Nucleic Acids Research*. 9:2989-2998.

Ishikawa, J., A. Yamashita, Y. Mikami, Y. Hoshino, H. Kurita, K. Hotta, T. Shiba, and M. Hattori. 2004. The complete genomic sequence of Nocardia farcinica IFM 10152. *Proceedings of the National Academy of Sciences of the United States of America*. 101:14925-14930.

Joshi, S.M., A.K. Pandey, N. Capite, S.M. Fortune, E.J. Rubin, and C.M. Sassetti. 2006. Characterization of mycobacterial virulence genes through genetic interaction mapping. *Proceedings of the National Academy of Sciences of the United States of America*. 103:11760-11765.

Kang, J.G., M.Y. Hahn, A. Ishihama, and J.H. Roe. 1997. Identification of sigma factors for growth phase-related promoter selectivity of RNA polymerases from Streptomyces coelicolor A3(2). *Nucleic Acids Research*. 25:2566-2573.

Kendall, S.L., M. Withers, C.N. Soffair, N.J. Moreland, S. Gurcha, B. Sidders, R. Frita, A. ten Bokum, G.S. Besra, J.S. Lott, and N.G. Stoker. 2007. A highly conserved transcriptional repressor controls a large regulon involved in lipid degradation in Mycobacterium smegmatis and Mycobacterium tuberculosis. *Molecular Microbiology*. 65:684-699.

Khan, N. 2009. *Acanthamoeba*: Biology and Pathogenesis. Caister Academic Press. viii + 290 pp.

Kieser, T., K.F. Chater, M.J. Bibb, M.J. Buttner, and D.A. Hopwood. 2000. Practical *Streptomyces* genetics. The John Innes Foundation.

Kilvington, S., T. Gray, J. Dart, N. Morlet, J.R. Beeching, D.G. Frazer, and M. Matheson. 2004. Acanthamoeba keratitis: The role of domestic tap water contamination in the United Kingdom. *Investigative Ophthalmology & Visual Science*. 45:165-169.

Kim, K., S.J. Lee, K.H. Lee, and D.B. Lim. 1998. Isolation and characterization of toluene-sensitive mutants from the toluene-resistant bacterium Pseudomonas putida GM73. *Journal of Bacteriology*. 180:3692-3696.

Kimura, M., Z.J. Jia, N. Nakayama, and S. Asakawa. 2008. Ecology of viruses in soils: Past, present and future perspectives. *Soil Science and Plant Nutrition*. 54:1-32.

Knol, J., K. Bodewits, G.I. Hessels, L. Dijkhuizen, and R. Van der Geize. 2008. 3-Keto-5 alpha-steroid Delta'-dehydrogenase from Rhodococcus erythropolis SQ1 and its orthologue in Mycobacterium tuberculosis H37Rv are highly specific enzymes that function in cholesterol catabolism. *Biochemical Journal*. 410:339-346.

Kodani, S., M.E. Hudson, M.C. Durrant, M.J. Buttner, J.R. Nodwell, and J.M. Willey. 2004. The SapB morphogen is a lantibiotic-like peptide derived from the product of the developmental gene ramS in Streptomyces coelicolor.

Proceedings of the National Academy of Sciences of the United States of America. 101:11448-11453.

Kumar, A., M. Bose, and V. Brahmachari. 2003. Analysis of expression profile of mammalian cell entry (mce) operons of Mycobacterium tuberculosis. *Infection and Immunity*. 71:6083-6087.

Kumar, A., A. Chandolia, U. Chaudhry, V. Brahmachari, and M. Bose. 2005. Comparison of mammalian cell entry operons of mycobacteria: in silico analysis and expression profiling. *Fems Immunology and Medical Microbiology*. 43:185-195.

Kunisawa, T. 2007. Gene arrangements characteristic of the phylum Actinobacteria. *Antonie Van Leeuwenhoek International Journal of General and Molecular Microbiology*. 92:359-365.

Labeda, D.P. 2010. Multilocus sequence analysis of phytopathogenic *Streptomyces* species. *IJSEM Paper in Press*.

Lamb, D.C., H. Ikeda, D.R. Nelson, J. Ishikawa, T. Skaug, C. Jackson, S. Omura, M.R. Waterman, and S.L. Kelly. 2003. Cytochrome P450 complement (CYPome) of the avermectin-producer Streptomyces avermitilis and comparison to that of Streptomyces coelicolor A3(2). *Biochemical and Biophysical Research Communications*. 307:610-619.

Lemgruber, L., P. Lupetti, W. De Souza, R.C. Vommaro, and B. da Rocha-Azevedo. 2010. The fine structure of the Acanthamoeba polyphaga cyst wall. *Fems Microbiology Letters*. 305:170-176.

Lerat, S., A.M. Simao-Beaunoir, and C. Beaulieu. 2009. Genetic and physiological determinants of Streptomyces scabies pathogenicity. *Mol. Plant Pathol.* 10:579-585.

Letek, M., P. Gonzalez, I. Macarthur, H. Rodriguez, T.C. Freeman, A. Valero-Rello, M. Blanco, T. Buckley, I. Cherevach, R. Fahey, A. Hapeshi, J. Holdstock, D. Leadon, J. Navas, A. Ocampo, M.A. Quail, M. Sanders, M.M. Scortti, J.F. Prescott, U. Fogarty, W.G. Meijer, J. Parkhill, S.D. Bentley, and J.A. Vazquez-

Boland. 2010. The genome of a pathogenic rhodococcus: cooptive virulence underpinned by key gene acquisitions. *PLoS Genet*. 6.

Li, H.R., Y. Yu, W. Luo, and Y.X. Zeng. 2010. Marisediminicola antarctica gen. nov., sp. nov., an actinobacterium isolated from the Antarctic. *International Journal of Systematic and Evolutionary Microbiology*. 60:2535-2539.

Lima, P., B. Sidders, L. Morici, R. Reader, R. Senaratne, N. Casali, and L.W. Riley. 2007. Enhanced mortality despite control of lung infection in mice aerogenically infected with a Mycobacterium tuberculosis mce1 operon mutant. *Microbes and Infection*. 9:1285-1290.

Liu, Z., Y. Li, L.Q. Zheng, Y.J. Huang, and W.J. Li. 2010. Saccharomonospora marina sp nov., isolated from an ocean sediment of the East China Sea. *International Journal of Systematic and Evolutionary Microbiology*. 60:1854-1857.

Lynch, M., M. O'Hely, B. Walsh, and A. Force. 2001. The probability of preservation of a newly arisen gene duplicate. *Genetics*. 159:1789-1804.

MacNeil, D.J., K.M. Gewain, C.L. Ruby, G. Dezeny, P.H. Gibbons, and T. Macneil. 1992. Analysis of *Streptomyces avermitilis* Genes Required for Avermectin Biosynthesis Utilizing a Novel Integration Vector. *Gene*. 111:61-68.

Marjanovic, O., Miyata, T., Goodridge, A., Kendall, L.V., Riley, L.W. 2009. *Mce2* operon mutant strain of *Mycobacterium tuberculosis* is attenuated in C57BL/6 mice. *Tuberculosis*.

Mazza, P., E.E. Noens, K. Schirner, N. Grantcharova, A.M. Mommaas, H.K. Koerten, G. Muth, K. Flardh, G.P. Van Wezel, and W. Wohlleben. 2006. MreB of Streptomyces coelicolor is not essential for vegetative growth but is required for the integrity of aerial hyphae and spores. *Molecular Microbiology*. 60:838-852.

McBride, J., P.R. Ingram, F.L. Henriquez, and C.W. Roberts. 2005. Development of colorimetric microtiter plate assay for assessment of antimicrobials against Acanthamoeba. *Journal of Clinical Microbiology*. 43:629-634.

McLean, K.J., D. Clift, D.G. Lewis, M. Sabri, P.R. Balding, M.J. Sutcliffe, D. Leys, and A.W. Munro. 2006. The preponderance of P450s in the Mycobacterium tuberculosis genome. *Trends in Microbiology*. 14:220-228.

McMahon, H.E.M., C.T. Kelly, and W.M. Fogarty. 1997. Effect of growth rate on alpha-amylase production by Streptomyces sp. IMD 2679. *Applied Microbiology and Biotechnology*. 48:504-509.

Mehling, A., U.F. Wehmeier, and W. Piepersberg. 1995. Nucleotide Sequences of Streptomycete 16S Ribosomal DNA - Towards a Specific Identification System for Streptomycetes Using PCR. *Microbiology-Uk*. 141:2139-2147.

Mersinias, V. 2003. Total RNA isolation from *Streptomyces* cultures with RNeasy protect bacteria kit. Vol. 2009. UniS *Streptomyces* microarray group.

Mohn, W.W., R. van der Geize, G.R. Stewart, S. Okamoto, J. Liu, L. Dijkhuizen, and L.D. Eltis. 2008. The Actinobacterial mce4 Locus Encodes a Steroid Transporter. *Journal of Biological Chemistry*. 283:35368-35374.

Moussatova, A., C. Kandt, M.L. O'Mara, and D.P. Tieleman. 2008. ATP-binding cassette transporters in Escherichia coli. *Biochim. Biophys. Acta-Biomembr.* 1778:1757-1771.

Murashige, T., & Skoog, F. 1962. A revised medium for rapid growth and bioassays with Tobacco tissue cultures. *Physiologia Plantarum*. 15.

Murray, J.F. 2005. Pulmonary complications of HIV-1 infection among adults living in sub-Saharan Africa. *International Journal of Tuberculosis and Lung Disease*. 9:826-835.

Naumova, I.B., A.S. Shashkov, E.M. Tul'skaya, G.M. Streshinskaya, Y.I. Kozlova, N.V. Potekhina, L.I. Evtushenko, and E. Stackebrandt. 2001. Cell wall teichoic acids: structural diversity, species specificity in the genus Nocardiopsis, and chemotaxonomic perspective. *FEMS Microbiology Reviews*. 25:269-283.

Newton, H.J., D.K.Y. Ang, I.R. van Driel, and E.L. Hartland. 2010. Molecular Pathogenesis of Infections Caused by Legionella pneumophila. *Clinical Microbiology Reviews*. 23:274-298.

Nguyen, H.T., K.A. Wolff, R.H. Cartabuke, S. Ogwang, and L. Nguyen. 2010. A lipoprotein modulates activity of the MtrAB two-component system to provide intrinsic multidrug resistance, cytokinetic control and cell wall homeostasis in Mycobacterium. *Molecular Microbiology*. 76:348-364.

Niederweis, M., O. Danilchanka, J. Huff, C. Hoffmann, and H. Engelhardt. 2010. Mycobacterial outer membranes: in search of proteins. *Trends in Microbiology*. 18:109-116.

Nodwell, J.R., R. Yang, D. Kuo, and R. Losick. 1999. Extracellular complementation and the identification of additional genes involved in aerial mycelium formation in Streptomyces coelicolor. *Genetics*. 151:569-584.

O'Riordan, M., and D.A. Portnoy. 2002. The host cytosol: front-line or home front? *Trends in Microbiology*. 10:361-364.

Ogata, H., S. Goto, K. Sato, W. Fujibuchi, H. Bono, and M. Kanehisa. 1999. KEGG: Kyoto Encyclopedia of Genes and Genomes. *Nucleic Acids Research*. 27:29-34.

Ohnishi, Y., J. Ishikawa, H. Hara, H. Suzuki, M. Ikenoya, H. Ikeda, A. Yamashita, M. Hattori, and S. Horinouchi. 2008. Genome sequence of the streptomycin-producing microorganism Streptomyces griseus IFO 13350. *Journal of Bacteriology*. 190:4050-4060.

Ohno, S. 1970. Gene Duplication as an Evolutionary Force. *In* Peeters, H. 39-42.

Okanishi, M., K. Suzuki, and H. Umezawa. 1974. Formation and reversion of streptomycete protoplasts: cultural conditions and morphological study. *J. Gen. Microbiol.* 80:389-400.

Oldham, M.L., A.L. Davidson, and J. Chen. 2008. Structural insights into ABC transporter mechanism. *Current Opinion in Structural Biology*. 18:726-733.

Paget, M., Wilson, J., Figurski, D. 2000. *In* Practical Streptomyces Genetics. T. Kieser, editor. 249.

Pandey, A.K., and C.M. Sassetti. 2008. Mycobacterial persistance requires the utilization of host cholesterol. *Proceedings of the National Academy of Sciences of the United States of America*. 105:4376-4380.

Pavlik, M., D. Pavlikova, J. Balik, and M. Neuberg. 2010. The contents of amino acids and sterols in maize plants growing under different nitrogen conditions. *Plant Soil and Environment*. 56:125-132.

Pieters, J., Gatfield, J. 2002. Hijacking the host: survival of pathogenic mycobacteria inside macrophages. *Trends in Microbiology*. 10:142-146.

Quintana, E.T., K. Wierzbicka, P. Mackiewicz, A. Osman, A.H. Fahal, M.E. Hamid, J. Zakrzewska-Czerwinska, L.A. Maldonado, and M. Goodfellow. 2008. Streptomyces sudanensis sp nov., a new pathogen isolated from patients with actinomycetoma. *Antonie Van Leeuwenhoek International Journal of General and Molecular Microbiology*. 93:305-313.

Rahman, O., L.G. Dover, and I.C. Sutcliffe. 2009. Lipoteichoic acid biosynthesis: two steps forwards, one step sideways? *Trends in Microbiology*. 17:219-225.

Redenbach, M., H.M. Kieser, D. Denapaite, A. Eichner, J. Cullum, H. Kinashi, and D.A. Hopwood. 1996. A set of ordered cosmids and a detailed genetic and physical map for the 8 Mb Streptomyces coelicolor A3(2) chromosome. *Molecular Microbiology*. 21:77-96.

Reichheld, S.E., Z. Yu, and A.R. Davidson. 2009. The induction of folding cooperativity by ligand binding drives the allosteric response of tetracycline repressor. *Proceedings of the National Academy of Sciences of the United States of America*. 106:22263-22268.

Rigali, S., F. Titgemeyer, S. Barends, S. Mulder, A.W. Thomae, D.A. Hopwood, and G.P. van Wezel. 2008. Feast or famine: the global regulator DasR links nutrient stress to antibiotic production by Streptomyces. *EMBO Rep.* 9:670-675.

Riley, L.W. 1995. Determinants of cell entry and intracellular survival of Mycobacterium tuberculosis *Trends in Microbiology*. 3:27 - 31.

Ripoll, F., S. Pasek, C. Schenowitz, C. Dossat, V. Barbe, M. Rottman, E. Macheras, B. Heym, J.L. Herrmann, M. Daffe, R. Brosch, J.L. Risler, and J.L. Gaillard. 2009. Non Mycobacterial Virulence Genes in the Genome of the Emerging Pathogen Mycobacterium abscessus. *PLoS One*. 4:12.

Rodriguez-Garcia, A., P. Combes, R. Perez-Redondo, M.C.A. Smith, and M.C.M. Smith. 2005. Natural and synthetic tetracycline-inducible promoters for use in the antibiotic-producing bacteria Streptomyces. *Nucleic Acids Research*. 33.

Ryding, N.J., M.J. Bibb, V. Molle, K.C. Findlay, K.F. Chater, and M.J. Buttner. 1999. New sporulation loci in Streptomyces coelicolor A3(2). *Journal of Bacteriology*. 181:5419-5425.

Saini, N.K., Sharma, M., Chandolia, A. 2008. Characterization of Mce4A protein of *Mycobacterium tuberculosis*: role in invasion and survival. *Bmc Microbiology*. 8.

Saitou, N., and M. Nei. 1987. The Neighbour-Joining Method - A New Method for Reconstructing Phylogenetic Trees. *Molecular Biology and Evolution*. 4:406-425.

Salah, I.B., E. Ghigo, and M. Drancourt. 2009. Free-living amoebae, a training field for macrophage resistance of mycobacteria. *Clin. Microbiol. Infect.* 15:894-905.

Sambrook, J., E.F. Fritsch, and T. Maniatis. 1989. Molecular Cloning a Laboratory Manual. Cold Spring Harbour Laboratory Press.

San Roman, S.A., P.D. Facey, L. Fernandez-Martinez, C. Rodriguez, C. Vallin, R. Del Sol, and P. Dyson. 2010. A heterodimer of EsxA and EsxB is involved in sporulation and is secreted by a type VII secretion system in Streptomyces coelicolor. *Microbiology-(UK)*. 156:1719-1729.

Santangelo, M.D., F. Blanco, E. Campos, M. Soria, M.V. Bianco, L. Klepp, A. Alito, O. Zabal, A. Cataldi, and F. Bigi. 2009. Mce2R from Mycobacterium tuberculosis represses the expression of the mce2 operon. *Tuberculosis*. 89:22-28.

Santangelo, M.D., Klepp, L., Nunez-Garcia, J. 2009. Mce3R, a TetR-type transcriptional repressor, controls the expression of a regulon involved in lipid metabolism in *Mycobacterium tuberculosis*. *Microbiology-(UK)*. 155:2245-2255.

Santangelo, M.P., F.C. Blanco, M.V. Bianco, L.I. Klepp, O. Zabal, A.A. Cataldi, and F. Bigi. 2008. Study of the role of Mce3R on the transcription of mce genes of Mycobacterium tuberculosis. *Bmc Microbiology*. 8.

Santangelo, M.P., J. Goldstein, A. Alito, A. Gioffre, K. Caimi, O. Zabal, M. Zumarraga, M.I. Romano, A.A. Cataldi, and F. Bigi. 2002. Negative transcriptional regulation of the mce3 operon in Mycobacterium tuberculosis. *Microbiology-(UK)*. 148:2997-3006.

Sassetti, C.M., D.H. Boyd, and E.J. Rubin. 2003. Genes required for mycobacterial growth defined by high density mutagenesis. *Molecular Microbiology*. 48:77-84.

Schmitz-Esser, S., E.R. Toenshoff, S. Haider, E. Heinz, V.M. Hoenninger, M. Wagner, and M. Horn. 2008. Diversity of bacterial endosymbionts of environmental Acanthamoeba isolates. *Applied and Environmental Microbiology*. 74:5822-5831.

Seghezzi, N., Amar, P., Koebmann, B. 2010. The construction of a library of synthetic promoters revealed some specific features of strong *Streptomyces* promoters. *Applied Genetics and Molecular Biotechnology*.

Senaratne, R., Sidders, B., Sequeira, P. 2008. *Mycobacterium tuberculosis* strains disrupted in *mce3* and *mce4* operons are attenuated in mice. *Journal of Medical Microbiology*. 57:164-170.

Shimono, N., L. Morici, N. Casali, S. Cantrell, B. Sidders, S. Ehrt, and L.W. Riley. 2003. Hypervirulent mutant of Mycobacterium tuberculosis resulting from disruption of the mce1 operon. *Proceedings of the National Academy of Sciences of the United States of America*. 100:15918-15923.

Shirling, E.B., & Gottlieb, D. 1966. Methods for Characterization of *Streptomyces* species. *International Journal of Systematic Bacteriology*. 16:313-340.

Singh, B., J. Ghosh, N.M. Islam, S. Dasgupta, and L.A. Kirsebom. 2010. Growth, cell division and sporulation in mycobacteria. *Antonie Van Leeuwenhoek International Journal of General and Molecular Microbiology*. 98:165-177.

Song, H., R. Sandie, Y. Wang, M.A. Andrade-Navarro, and M. Niederweis. 2008. Identification of outer membrane proteins of Mycobacterium tuberculosis. *Tuberculosis*. 88:526-544.

Stackebrandt, E., D. Witt, C. Kemmerling, R. Kroppenstedt, and W. Liesack. 1991. Designation of Streptomycete 16S and 23S Ribosomal-RNA-Based Target Regions for Oligonucleotide Probes. *Applied and Environmental Microbiology*. 57:1468-1477.

Suarez, J., C. Barbes, and C. Hardisson. 1980. Germination of Spores of *Micromonospora chalcea* - Physiological and Biochemical Changes. *Journal of General Microbiology*. 121:159-167.

Sun, J.H., A. Hesketh, and M. Bibb. 2001. Functional Analysis of relA and rshA, two relA/spoT homologues of Streptomyces coelicolor A3(2). *Journal of Bacteriology*. 183:3488-3498.

Sun, J.H., G.H. Kelemen, J.M. Fernandez-Abalos, and M.J. Bibb. 1999. Green fluorescent protein as a reporter for spatial and temporal gene expression in Streptomyces coelicolor A3(2). *Microbiology-Uk*. 145:2221-2227.

Sun Y, C.Y., Mai V, Farmerie W, Yu F, Li J, Goodison S. 2010. Advanced computational algorithms for microbial community analysis using massive 16S rRNA sequence data. *Nucleic Acids Research*. 38.

Sutcliffe, I.C. 2011. New insights into the distribution of WXG100 protein secretion systems. *Antonie Van Leeuwenhoek*. 99:127-131.

Sutcliffe, l.C., and D.J. Harrington. 2004. Lipoproteins of Mycobacterium tuberculosis: an abundant and functionally diverse class of cell envelope components. *FEMS Microbiology Reviews*. 28:645-659.

Swanson, M.M., G. Fraser, T.J. Daniell, L. Torrance, P.J. Gregory, and M. Taliansky. 2009. Viruses in soils: morphological diversity and abundance in the rhizosphere. *Ann. Appl. Biol.* 155:51-60.

Tamura, K., J. Dudley, M. Nei, and S. Kumar. 2007. MEGA4: Molecular evolutionary genetics analysis (MEGA) software version 4.0. *Molecular Biology and Evolution*. 24:1596-1599.

Teichmann, S.A., and M.M. Babu. 2004. Gene regulatory network growth by duplication. *Nature Genetics*. 36:492-496.

ten Bokum, A.M.C., F. Movahedzadeh, R. Frita, G.J. Bancroft, and N.G. Stoker. 2008. The case for hypervirulence through gene deletion in Mycobacterium tuberculosis. *Trends in Microbiology*. 16:436-441.

Thomaides, H.B., E.J. Davison, L. Burston, H. Johnson, D.R. Brown, A.C. Hunt, J. Errington, and L. Czaplewski. 2007. Essential bacterial functions encoded by gene pairs. *Journal of Bacteriology*. 189:591-602.

Thomas, G.H. 2010. Homes for the orphans: utilization of multiple substrate-binding proteins by ABC transporters. *Molecular Microbiology*. 75.

Thompson, B.J., D.A. Widdick, M.G. Hicks, G. Chandra, I.C. Sutcliffe, T. Palmer, and M.I. Hutchings. 2010. Investigating lipoprotein biogenesis and function in the model Gram-positive bacterium Streptomyces coelicolor. *Molecular Microbiology*. 77:943-957.

Thompson, C.J., J.M. Ward, and D.A. Hopwood. 1980. DNA Cloning in Streptomyces - Resistance Genes from Antibiotic-Producing Species. *Nature*. 286:525-527.

Tokala, R.K., J.L. Strap, C.M. Jung, D.L. Crawford, M.H. Salove, L.A. Deobald, J.F. Bailey, and M.J. Morra. 2002. Novel plant-microbe rhizosphere interaction involving Streptomyces lydicus WYEC108 and the pea plant (Pisum sativum). *Applied and Environmental Microbiology*. 68:2161-2171.

Tortoli, E. 2006. The new mycobacteria: an update. *Fems Immunology and Medical Microbiology*. 48:159-178.

Traag, B.A., A. Driks, P. Stragier, W. Bitter, G. Broussard, G. Hatfull, F. Chu, K.N. Adams, L. Ramakrishnan, and R. Losick. 2010. Do mycobacteria produce endospores? *Proceedings of the National Academy of Sciences of the United States of America*. 107:878-881.

Tucker, N.P., M.G. Hicks, T.A. Clarke, J.C. Crack, G. Chandra, N.E. Le Brun, R. Dixon, and M.I. Hutchings. 2008. The Transcriptional Repressor Protein NsrR Senses Nitric Oxide Directly via a [2Fe-2S] Cluster. *PLoS One*. 3.

Vaillancourt, P., G.L. Costa, and M.P. Weiner. 1994. Vector Systems for Directional and Bidirectional Cloning of PCR-Generated DNA Fragments and High-Level Protein Expression. *Abstr. Pap. Am. Chem. Soc.* 207:123-BIOT.

Volkman, H.E., H. Clay, D. Beery, J.C.W. Chang, D.R. Sherman, and L. Ramakrishnan. 2004. Tuberculous granuloma formation is enhanced by a Mycobacterium virulence determinant. *Plos Biology*. 2:1946-1956.

Waterfield, N.R., M. Sanchez-Contreras, I. Eleftherianos, A. Dowling, G. Yang, P. Wilkinson, J. Parkhill, N. Thomson, S.E. Reynolds, H.B. Bode, S. Dorus, and R.H. Ffrench-Constant. 2009. Rapid Virulence Annotation (RVA): Identification of virulence factors using a bacterial genome library and multiple invertebrate hosts (vol 105, pg 15967, 2008). *Proceedings of the National Academy of Sciences of the United States of America*. 106:2083-2083.

WHO. 2010. Global tuberculosis control report 2010. World Health Organisation.

Widdick, D.A., K. Dilks, G. Chandra, A. Bottrill, M. Naldrett, M. Pohlschroder, and T. Palmer. 2006. The twin-arginine translocation pathway is a major route of protein export in Streptomyces coelicolor. *Proceedings of the National Academy of Sciences of the United States of America*. 103:17927-17932.

Widdick, D.A., M.G. Hicks, B.J. Thompson, A. Tschumi, G. Chandra, I.C. Sutcliffe, J.K. Bruelle, P. Sander, T. Palmer, and M.I. Hutchings. 2011. Dissecting the complete lipoprotein biogenesis pathway in Streptomyces scabies. *Molecular Microbiology*. 80:1395-1412.

Wu, G., L. Nie, and W. Zhang. 2006. Predicted highly expressed genes in Nocardia farcinica and the implication for its primary metabolism and nocardial virulence. *Antonie Van Leeuwenhoek*. 89:135-146.

Xiang, H.Y., N. Takaya, and T. Hoshino. 2006. Novel cholesterol esterase secreted by Streptomyces persists during aqueous long-term storage. *J. Biosci. Bioeng.* 101:19-25.

Xu, J., Y. Wang, S.J. Xie, J. Xiao, and J.S. Ruan. 2009. Streptomyces xiamenensis sp nov., isolated from mangrove sediment. *International Journal of Systematic and Evolutionary Microbiology*. 59:472-476.

Xue, L.J., M.M. Cao, J. Luan, H. Ren, X. Pan, J. Cao, and Z.T. Qi. 2007. Mammalian cell entry protein of Mycobacterium tuberculosis induces the proinflammatory response in RAW 264.7 murine macrophage-like cells. *Tuberculosis*. 87:185-192.

Yam, K., D'Angelo, I., Kalsheuer, R., Zhu, H., Wang, J., Snieckus, V., Ly, L.H., Converse, P.J., Jacobs, W.R., Strynadka, N., Eltis, L.D. 2009. Studies of a ring-cleaving dioxygenase illuminate the role of cholesterol metabolism in the pathogenesis of *Mycobacterium tuberculosis*. *Plos Pathogens*. 5.

Yamamura, H., T. Tamura, Y. Sakiyama, and S. Harayama. 2007. Nocardia amamiensis sp nov., isolated from a sugar-cane field in Japan. *International Journal of Systematic and Evolutionary Microbiology*. 57:1599-1602.

Yamasaki, M., M. Redenbach, and H. Kinashi. 2001. Integrated structures of the linear plasmid SCP1 in two bidirectional donor strains of Streptomyces coelicolor A3(2). *Molecular and General Genetics*. 264:634-642.

Yang, X.X., E. Dubnau, I. Smith, and N.S. Sampson. 2007. Rv1106c from Mycobacterium tuberculosis is a 3 beta-hydroxysteroid dehydrogenase. *Biochemistry*. 46:9058-9067.

Zhi, X.Y., Li, W.J., Stackebrandt, E. 2009. An update of the structure and 16S rRNA gene sequence-based definition of higher ranks of the class Actinobacteria, with the proposal of two new suborders and four new families and emended descriptions of the existing higher taxa. *International Journal of Systematic and Evolutionary Microbiology*. 59:589-608.